SR Monitor – Special topics

T. Mitsuhashi

Classical Optics is disappearing from curriculum of Universities now!

Some geometrical optics can find in high school physics……..

You can buy or find not kind textbooks.

I try to introduce classical optics useful for SR monitor.

Story of my talk

1. Introduction

2. SR monitor based on visible SR

   - Extraction of visible SR and optical path to dark room key components and it's design

   - How to identify wavefront error

3. Common equipments use in SR monitor

4. Optics for focusing system

   - Geometrical optics of focusing system
   - Wave optics of focusing system

If I will have further time, I will add followings;

- **Application of Adaptive optics to correct thermal deformation of extraction mirror**
- **Dynamical observation of beam profile with high-speed gated camera**
- **Streak camera technique for longitudinal profile measurement**
- **Optical phase space monitor by focusl system and afocal system**
- **1st order spatial Interferometry beam size measurement**
- **Beam halo measurement with the Coronagraph**

5. SR monitor based on X-ray

- Pin-hole camera
- Fresnel zone plate

Not include SR theory, please see some other text.

1. Introduction

The SR monitor is beam instrumentation to measure the transverse and longitudinal profile, size, etc. statistically, or dynamically using optical technique with the synchrotron radiation.

1. **Light source is normally SR emitted from the bending magnet.**
2. **Visible SR   380nm-800nm.**
3. **X-ray SR   0.05-0.3nm.**

VUV region is not used because of difficulty in handling.

Based on Visible Synchrotron radiation

Transverse

Transverse beam profile or size diagnostics

Imaging

geometrical optics

Interferometry

Wave optics

1^{st} and 2ed order spatial coherence

Transverse beam profile or size diagnostics

light as photon

light as Wave

Imaging

Interferometry

Transverse beam profile or size diagnostics

light as photon

light as Wave

Imaging

$\Delta\theta/\lambda * \Delta x \geq 1$

Interferometry

$2\ \Delta\phi * \Delta N \geq 1$

Transverse beam profile or size diagnostics

light as photon

Imaging

$\Delta\theta/\lambda * \Delta x$

50μm

light as Wave

Interferometry

$\Delta\phi * \Delta N$

2μm

Key point is wavefront error

Longitudinal

Longitudinal beam profile or size diagnostics

imaging

Streak camera

2ed order coherence

(1st order coherence)

Intensity interferometry

Auto correlation

Cross correlation

Longitudinal beam profile or size diagnostics

imaging

Streak

2-3ps

200fs

Typical streak camera

fs streak camera

2ed ord

Limited by glass dispersion

Intensity interferometry 100fs

Auto correlation

Cross correlation

Influenced by timing jitter between two inputs

Based on X-ray synchrotron radiation for submicron beam size measurement

Transverse beam profile or size diagnostics

Imaging

Pinhole camera

Fresnel zone plate

K-B mirror (Kirkpatrick-Batz mirror)

Interferometry

X-ray interferomter

Transverse beam profile or size diagnostics

Geometrical optics

1^{st} and 2ed order spatial coherence

Imaging

- Pinhole camera
- Fresnel zone plate
- K-B mirror (Kirkpatrick-Batz mirror)

Few 100nm

Interferometry

- X-ray interferomter

Sub nm to few nm

Key point is wavefront error

Transverse beam profile or size diagnostics

Geometrical optics

1st and 2ed order spatial coherence

Imaging	**Interferometry**
Fresnel zone plate	**X-ray interferomter**
K-B mirror (Kirkpatrick-Batz mirror)	
Few 100nm	**Sub nm to few nm**

2. SR monitor based on visible SR

Extraction of visible SR
and
Optical path to dark room
Key components and it’s design

Set up of SR monitor

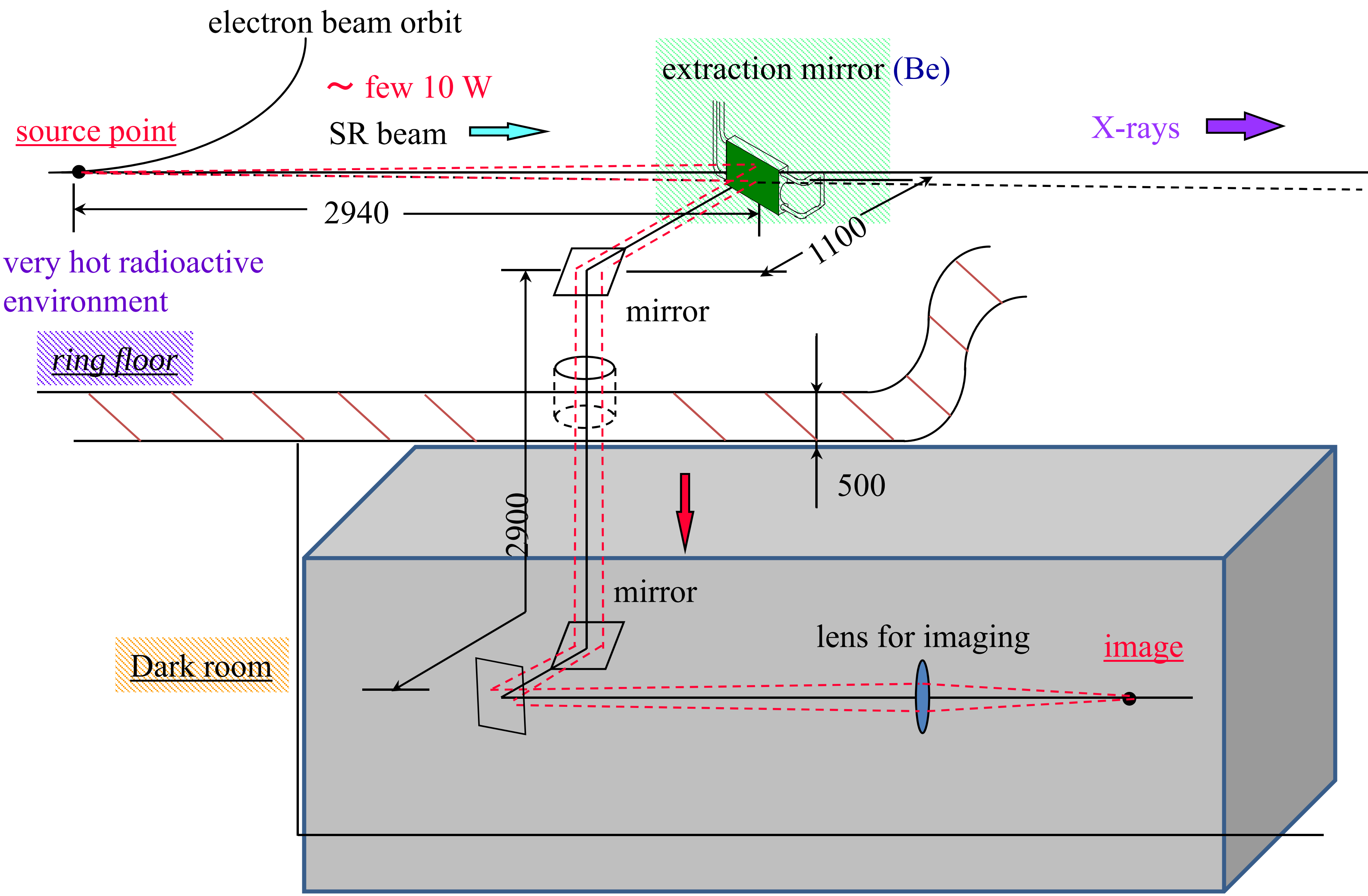

Optical path layout at KEK B-factory

Total length is about 40m

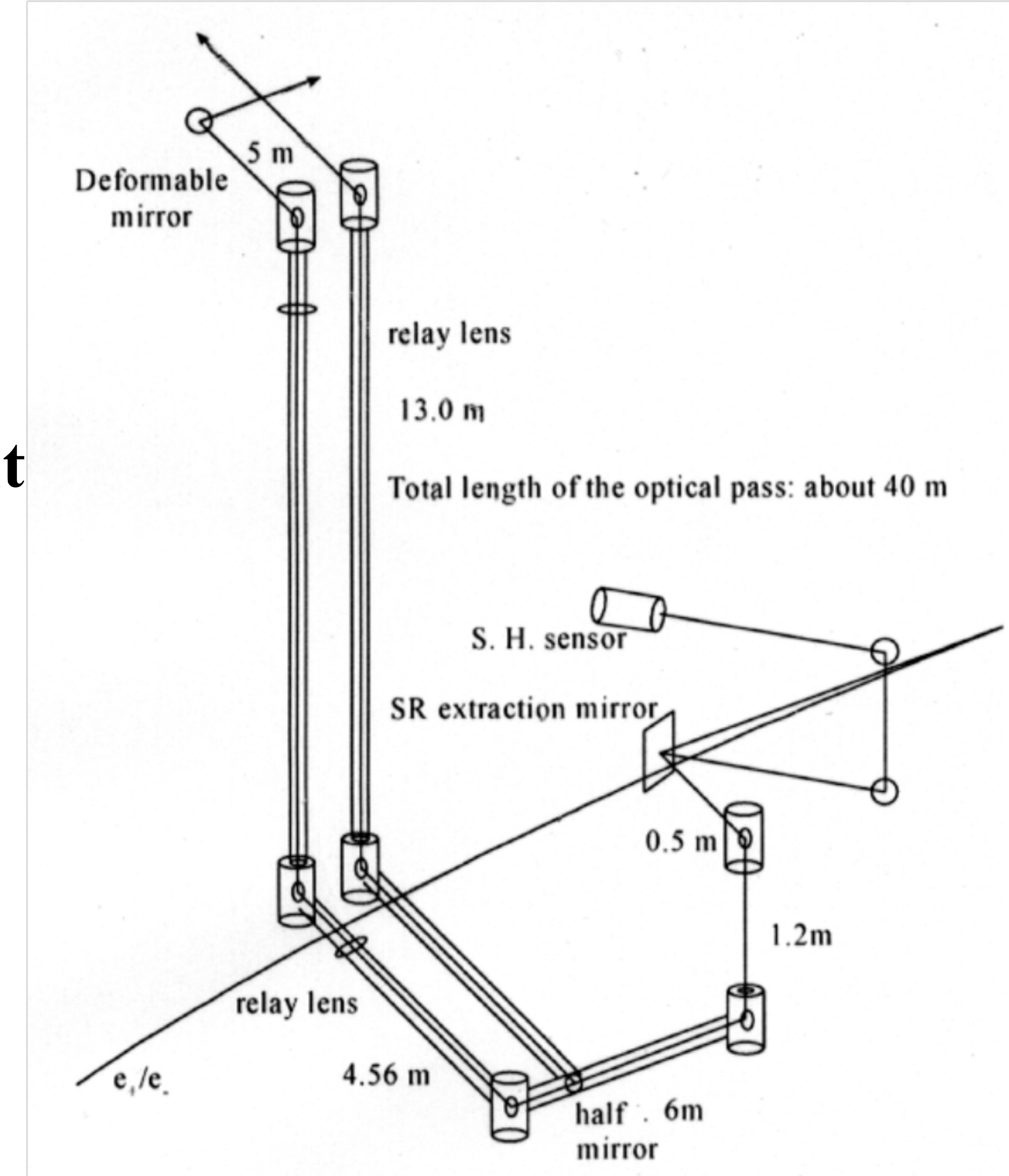

Extraction mirror design

Beryllium extraction mirror

Photon Factory   E=2.5GeV, ρ=8.66m

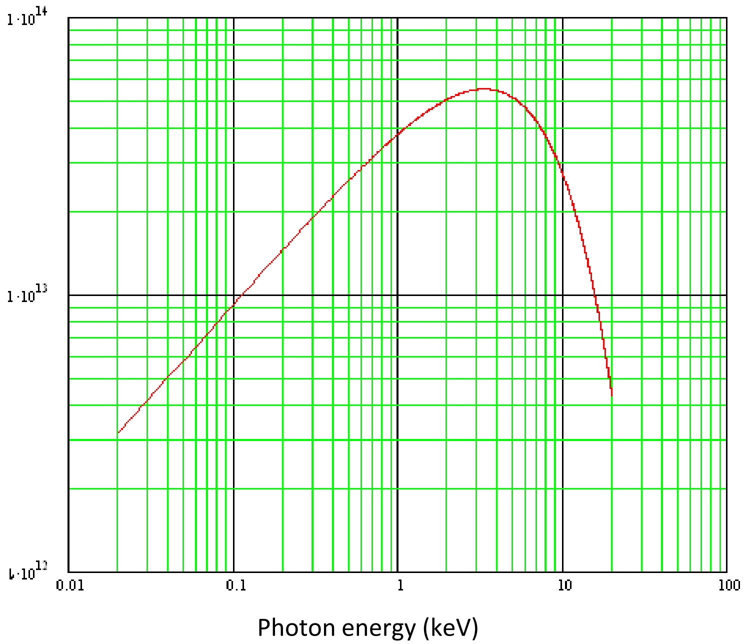

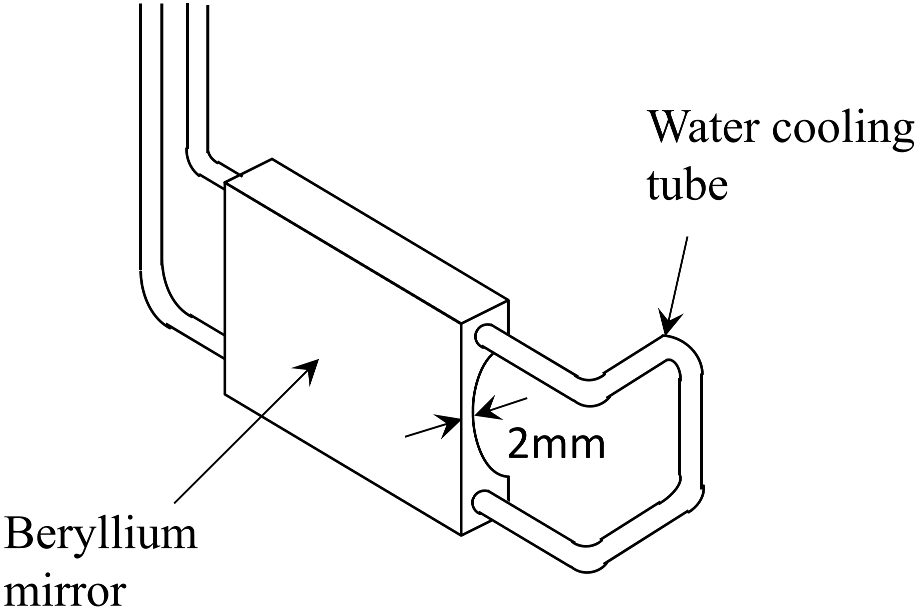

Angular distribution of SR at 500nm

2.5GeV
ρ=8.66m

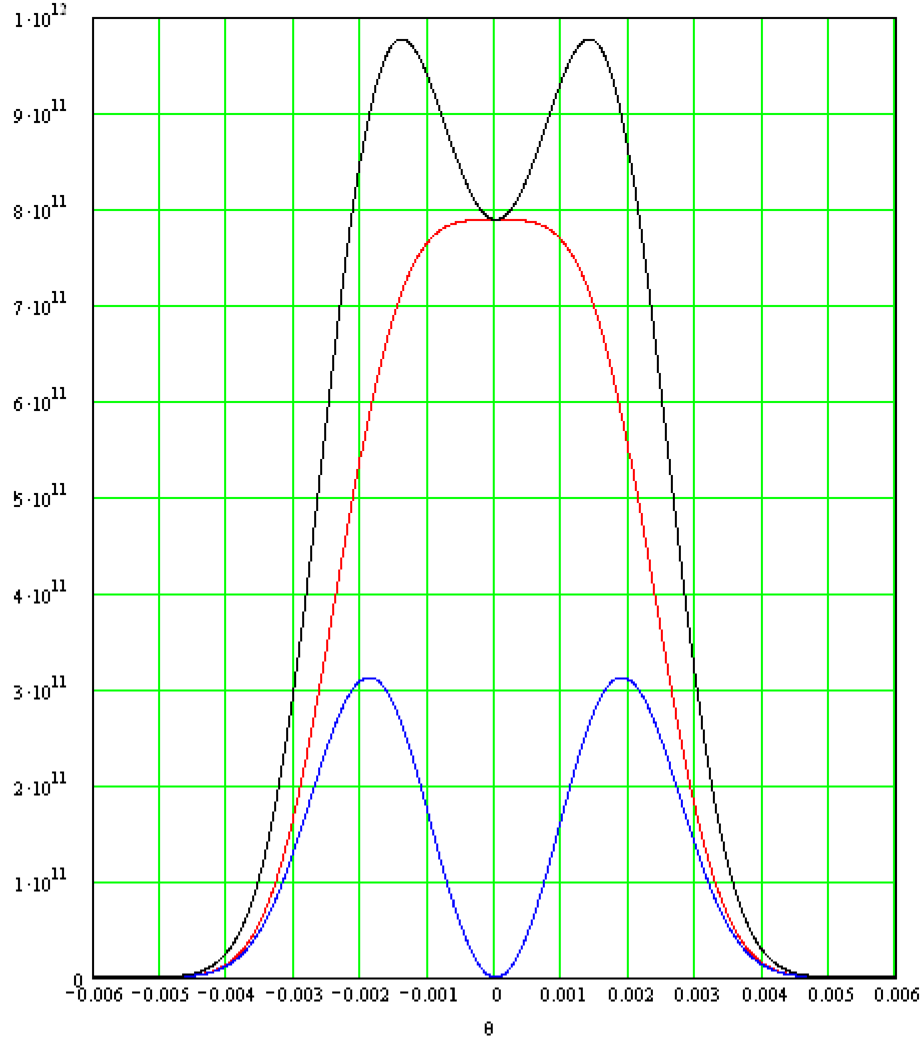

Beryllium extraction mirror for the B-factory
E=3.5GeV, ρ=65m

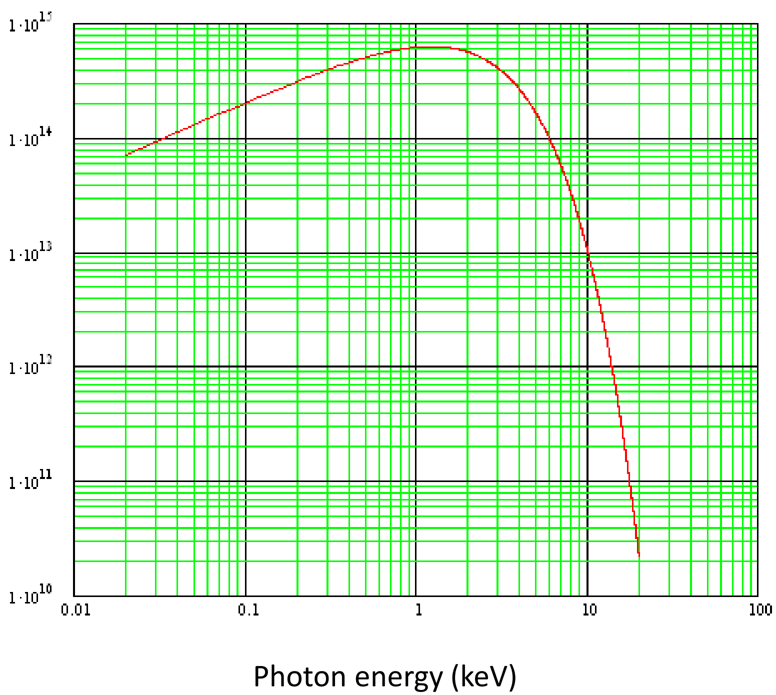

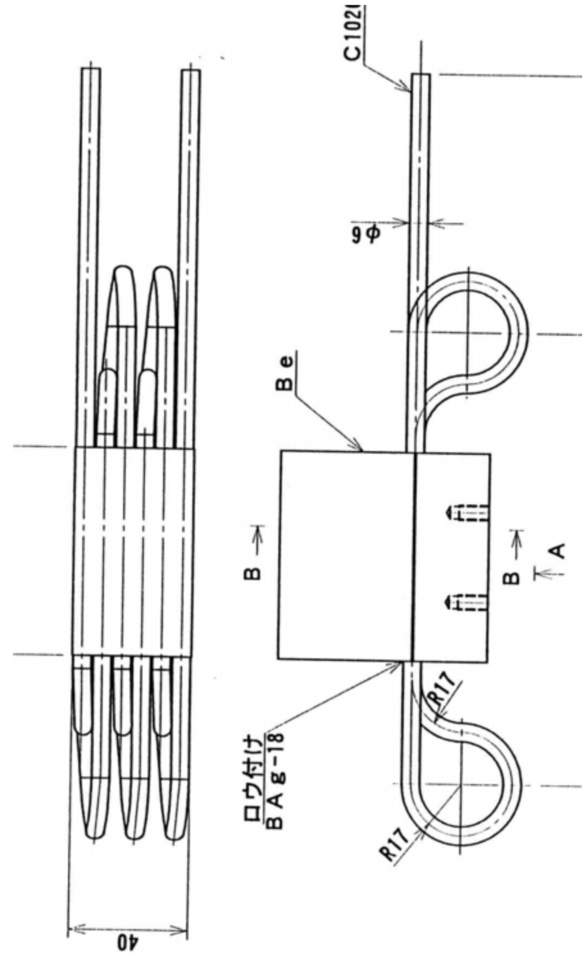

500nm

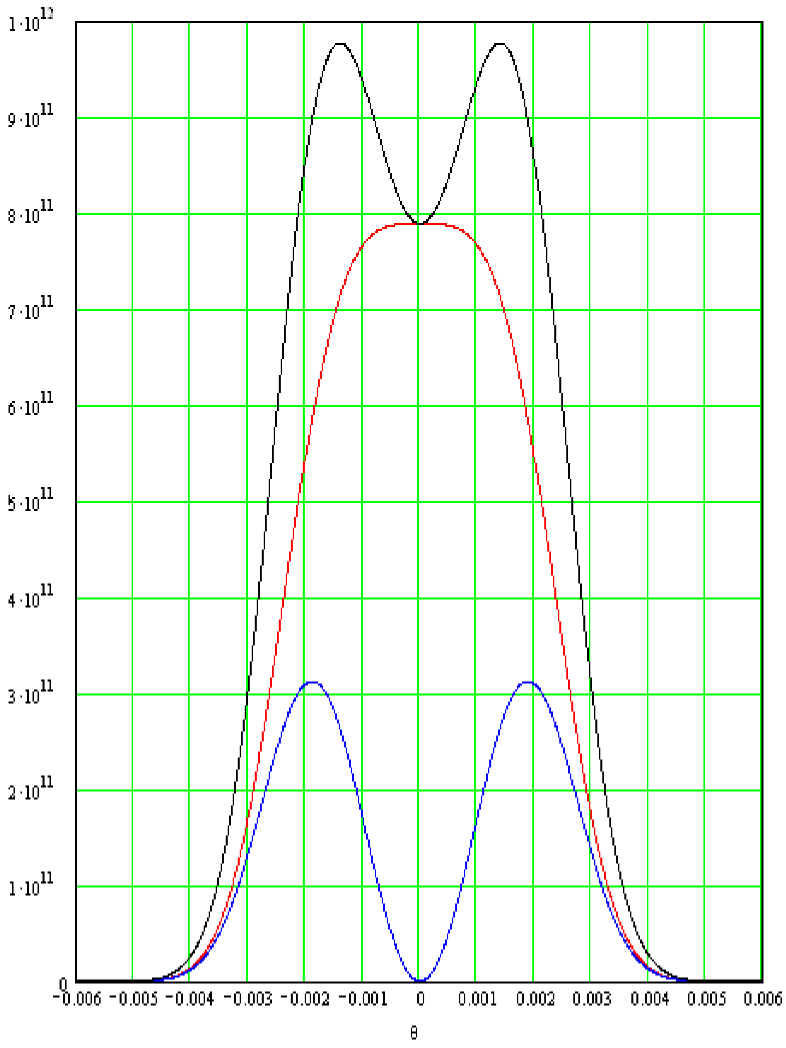

$1 \cdot 10^{12}$
$9 \cdot 10^{11}$
$8 \cdot 10^{11}$
$7 \cdot 10^{11}$
$6 \cdot 10^{11}$
$5 \cdot 10^{11}$
$4 \cdot 10^{11}$
$3 \cdot 10^{11}$
$2 \cdot 10^{11}$
$1 \cdot 10^{11}$
0
−0.006 −0.005 −0.004 −0.003 −0.002 −0.001 0 0.001 0.002 0.003 0.004 0.005 0.006
θ

0.1nm

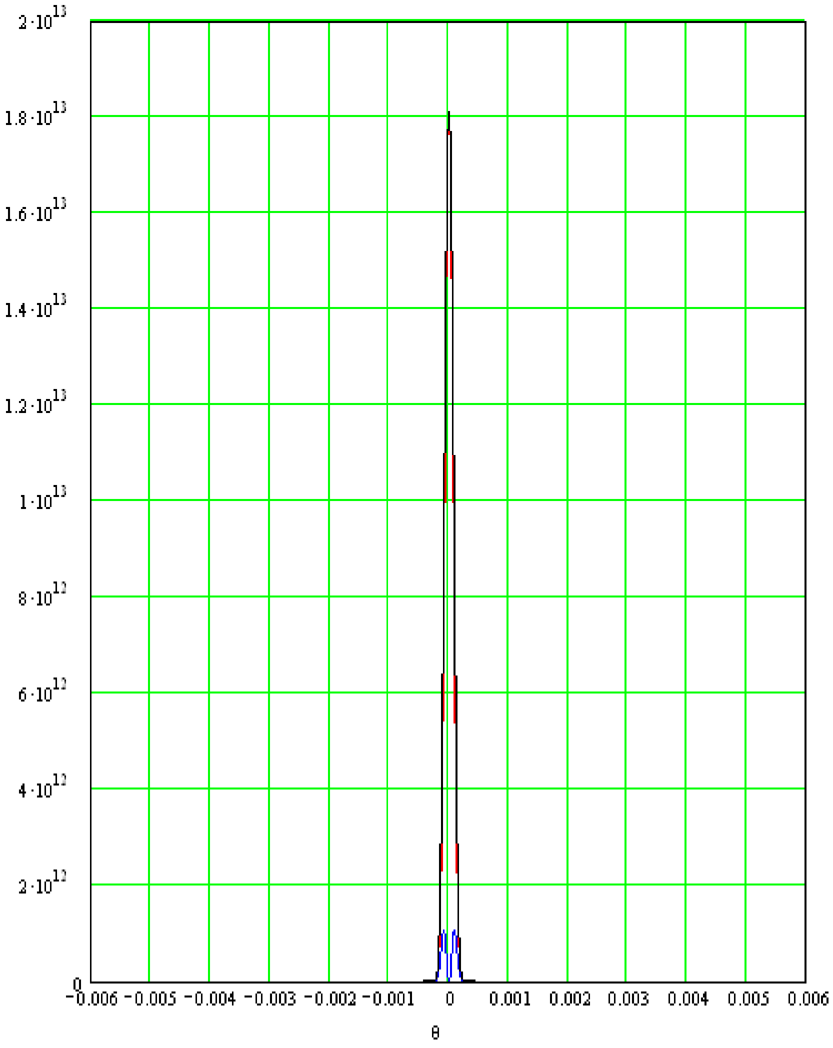

$2 \cdot 10^{13}$
$1.8 \cdot 10^{13}$
$1.6 \cdot 10^{13}$
$1.4 \cdot 10^{13}$
$1.2 \cdot 10^{13}$
$1 \cdot 10^{13}$
$8 \cdot 10^{12}$
$6 \cdot 10^{12}$
$4 \cdot 10^{12}$
$2 \cdot 10^{12}$
0
−0.006 −0.005 −0.004 −0.003 −0.002 −0.001 0 0.001 0.002 0.003 0.004 0.005 0.006
θ

Extraction mirror with X-ray absorber

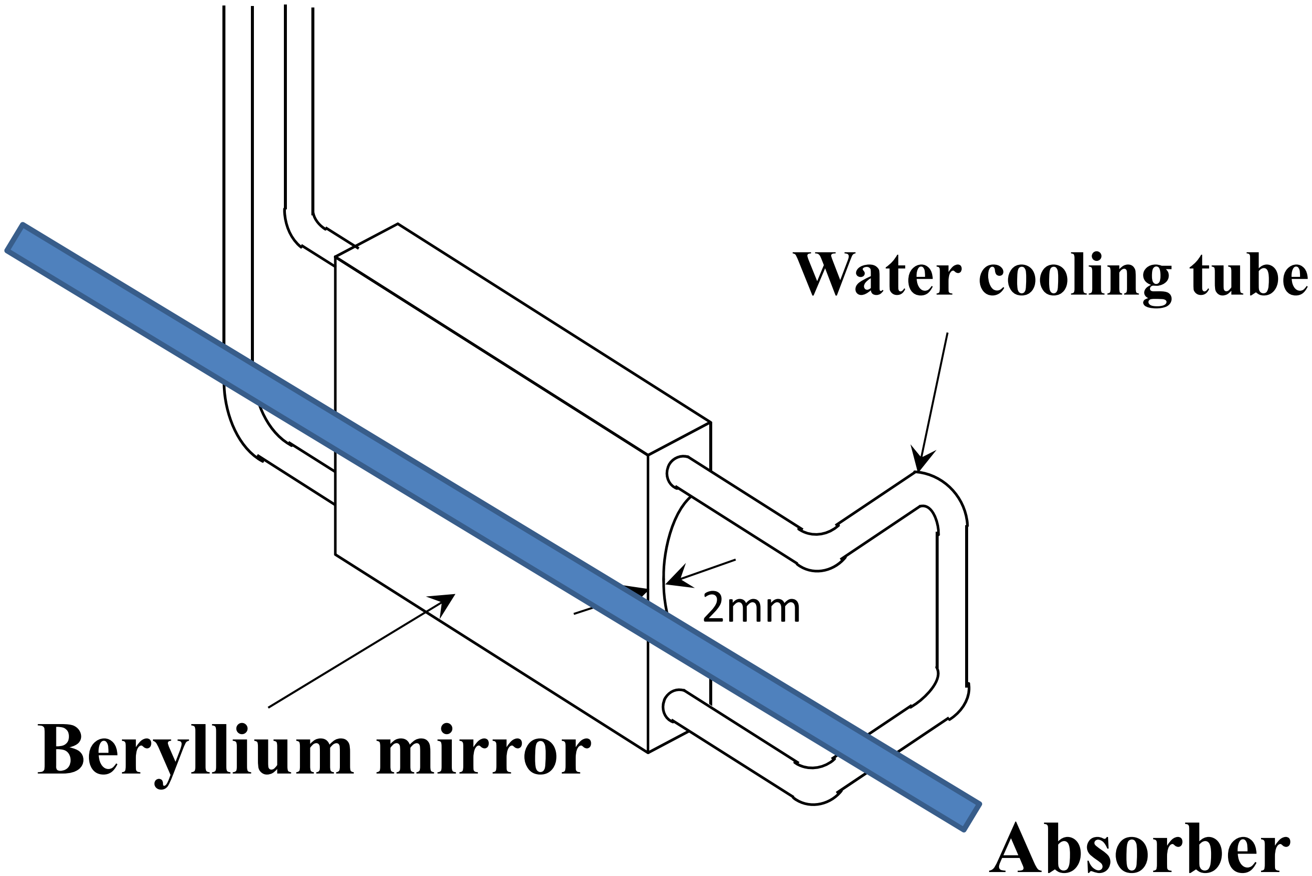

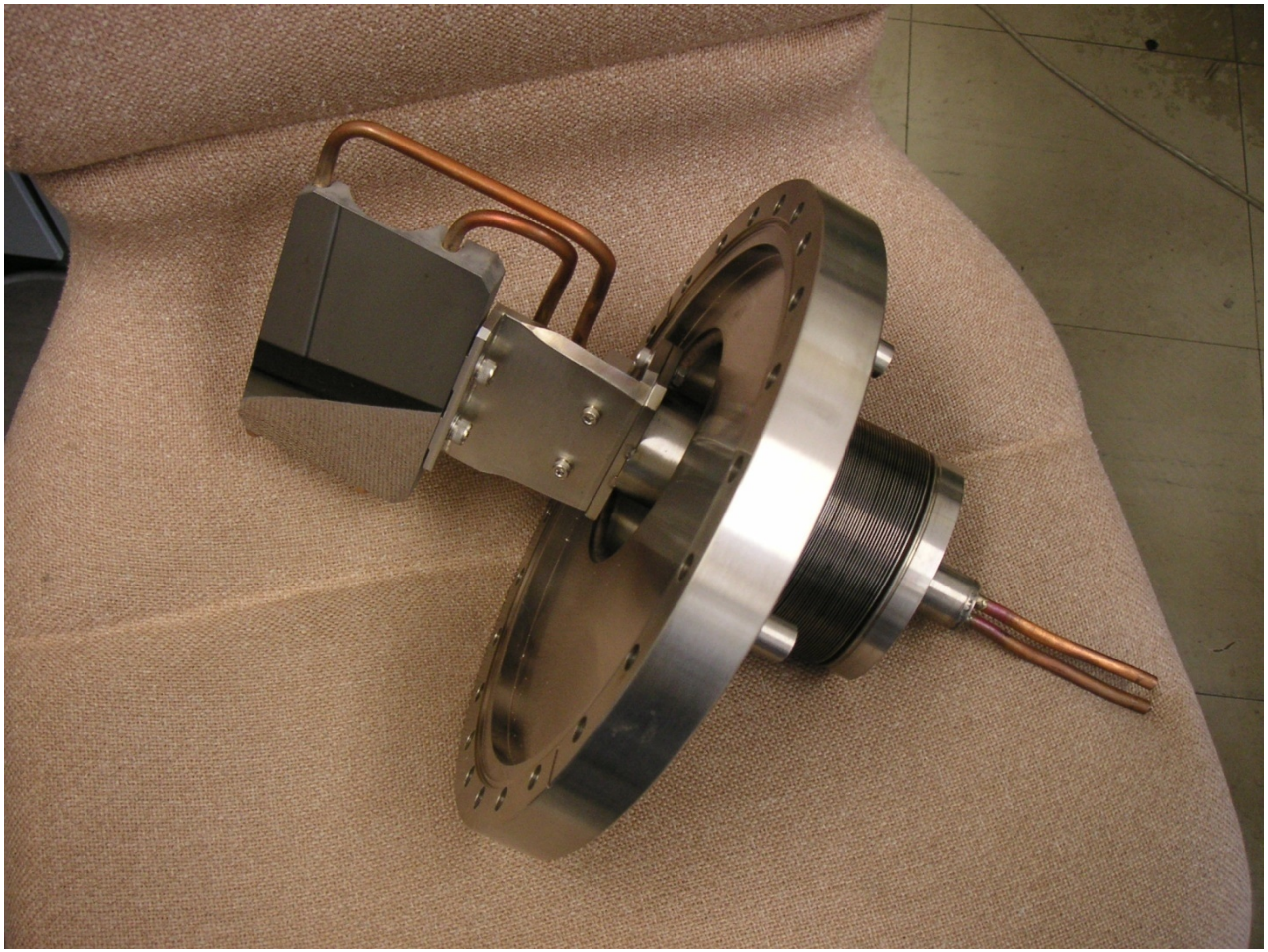

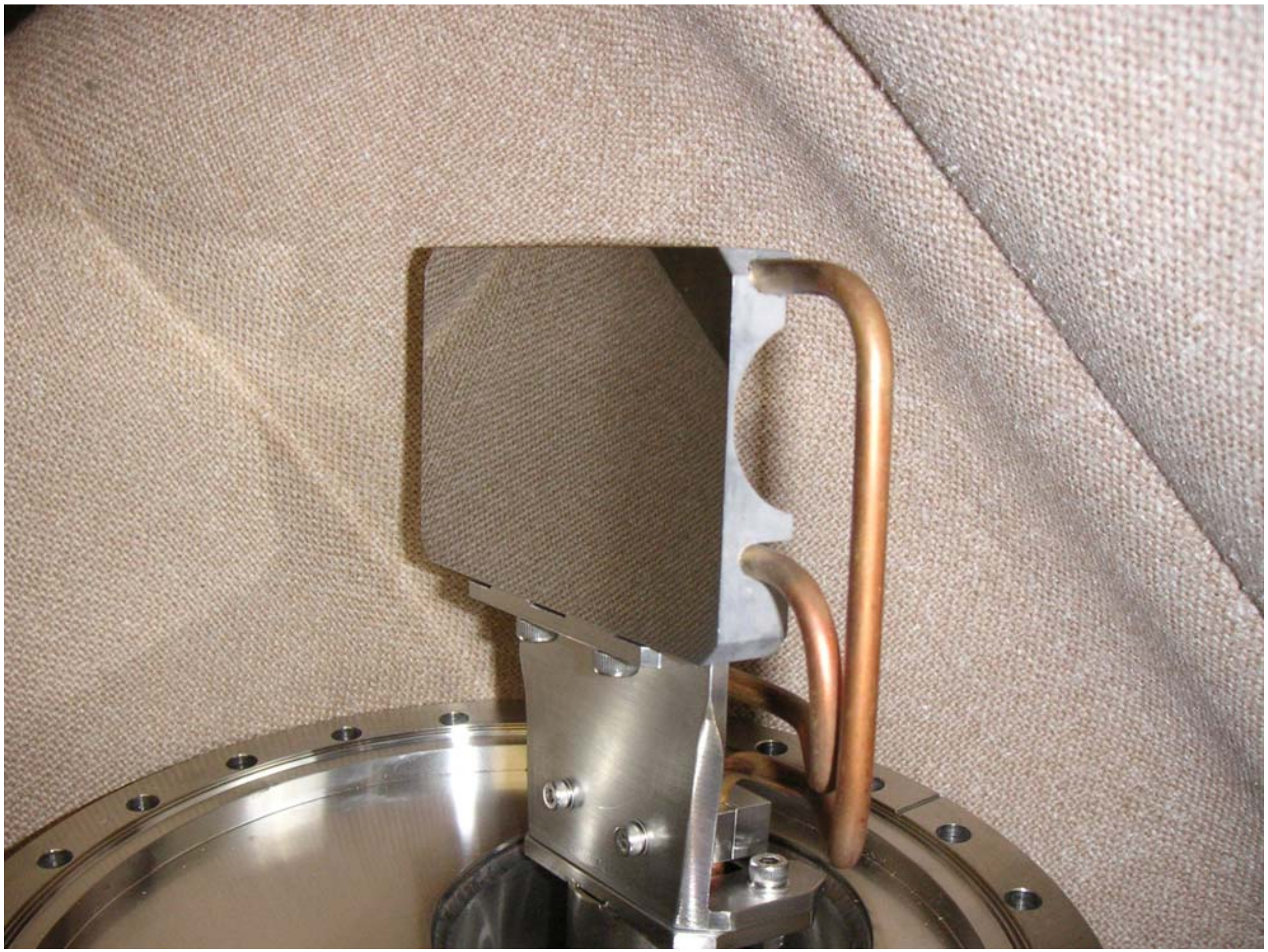


'98 9 27


'98 7 20

The l/10 glass window for the extraction of visible SR

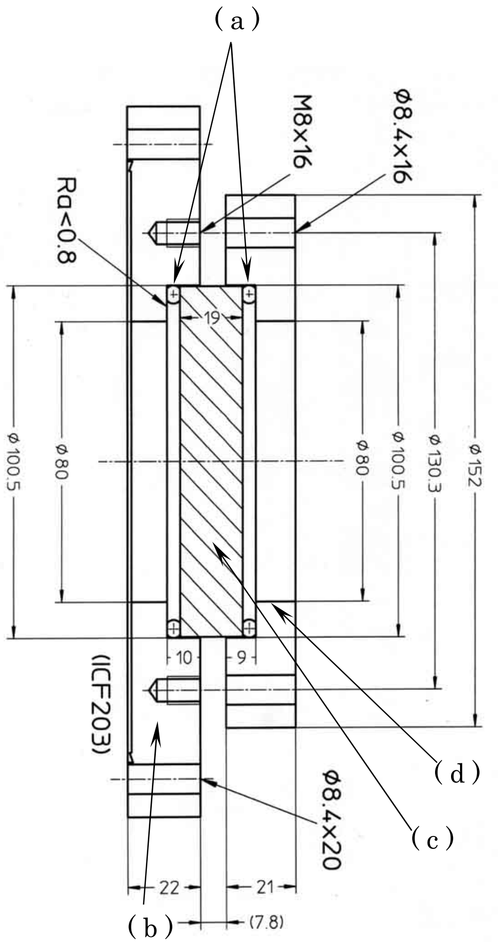

General design of the glass window. In this figure, (a): metal O-ring, (b): vacuum-side conflat flange, (c): optical glass flat, (d): air-side flange.

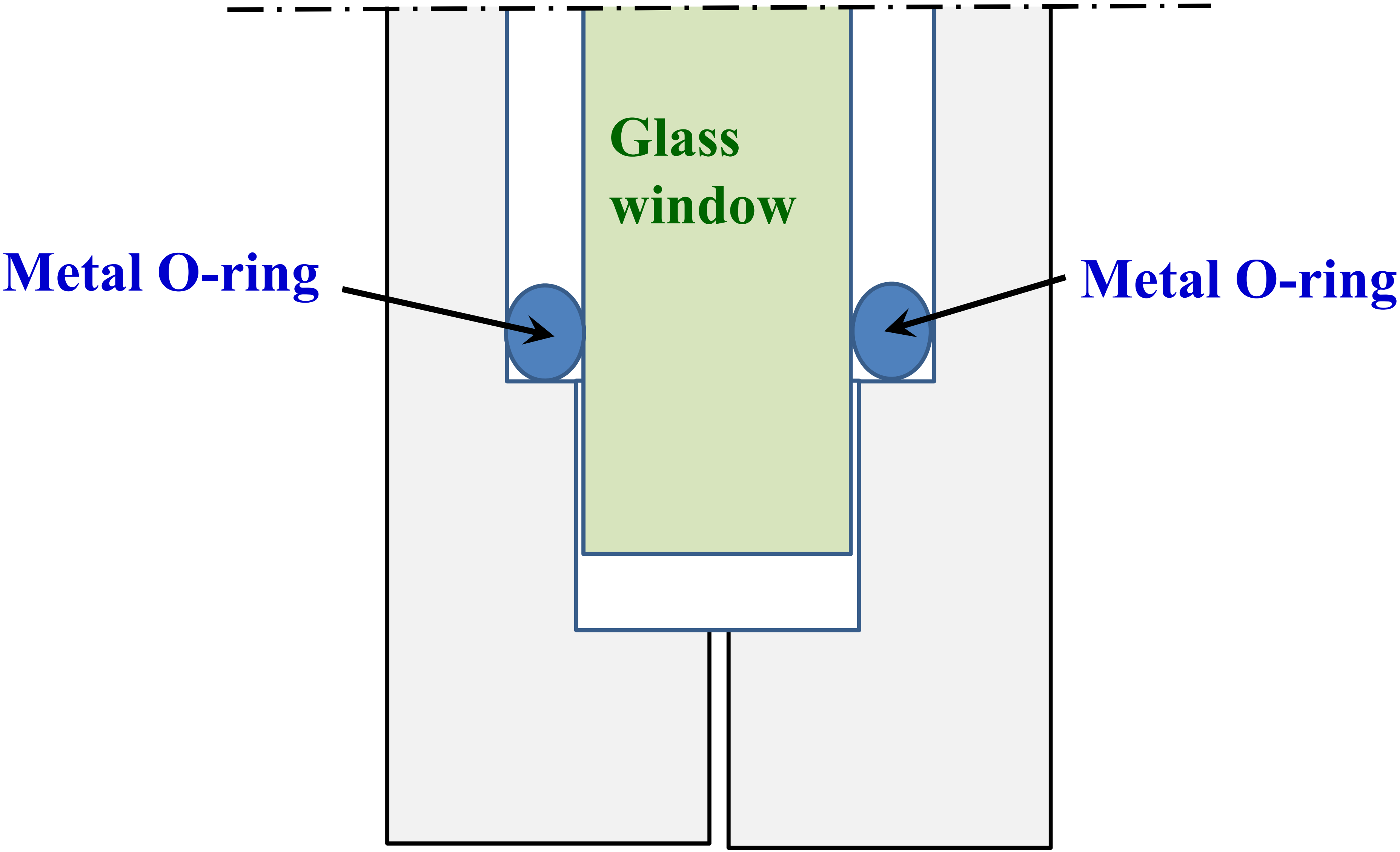
Glass window
Metal O-ring
Metal O-ring

Mirror with its holder used for the optical path

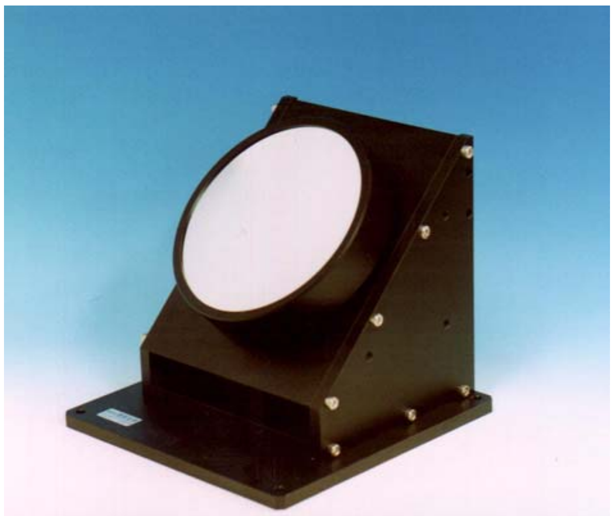

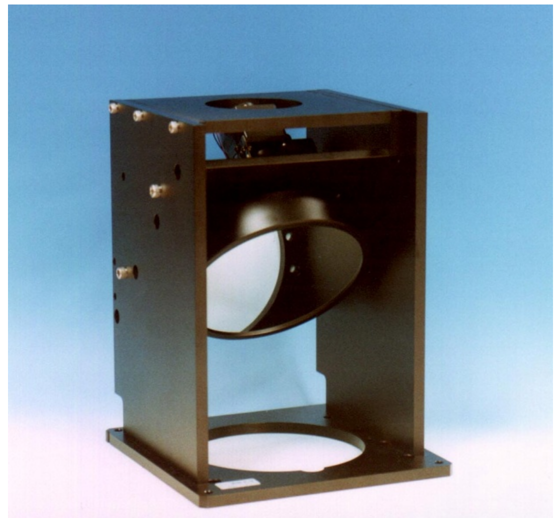

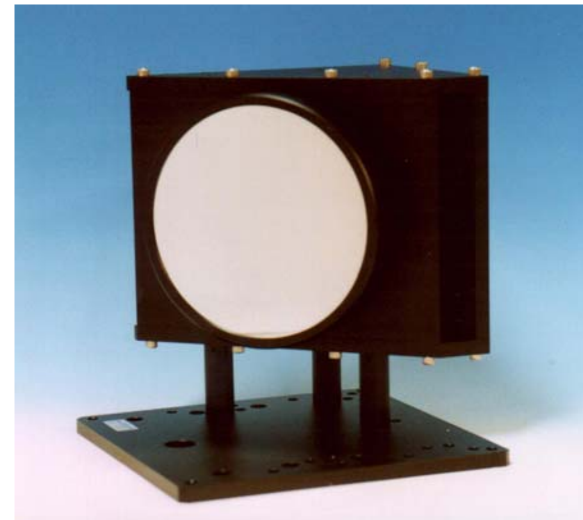

Surface quality: λ/10

Installation of optical path ducts and boxes at the KEK B-factory

Relay lens installed in the optical path duct

How to identify wavefront error

1. **Fieau interferometer**

2. **Schack-Hartmann method**

3. **Ray tracing using Hartmann mask**

1. **Fieau interferometer**
   1st order coherence

2. **Schack-Hartmann method**
   Geometrical optics

3. **Ray tracing using Hartmann mask**
   Geometrical optics

1. Fizeau interferometer

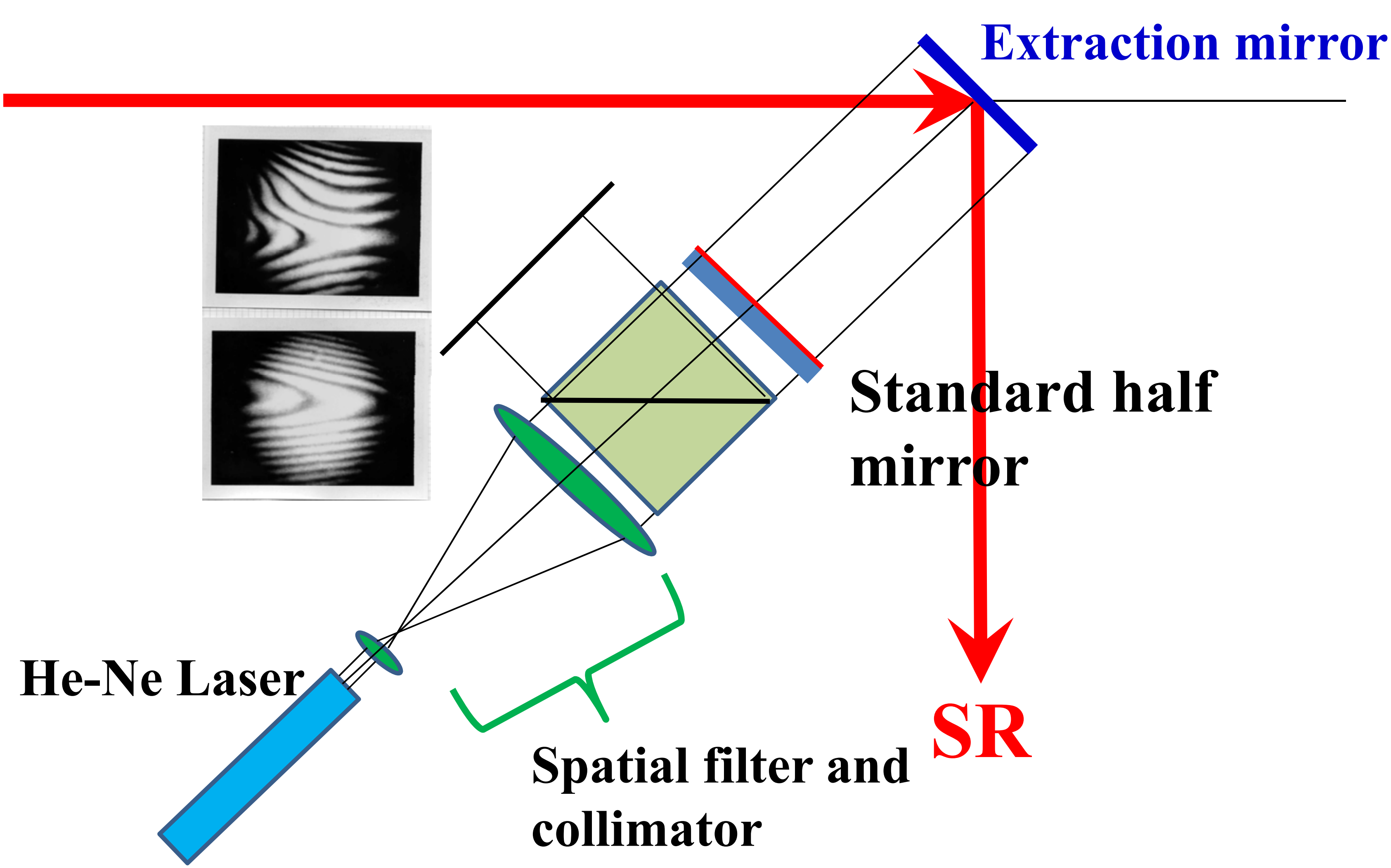

Surface of Be mirror

without beam

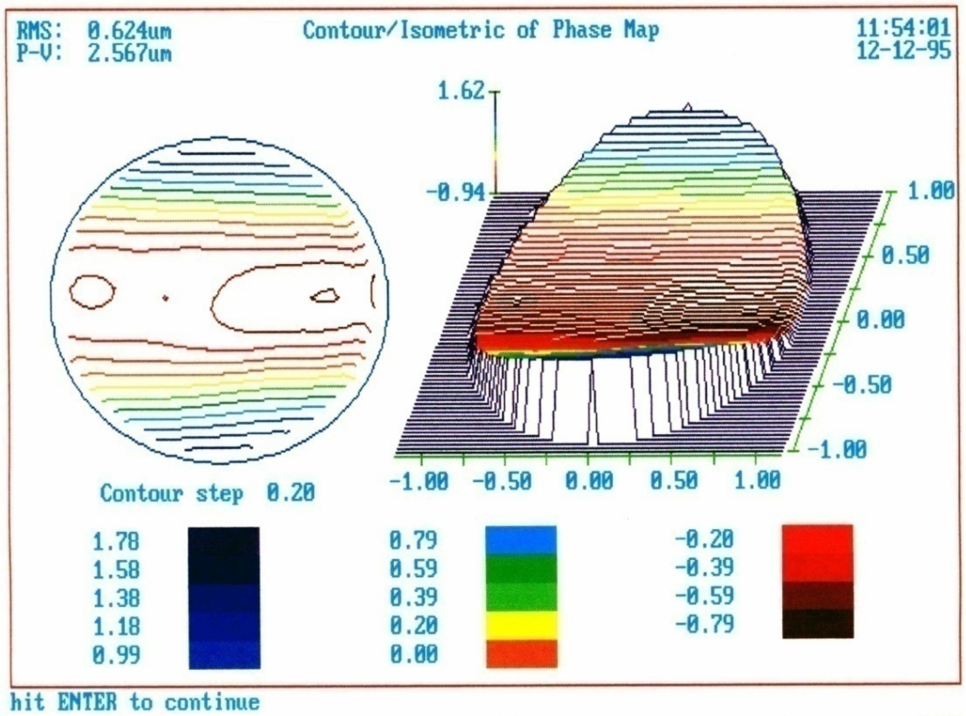

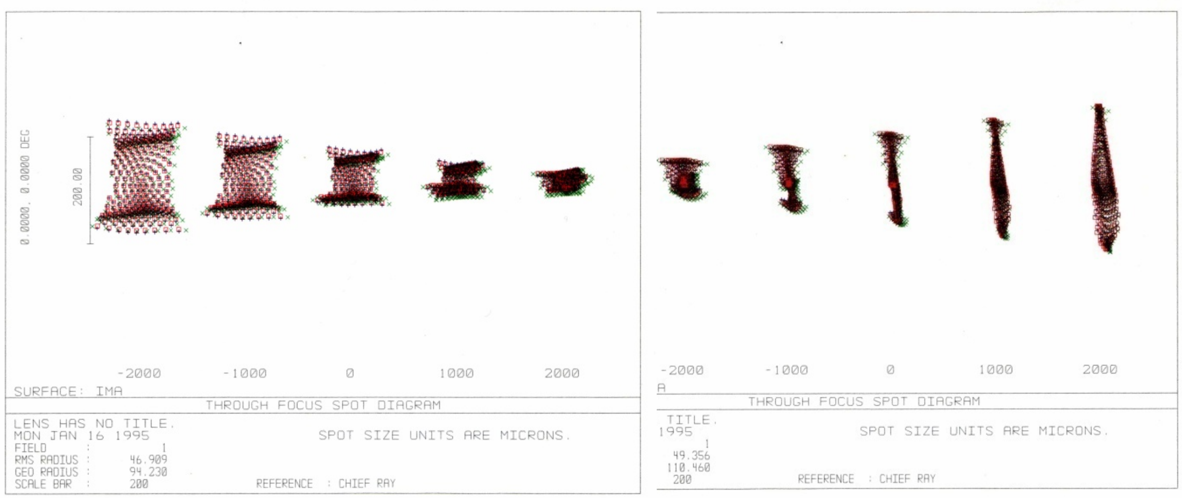

Surface of Be mirror

50mA

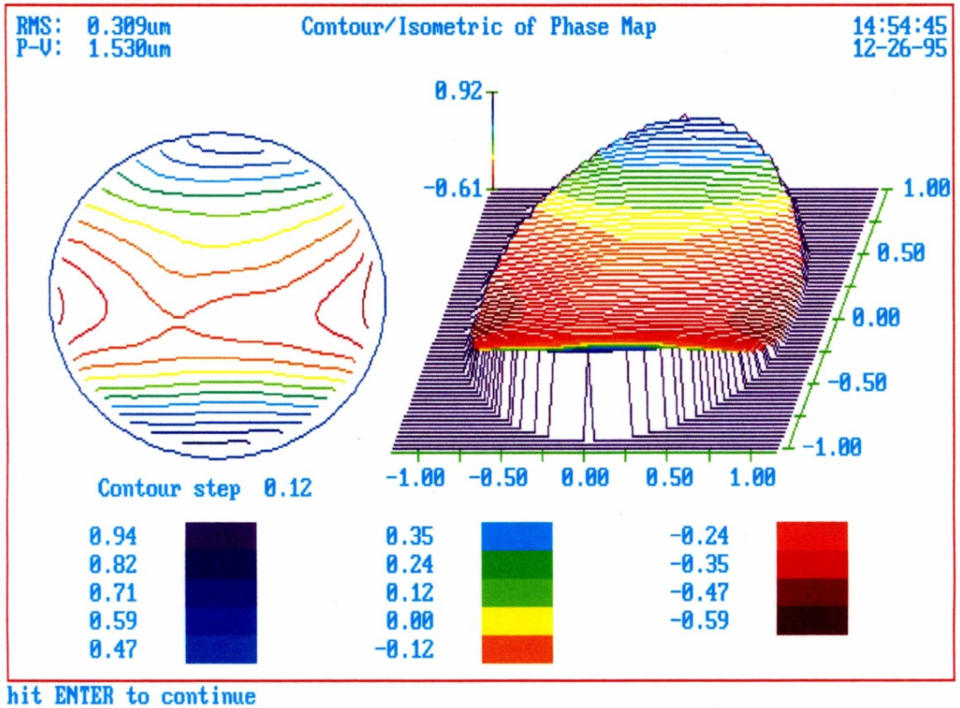

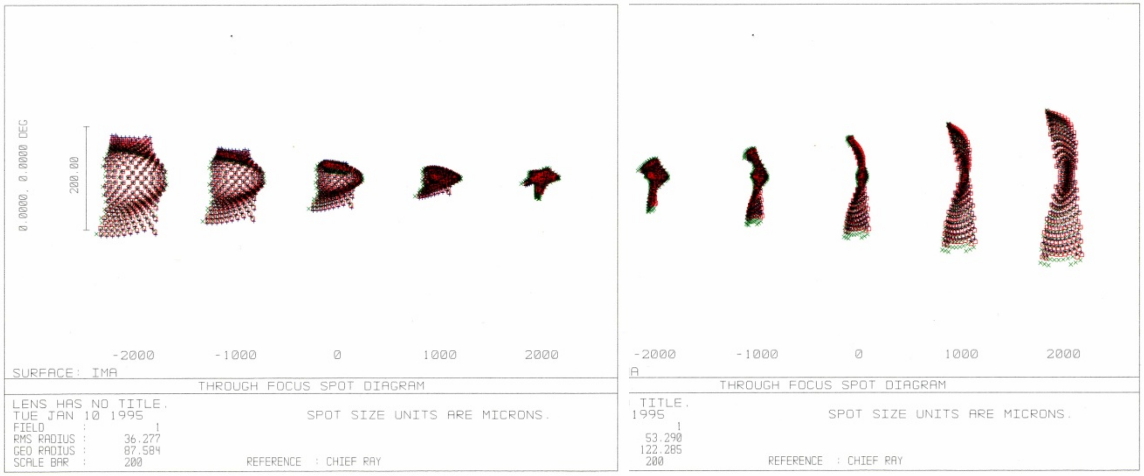

Surface of Be mirror

75mA

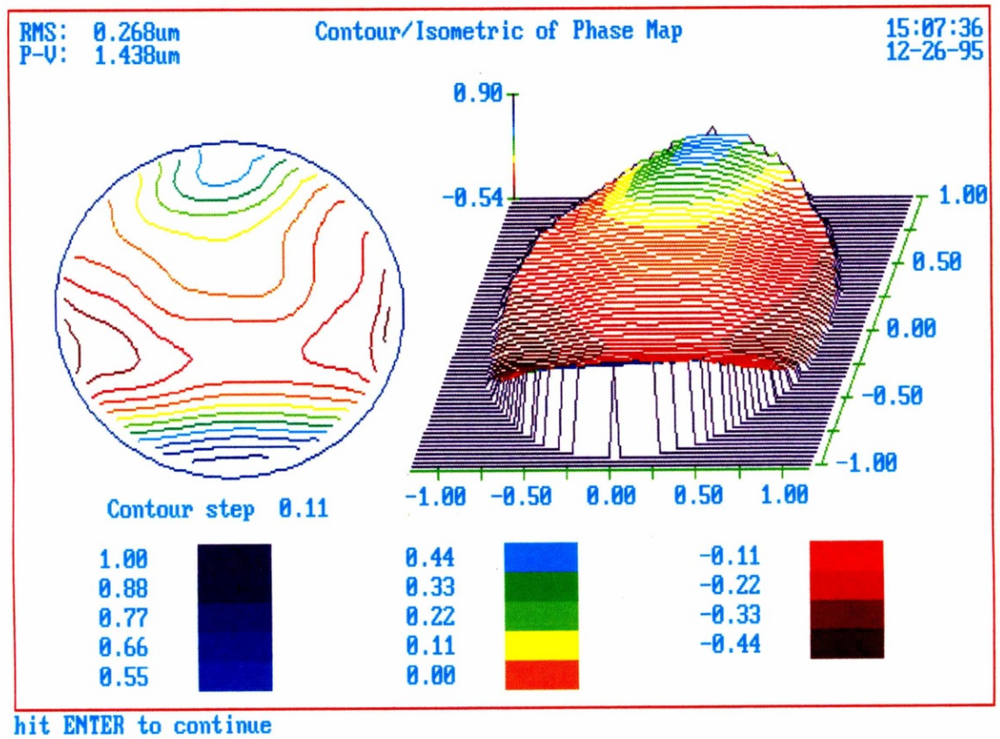

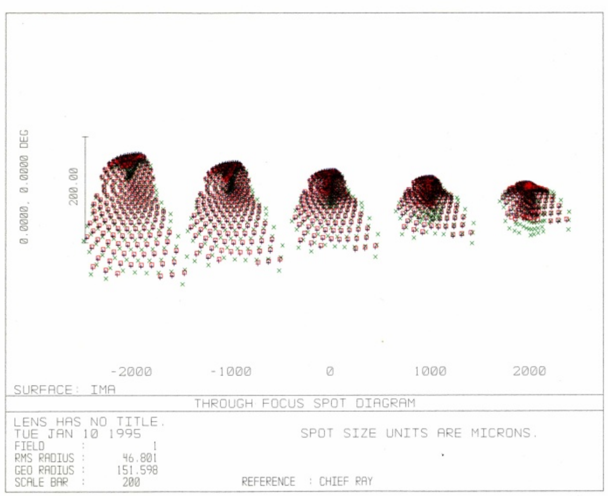

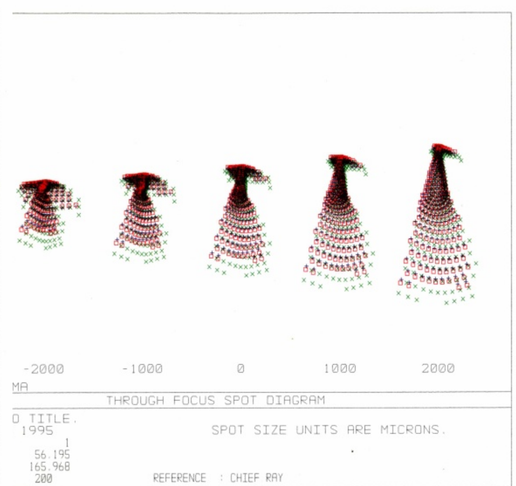

Surface of Be mirror

125mA

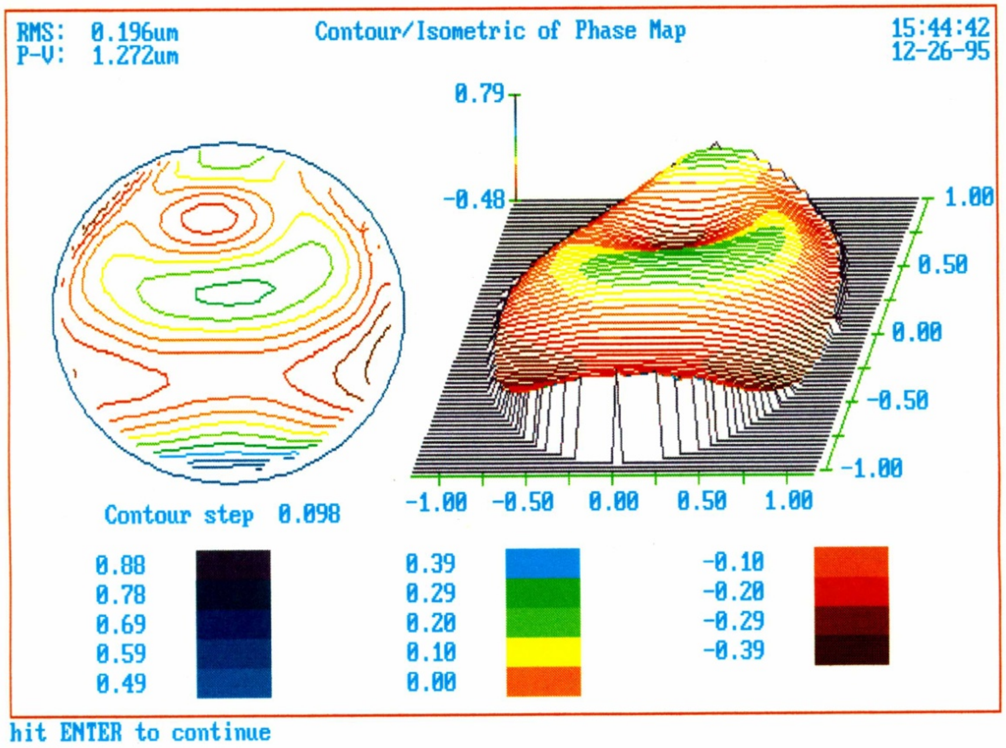

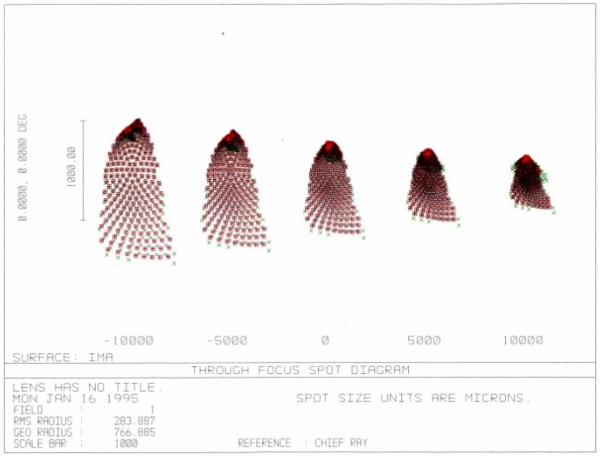

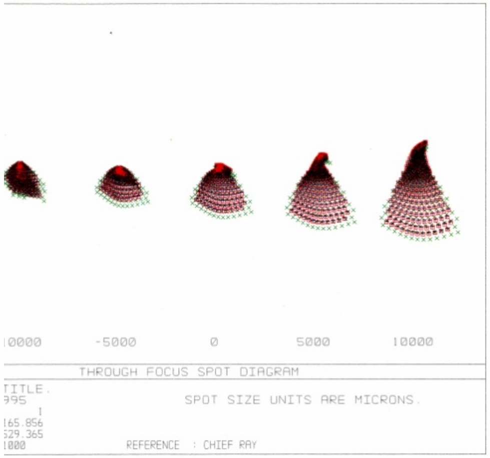

2. Schack-Hartmann method

$$\frac{dW(x)}{dx} = -\frac{\Delta x}{f}$$

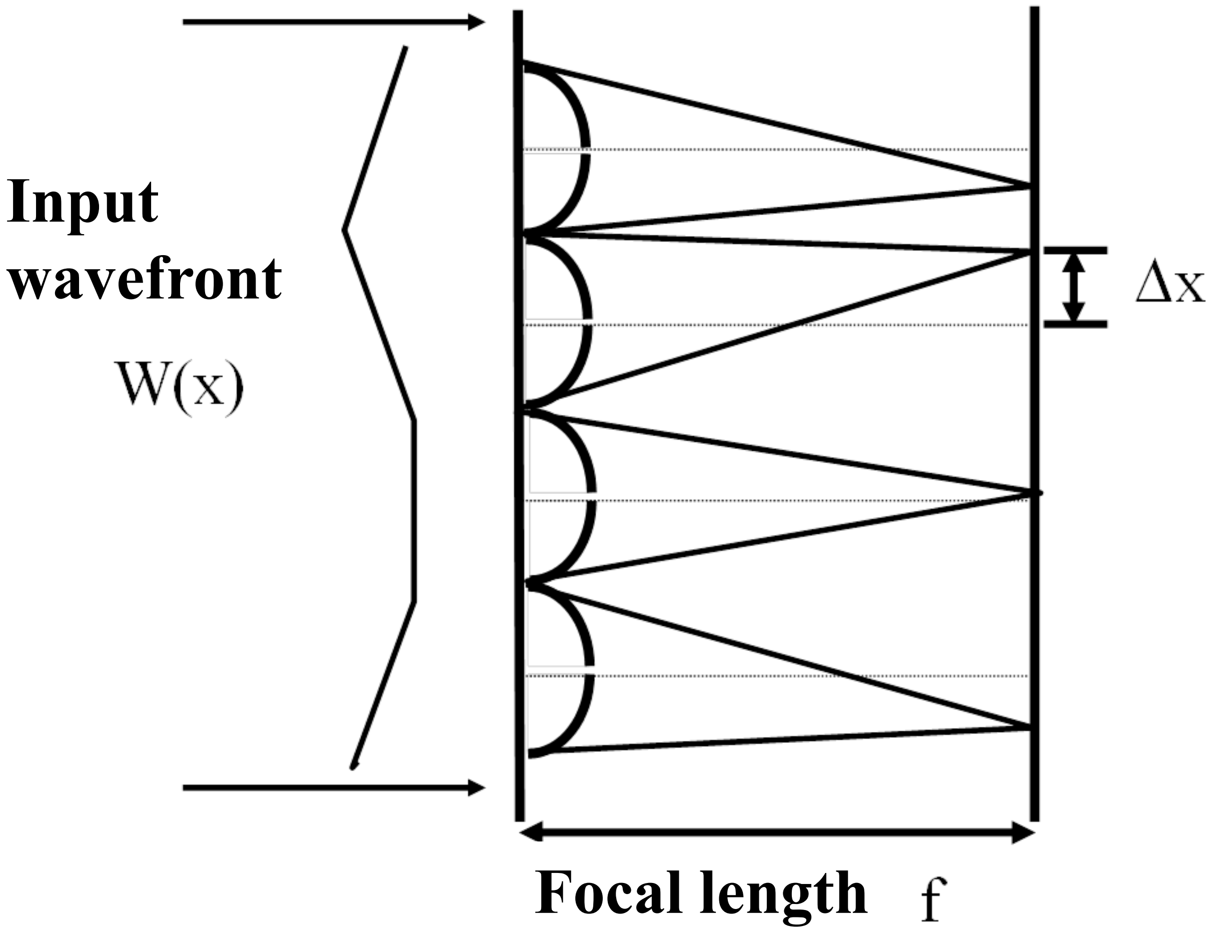

Practical set up of Schack-Hartmann method

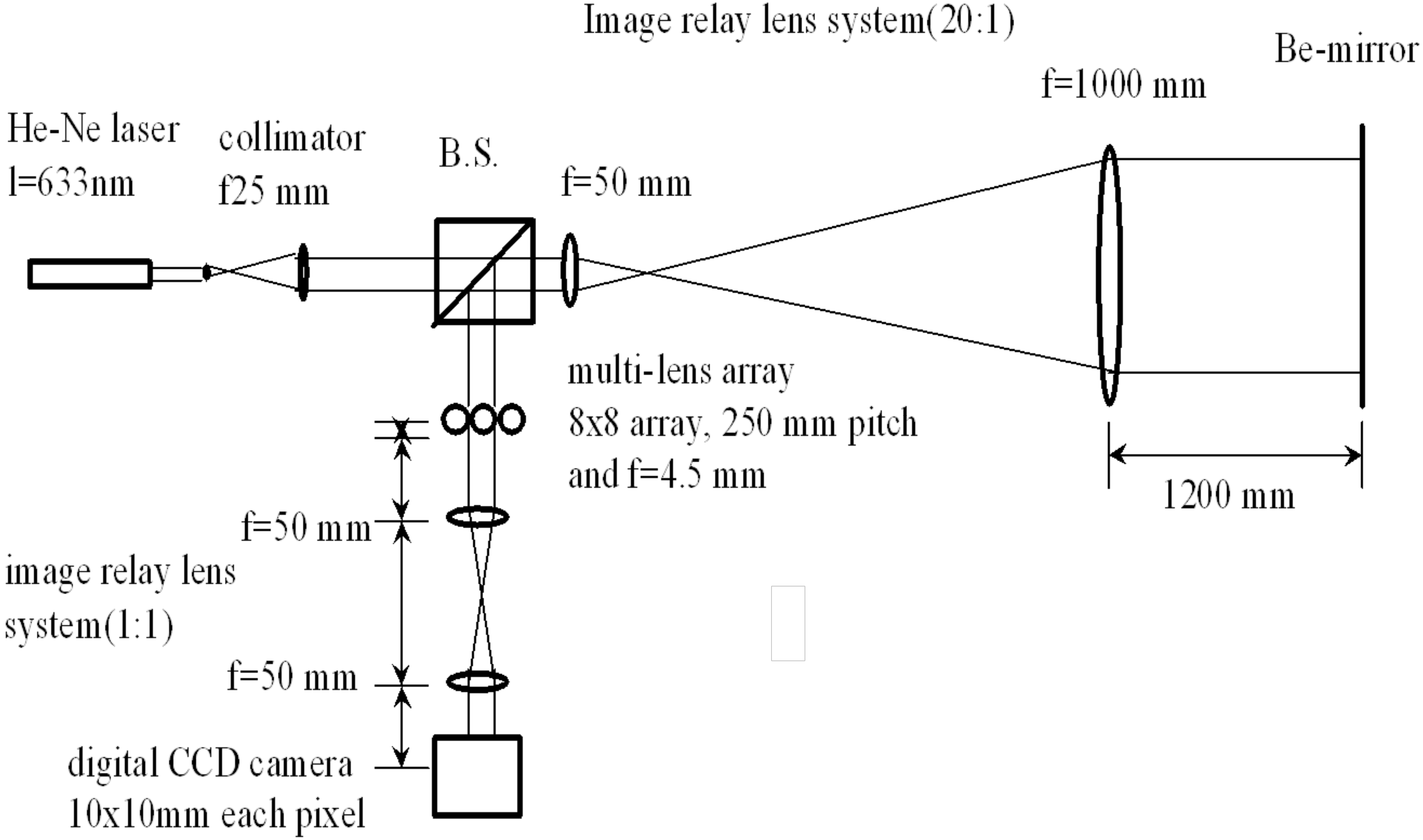

Projection optics

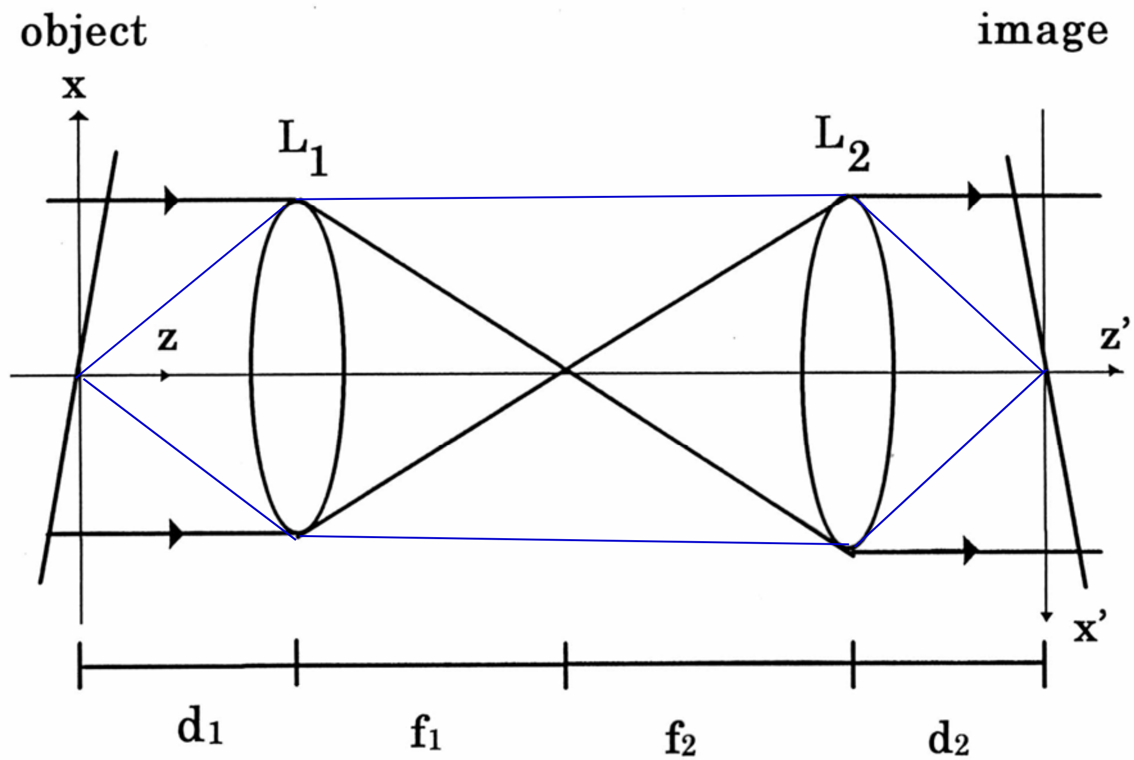

$$d_2 = (f_1 + f_2)\left(\frac{f_2}{f_1}\right) - d_1\left(\frac{f_2}{f_1}\right)^2$$

Magnification $$\frac{1}{m} = \frac{x'}{x} = \frac{f_2}{f_1}$$

Gradient on image $$\frac{dz'}{dx'} = m\frac{dz}{dx}$$

Local gradients on mirror are magnified by angular magnification of relay system

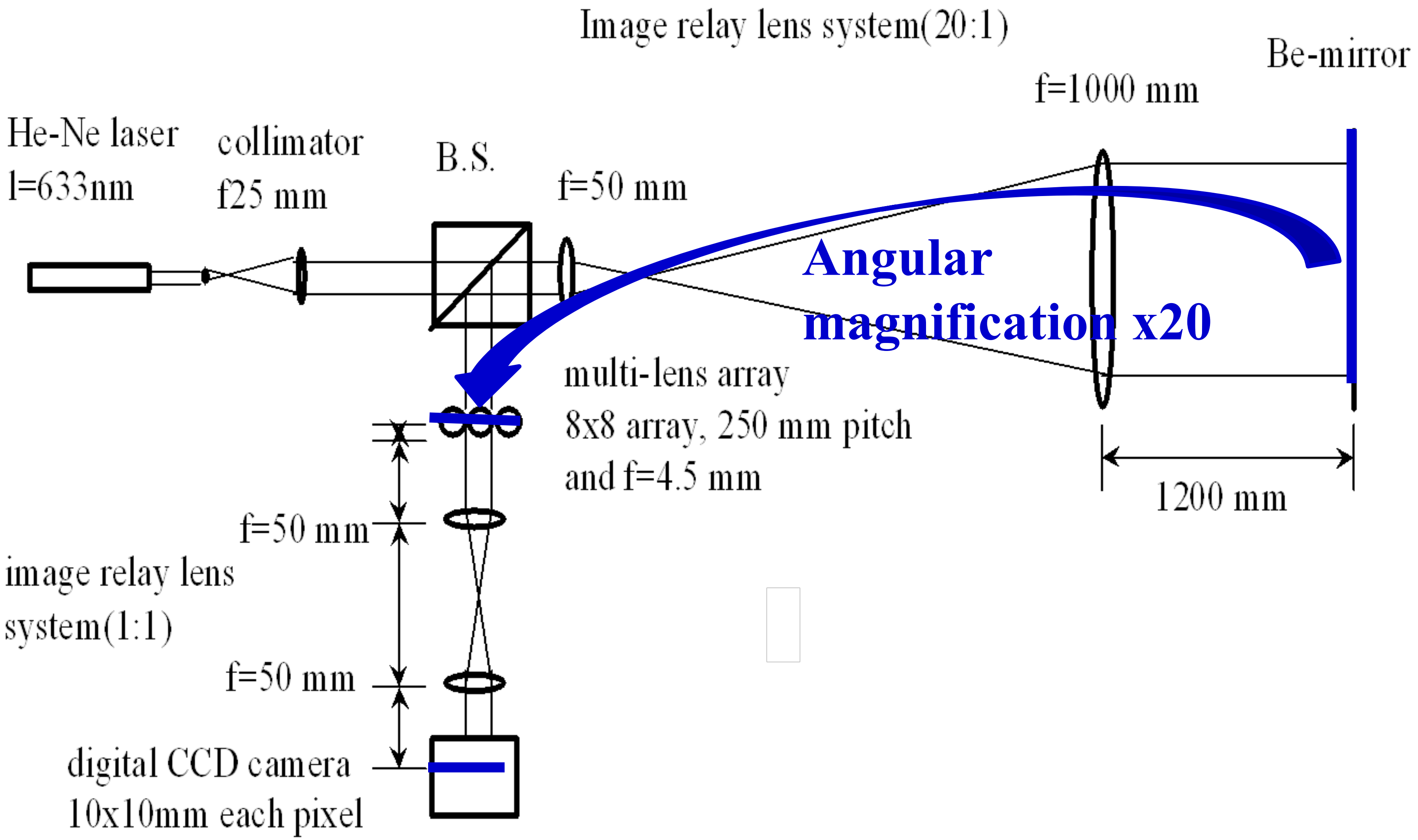

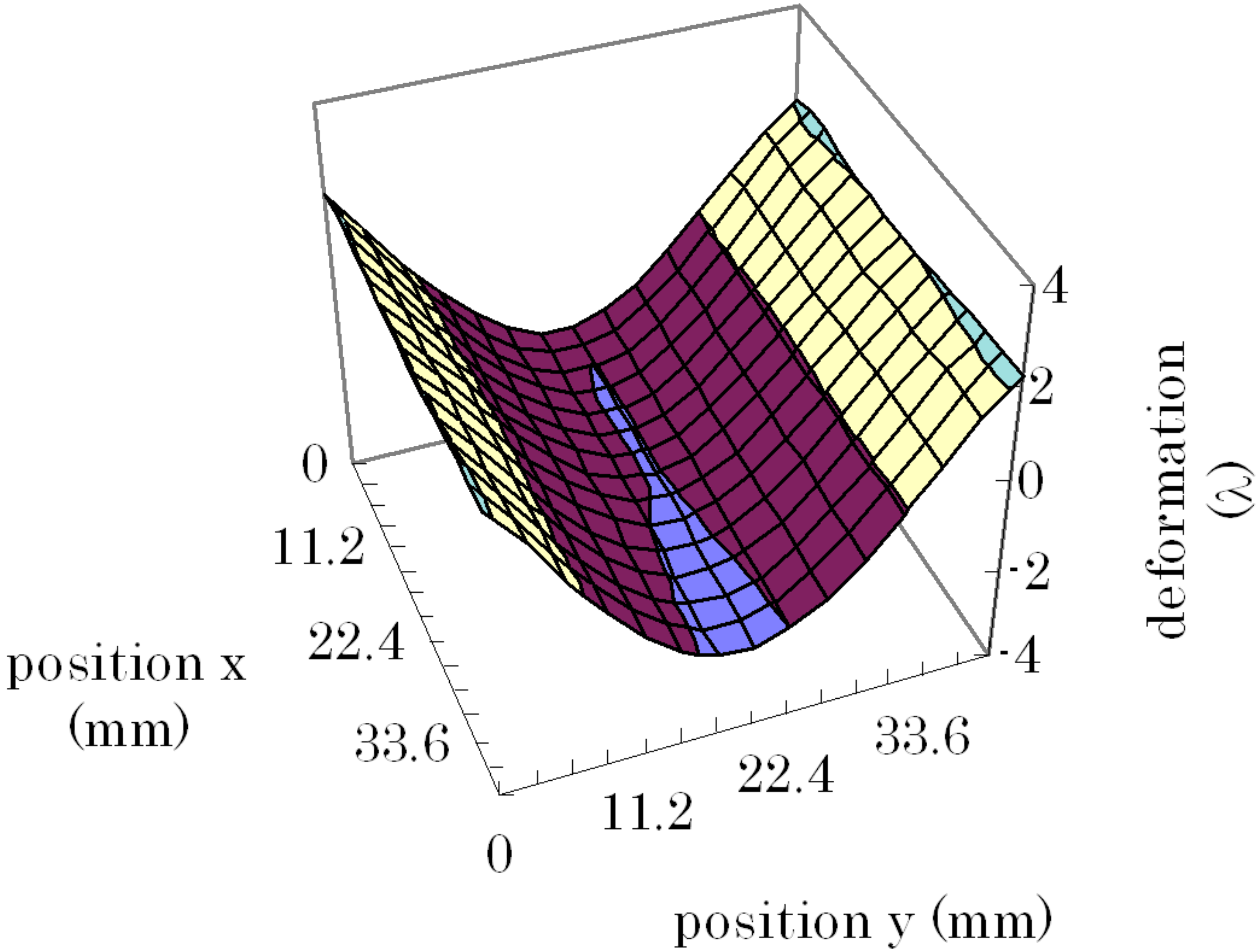

0
11.2
22.4
33.6
position x
(mm)
0
11.2
22.4
33.6
position y (mm)
4
2
0
-2
-4
deformation
(λ)

3. Ray tracing by Hartmann mask

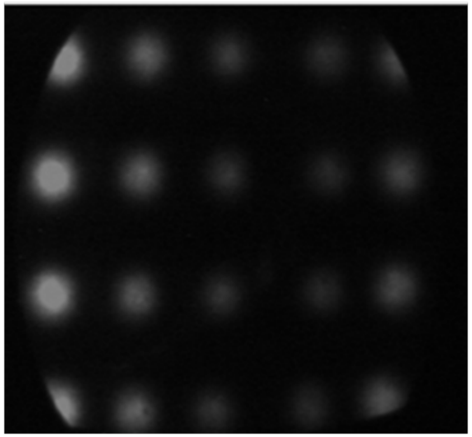

Projection of rays

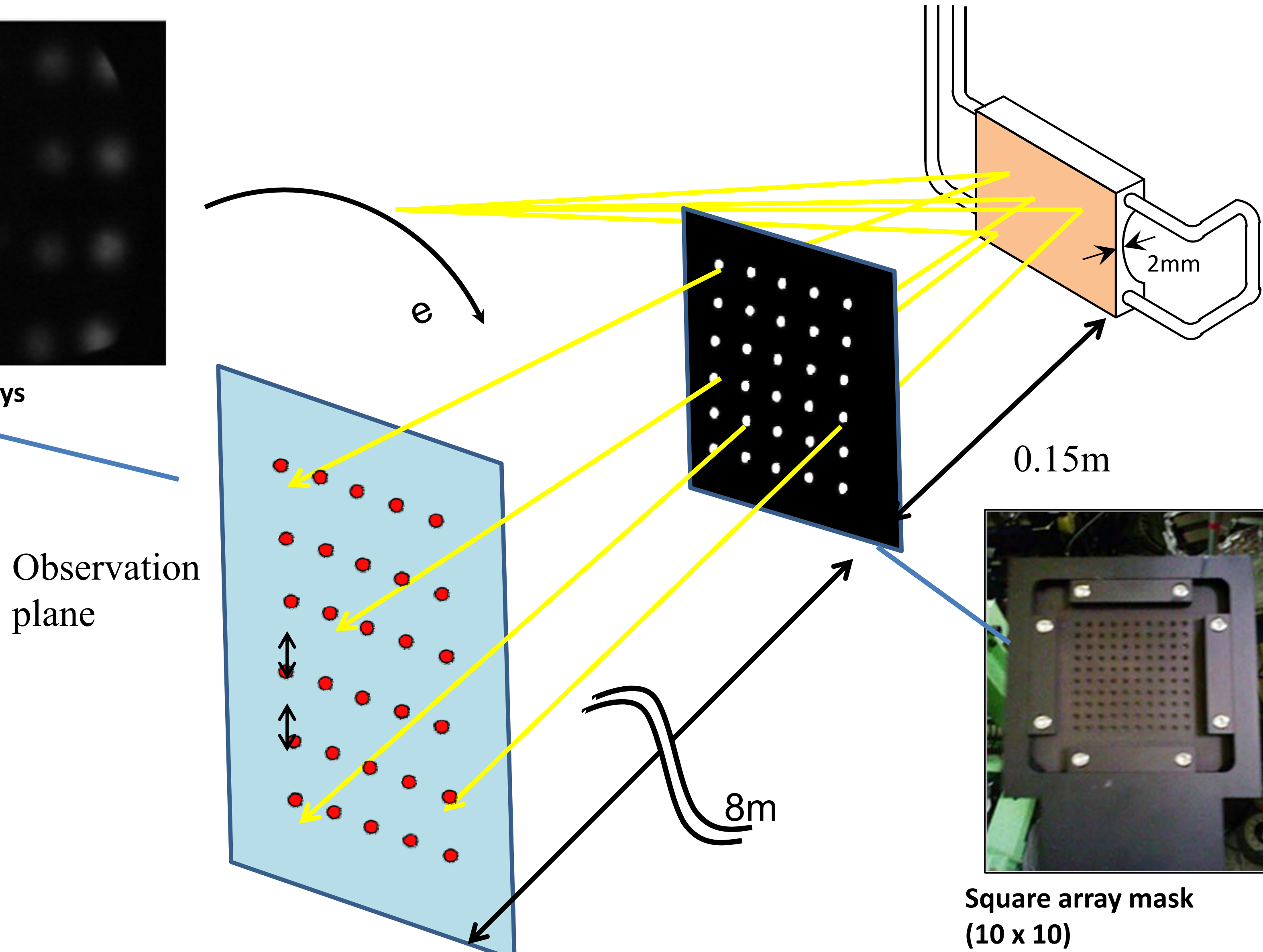

Square array mask (10 x 10)

Ray tracing by Hartmann mask

Displacement of spots due to local gradients on mirror are magnified by long optical lever

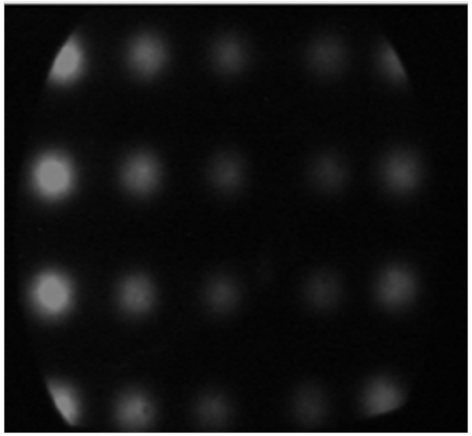

Projection of rays

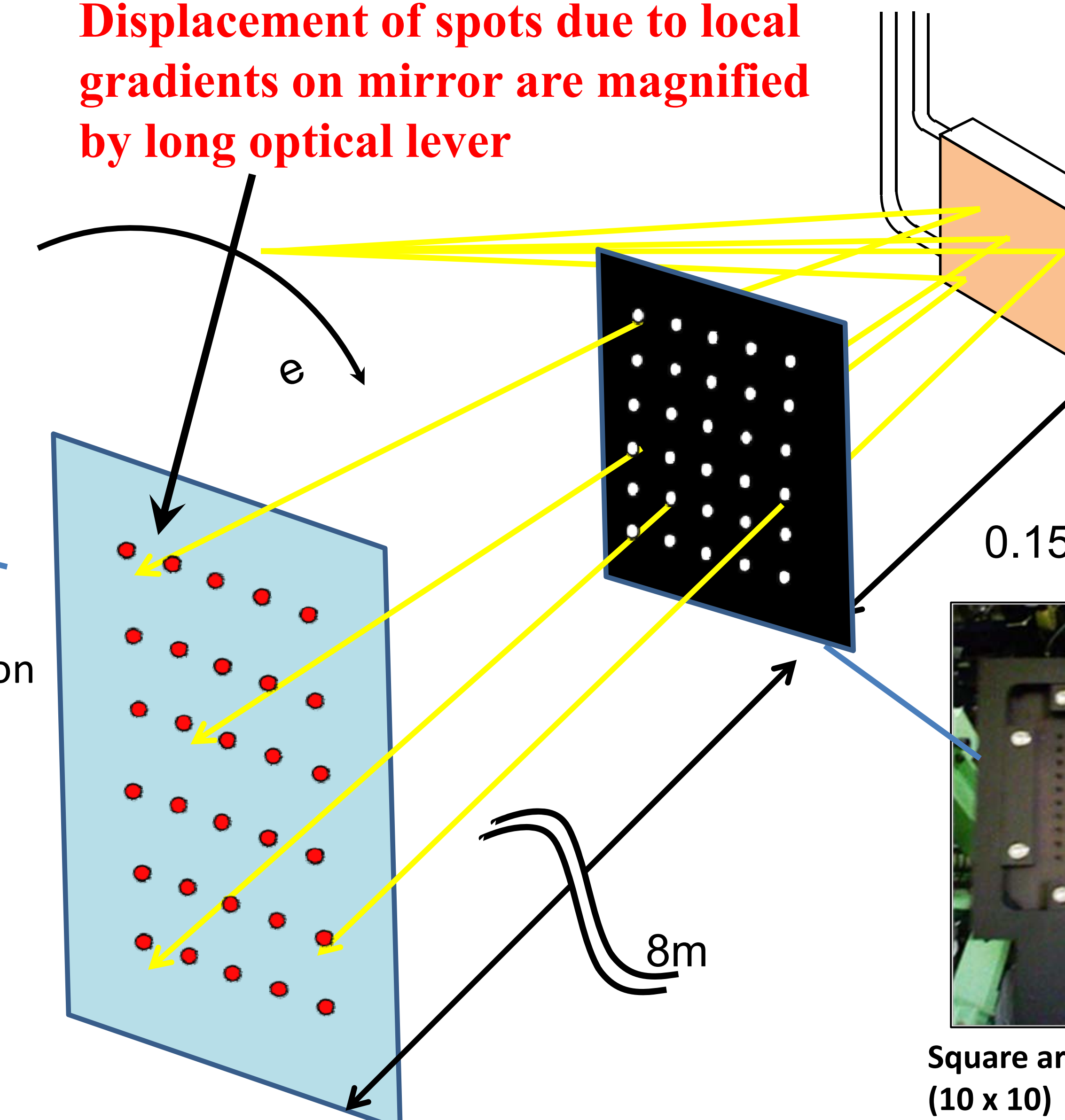

Square array mask (10 x 10)

Characterization of mirror deformation due to SR irradiation by the use of Hartmann screen

Hartmann square screen
Diameter of hole 1mm
10x10, 5mm spacing

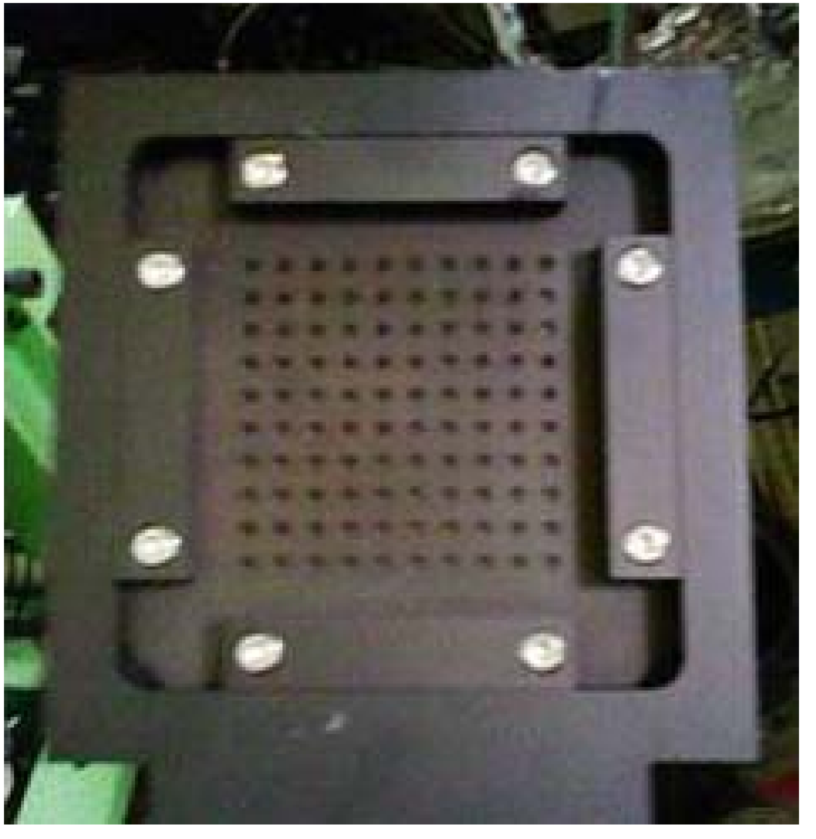

Spots pattern on observation plane by square hole array

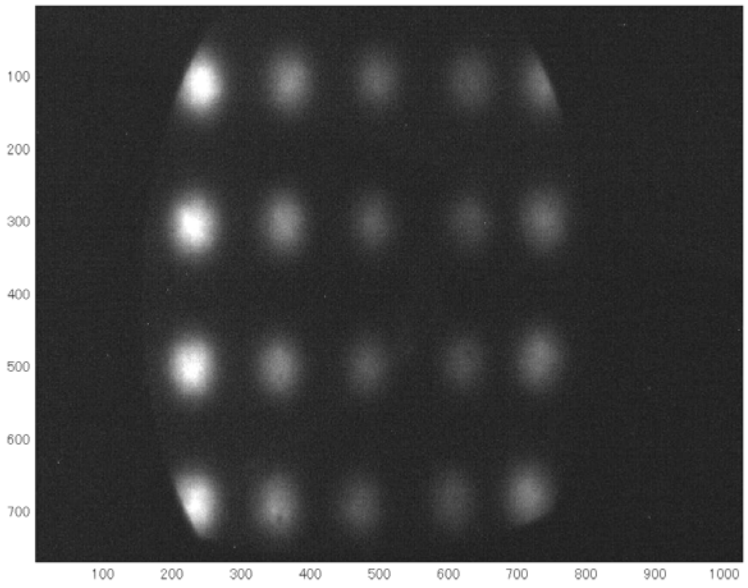

280mA

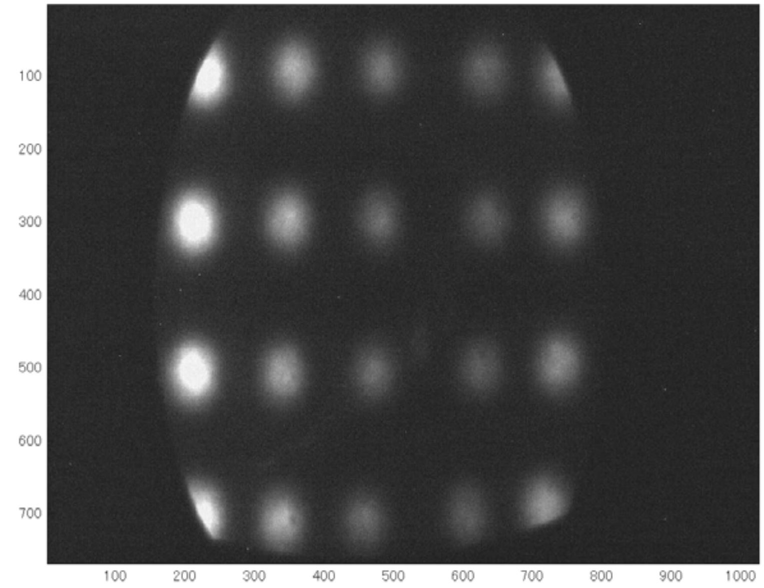

450mA

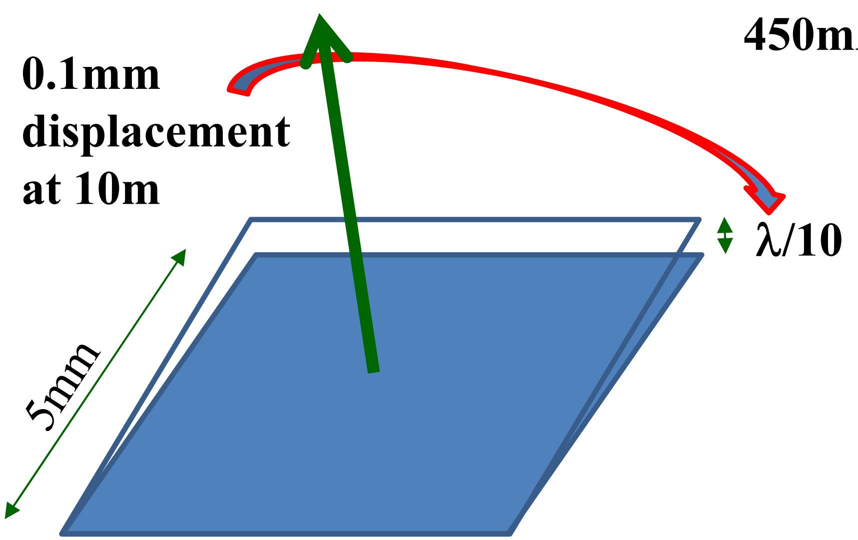

Wavefront error due to thermal deformation of extraction mirror From 300mA to 450mA at the Photon Factory, KEK

Let's put wavefront at 300mA into null, and observe wavefront distortion

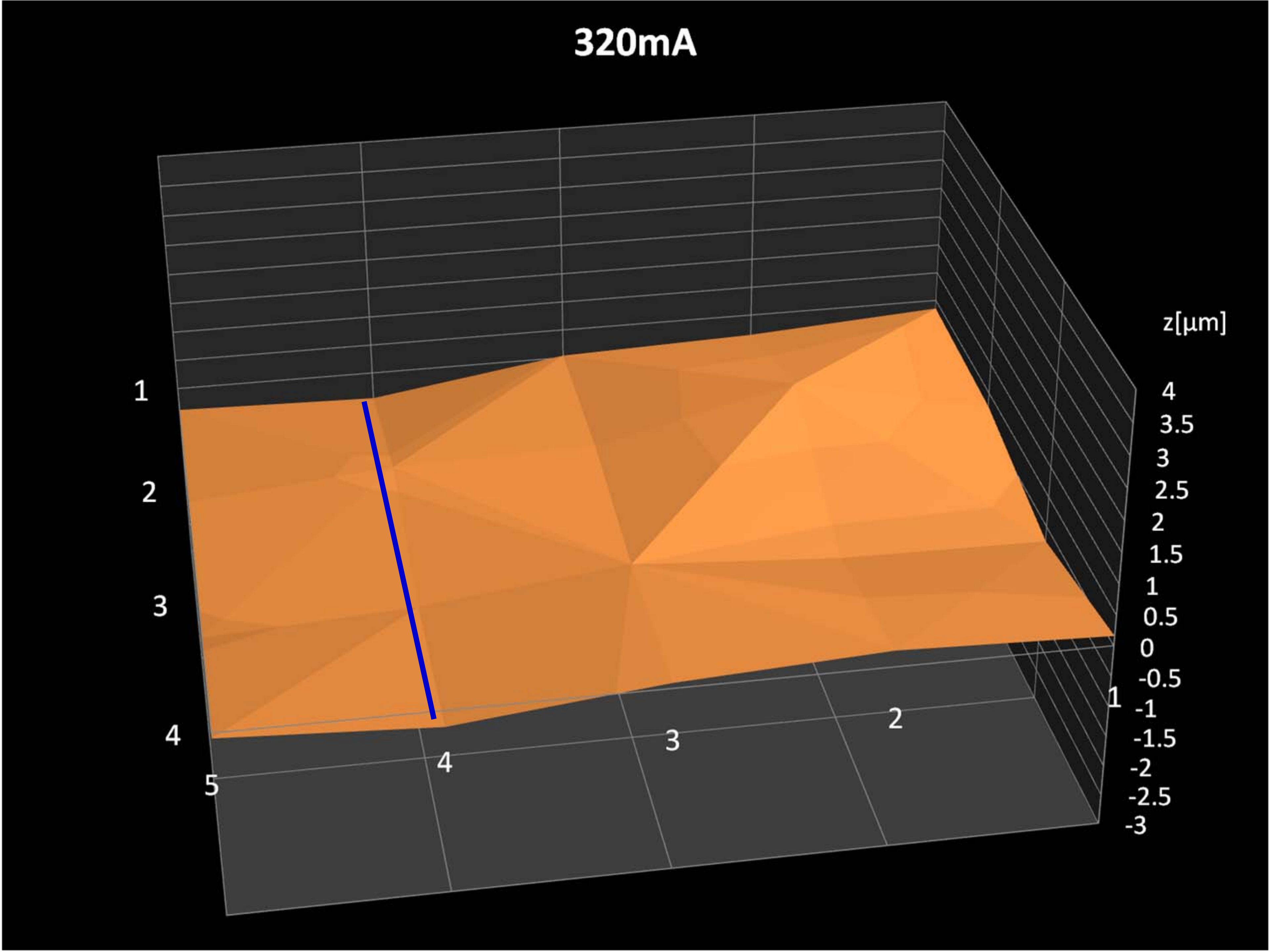

320mA
z[µm]
4
3.5
3
2.5
2
1.5
1
0.5
0
-0.5
-1
-1.5
-2
-2.5
-3
1
2
3
4
5
4
3
2
1

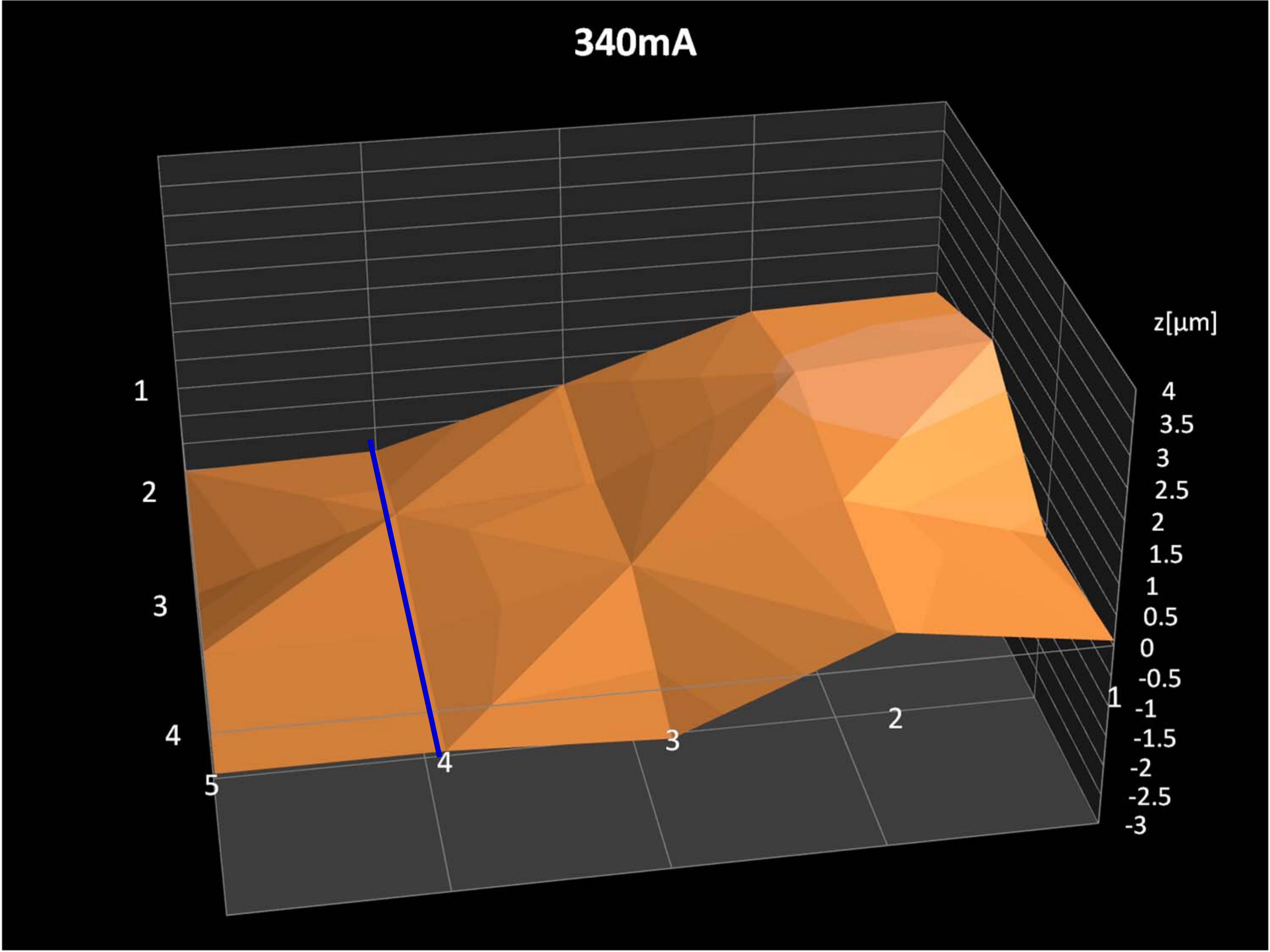

340mA
z[µm]
4
3.5
3
2.5
2
1.5
1
0.5
0
-0.5
-1
-1.5
-2
-2.5
-3
1
2
3
4
5
4
3
2
1

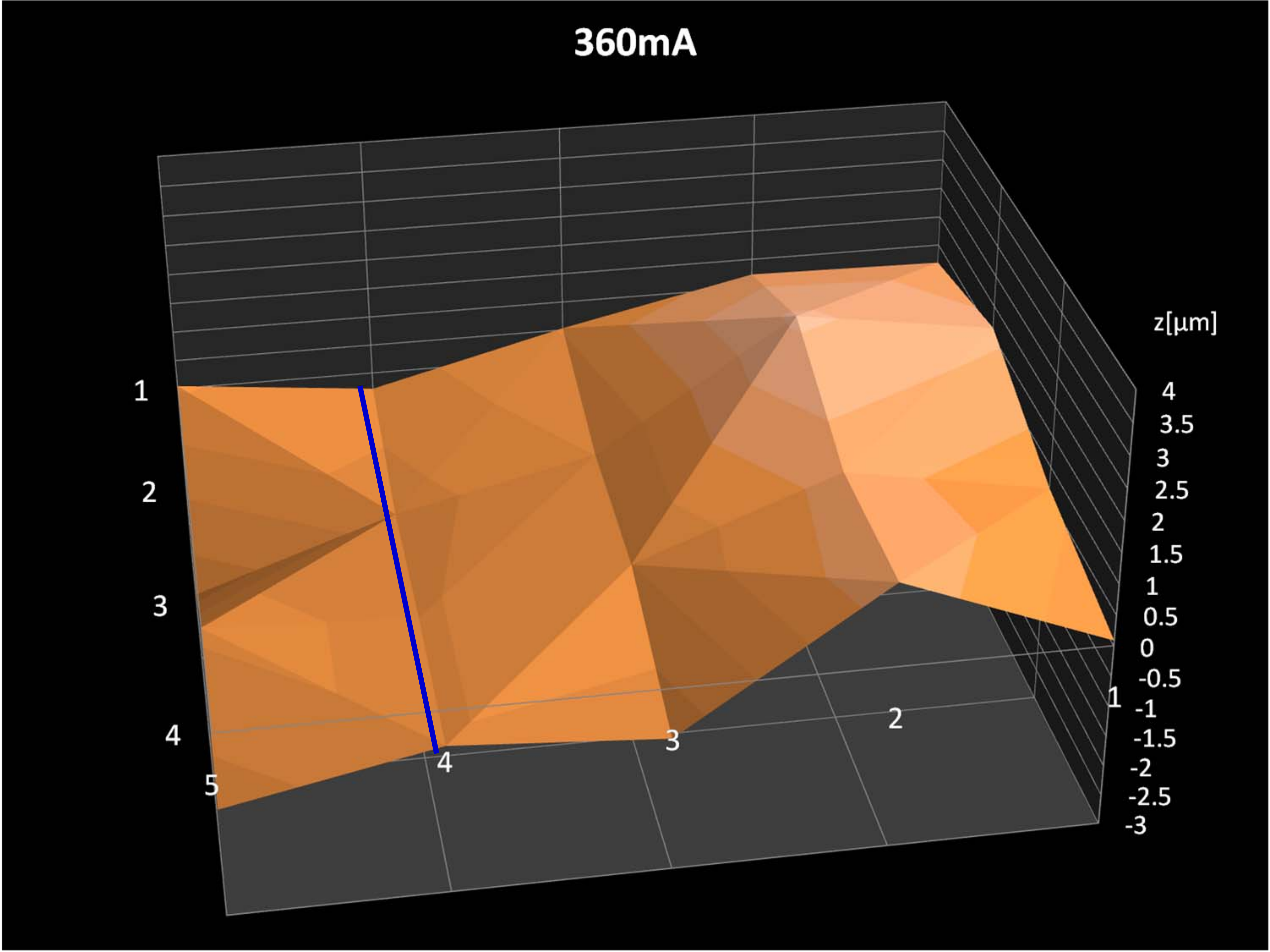
360mA
z[µm]
4
3.5
3
2.5
2
1.5
1
0.5
0
-0.5
-1
-1.5
-2
-2.5
-3
1
2
3
4
5
1
2
3
4

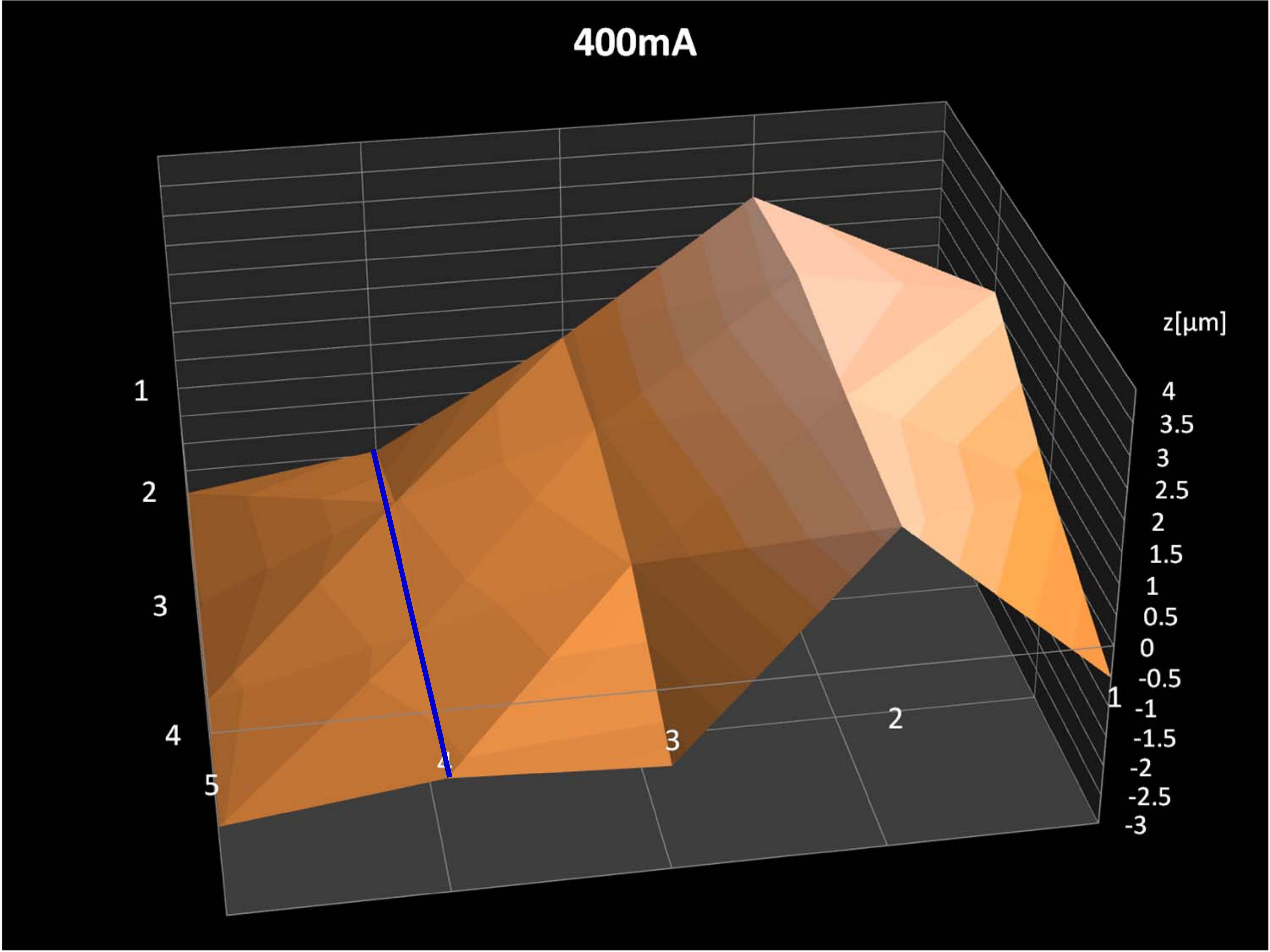

400mA
z[µm]
4
3.5
3
2.5
2
1.5
1
0.5
0
-0.5
-1
-1.5
-2
-2.5
-3
1
2
3
4
5
1
2
3
4

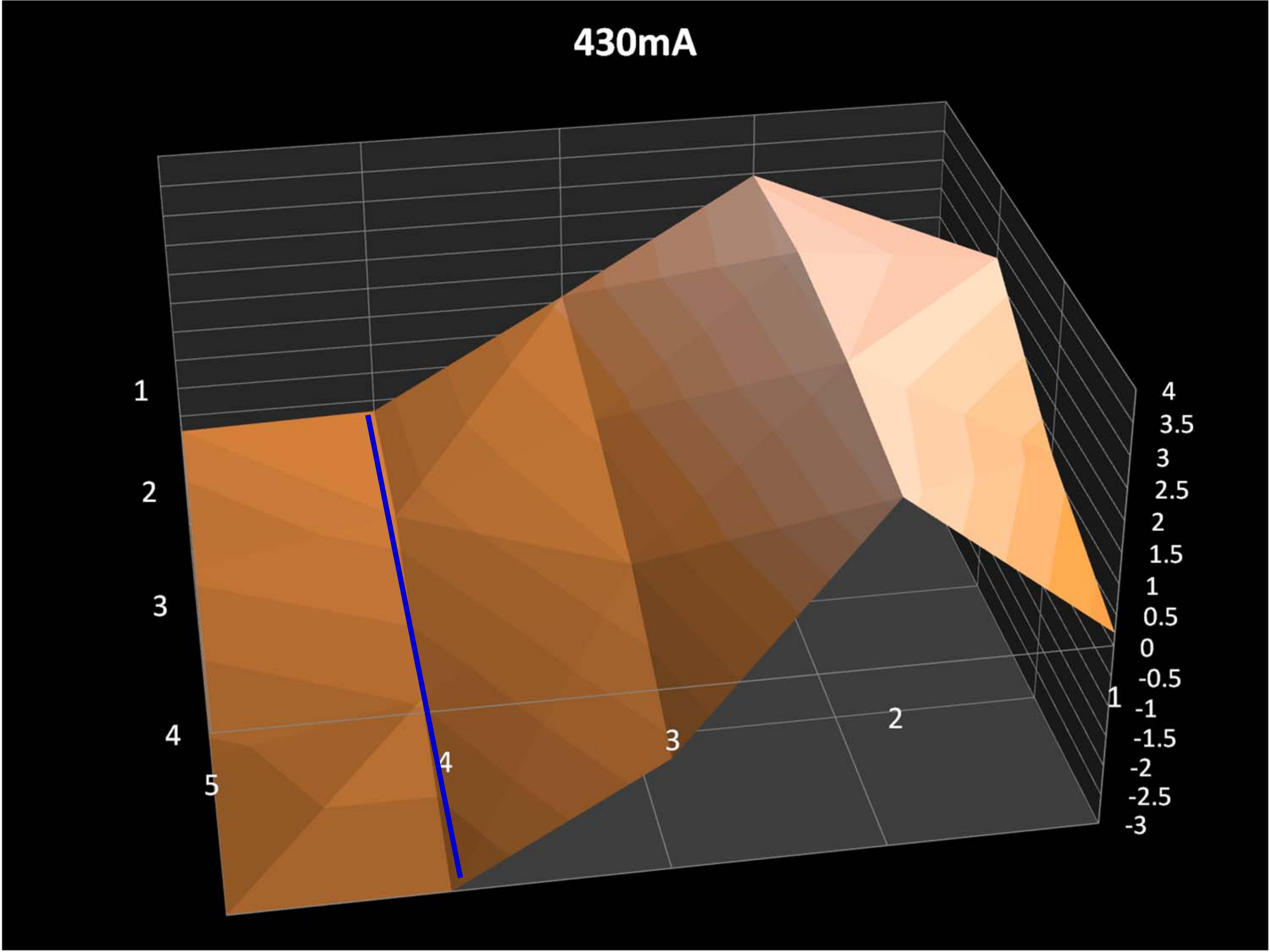

430mA
1
2
3
4
5
4
3
2
1
4
3.5
3
2.5
2
1.5
1
0.5
0
-0.5
-1
-1.5
-2
-2.5
-3

450mA

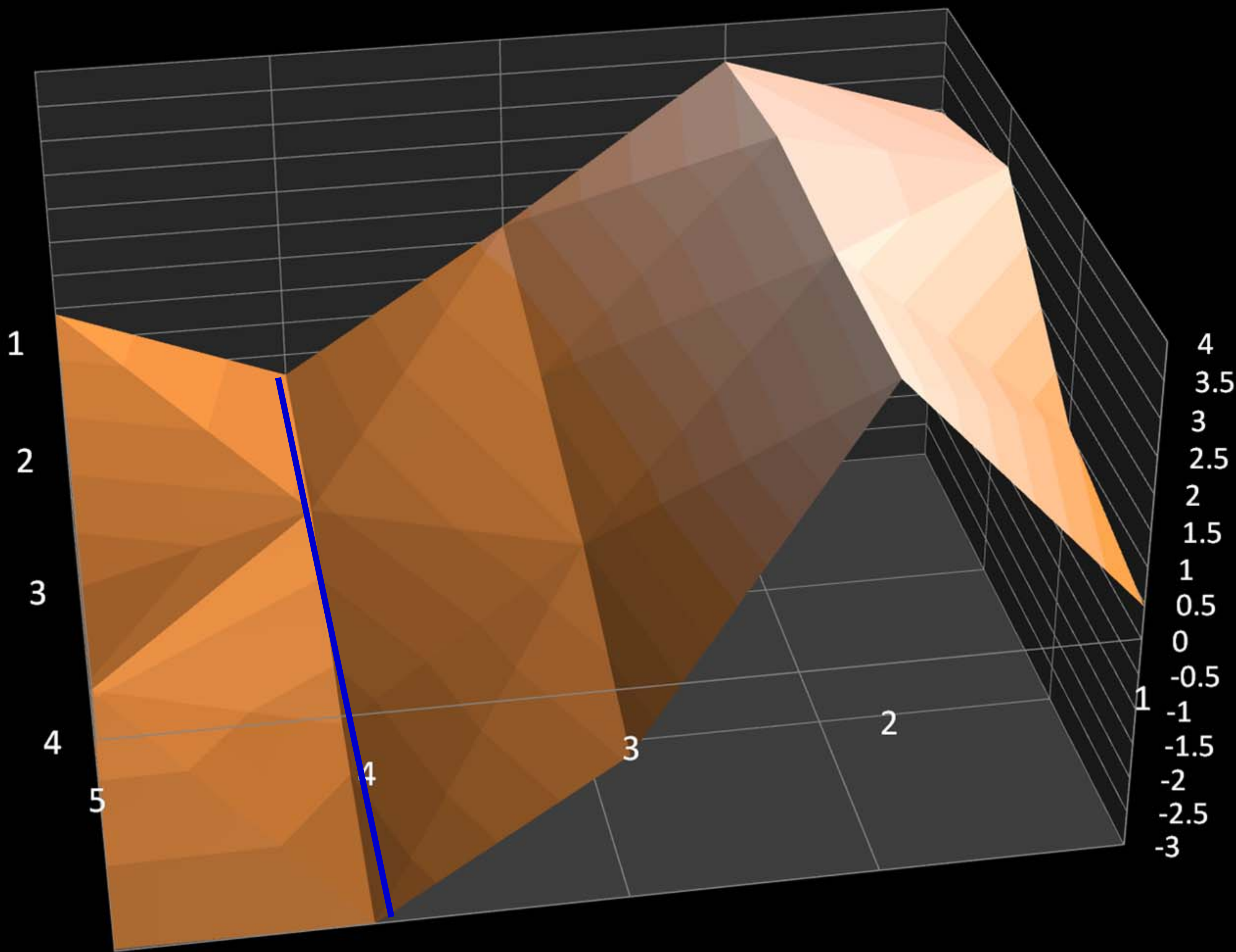

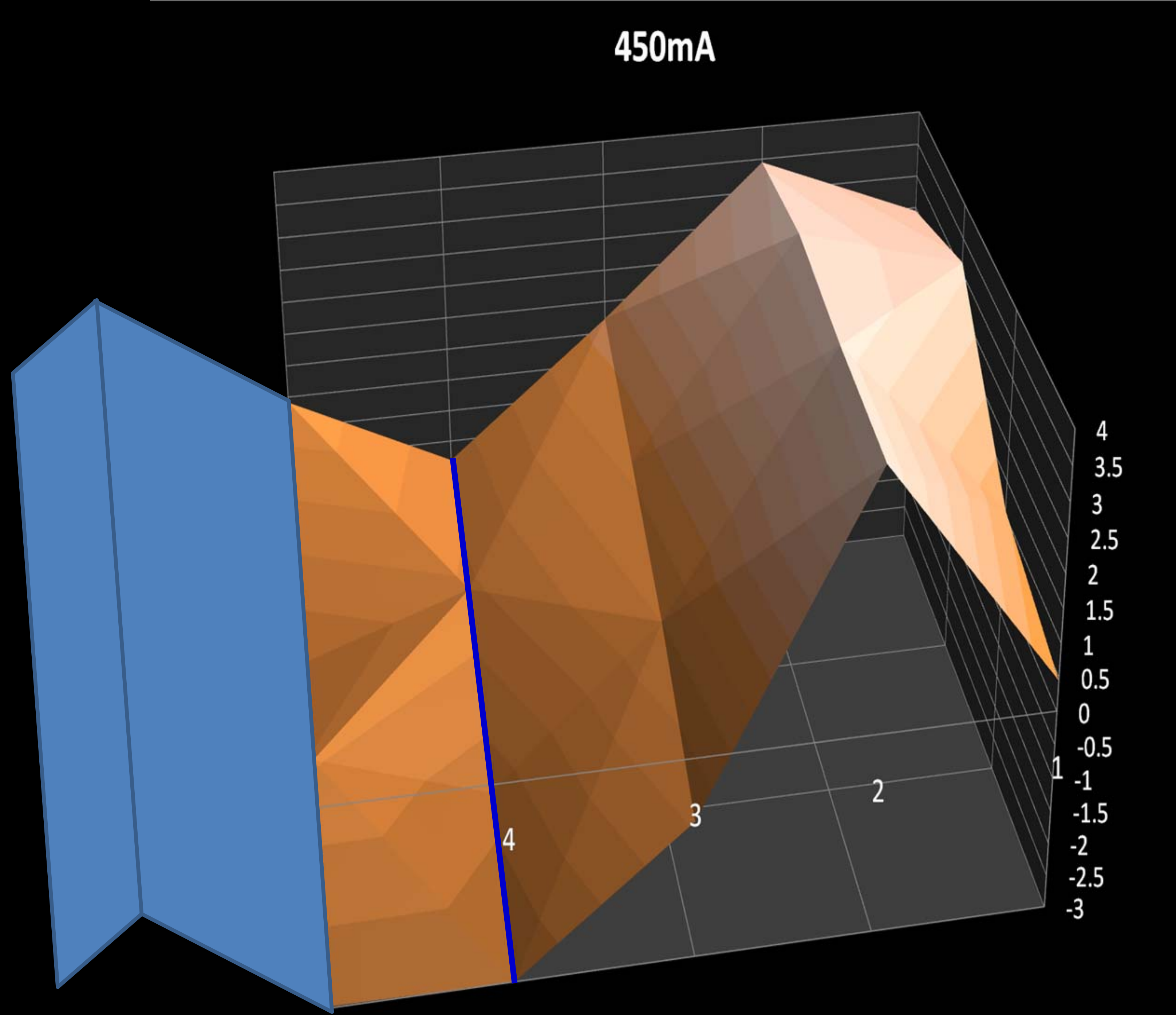
450mA
4
3.5
3
2.5
2
1.5
1
0.5
0
-0.5
-1
-1.5
-2
-2.5
-3
1
2
3
4

Comparison of these methods to identify the wavefront distortion

1. Fizeau interferometer

- **Coherent method:** very week for floor vibrations
- **Sensitivity:** $\lambda/5$- $\lambda/10$(depend on reference plate)
- **Device location:** In front of mirror
- **Optical path:** Not included
- **Other:** Non destructive, Expensive

2.Shack-Hartmann

- **Incoherent method:** strong for floor vibrations
- **Sensitivity:** $\lambda/5$- $\lambda/10$ (depends on angular magnification)
- **Device location:** In front of mirror
- **Optical path:** Not included
- **Other:** Non destructive, Expensive

3.Hartmann screen

- **Incoherent method:** strong for floor vibrations
- **Sensitivity:** $\lambda/5$- $\lambda/10$ (depends on optical lever length)
- **Device location:** Mask locates in front of mirror
- **Optical path:** Included
- **Other:** Destructive, Cheep

3. Common equipments in down stream of optical path

focusing system to observe the beam image

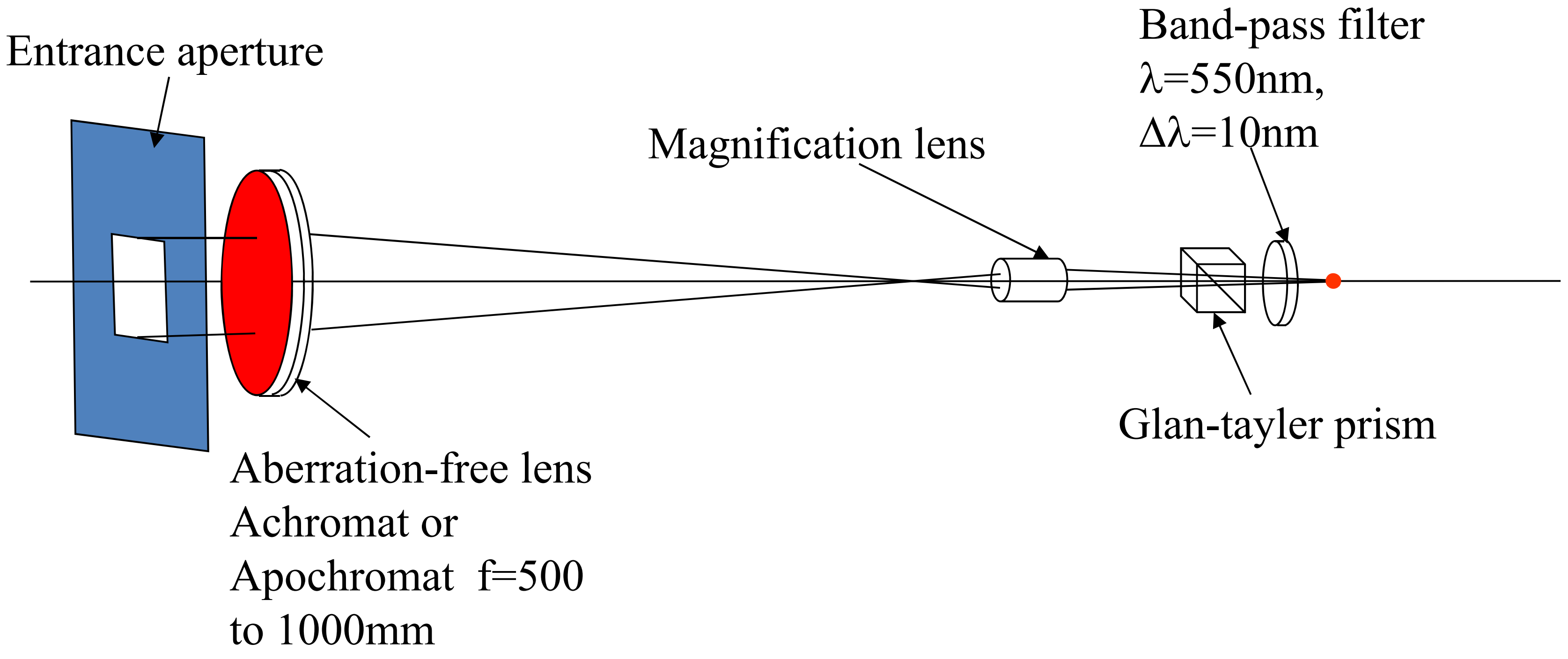

Typical image of the beam

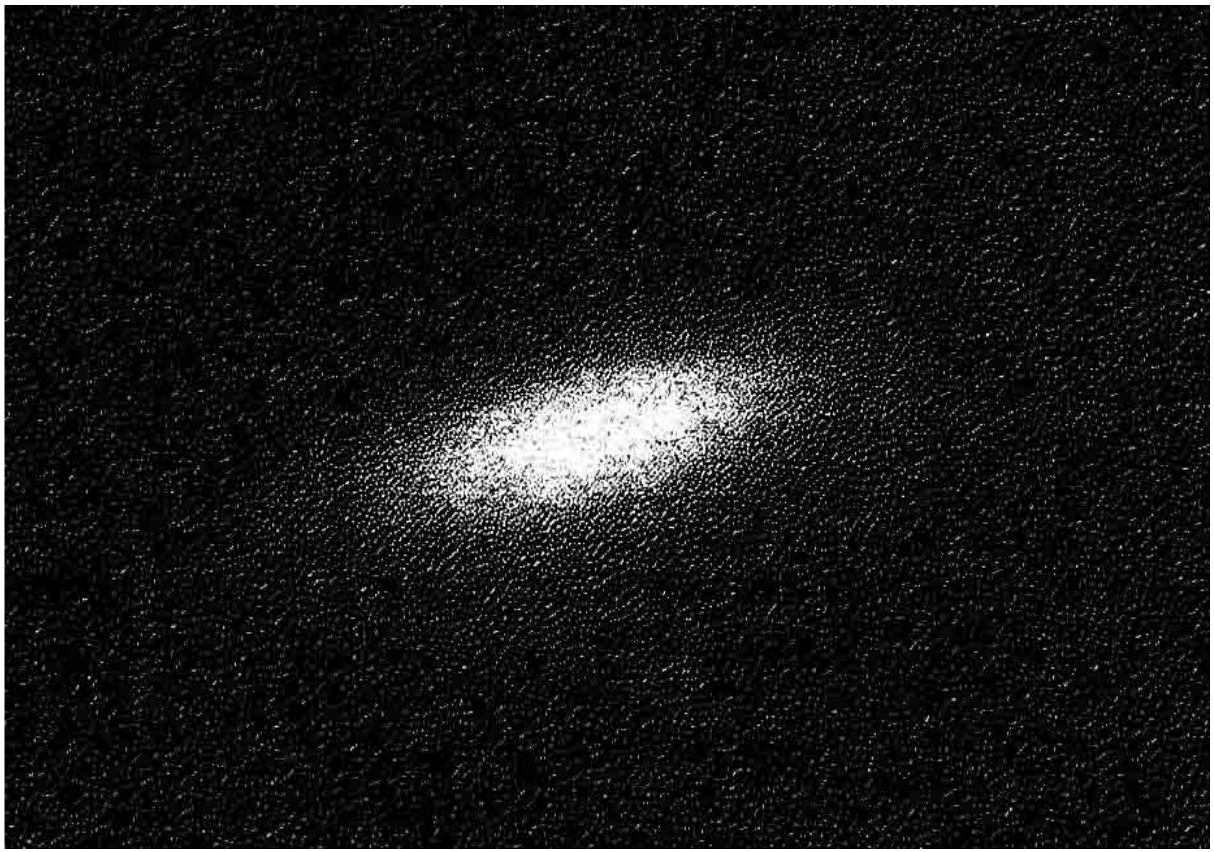

Double slit interferometer to measure beam size using 1st order spatial coherence

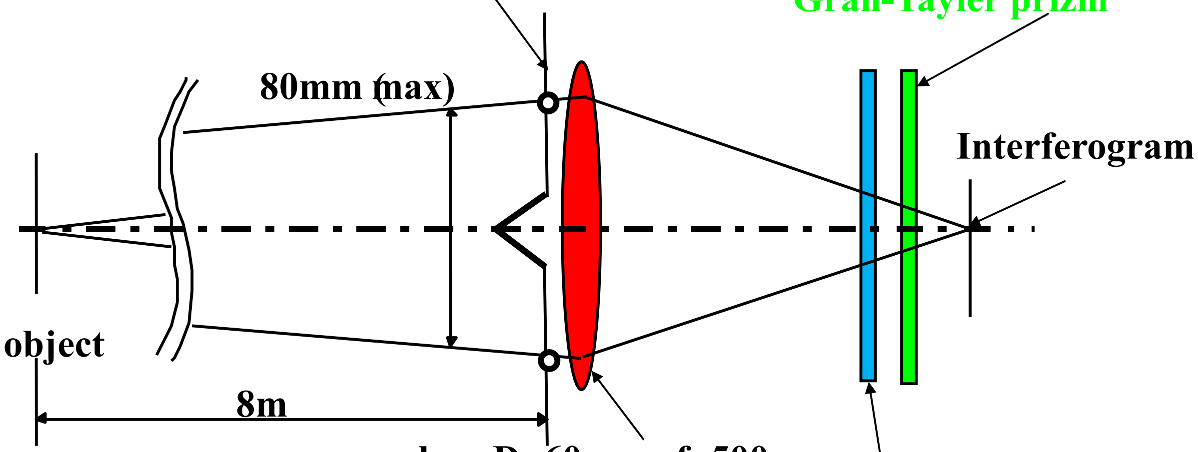

The intensity of the interferogram is given by;

$$I(y,D)=\int (I_1+I_2)\cdot\left\{\sin c\left(\frac{\pi\cdot a\cdot y\cdot\chi(D)}{\lambda\cdot f}\right)\right\}^2\cdot\left\{1+\gamma\cdot\cos\left(k\cdot D\cdot\left(\frac{y}{f}+\psi\right)\right)\right\}d\lambda$$

$$\gamma=\left(\frac{2\cdot\sqrt{I_1\cdot I_2}}{I_1+I_2}\right)\cdot\left(\frac{I_{\max}-I_{\min}}{I_{\max}+I_{\min}}\right)\quad,\quad \psi=\tan^{-1}\frac{S(D)}{C(D)}$$

Typical interferograms measured by SR interferometer

$\lambda = 550nm$

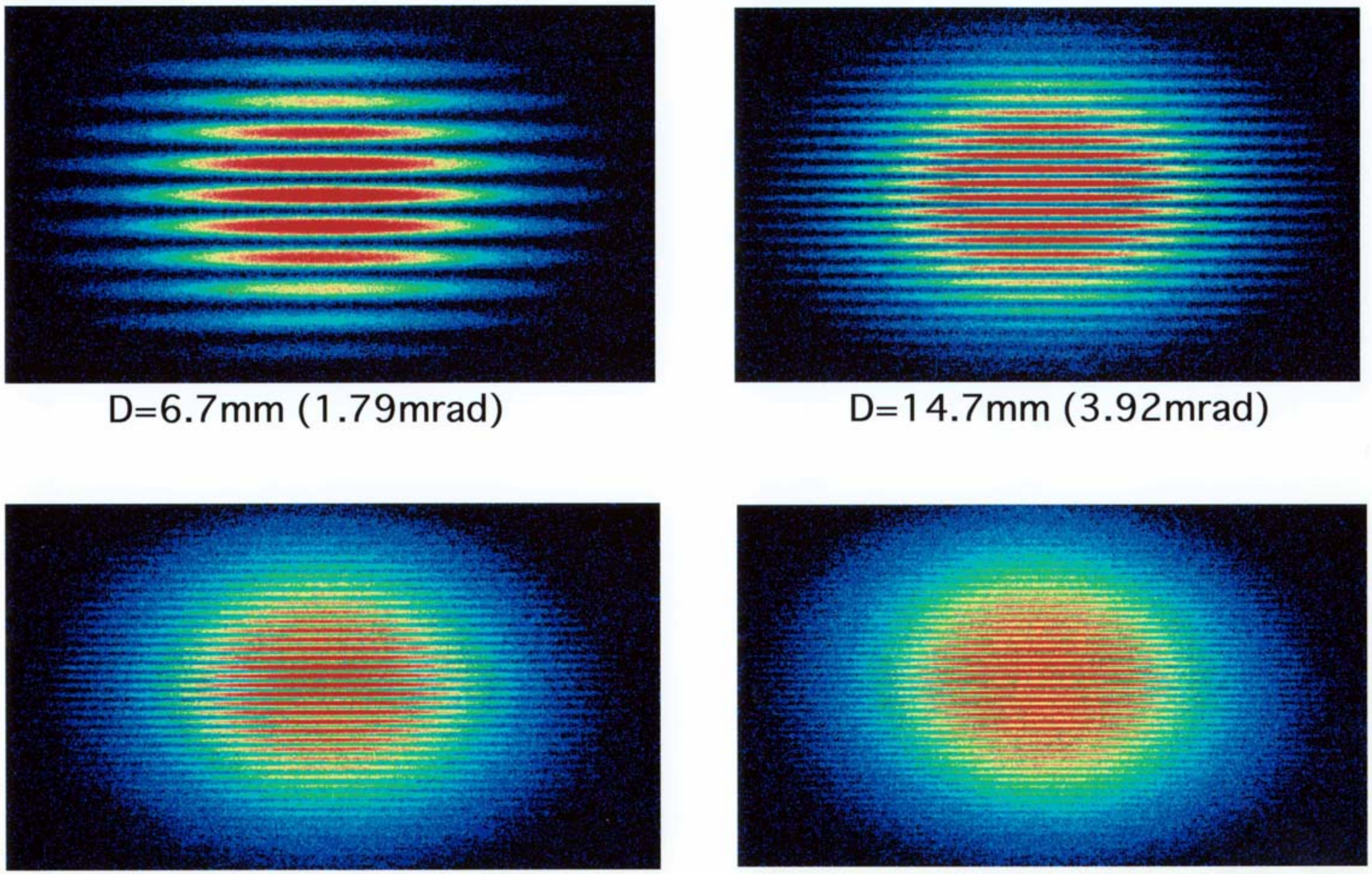

D=6.7mm (1.79mrad)

D=14.7mm (3.92mrad)

D=22.7mm (6.05mrad)

D=28.7mm (7.65mrad)

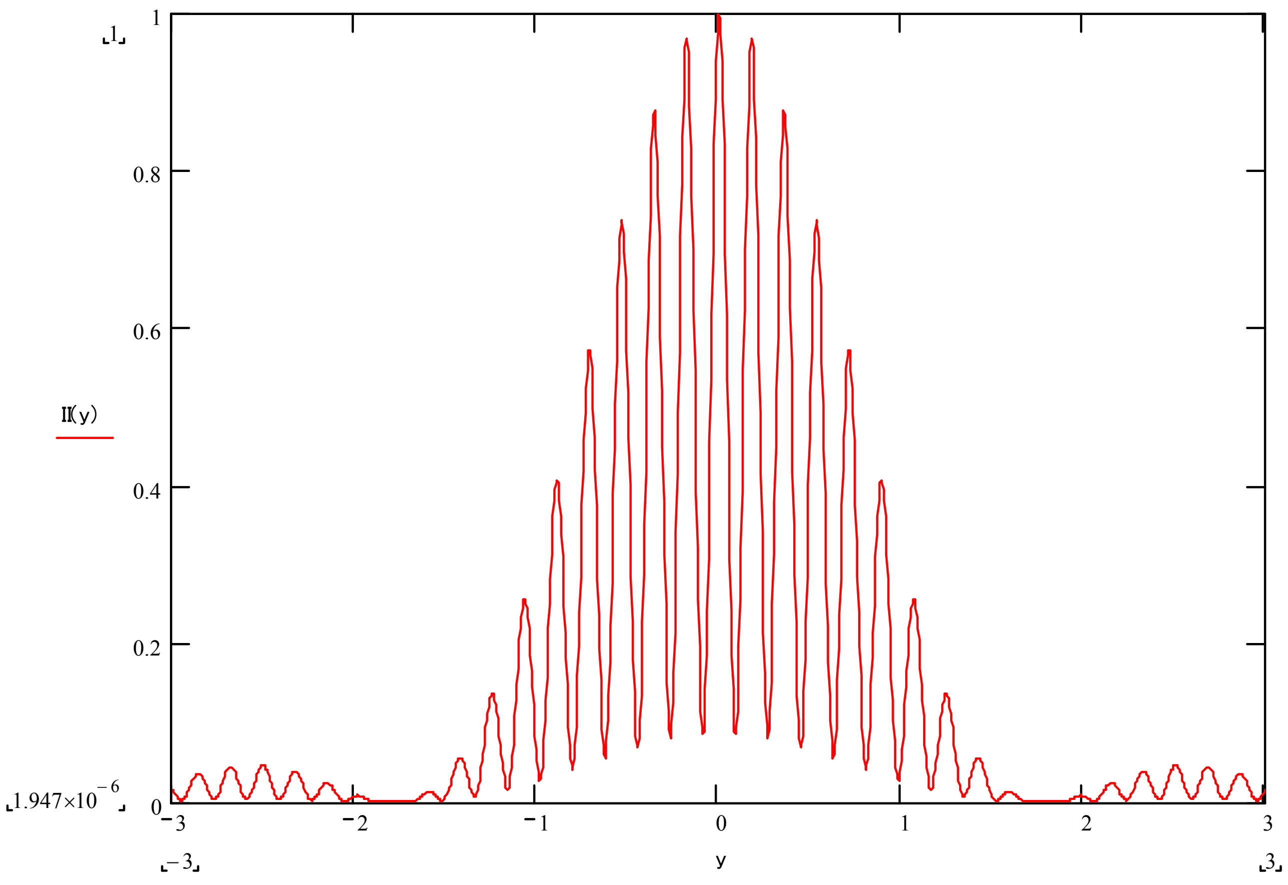
1
0.8
0.6
0.4
0.2
0
II(y)
1.947×10^−6
−3
−2
−1
0
1
2
3
y

Beam size measurement by SR interferometer

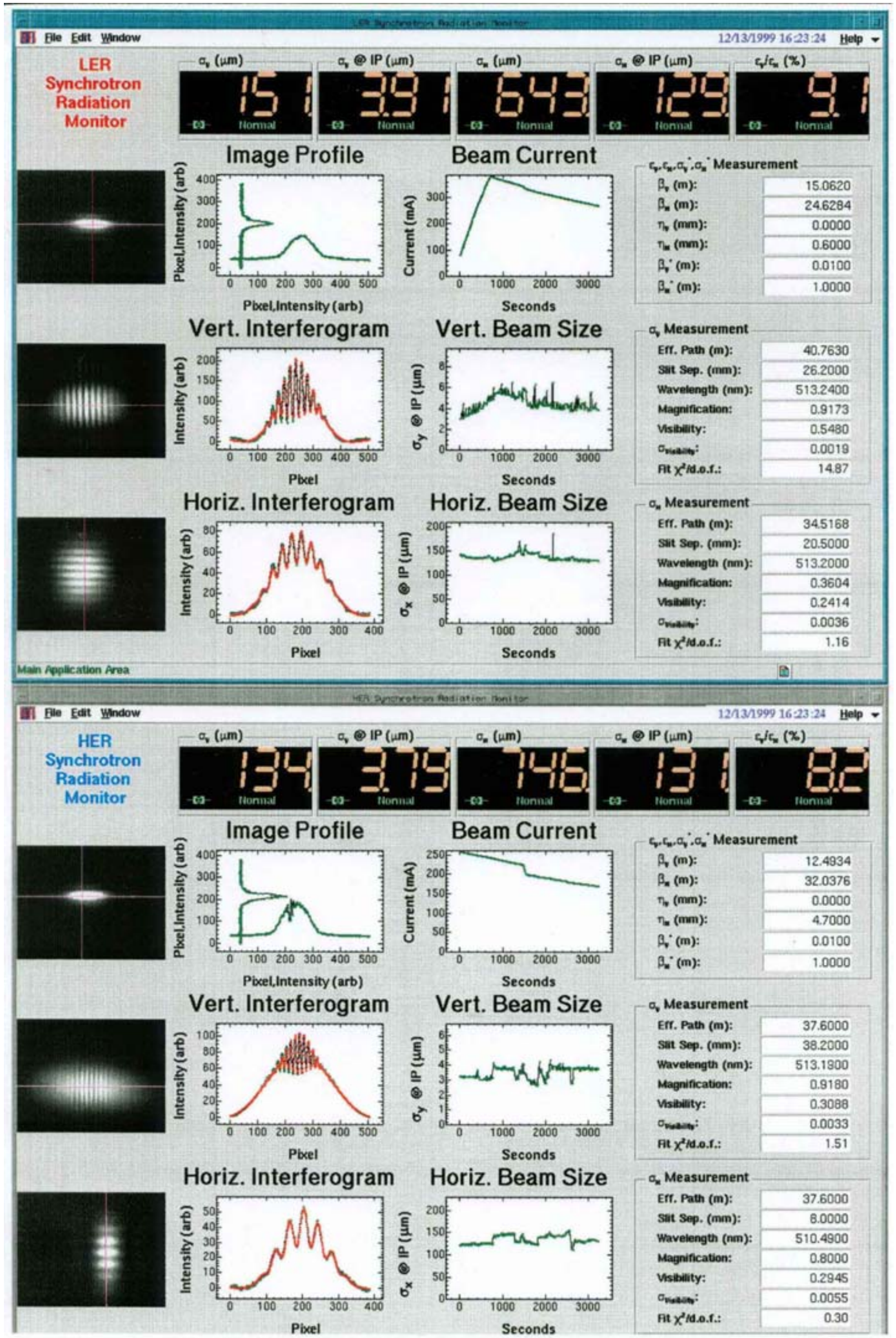

Streak camera to measure longitudinal profile

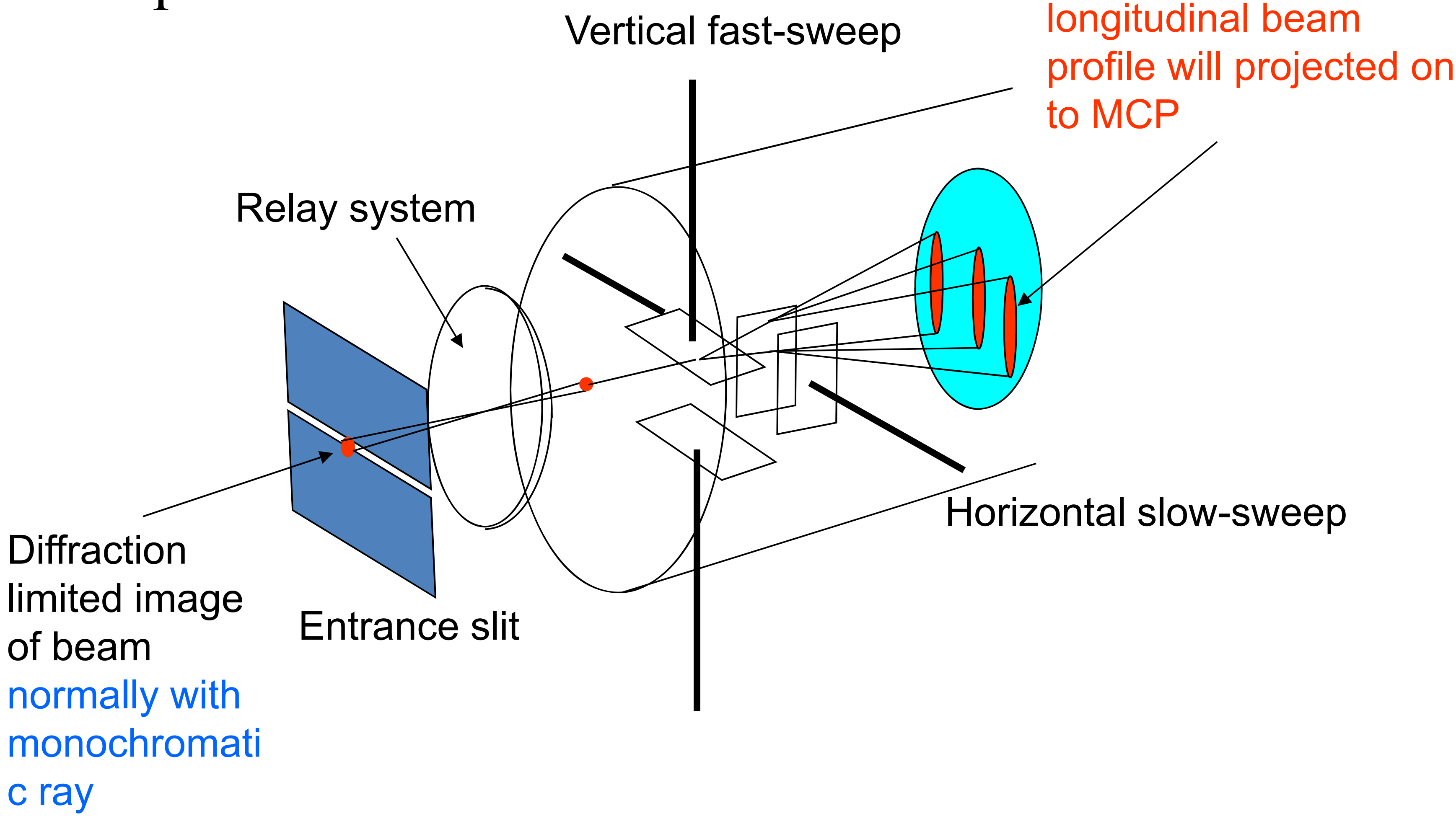

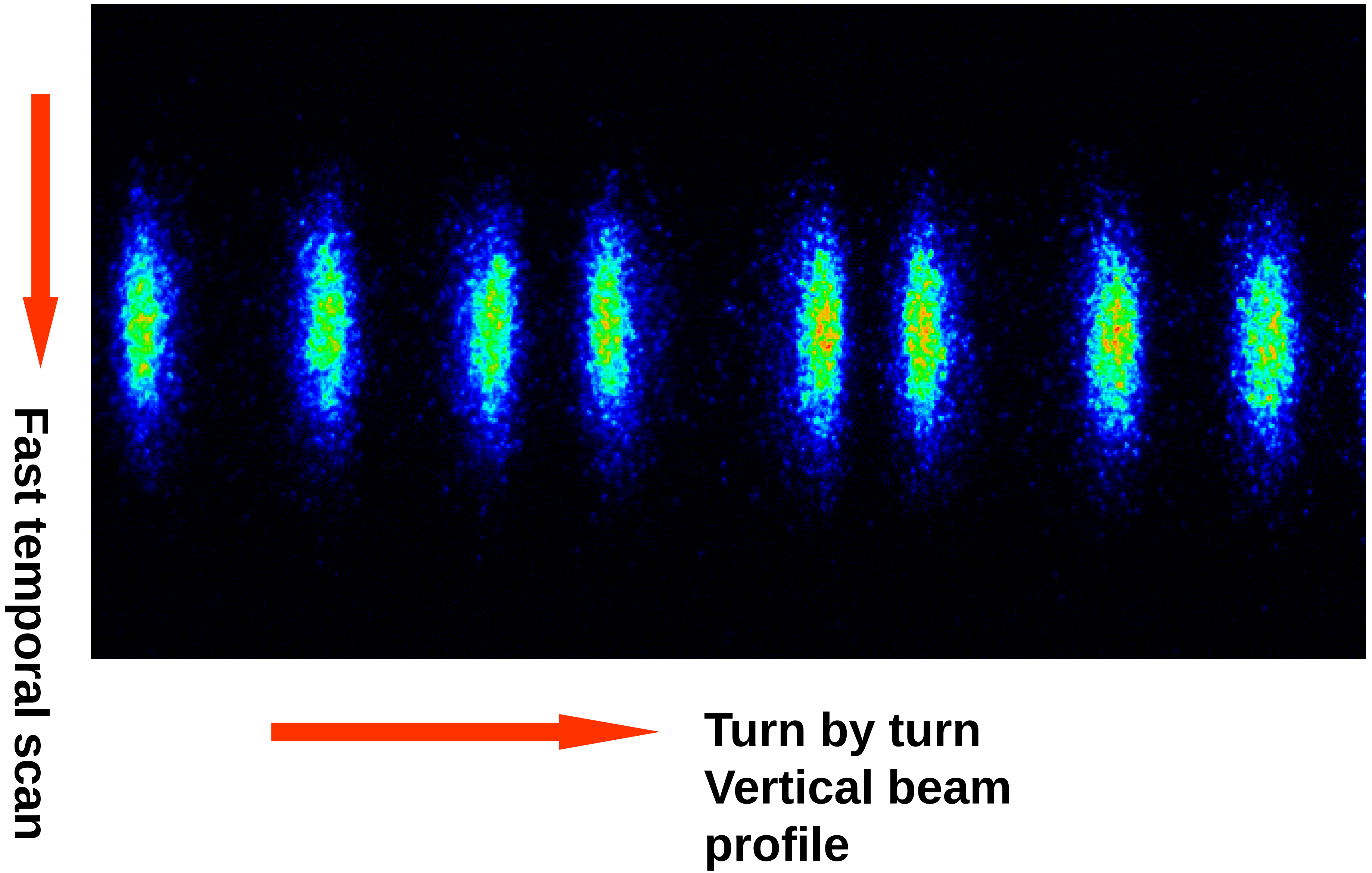

Fast temporal scan
Turn by turn
Vertical beam
profile

Dynamical observation of beam profile with high-speed gated camera

Function of high-speed gated camera

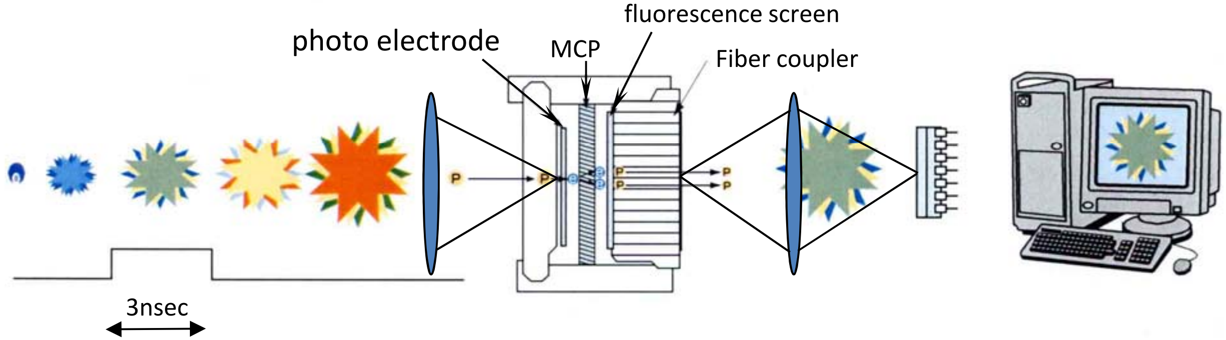

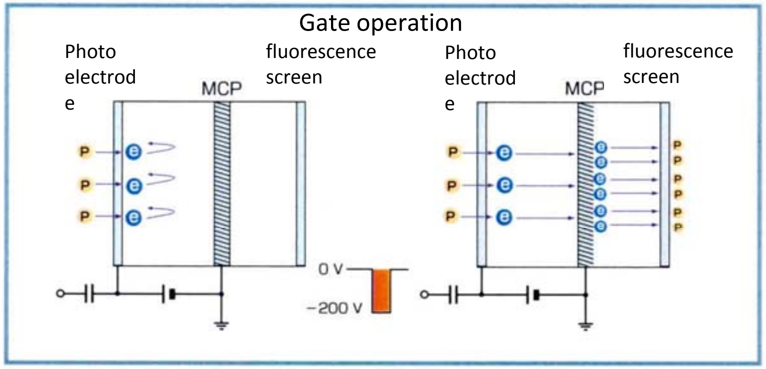

Turn by turn image of injected beam into storage ring

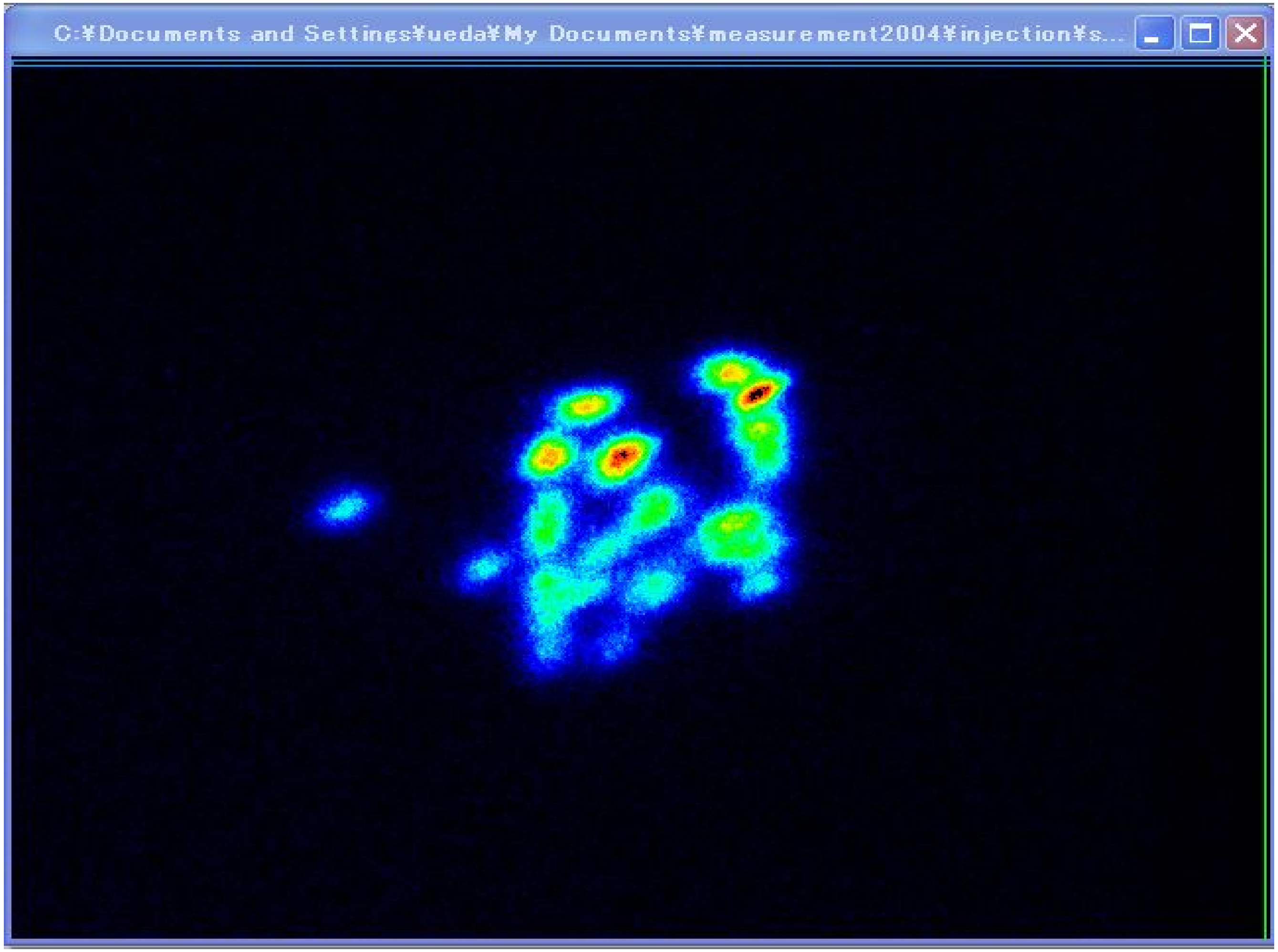

Observation of beam halo with corona graph

Optical system of Lyott's corona graph

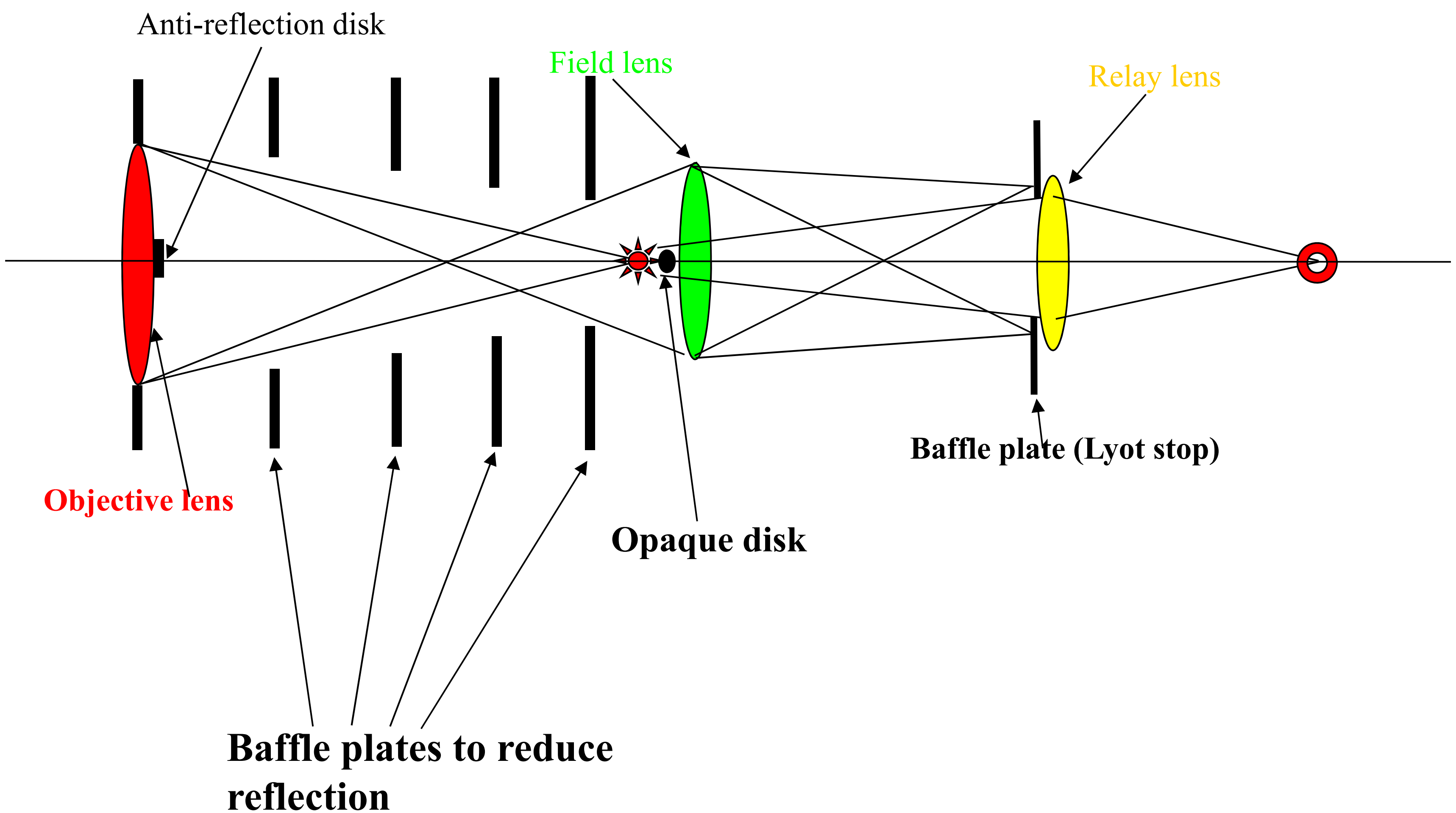

Image of beam profile without the opaque disk. Exposure time of CCD camera is 10msec.

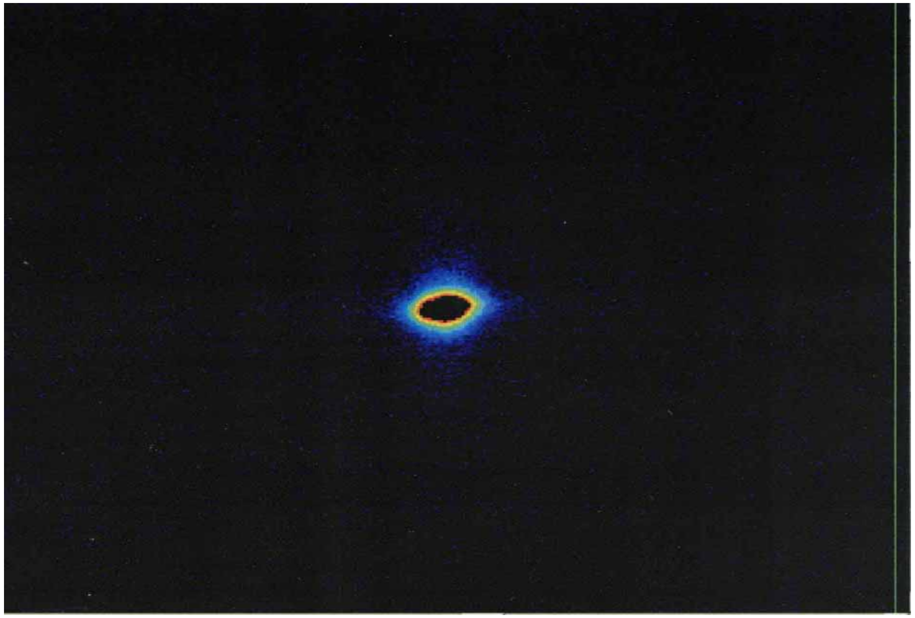

Image of beam tail with the opaque disk. Transverse magnification is same as in Fig.6. Exposure time of CCD camera is 10msec.

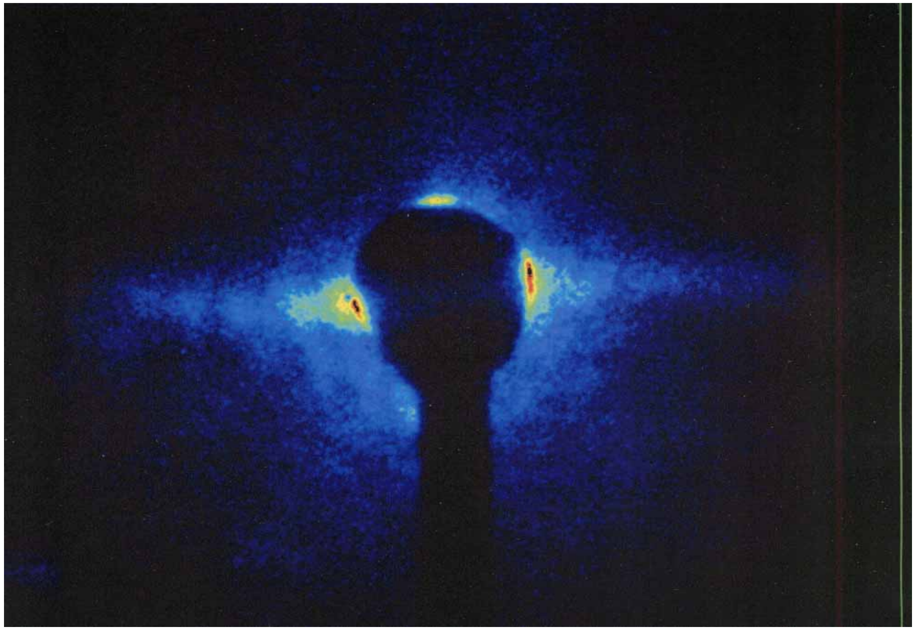

Focusing components are used everywhere in the SR monitor!

Optics to understand focusing system is most important issue in the SR monitor

3. Optics for focusing system

Geometrical optics of focusing system

Focusing system with lens

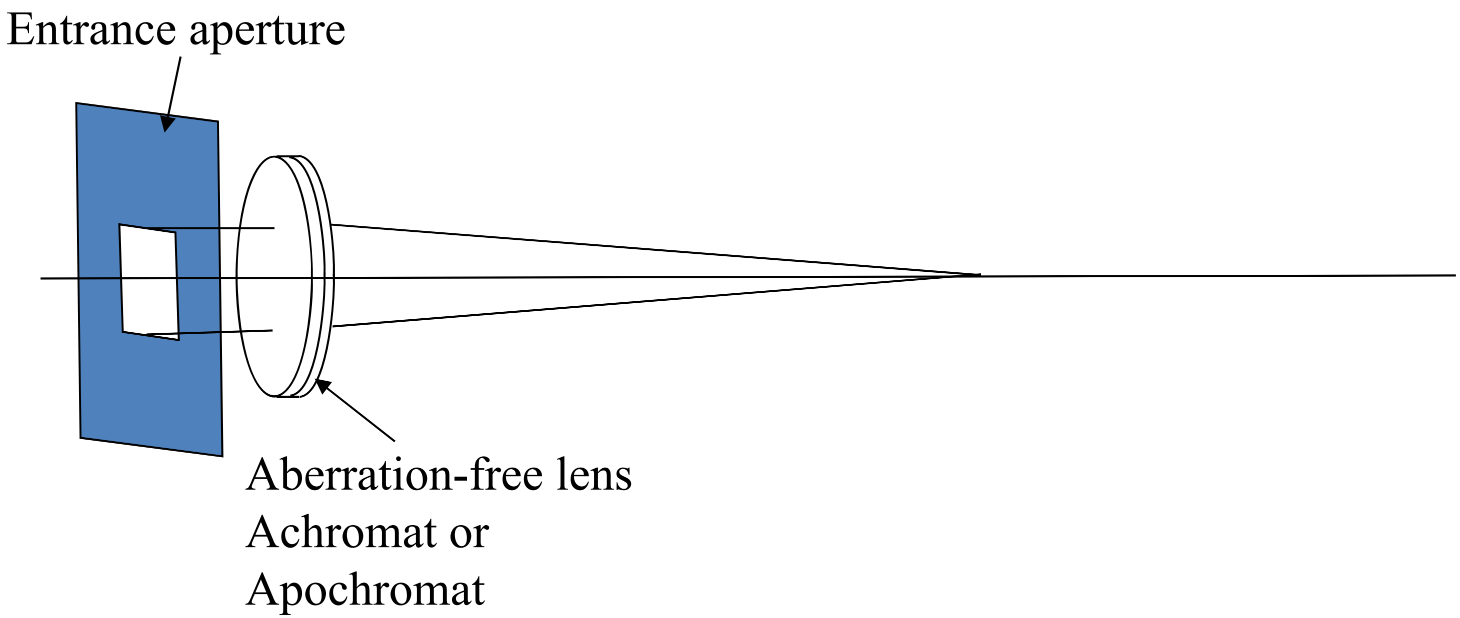

Practical focusing system for SR monitor

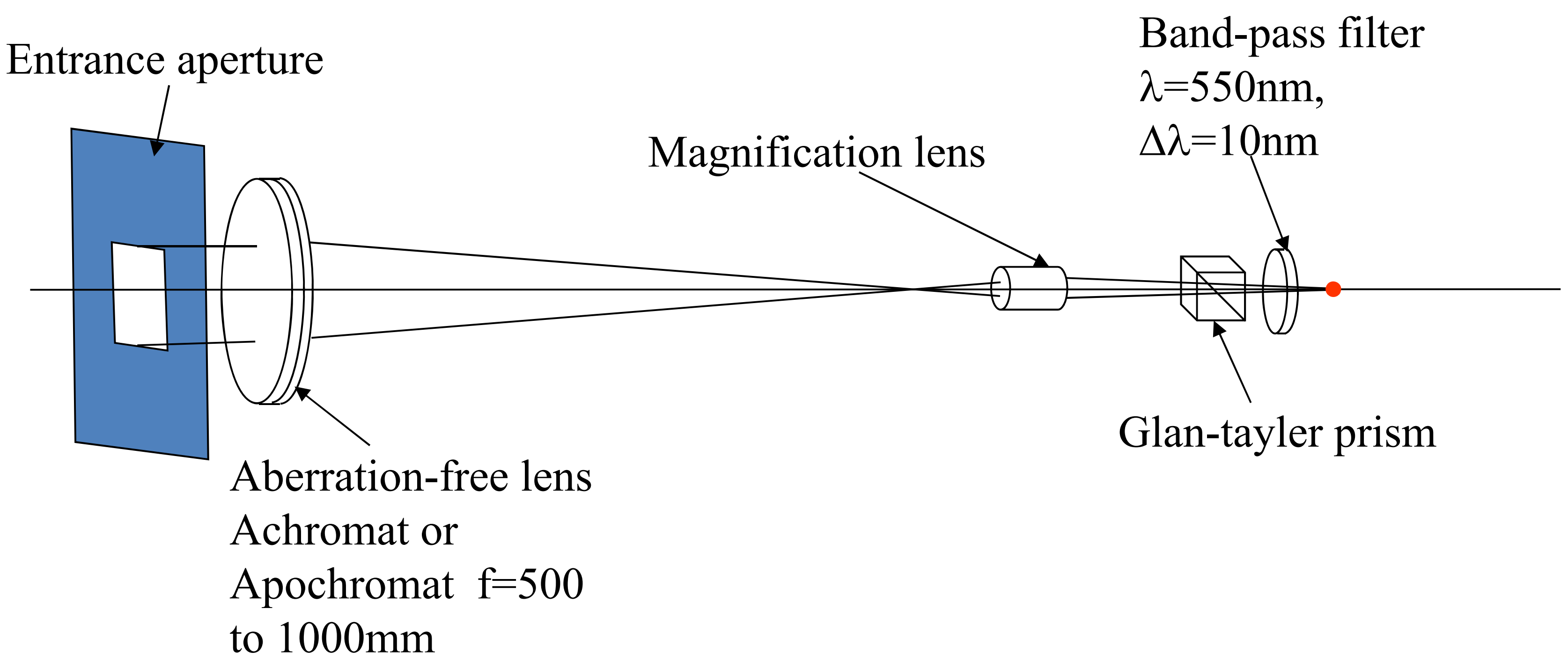

Herschelian arrangement of optics

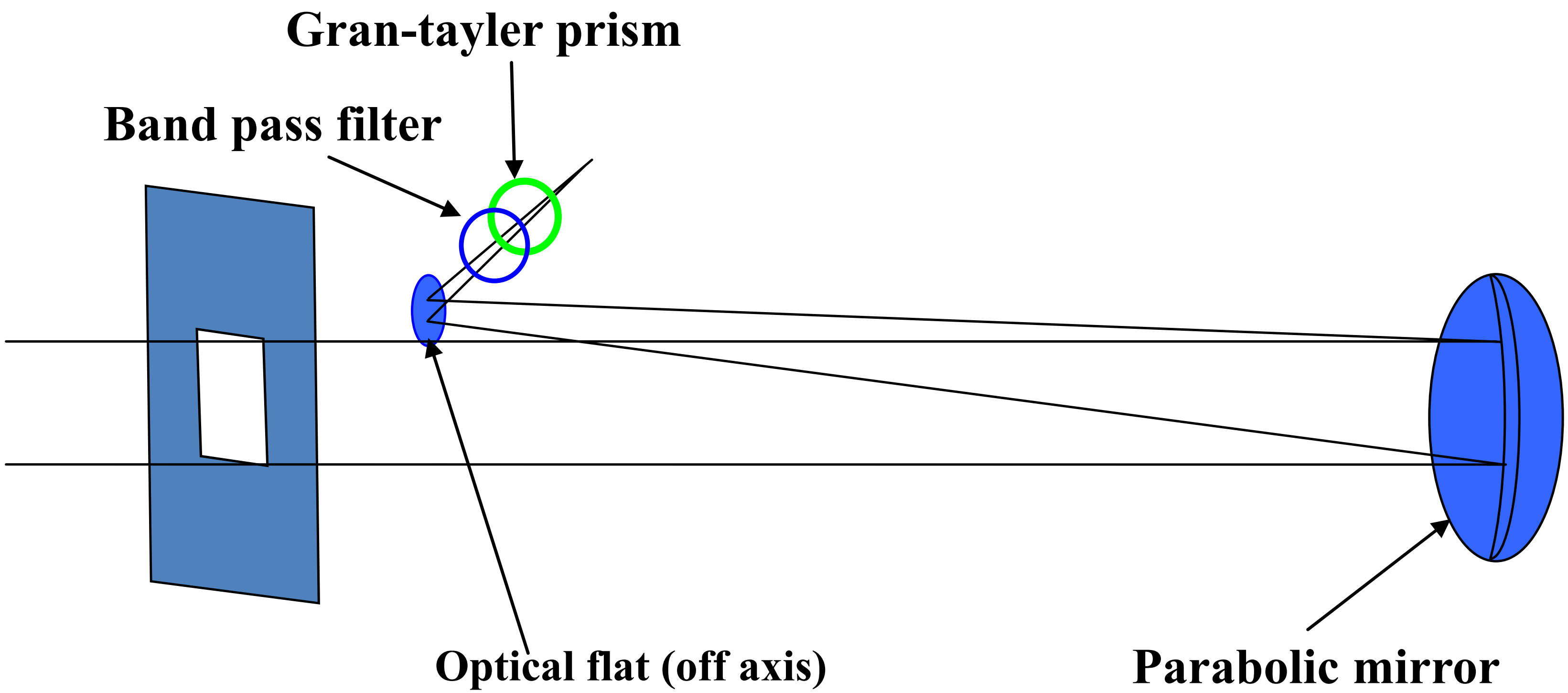

Newton's equation

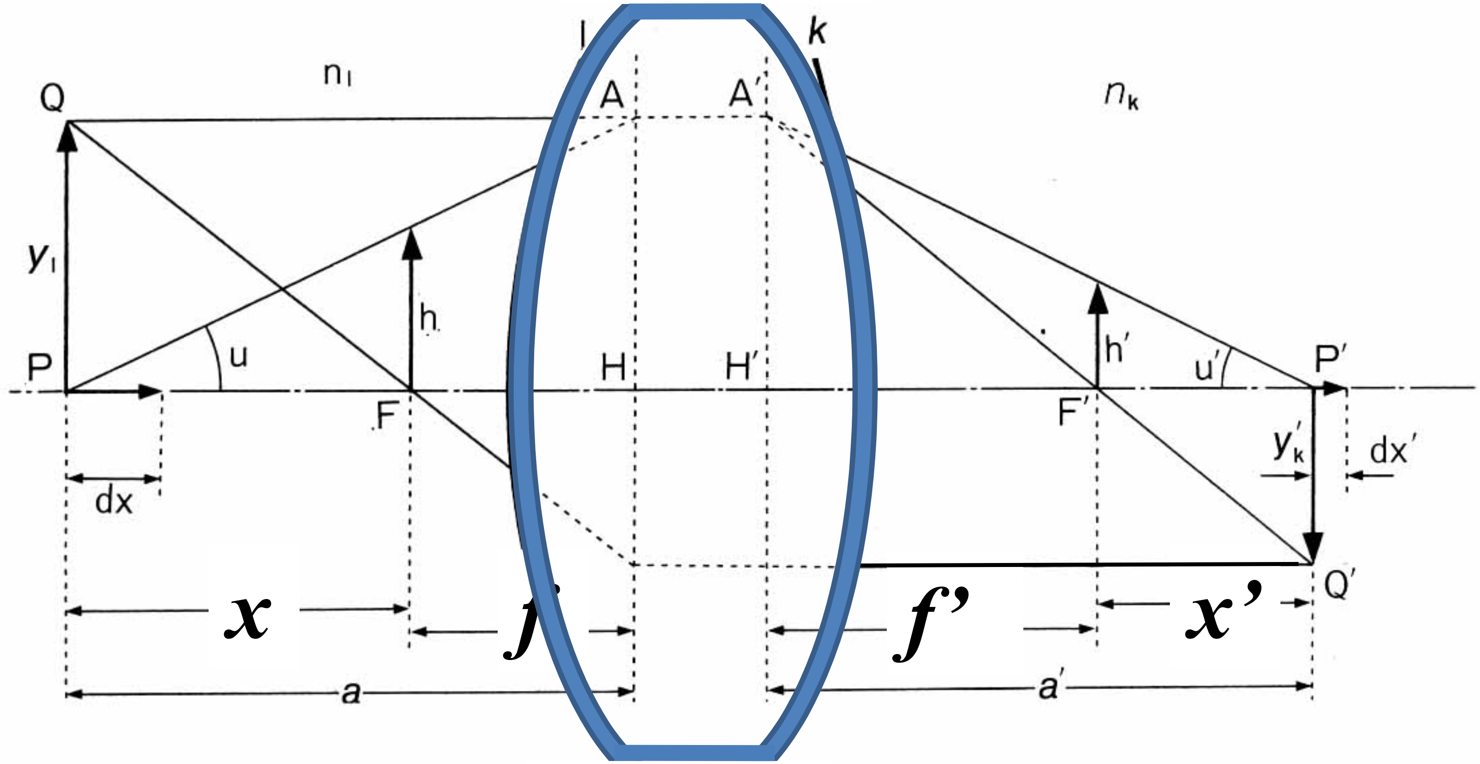

$$\beta = \frac{y'_k}{y_1} = -\frac{x'}{f'} = \frac{f}{x}$$

Conjugation points

P: front focus point

P': back focus point

H: front principal point

H': back principal point

In the focusing system which used in SR monitor, image will appear in narrow field on-axis.

In this case, most important aberration is on-axis spherical aberration.

For understanding the spherical aberration, let us start with focusing mirror system by ellipsoidal surface.

Spherical aberration

1. Ellipsoidal surface

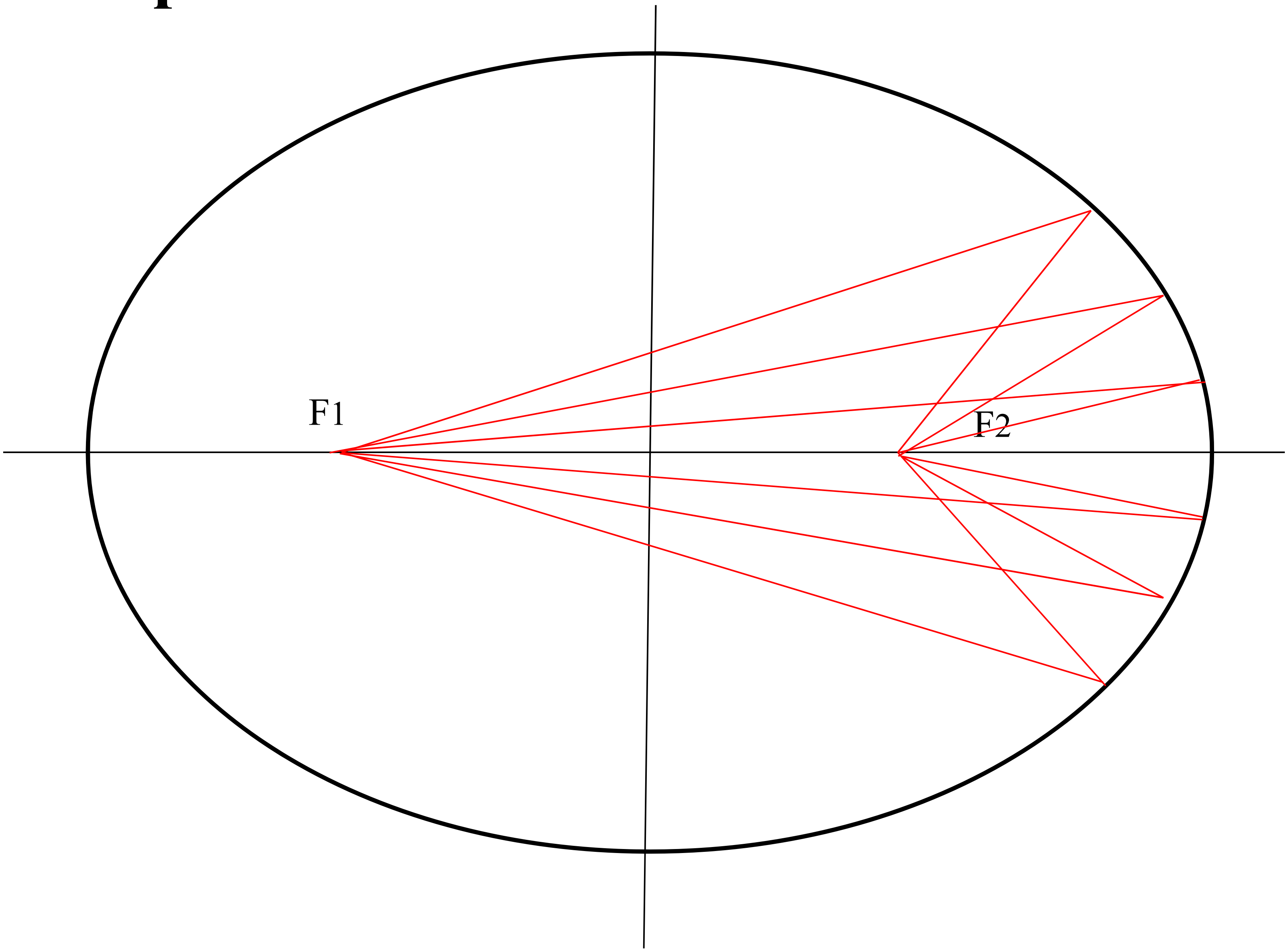

1. Ellipsoidal surface

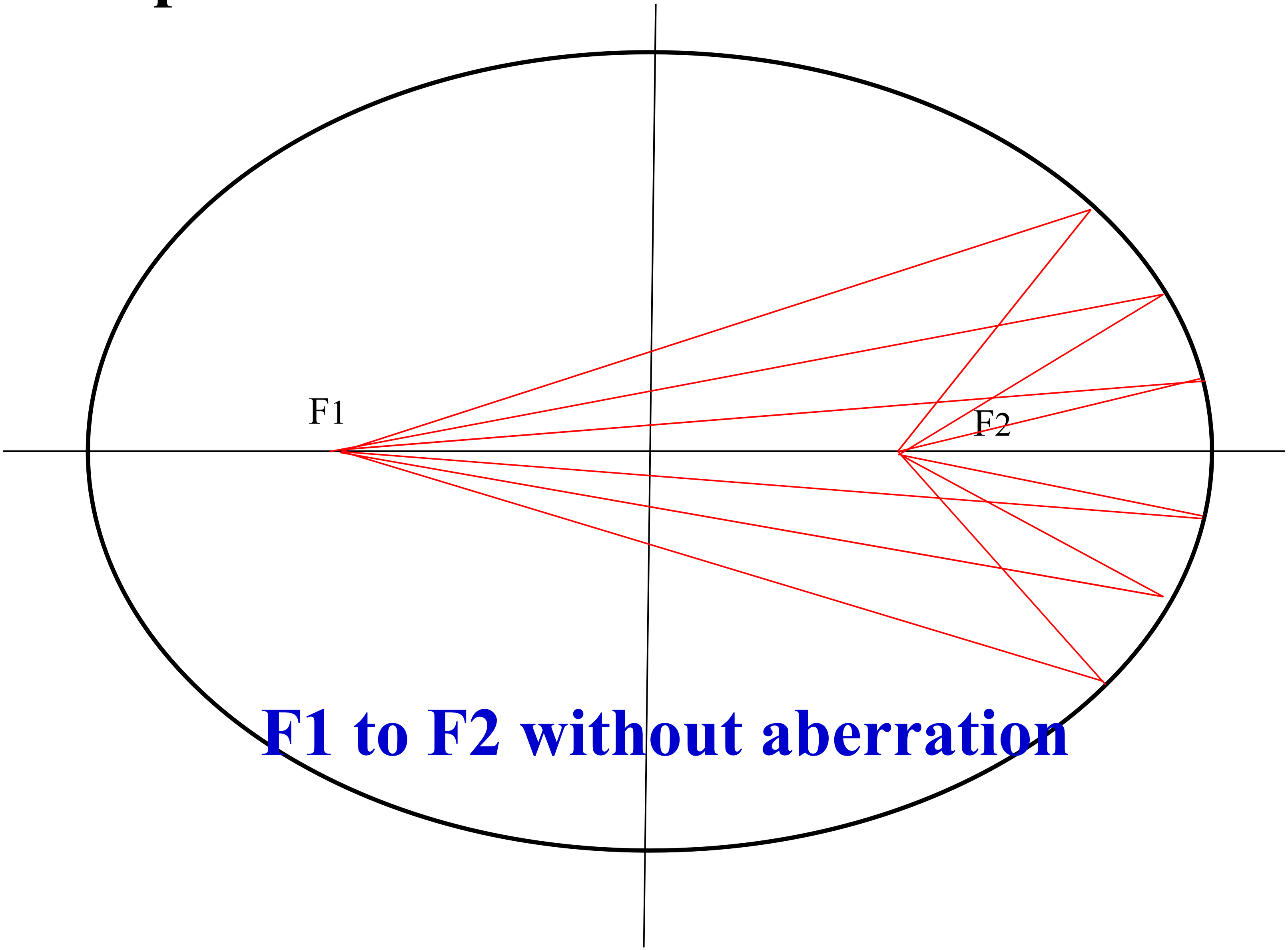

F1 to F2 without aberration

2.Spherical surface

F1=F2=F

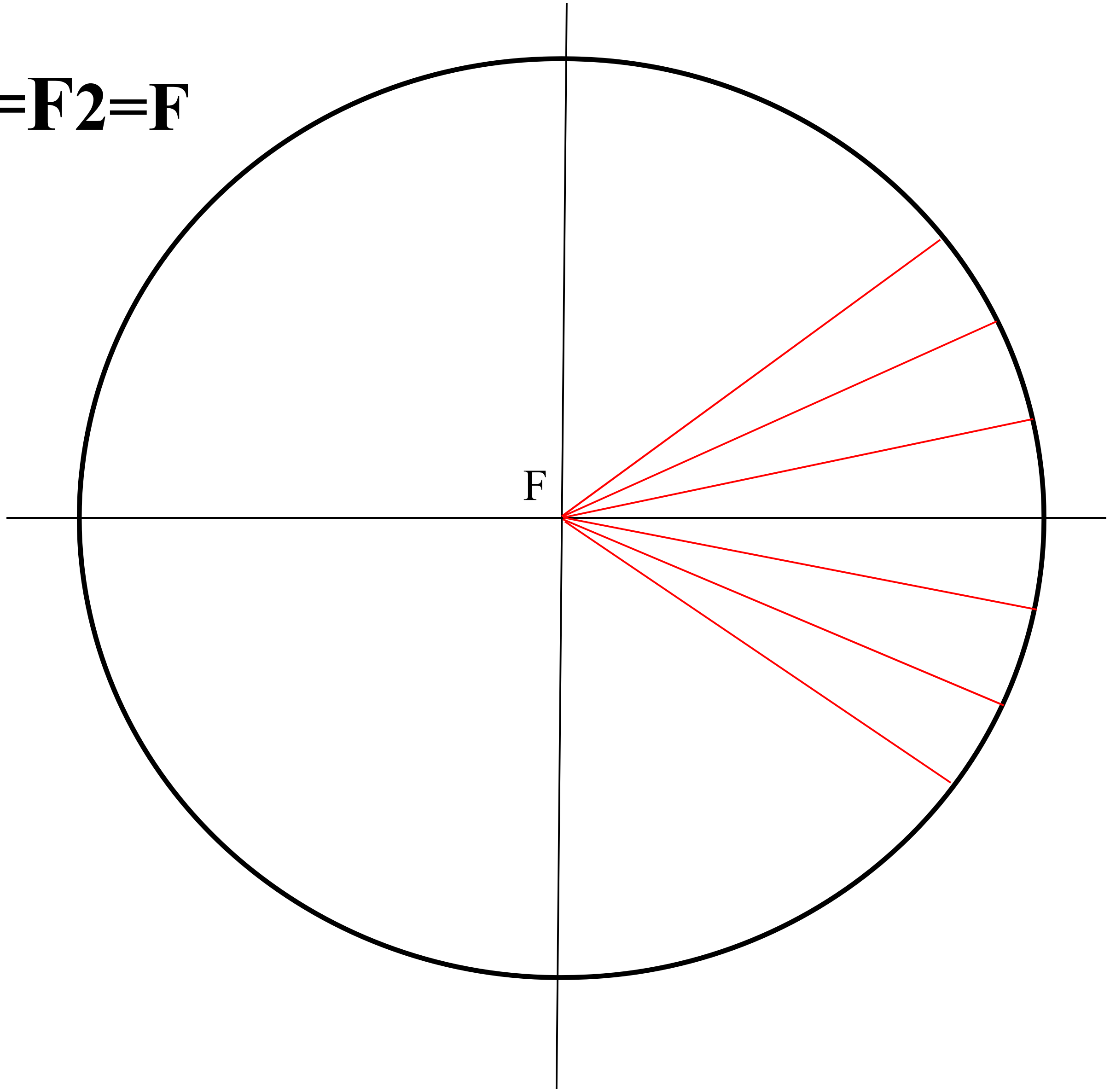

2.Spherical surface

F1=F2=F

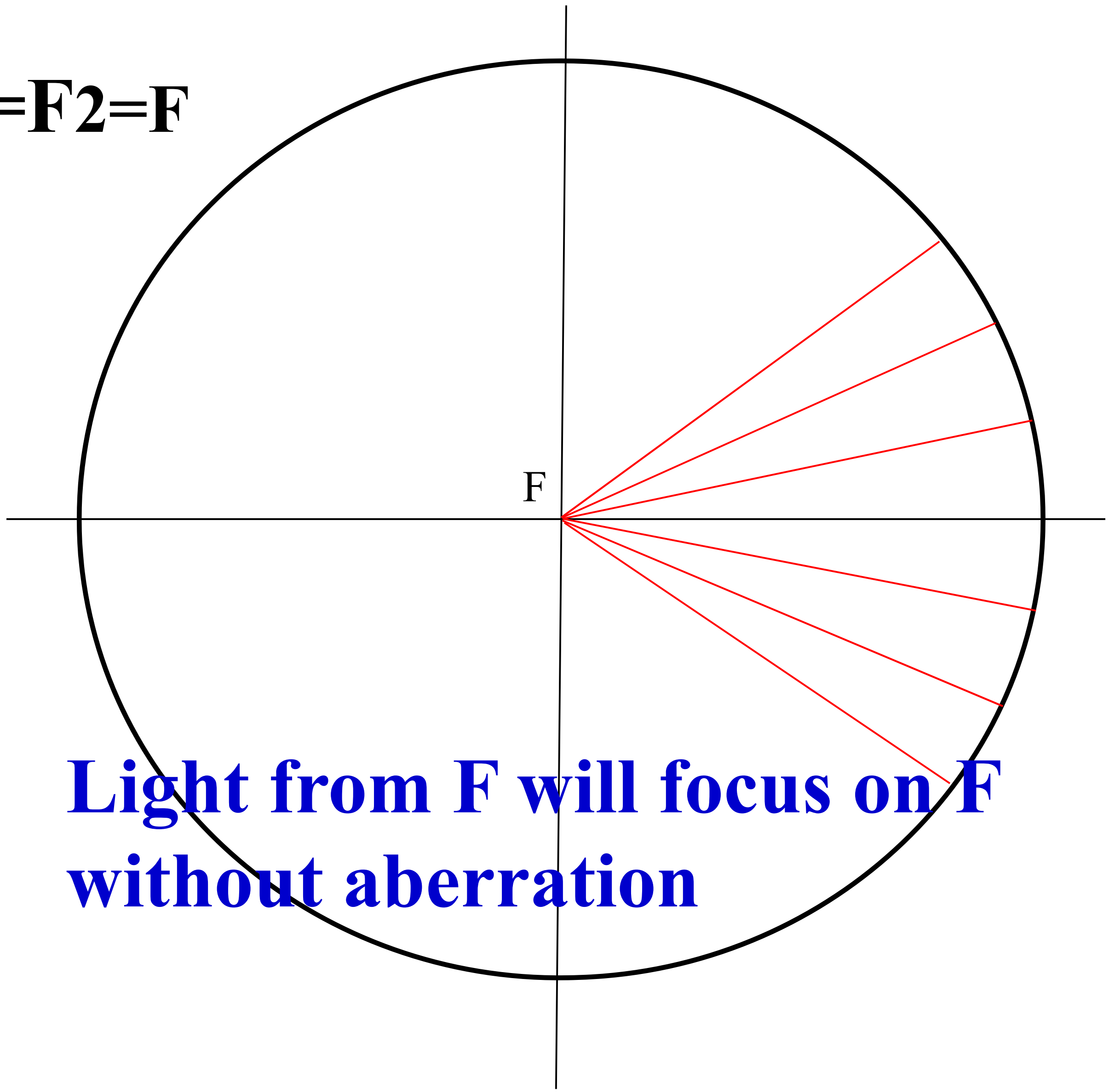

Light from F will focus on F without aberration

Parabolic surface

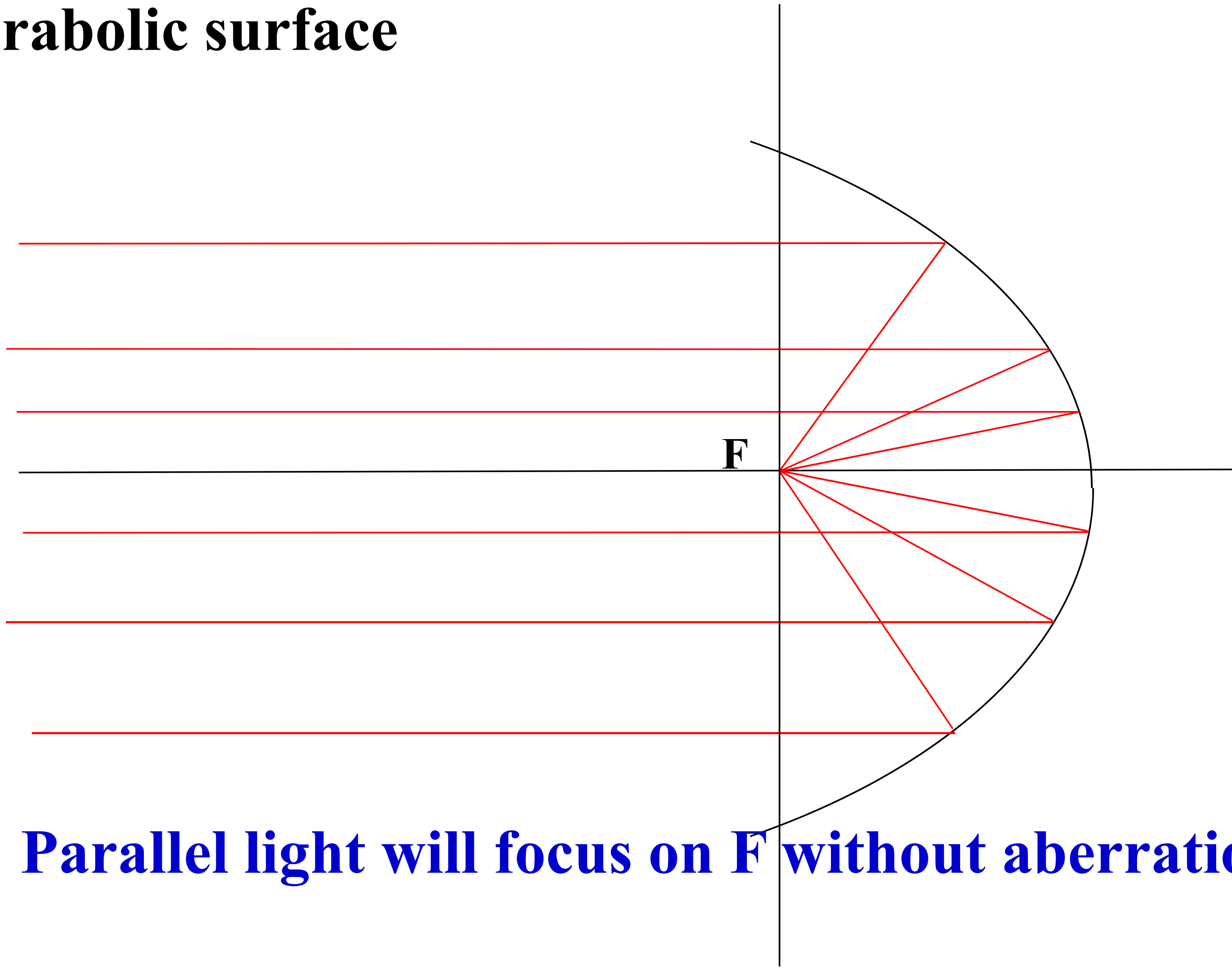

Parallel light will focus on F without aberration

Parabolic surface

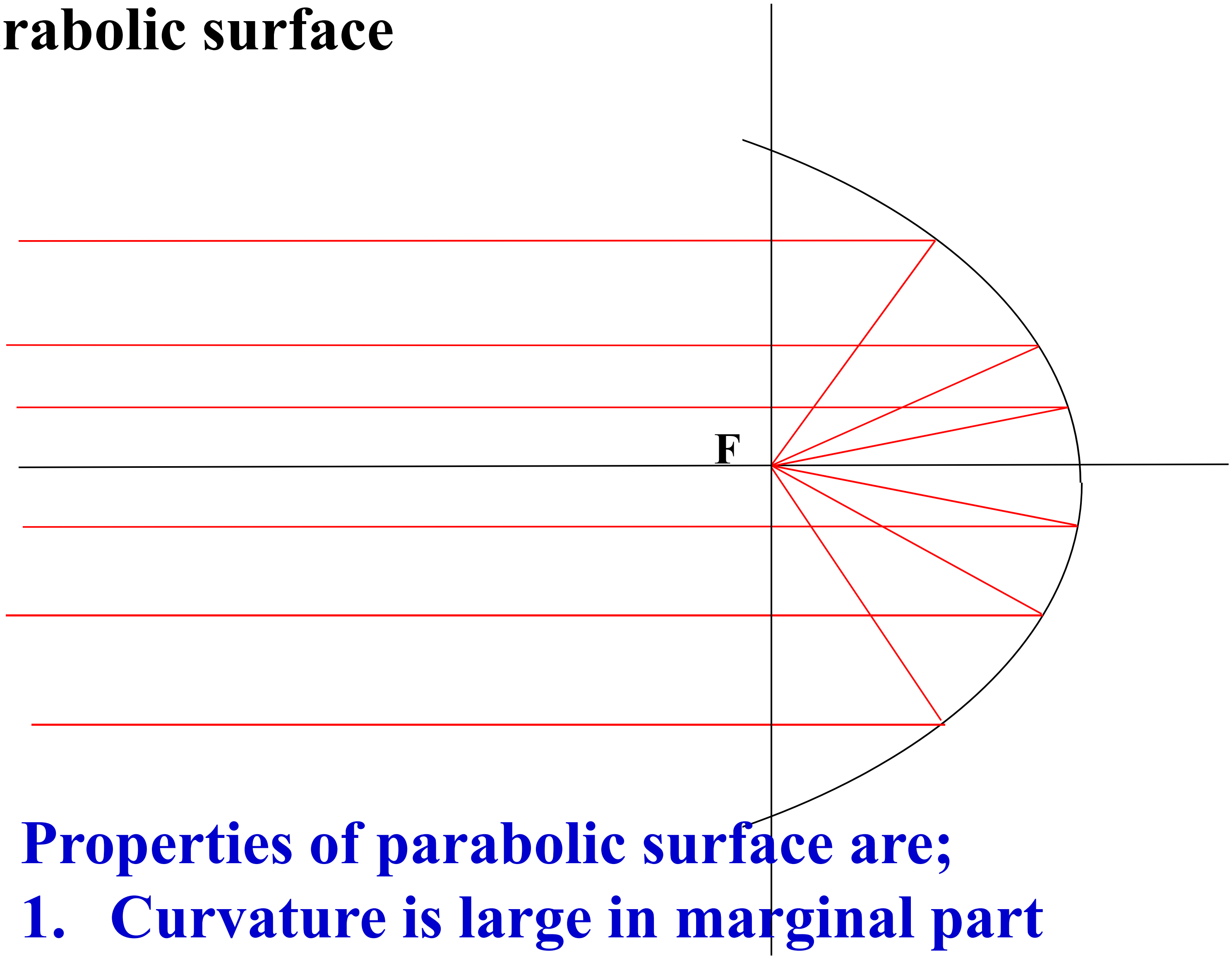

Properties of parabolic surface are;

1. **Curvature is large in marginal part**
2. **Curvature is small in paraxial part**

If the parallel light will come to spherical surface,

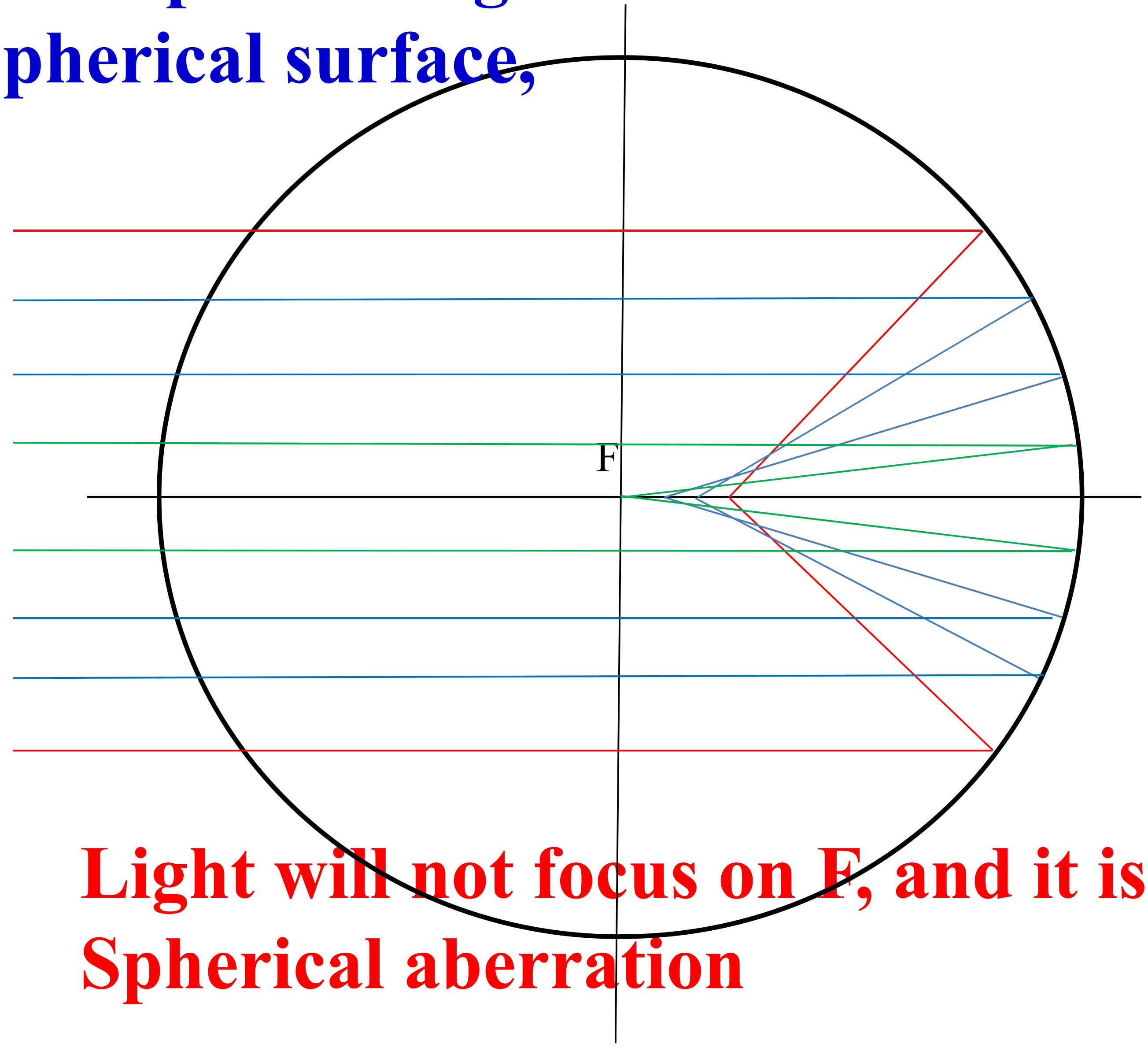

Light will not focus on F, and it is Spherical aberration

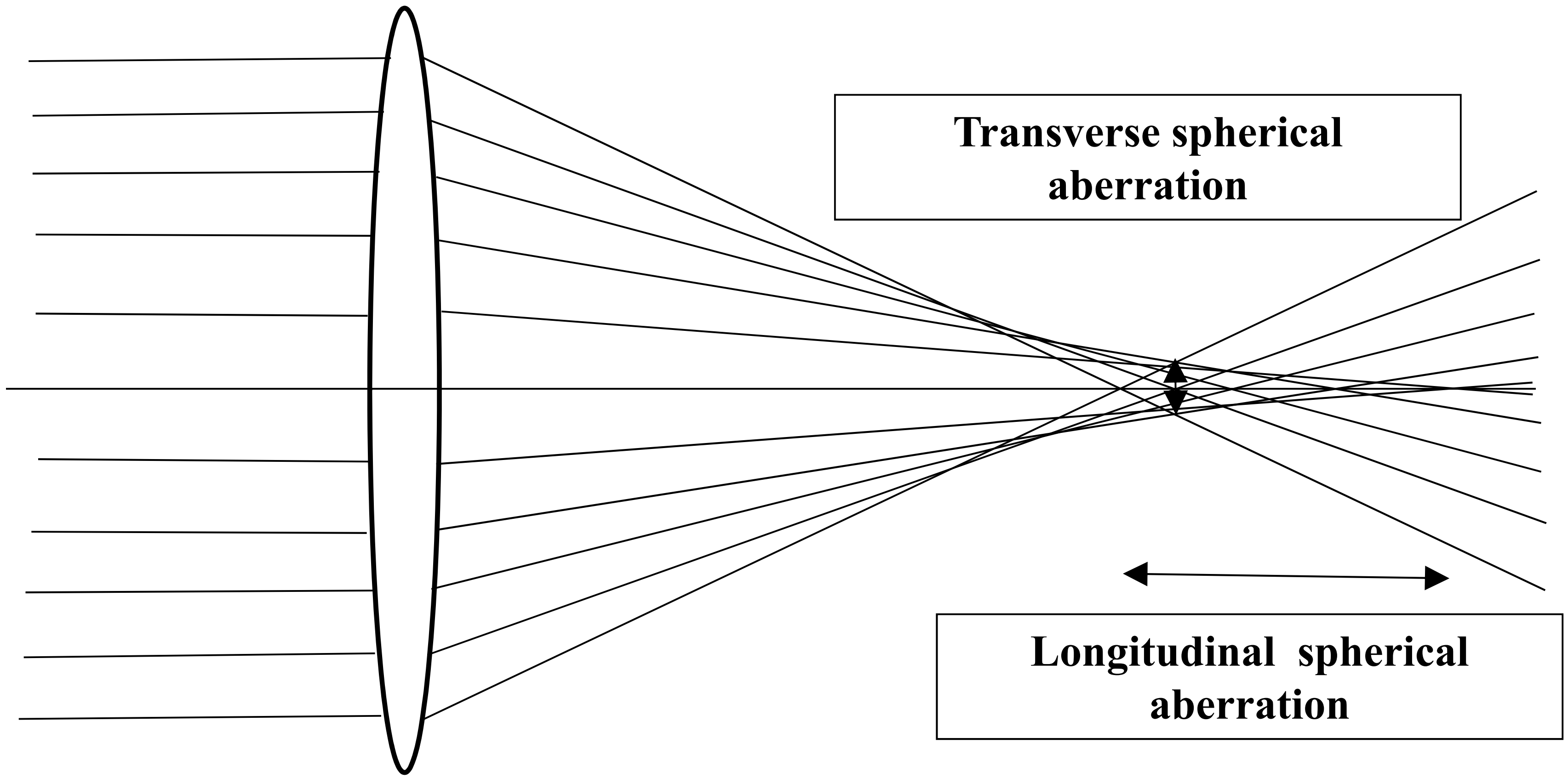
Transverse spherical aberration
Longitudinal spherical aberration

At average focus point, spherical aberration Looks;

How to correct spherical aberration?

Off course, we shall use non-spherical surface for reflective system,

but

How in the refractive system?

Spherical aberration

Focusing lens **+Spherical aberration**

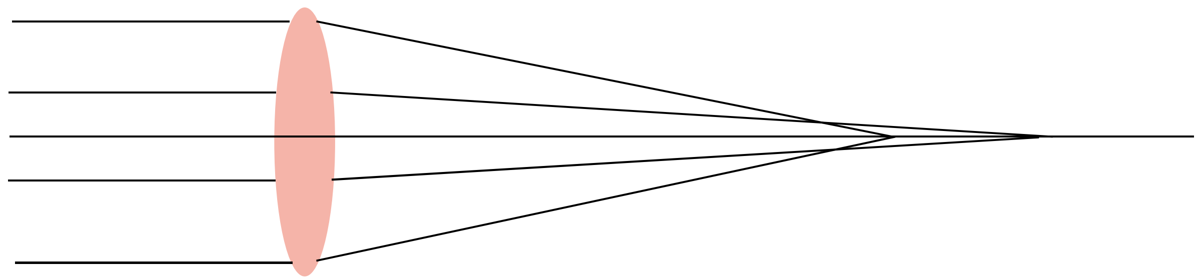

Defocusing lens **-Spherical aberration**

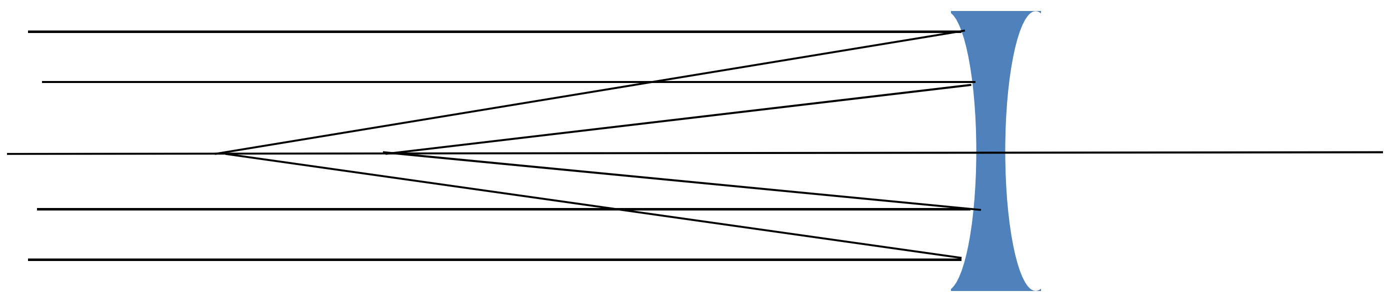

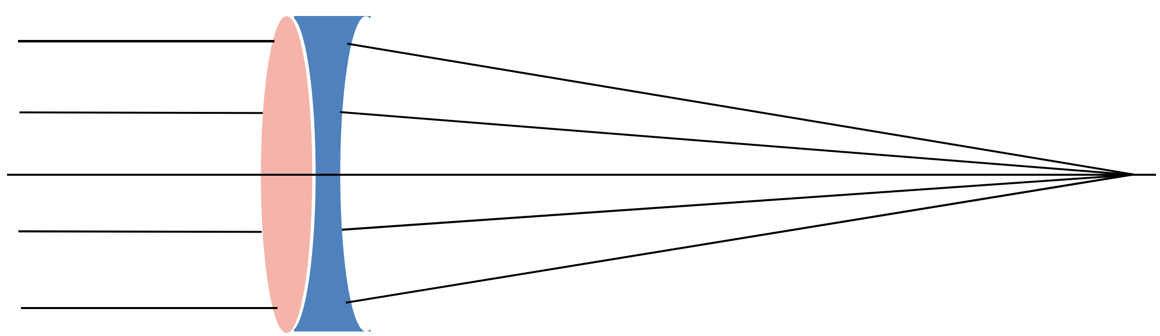

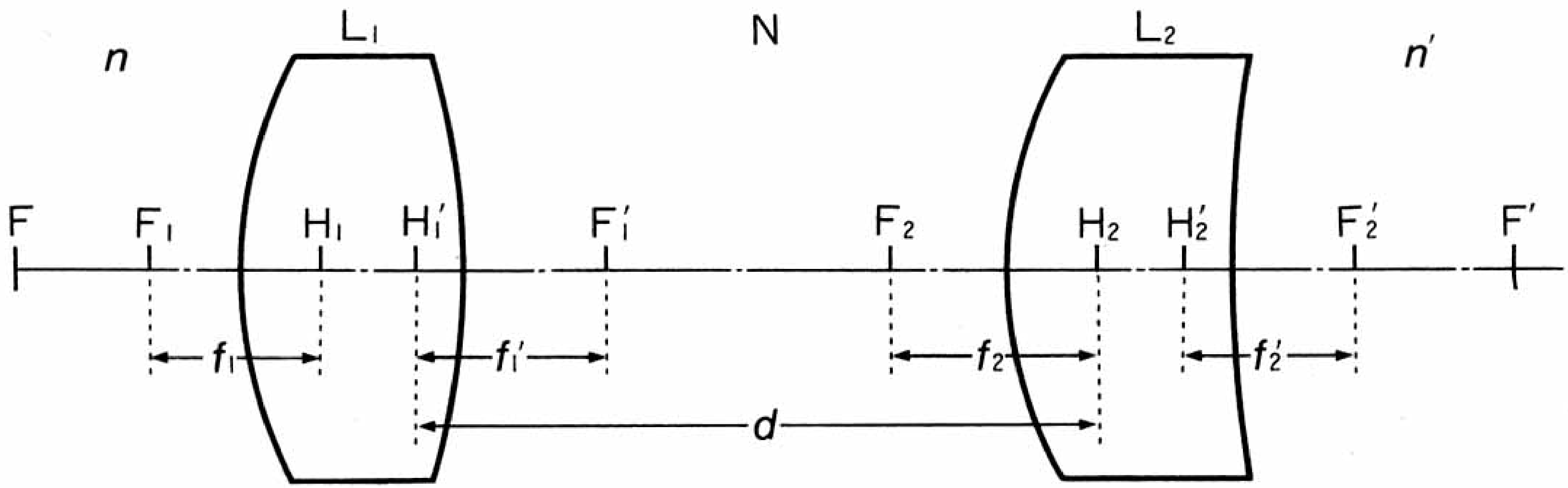

Front focus $$f = \frac{f_1 \cdot f_2}{f'_1 + f_2 - d}$$

d≠0

***f, f'*≠∞**

Back focus $$f' = \frac{f'_1 \cdot f'_2}{f'_1 + f'_2 - d}$$

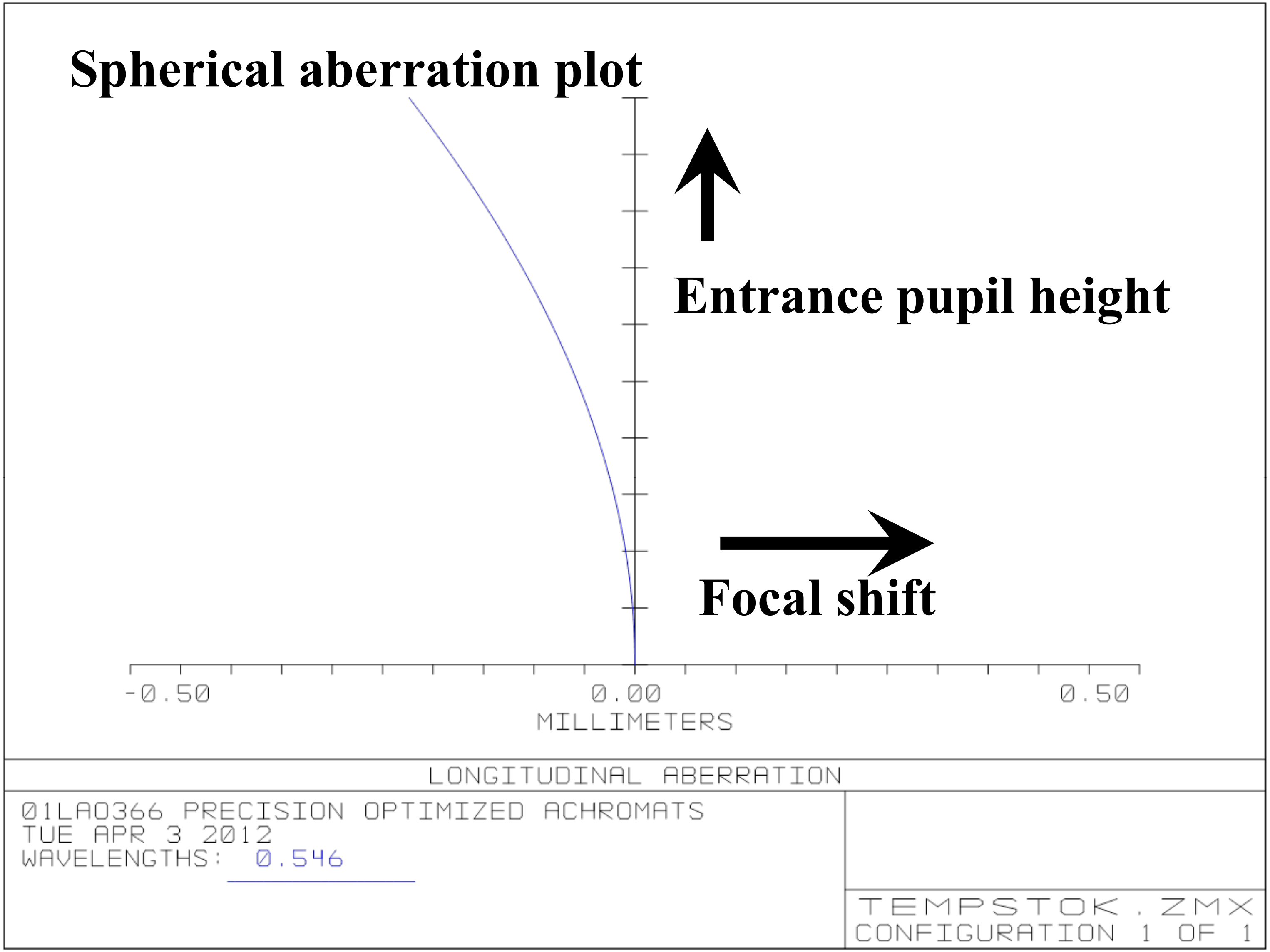
Spherical aberration plot
Entrance pupil height
Focal shift
-0.50
0.00
0.50
MILLIMETERS
LONGITUDINAL ABERRATION
01LA0366 PRECISION OPTIMIZED ACHROMATS
TUE APR 3 2012
WAVELENGTHS: 0.546
TEMPSTOK.ZMX
CONFIGURATION 1 OF 1

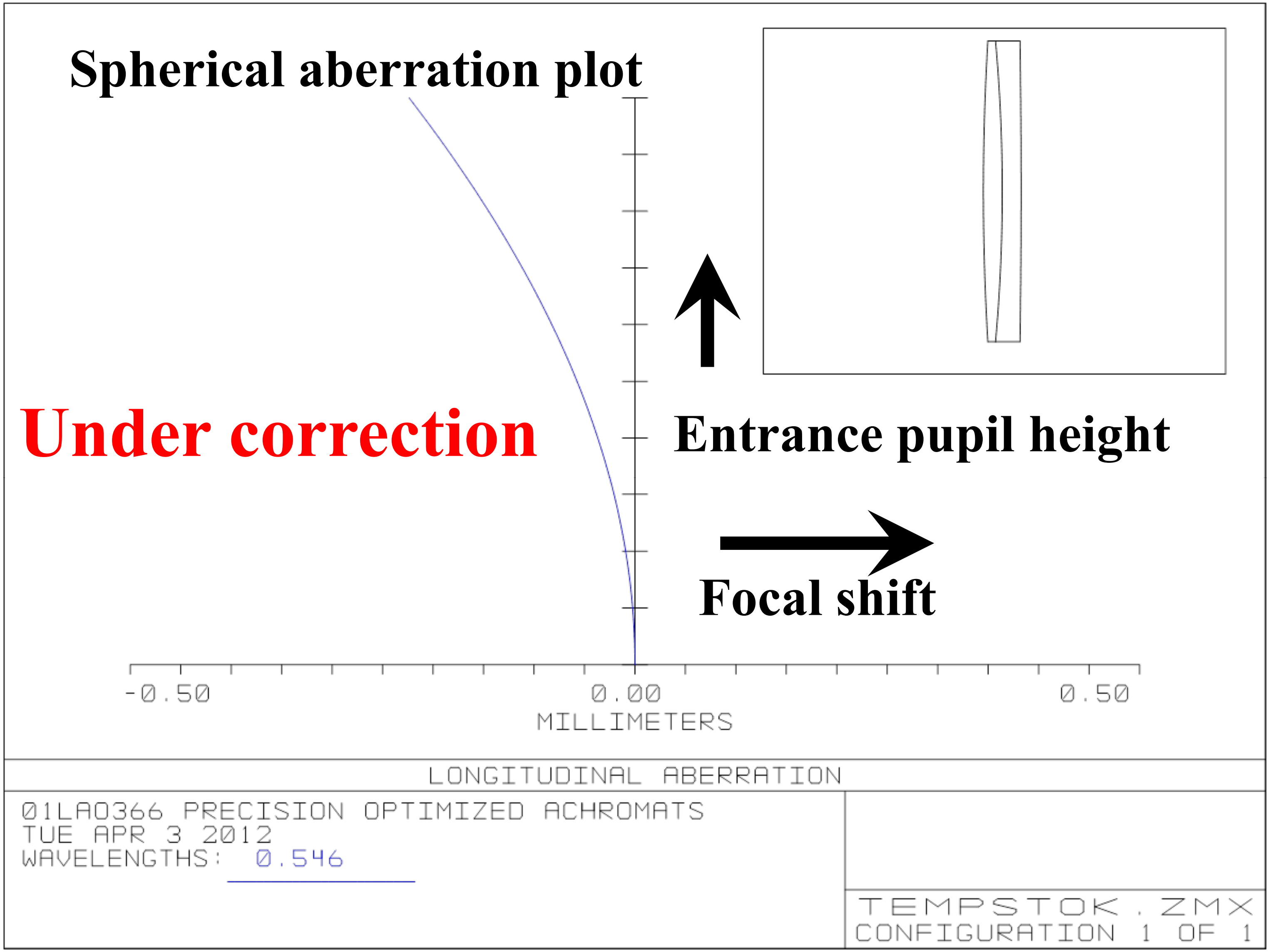

Spherical aberration plot
Under correction
Entrance pupil height
Focal shift
-0.50
0.00
0.50
MILLIMETERS
LONGITUDINAL ABERRATION
01LAO366 PRECISION OPTIMIZED ACHROMATS
TUE APR 3 2012
WAVELENGTHS: 0.546
TEMPSTOK.ZMX
CONFIGURATION 1 OF 1

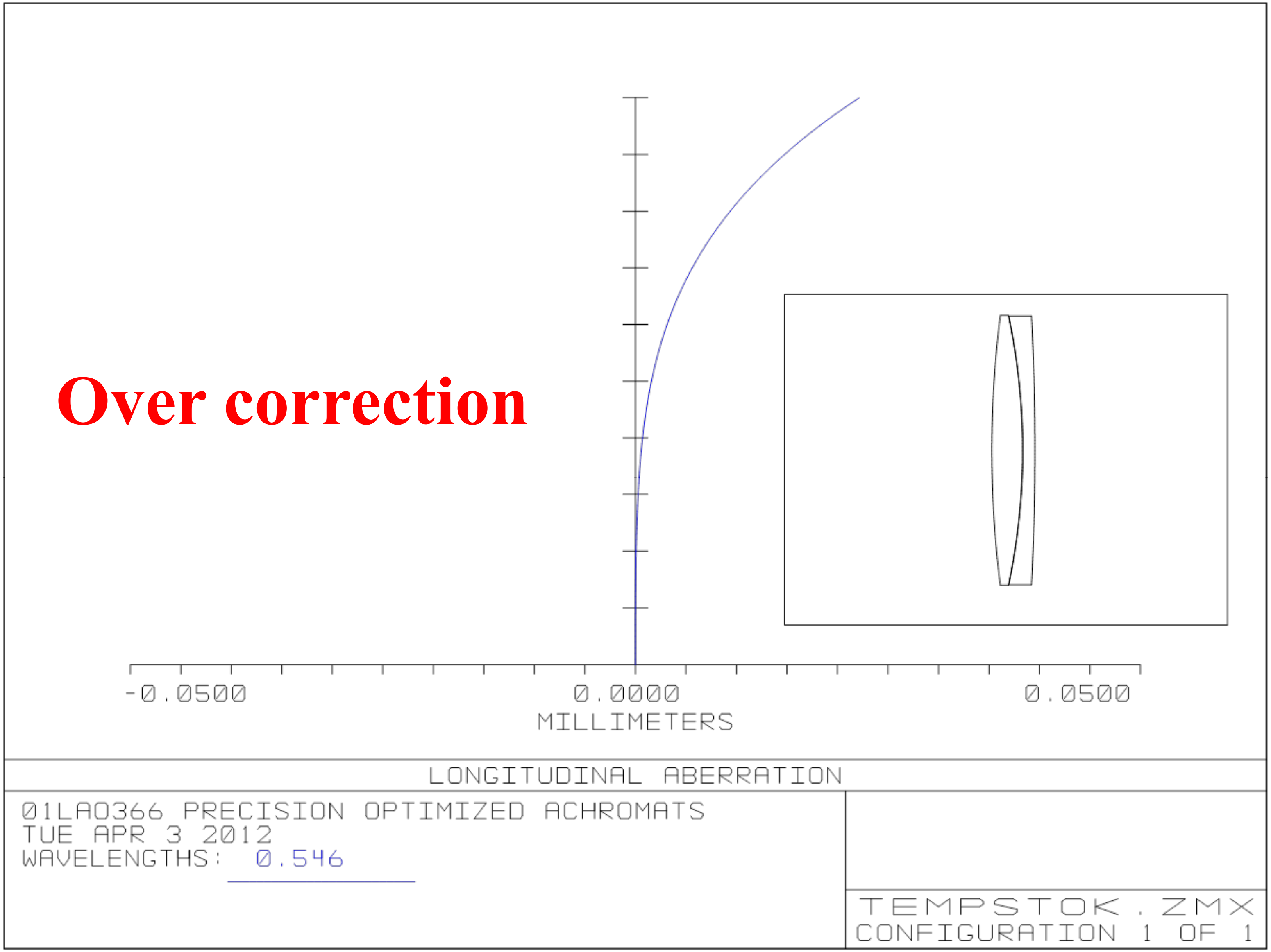
Over correction
-0.0500
0.0000
0.0500
MILLIMETERS
LONGITUDINAL ABERRATION
01LA0366 PRECISION OPTIMIZED ACHROMATS
TUE APR 3 2012
WAVELENGTHS: 0.546
TEMPSTOK.ZMX
CONFIGURATION 1 OF 1

Under correction

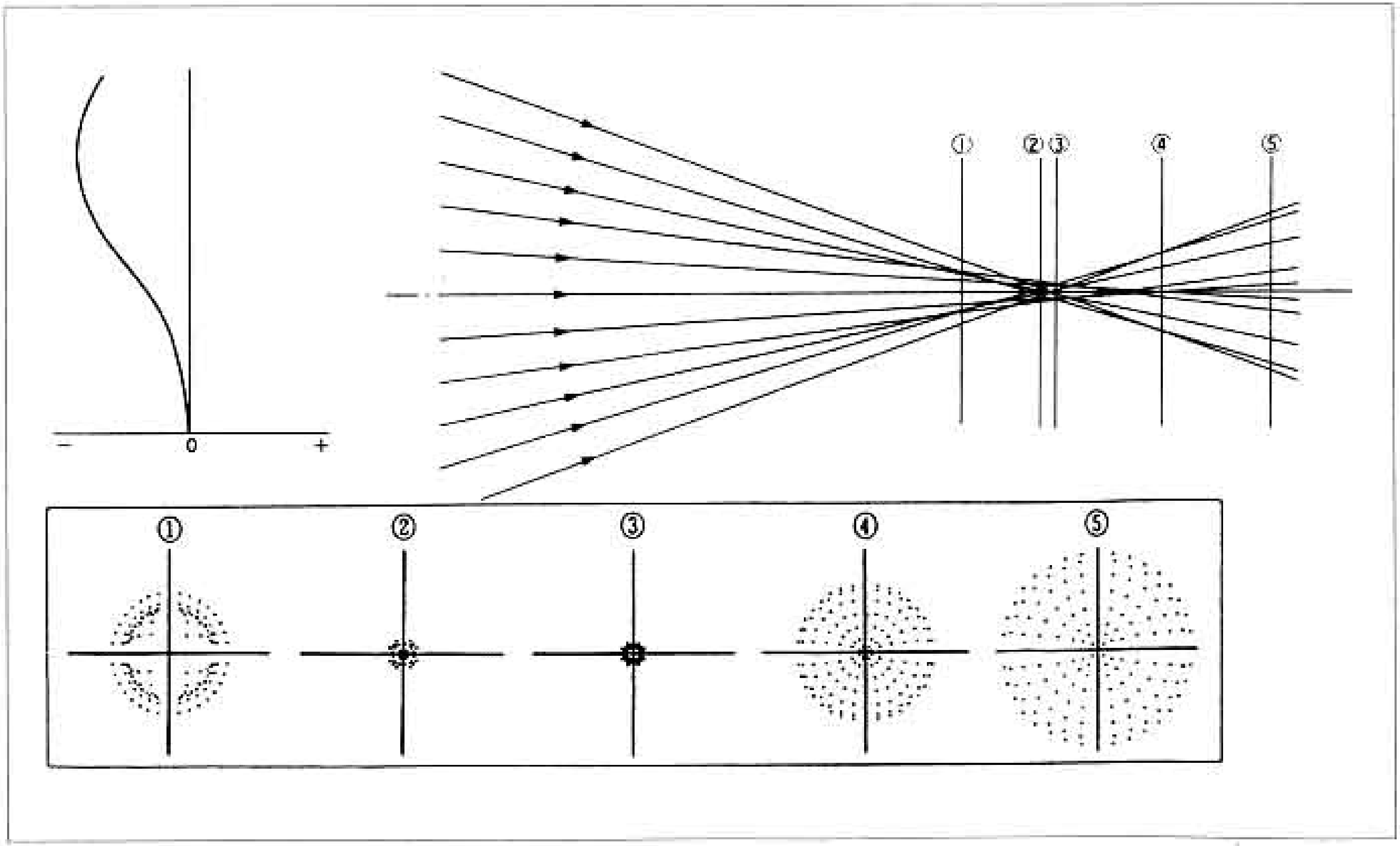

Full correction

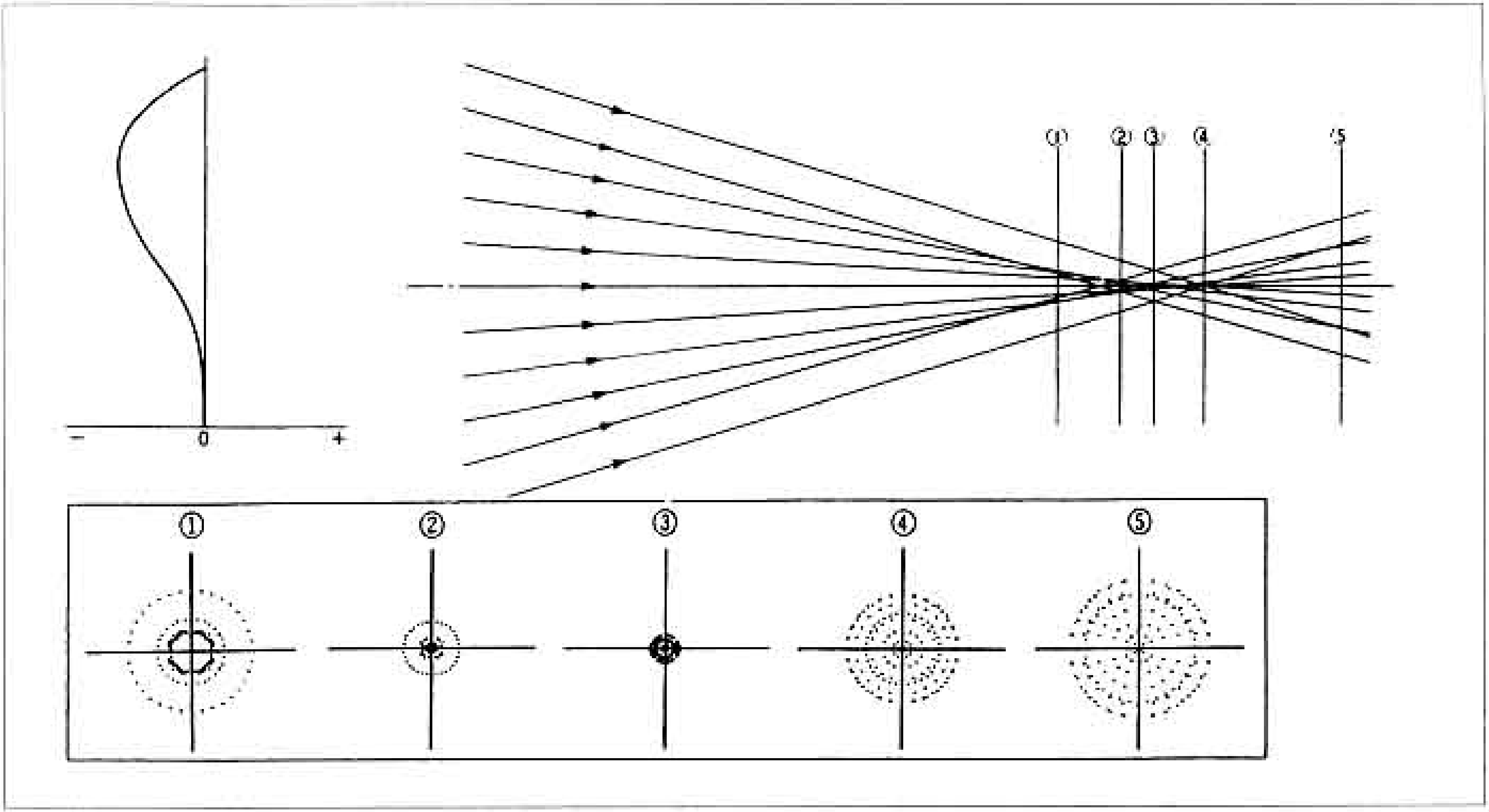

Over correction

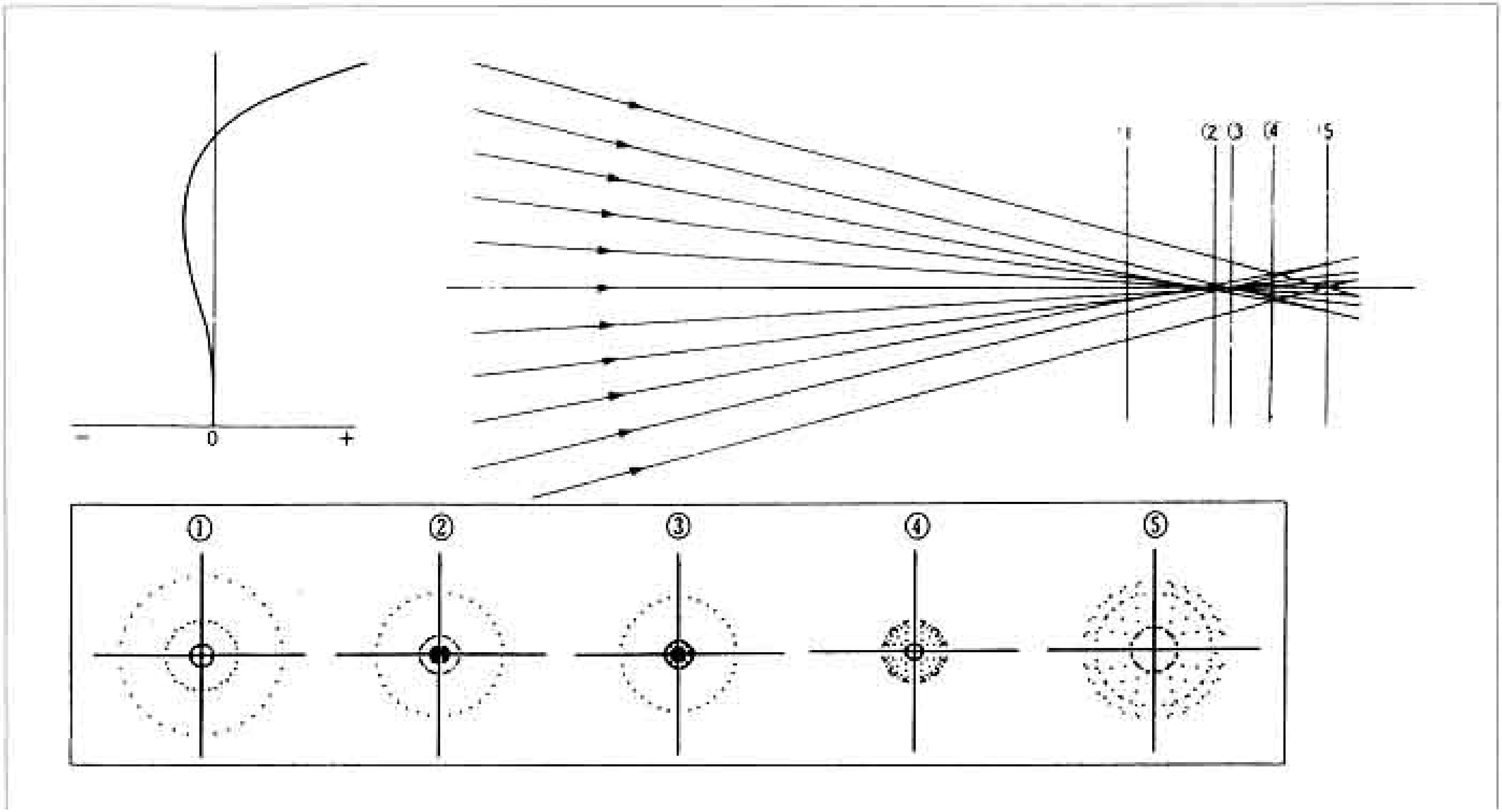

Chromatic aberration

Wave length dependence of refractive index

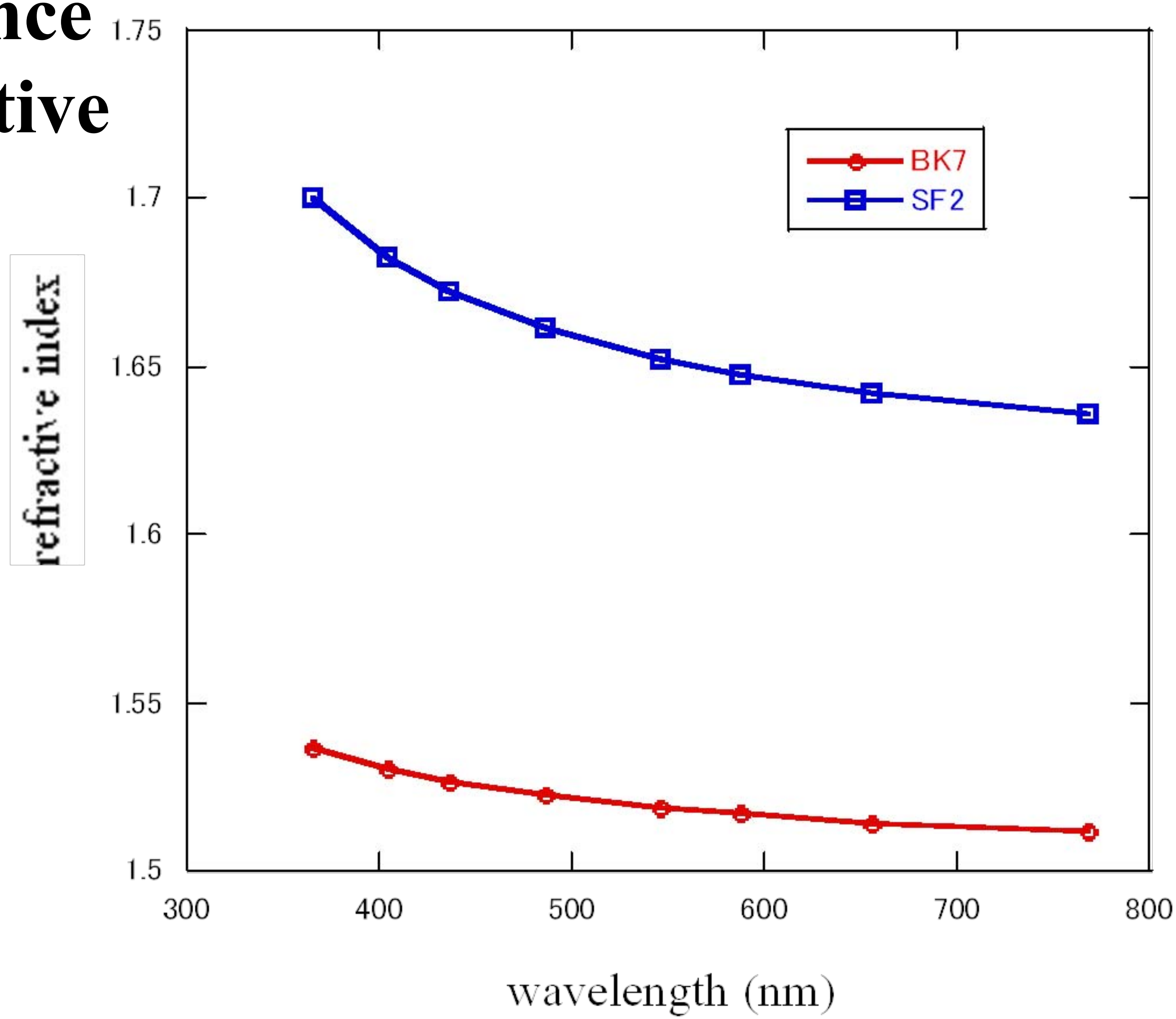

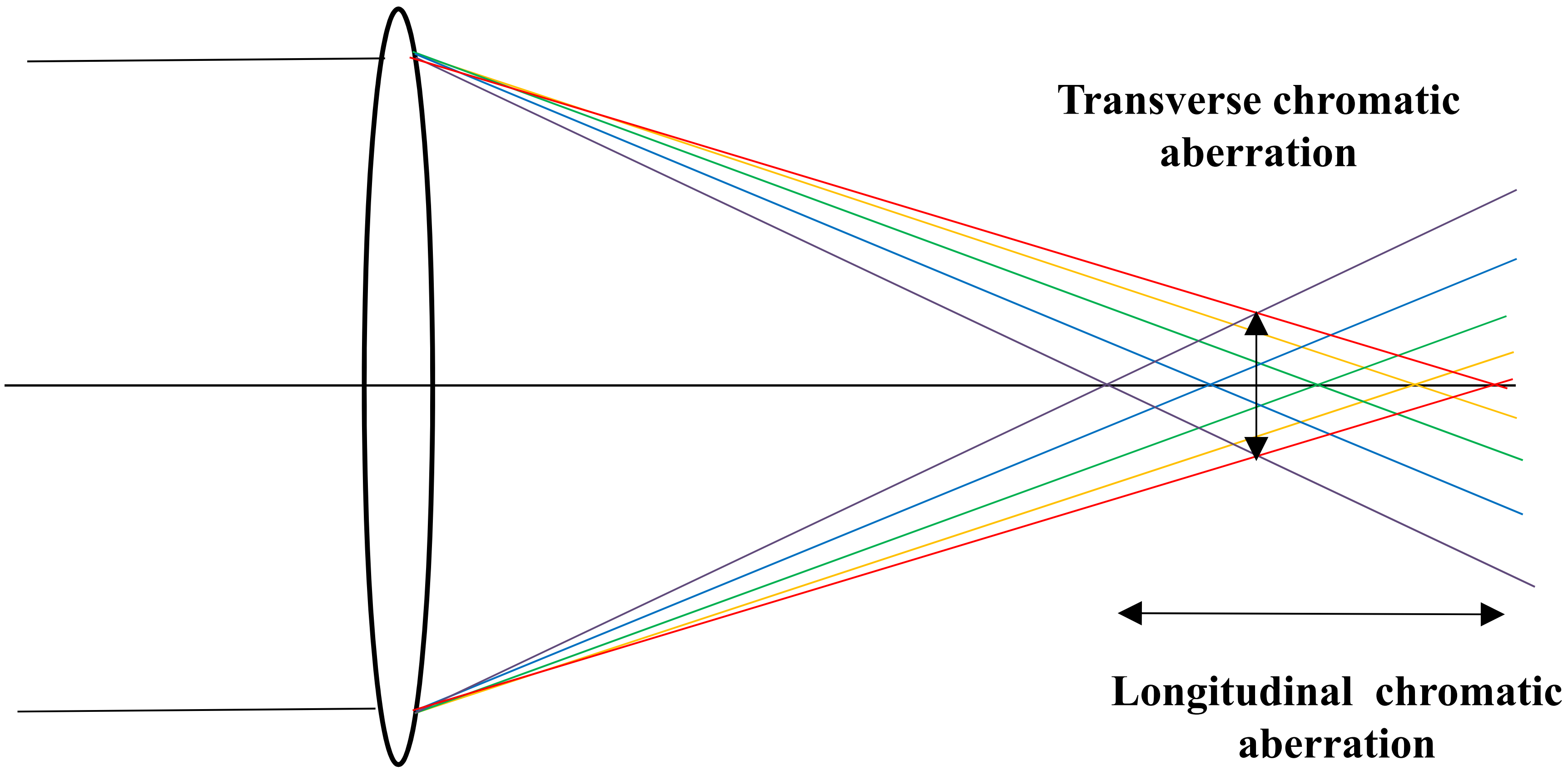
Transverse chromatic aberration
Longitudinal chromatic aberration

Concept of achromatic lens

Focusing lens +dispersion

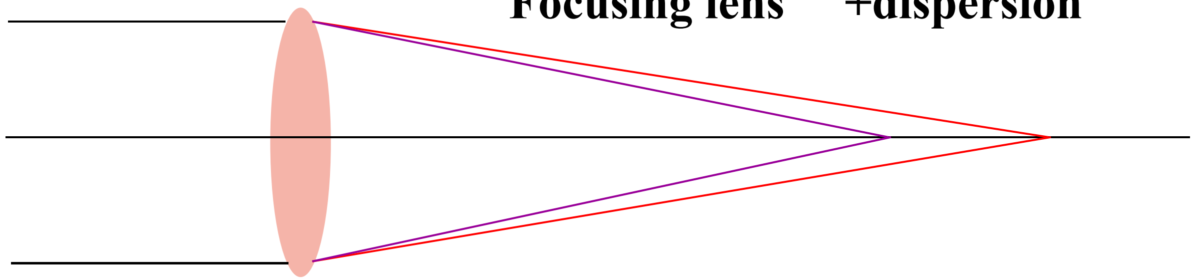

Defocusing lens -dispersion

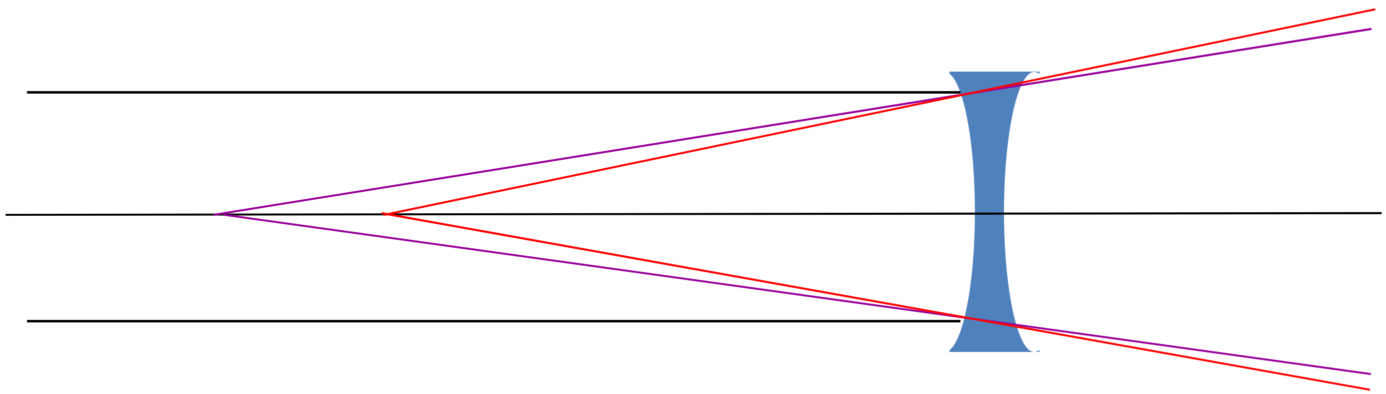

Certain combination of focusing and defocusing lens can cancel focal shift

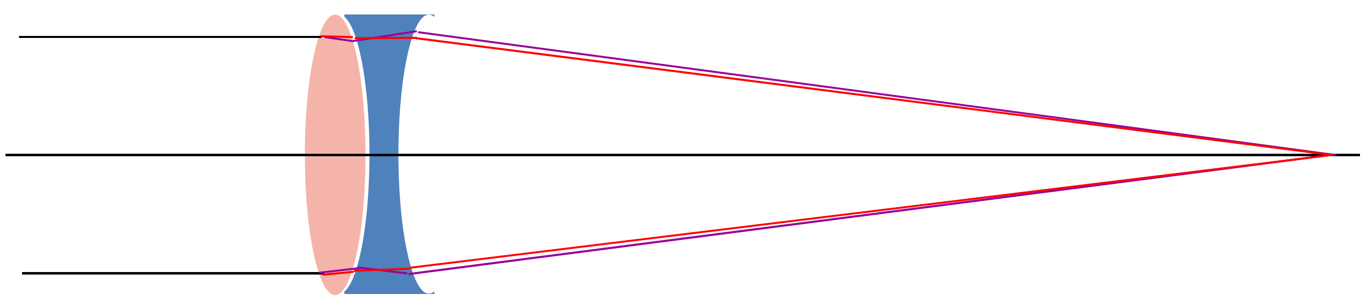

Chromatic aberration plot

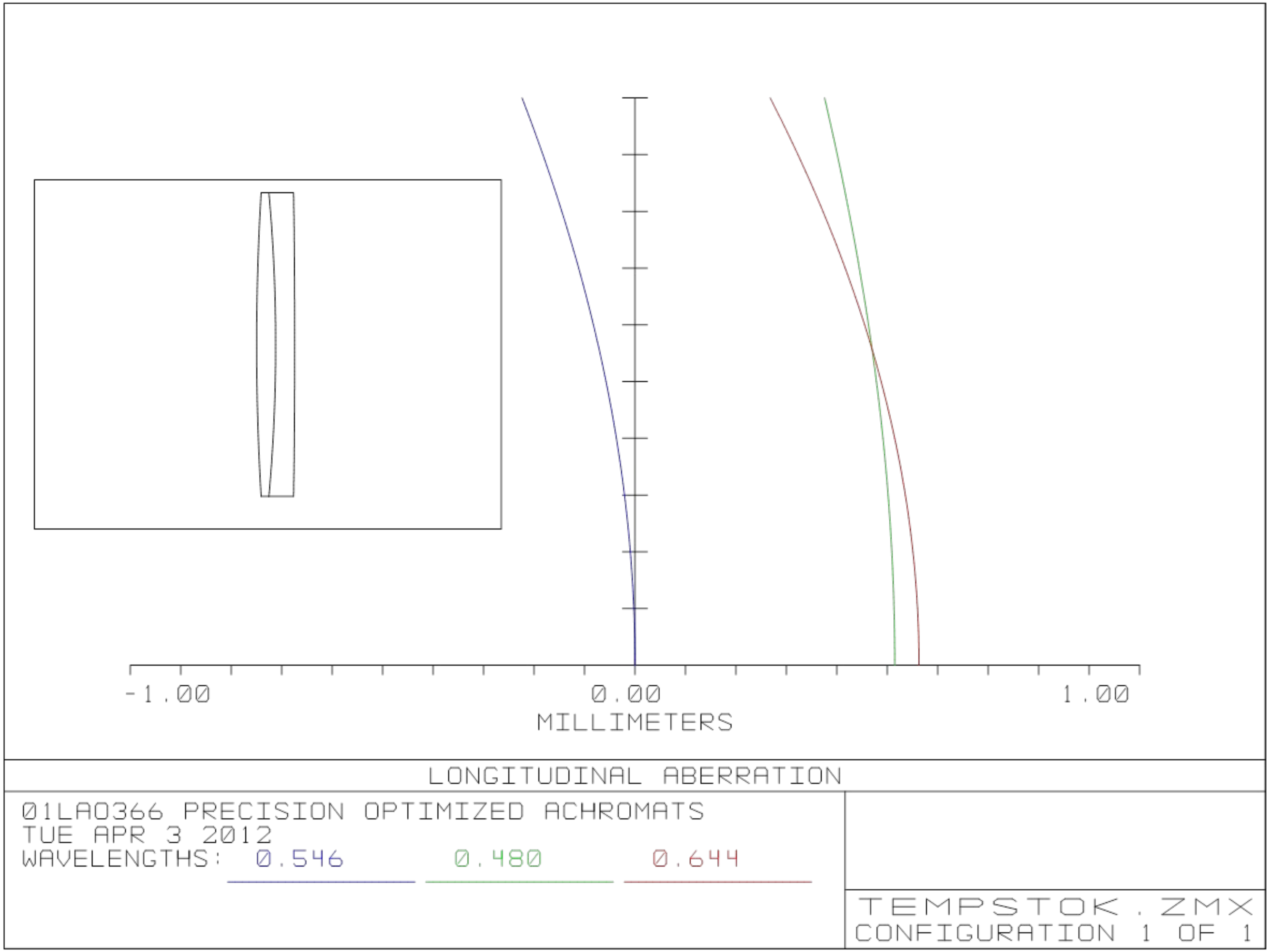

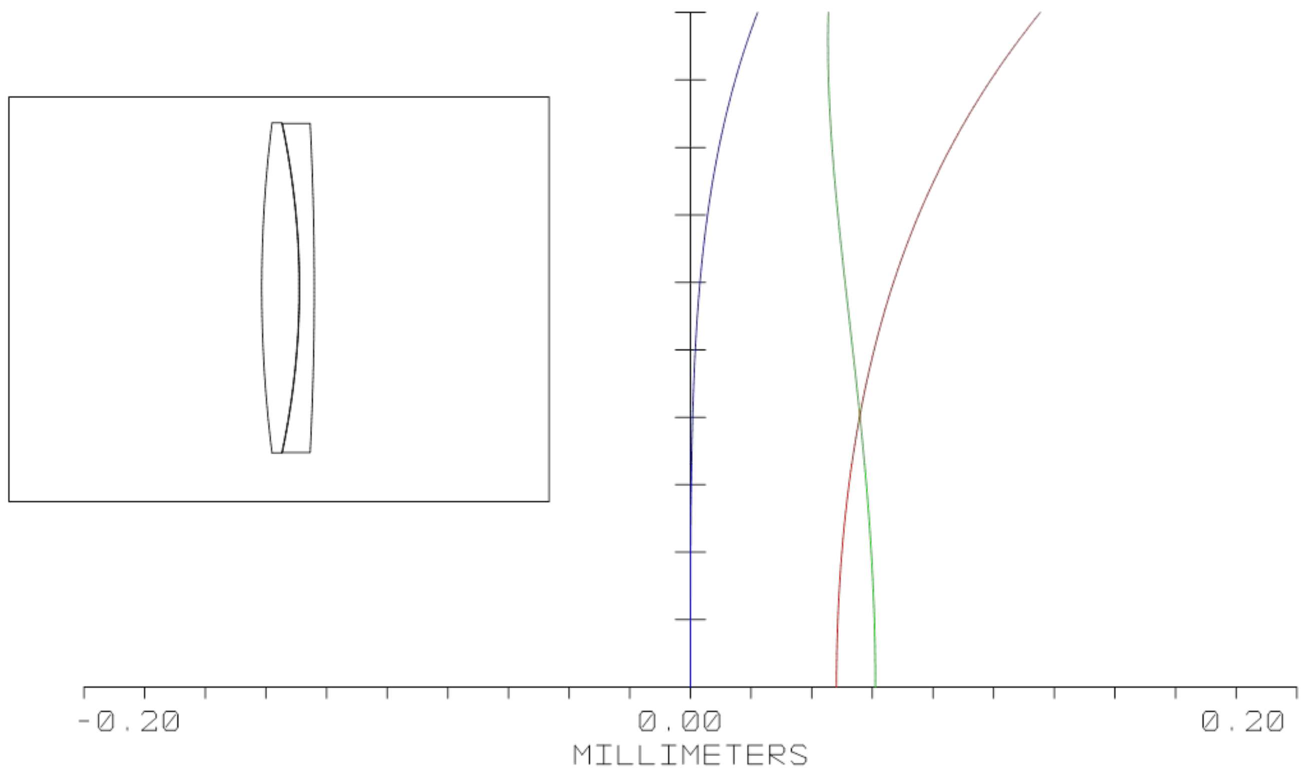

LONGITUDINAL ABERRATION

01LA0366 PRECISION OPTIMIZED ACHROMATS
TUE APR 3 2012
WAVELENGTHS: 0.546 0.644 0.480

TEMPSTOK.ZMX
CONFIGURATION 1 OF 1

Astigmatism
due to
troidal focusing power

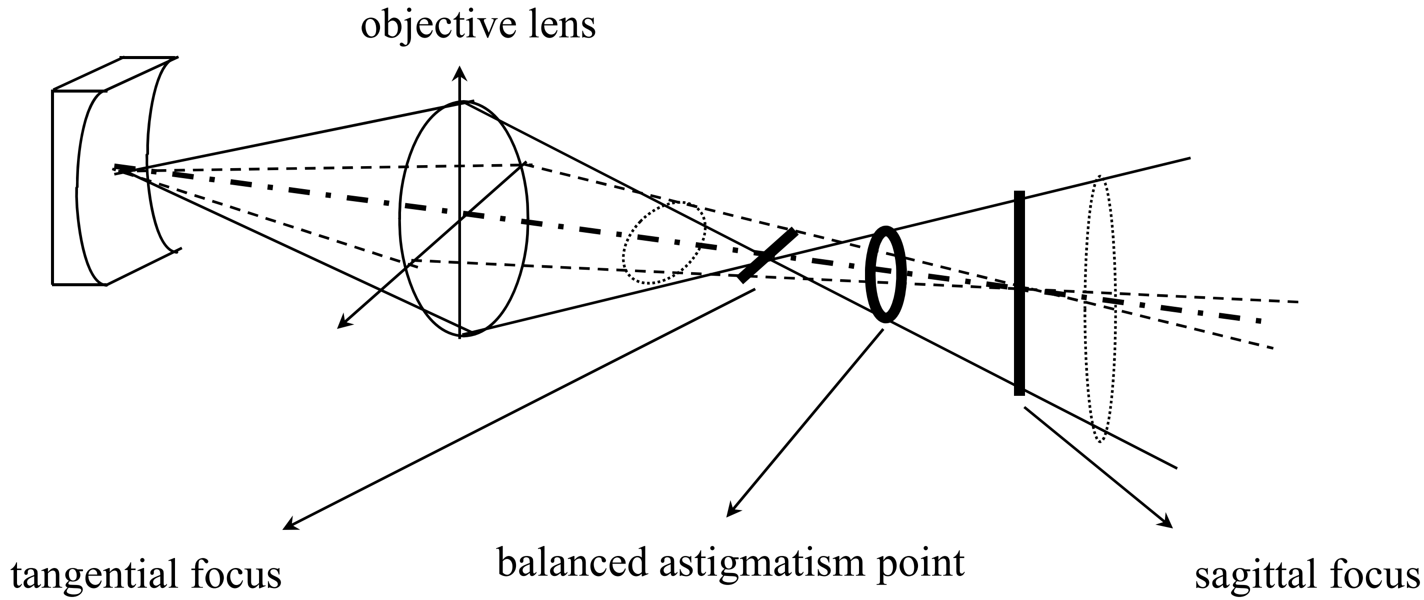
objective lens
tangential focus
balanced astigmatism point
sagittal focus

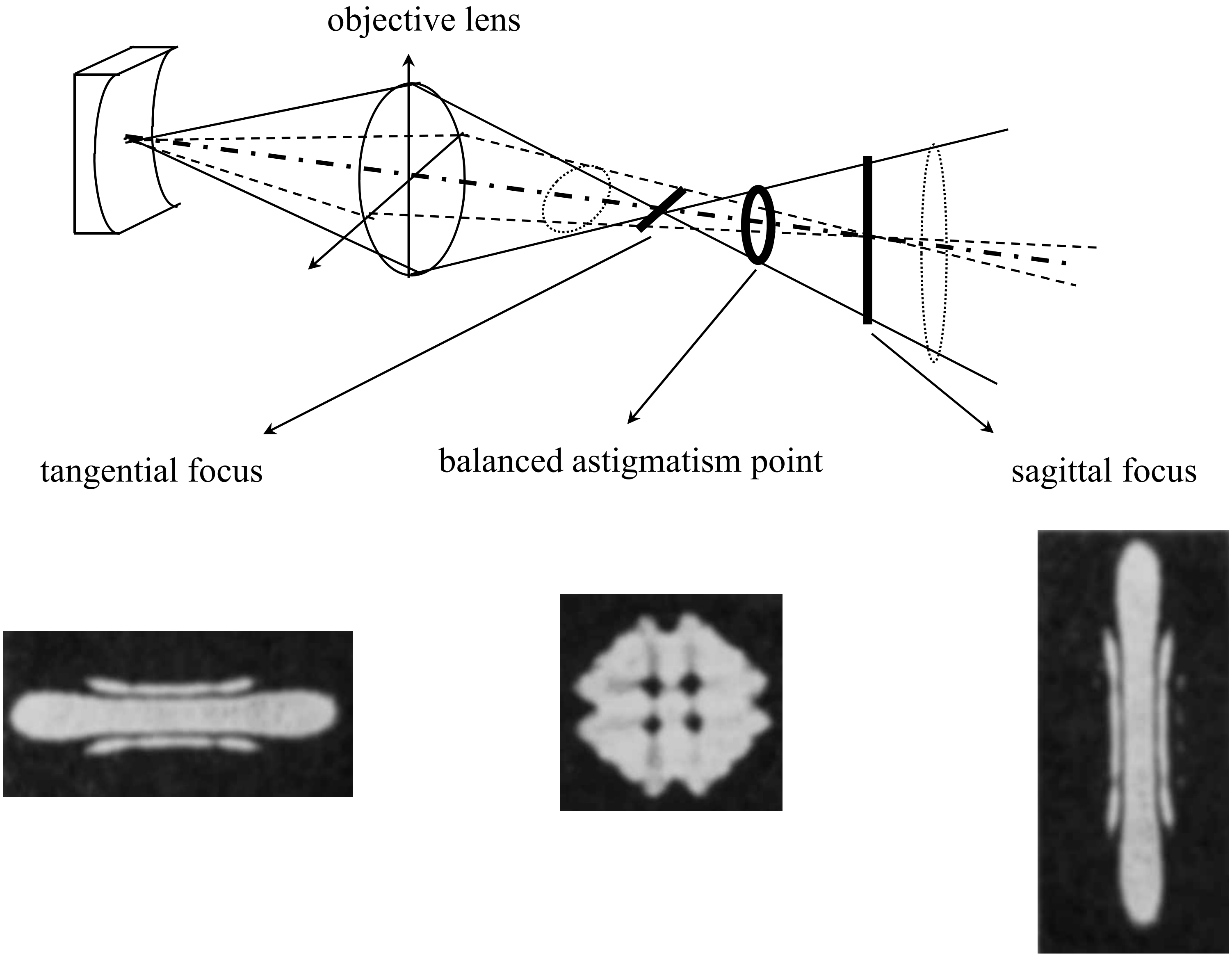
objective lens
tangential focus
balanced astigmatism point
sagittal focus

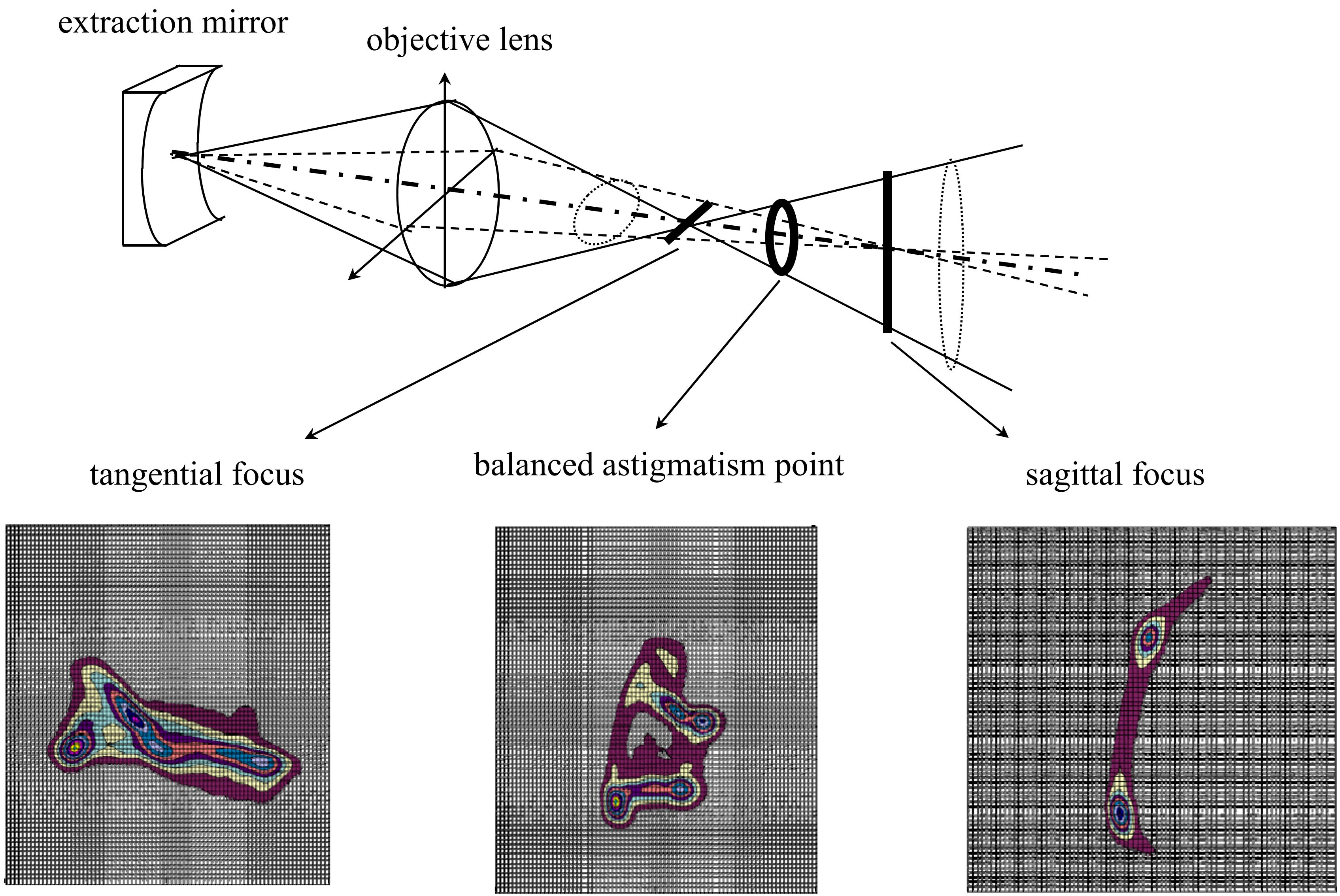
extraction mirror
objective lens
tangential focus
balanced astigmatism point
sagittal focus

Comma
due to
tilted incidence

Input ray with incident angle of ω

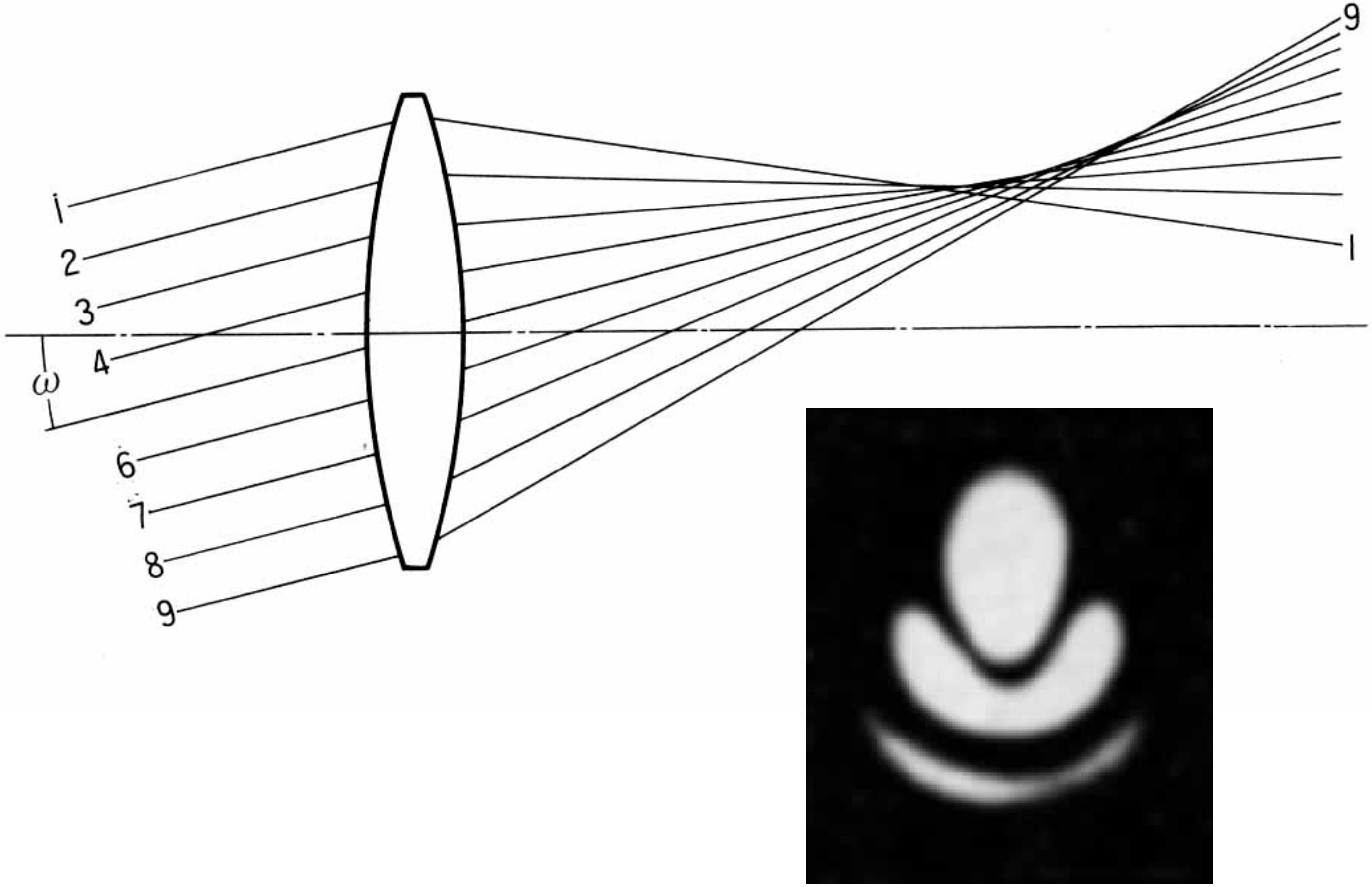

Alignment error (tilt) of lens also produce comma

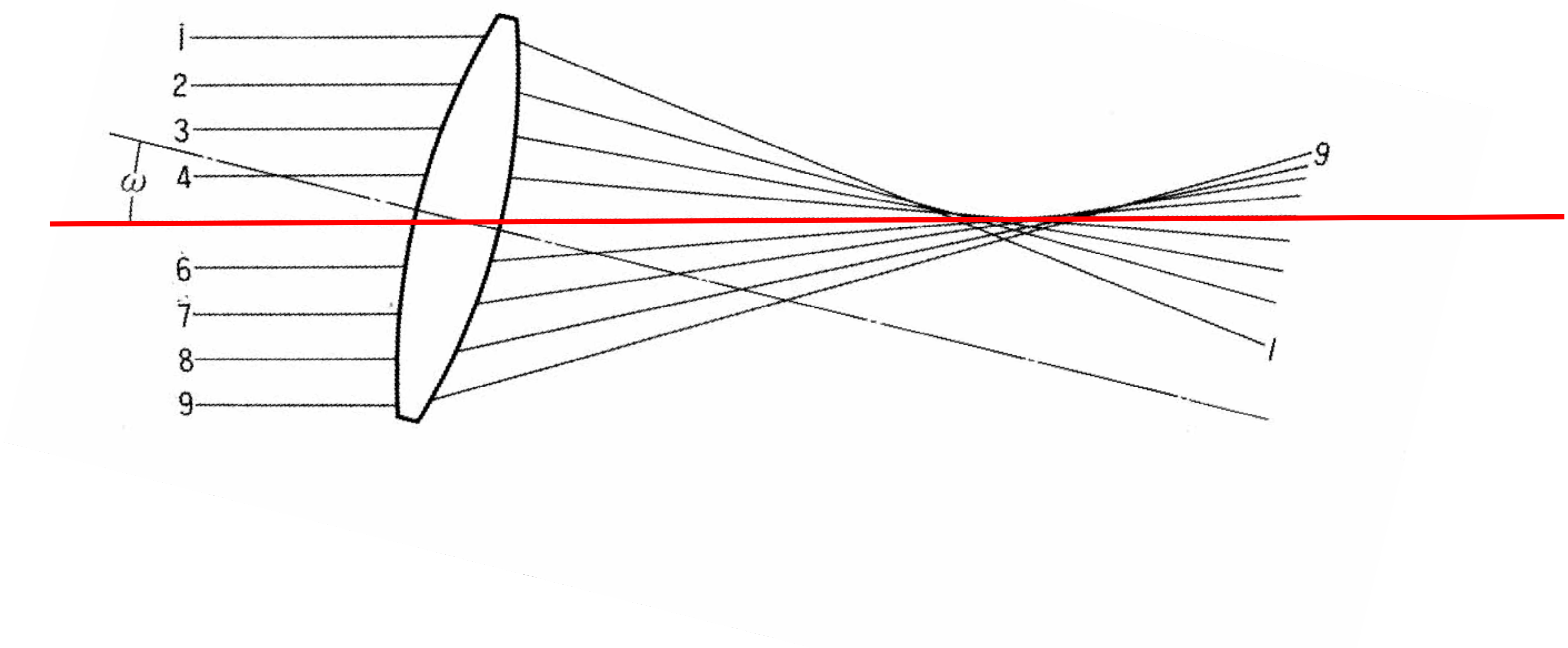

Alignment error (tilt) of lens also produce comma

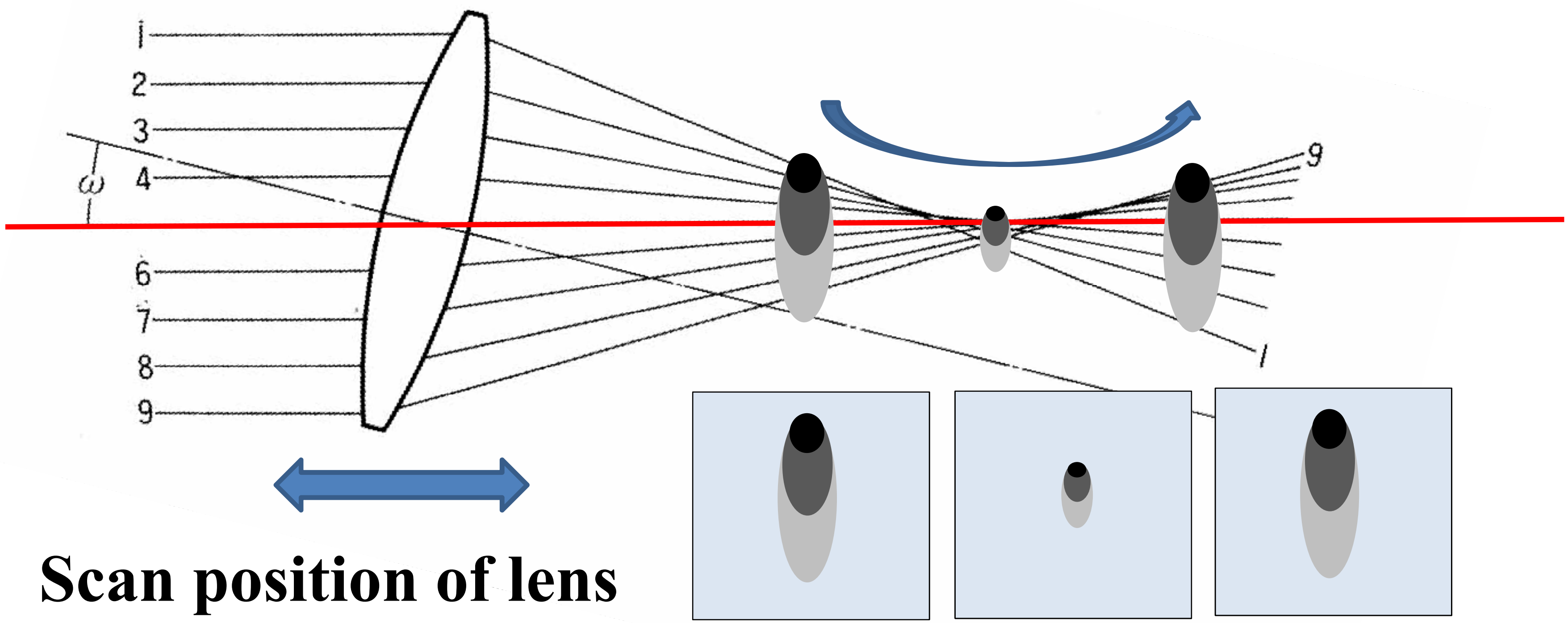

Scan position of lens

Lens has often has a wedge component!

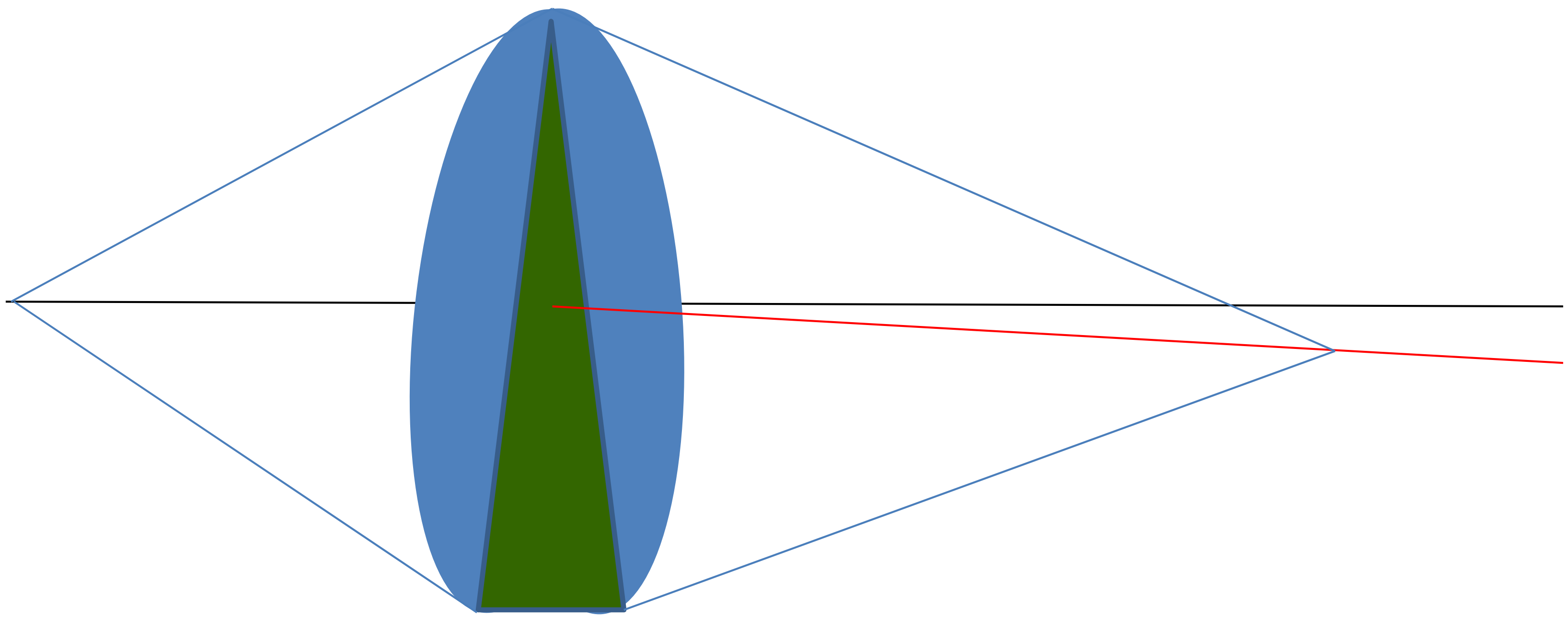

Scan position of lens

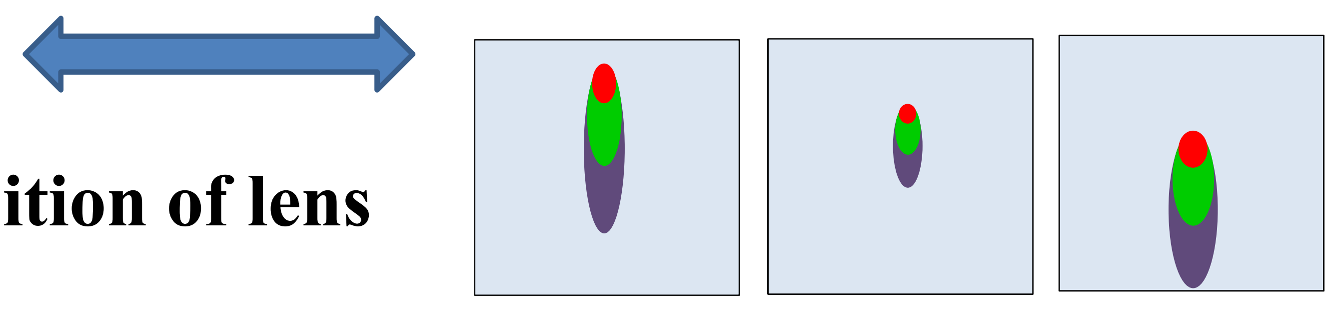

Wave optics of focusing system

Diffraction

Diffraction geometry

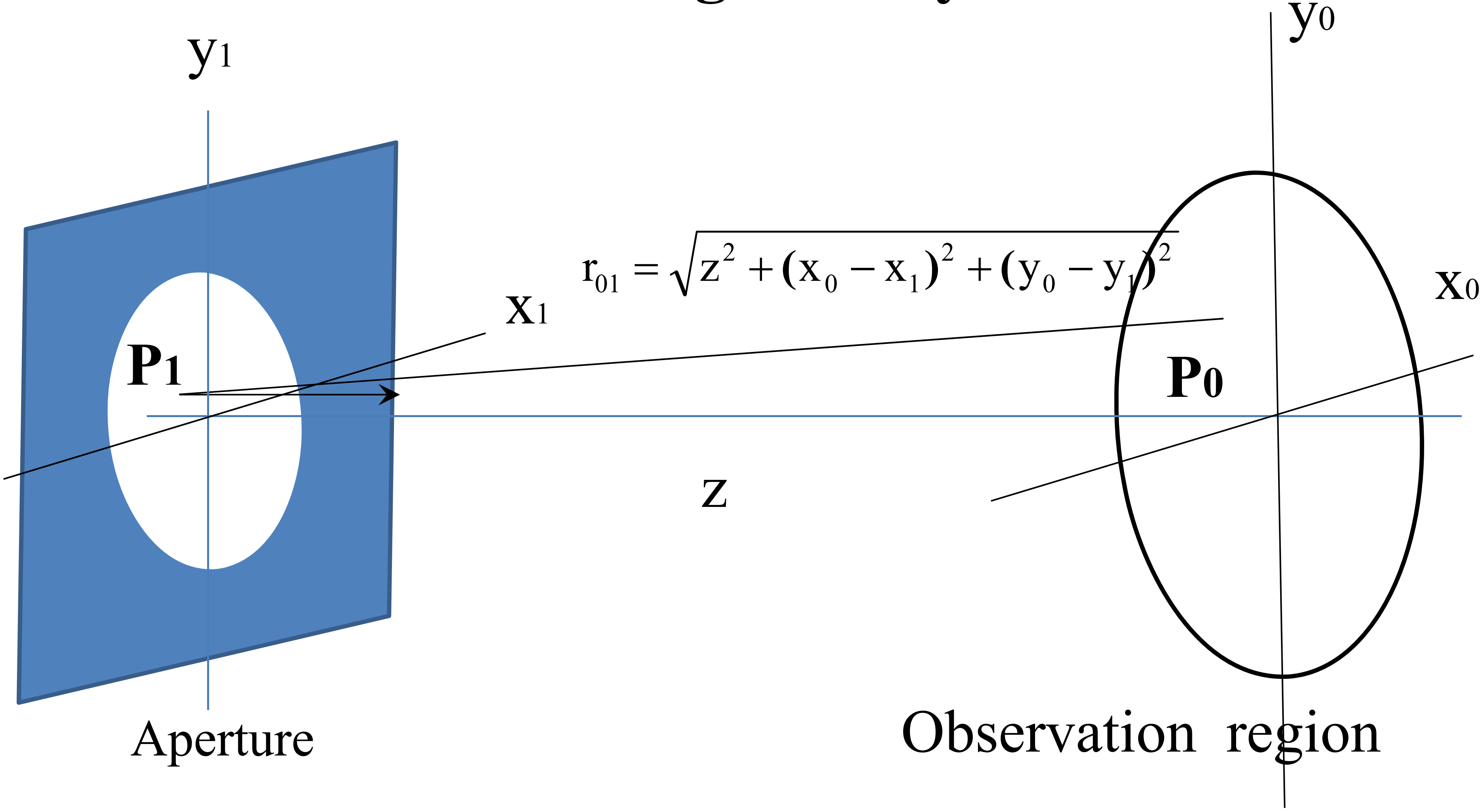

$$\mathbf{U}(p_0) = \iint_{\Sigma} \mathbf{h}(P_0, P_1)\, \mathbf{U}(P_1)\, dx_1 dy_1$$

$$\mathbf{h}(P_0, P_1) = \frac{1}{i \cdot \lambda} \frac{\exp(i \cdot k \cdot r_{01})}{r_{01}} \cos(\vec{n}, \vec{r}_{01})$$

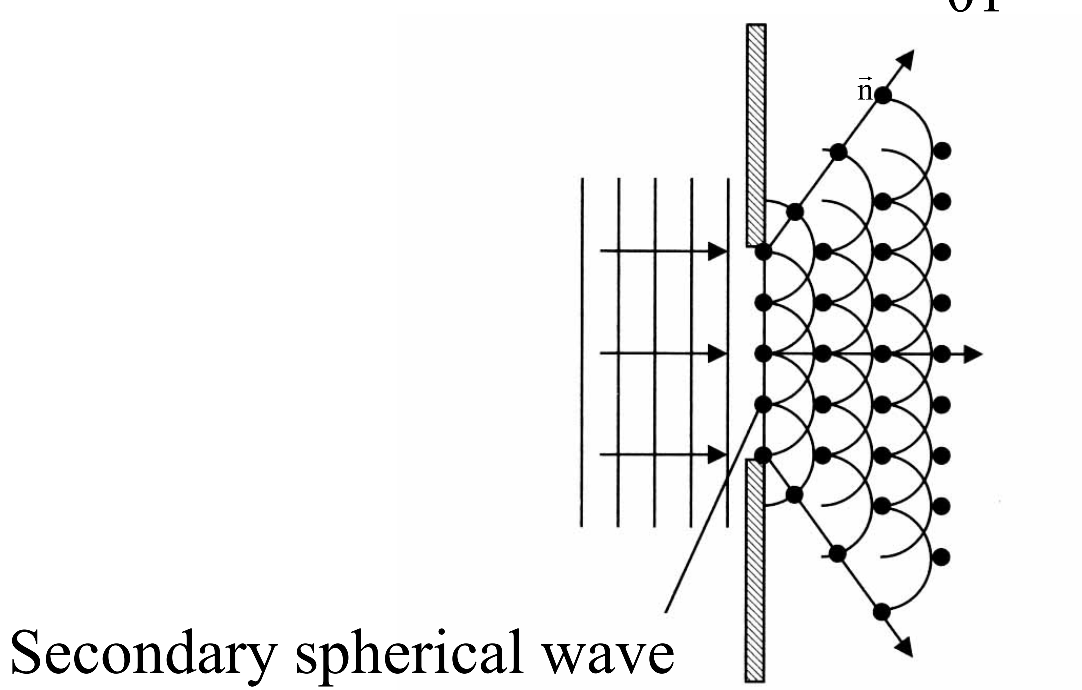

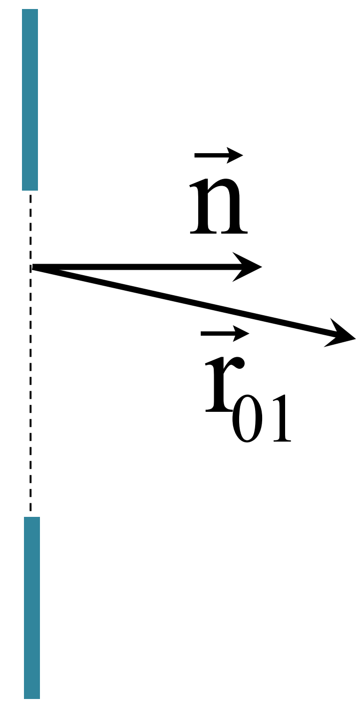

Paraxial approximation

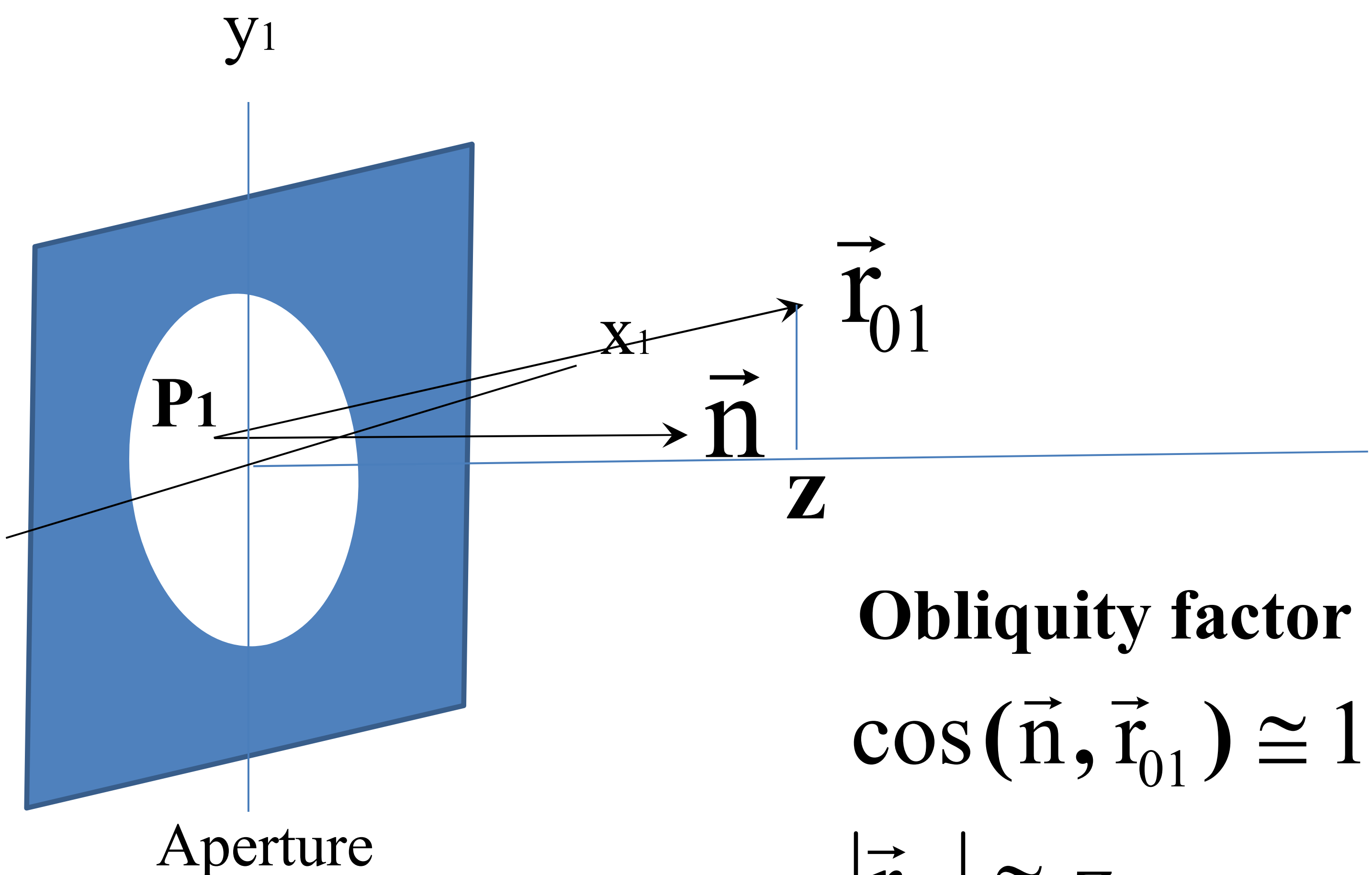

Obliquity factor

$$\cos(\vec{n}, \vec{r}_{01}) \cong 1$$

$$\left|\vec{r}_{01}\right| \cong z$$

The Fresnel approximation

$$r_{01} = \sqrt{z^2 + (x_0 - x_1)^2 + (y_0 - y_1)^2}$$

$$= z\sqrt{1 + \left(\frac{x_0 - x_1}{z}\right)^2 + \left(\frac{y_0 - y_1}{z}\right)^2}$$

$$\cong z\left[1 + \frac{1}{2}\left(\frac{x_0 - x_1}{z}\right)^2 + \frac{1}{2}\left(\frac{y_0 - y_1}{z}\right)^2\right]$$

Spherical $\Rightarrow$ Quadratic phase factor

$$\mathbf{h}(x_0, y_0 : x_1, y_1) = \frac{\exp(ikz)}{i\lambda z} \boxed{\exp\left[\frac{ik}{2z}\left[(x_0 - x_1)^2 + (y_0 - y_1)^2\right]\right]}$$

Quadratic wave

$$\boxed{\begin{aligned} &= \frac{\exp(ikz)}{i\lambda z} \exp\left[\frac{ik}{2z}\left[x_0^{\,2} + y_0^{\,2}\right]\right] \exp\left[\frac{ik}{2z}\left[x_1^{\,2} + y_1^{\,2}\right]\right] \\ &\quad \times \exp\left[\frac{ik}{2z}\left[x_0 x_1 + y_0 y_1\right]\right] \end{aligned}}$$

Fresnel diffraction

The Fraunhofer approximation

Very long z

$$\frac{ik}{2z}\left[x_1^{\,2}+y_1^{\,2}\right] << 1$$

$$\exp\left[\frac{ik}{2z}\left[x_1^{\,2}+y_1^{\,2}\right]\right] \cong 1$$

$$\mathbf{h}(x_0, y_0 : x_1, y_1) = \exp\frac{\exp(ikz)}{i\lambda z}\exp\left[\frac{ik}{2z}\left[x_0^{\,2}+y_0^{\,2}\right]\right]$$

Plane wave

$$\times \boxed{\exp\left[\frac{ik}{2z}\left[x_0x_1+y_0y_1\right]\right]}$$

Fraunhofer diffraction

Diffraction by slit   height 10mm

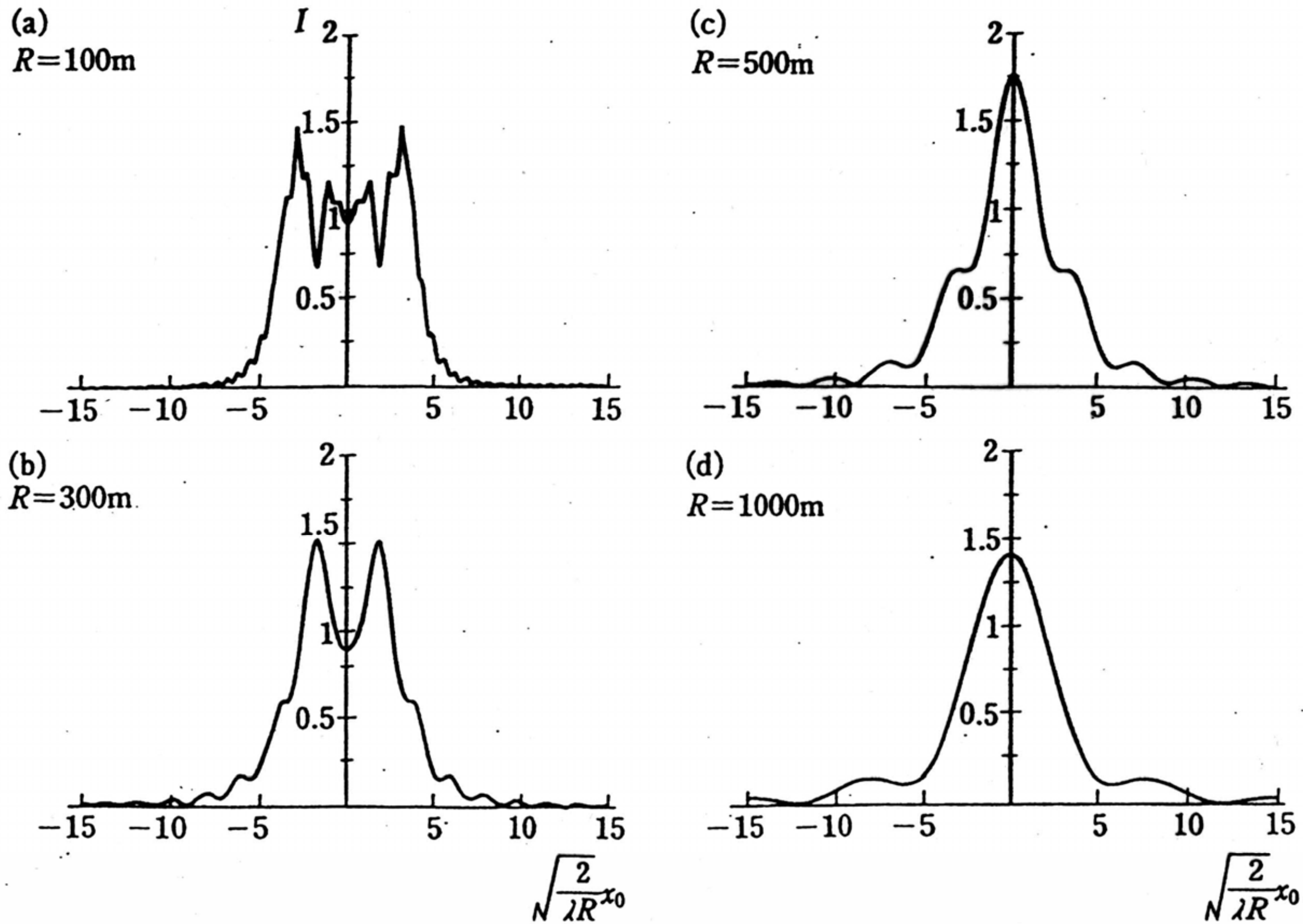

Propagation of light in free space by few 10m

Fresnel diffraction!

Fraunhofer diffraction: few km

Pupil with Lens

Pupil with Lens

Paraxial Lens transfer function t_l

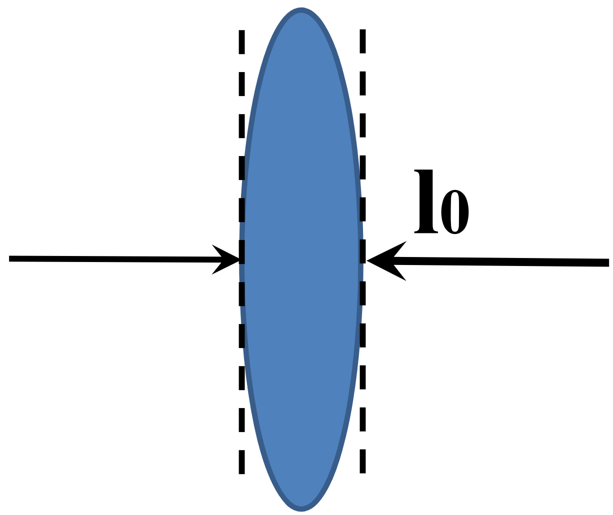

$$\mathbf{t}_l(x, y) = \exp(ikl_0)\exp[ik(n-1)l_0]\exp\left(-i\frac{k}{2f}\left(x^2+y^2\right)\right)$$

Physical meaning of paraxial lens transfer function

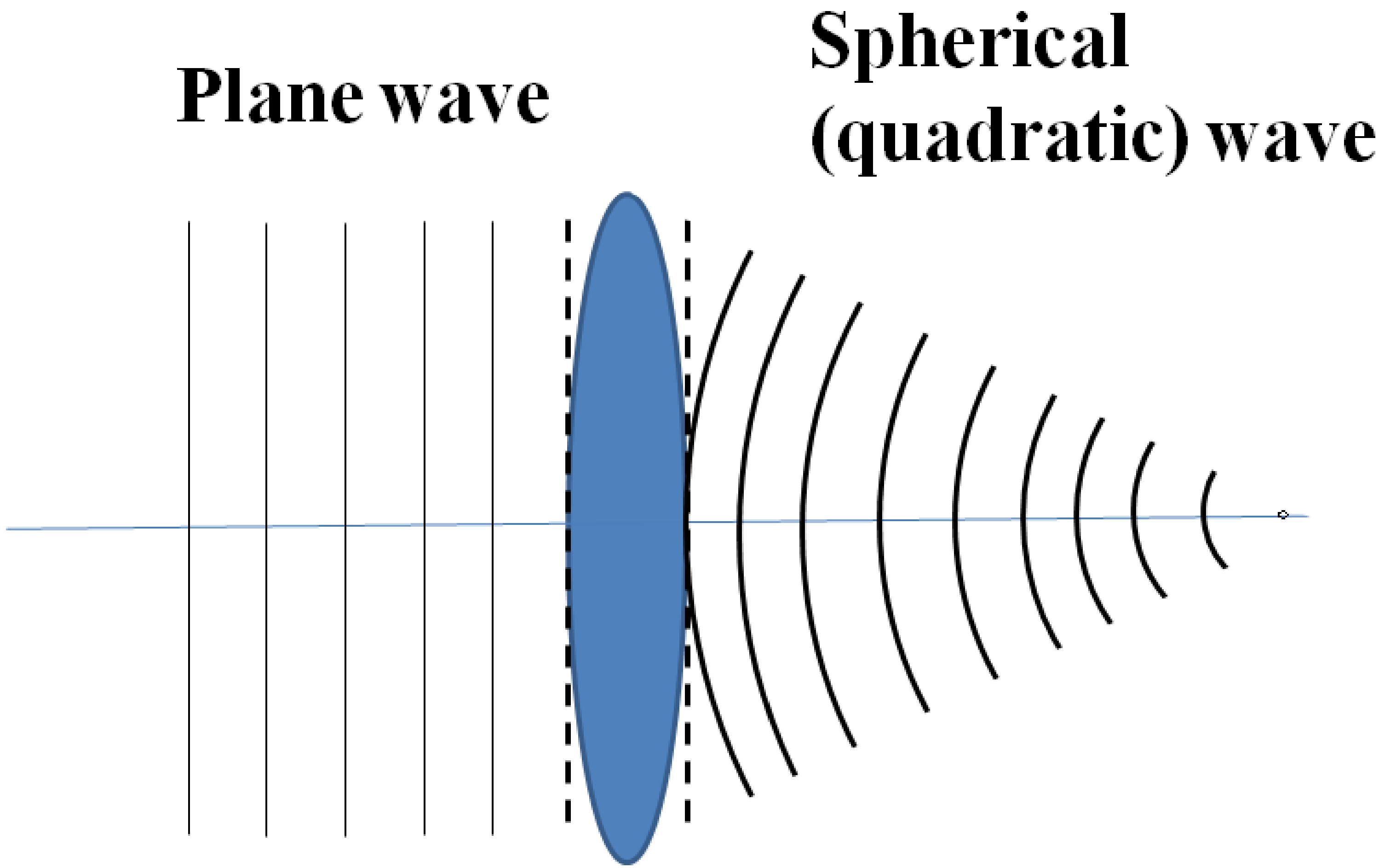

Diffraction with lens

Step 1
Paraxial lens transform of input U_l

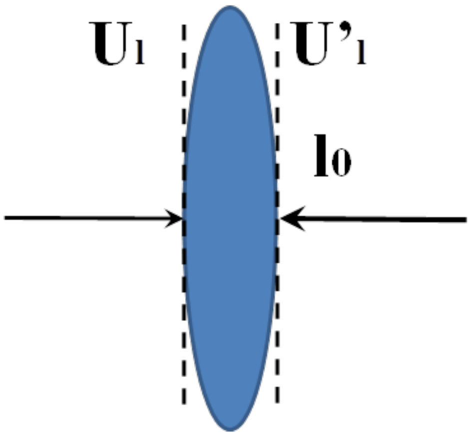

Step 1
Fresnel Transform of U'_l

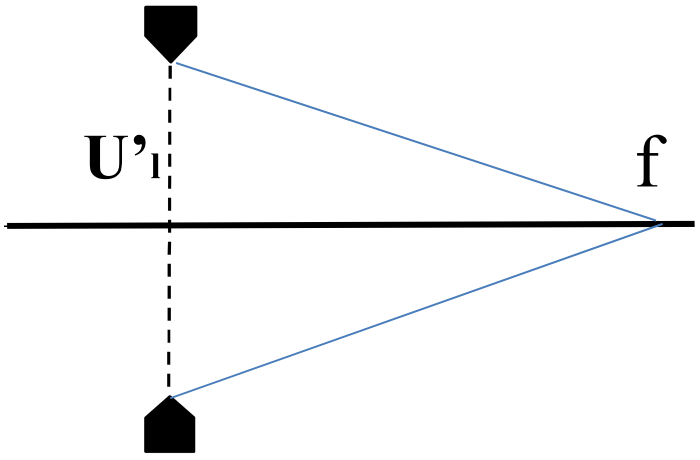

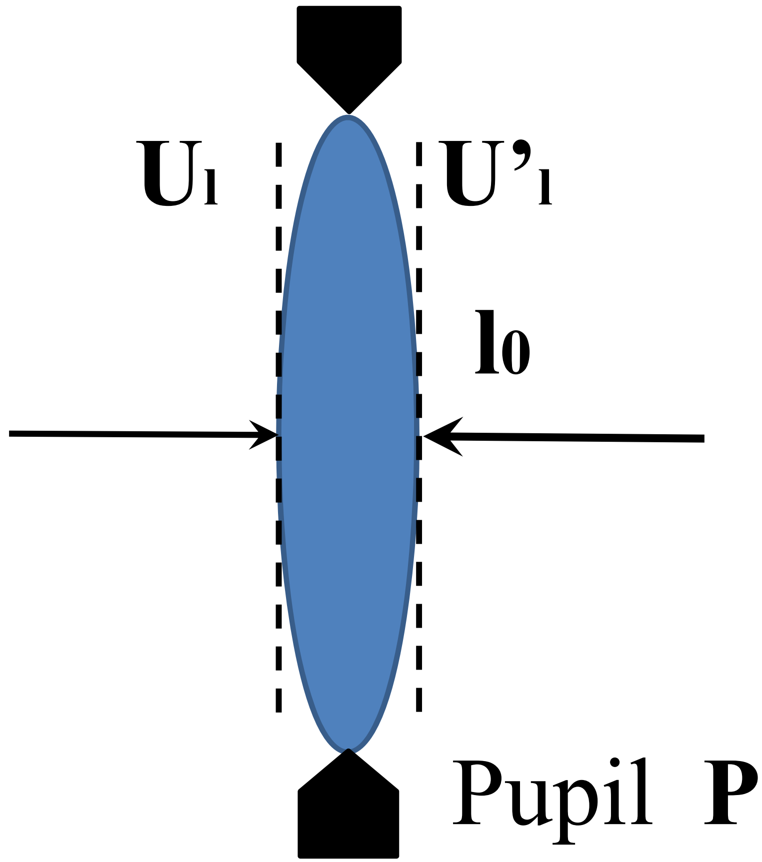

$$\mathbf{U}'_1(x,y) = \mathbf{P}(x,y)\,t_1(x,y)\,\mathbf{U}_1(x,y)$$

$$= \mathbf{P}(x,y)\,\mathbf{U}_1(x,y)\exp\left[-i\frac{k}{2f}\left(x^2+y^2\right)\right]$$

$$U_f(x_f, y_f) = \frac{\exp\left[i\frac{k}{2f}\left(x^2{}_f + y^2{}_f\right)\right]}{i\lambda f}$$

$$\times \iint_\Sigma U_1(x,y) \exp\left(-i\frac{k}{2f}\left(x^2+y^2\right)\right) \boxed{\exp\left(i\frac{k}{2f}\left(x^2+y^2\right)\right)} \exp\left[\frac{ik}{2f}\left[xx_f + yy_f\right]\right] dxdy$$

Lens transfer function

Quadratic wave

As the result;

$$\mathbf{U}_f(\mathbf{x}_f, \mathbf{y}_f) = \frac{\exp\left[i\frac{k}{2f}\left(x^2{}_f + y^2{}_f\right)\right]}{i\lambda f}$$

Plane wave

$$\times \iint \mathbf{U}_1(x,y)\mathbf{P}(x,y) \boxed{\exp\left[\frac{ik}{2f}\left[xx_f + yy_f\right]\right]} dxdy$$

$$U_f(x_f, y_f) = \frac{\exp\left[i\frac{k}{2f}\left(x^2{}_f + y^2{}_f\right)\right]}{i\lambda f}$$

$$\times \iint_\Sigma U_1(x,y) \exp\left(-i\frac{k}{2f}\left(x^2 + y^2\right)\right) \boxed{\exp\left(i\frac{k}{2f}\left(x^2 + y^2\right)\right)} \exp\left[\frac{ik}{2f}\left[xx_f + yy_f\right]\right] dxdy$$

Lens transfer function

Quadratic wave

As the result;

Fourier transform of pupil function

$$U_f(x_f, y_f) = \frac{\exp\left[i\frac{k}{2f}\left(x^2{}_f \right.\right.}{i\lambda f}$$

Plane wave

$$\times \iint U_1(x,y) P(x,y) \boxed{\exp\left[\frac{ik}{2f}\left[xx_f + yy_f\right]\right]} dxdy$$

Diffraction on image plane

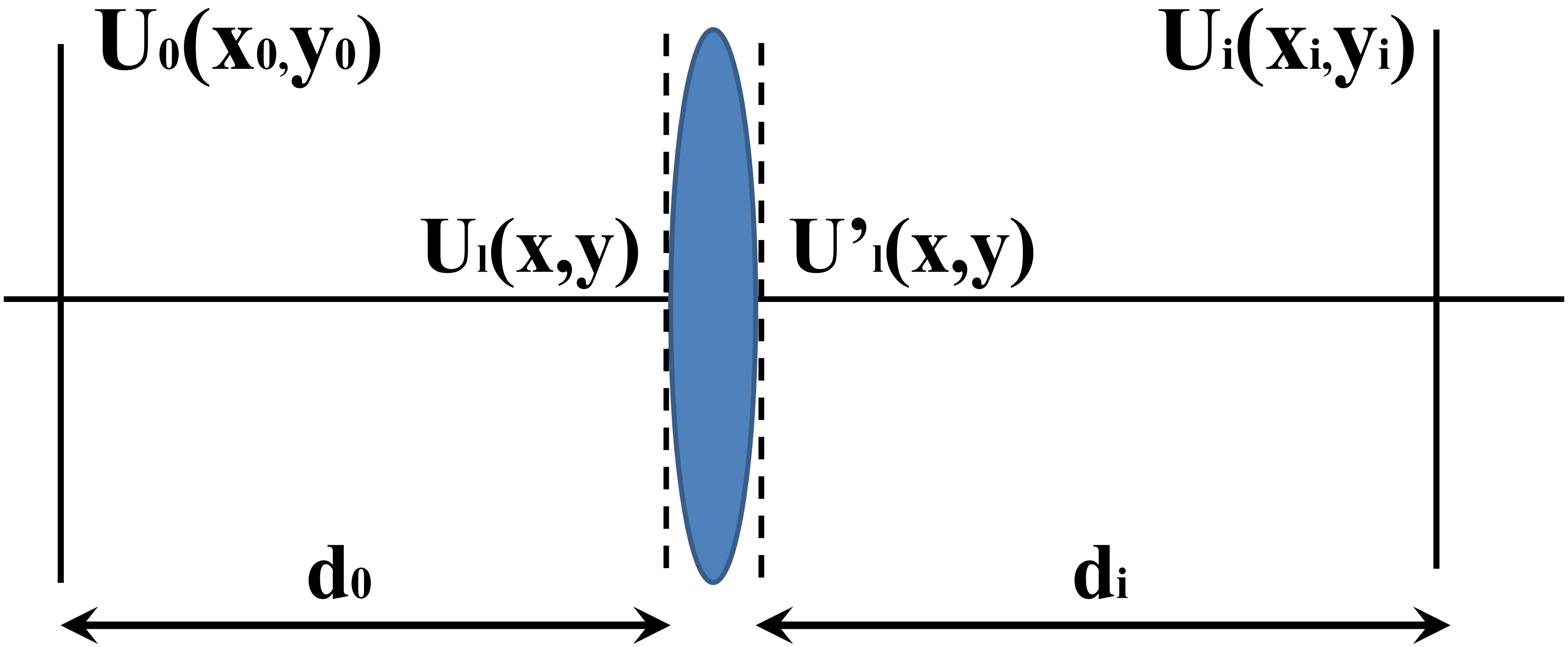

1. $U_0(x_0,y_0) \longrightarrow U_1(x,y)$

Fresnel transform

$$U_1(x,y)=\iint U_0(x_0,y_0)\boxed{\exp\left(i\frac{k}{2d_0}\left(x^2+y^2\right)\right)\exp\left[\frac{ik}{2d_0}\left[x_0x+y_0y\right]\right]dx_0dy_0}$$

2. $U_1(x,y) \longrightarrow U'_1(x,y)$

Lens transform

$$U'_1(x,y)=t(x,y)U_1(x,y)$$

$$=\iint U'_1(x,y)\,\mathbf{P}(x,y)\boxed{\exp\left(-i\frac{k}{2f}\left(x^2+y^2\right)\right)}\exp\left(i\frac{k}{2d_0}\left(x^2+y^2\right)\right)$$

$$\times\exp\left[\frac{ik}{2d_0}\left[x_0x+y_0y\right]\right]dx_0dy_0$$

3. $U'_1(x,y) \longrightarrow U_i(x_i,y_i)$

Fresnel transform

$$U_i(x_i, y_i) = \iint U'_1(x, y)\boxed{\exp\left(i\frac{k}{2di}\left(x^2 + y^2\right)\right)}$$

$$\boxed{\times \exp\left[\frac{ik}{2di}\left[xx_i + yy_i\right]\right]}dxdy$$

Then, h is given by;

$$\mathbf{h}(x_0, y_0 : x_i, y_i) = \iint \mathbf{U'}_1(x, y)\,\mathbf{P}(x, y) \exp\left(i\frac{k}{2di}\left(x^2 + y^2\right)\right) \exp\left(i\frac{k}{2d_0}\left(x^2 + y^2\right)\right)$$

$$\times \exp\left(-i\frac{k}{2f}\left(x^2 + y^2\right)\right) \exp\left[\frac{ik}{2d_0}\left[x_0 x + y_0 y\right]\right] \exp\left[\frac{ik}{2di}\left[x x_i + y y_i\right]\right] dxdy$$

Tidy up the equation;

$$= (\text{Quadratic phase factor}) \times \iint \mathbf{P}(x, y) \exp\left[i\frac{k}{2}\left(\frac{1}{d_0} + \frac{1}{d_i} - \frac{1}{f}\right)\left(x^2 + y^2\right)\right]$$

$$\times \exp\left[-ik\left(\left(\frac{x_0}{d_0} + \frac{x_i}{d_i}\right)x + \left(\frac{y_0}{d_0} + \frac{y_i}{d_i}\right)y\right)\right] dxdy$$

physical meaning is not clear!

Then, h is given by;

$$\mathbf{h}(x_0, y_0 : x_i, y_i) = \iint \mathbf{U'}_1(x,y)\,\mathbf{P}(x,y) \exp\left(i\frac{k}{2di}(x^2+y^2)\right)\exp\left(i\frac{k}{2d_0}(x^2+y^2)\right)$$

$$\times \exp\left(-i\frac{k}{2f}(x^2+y^2)\right)\exp\left[\frac{ik}{2d_0}[x_0x+y_0y]\right]\exp\left[\frac{ik}{2di}[xx_i+yy_i]\right]dxdy$$

$$= (\text{Quadratic phase factor}) \times \iint \mathbf{P}(x,y)\exp\left[i\frac{k}{2}\left(\frac{1}{d_0}+\frac{1}{d_i}-\frac{1}{f}\right)(x^2+y^2)\right]$$

$$\times \exp\left[-ik\left(\left(\frac{x_0}{d_0}+\frac{x_i}{d_i}\right)x+\left(\frac{y_0}{d_0}+\frac{y_i}{d_i}\right)y\right)\right]dxdy$$

What is physical meaning of this term?

Return to geometrical optics;

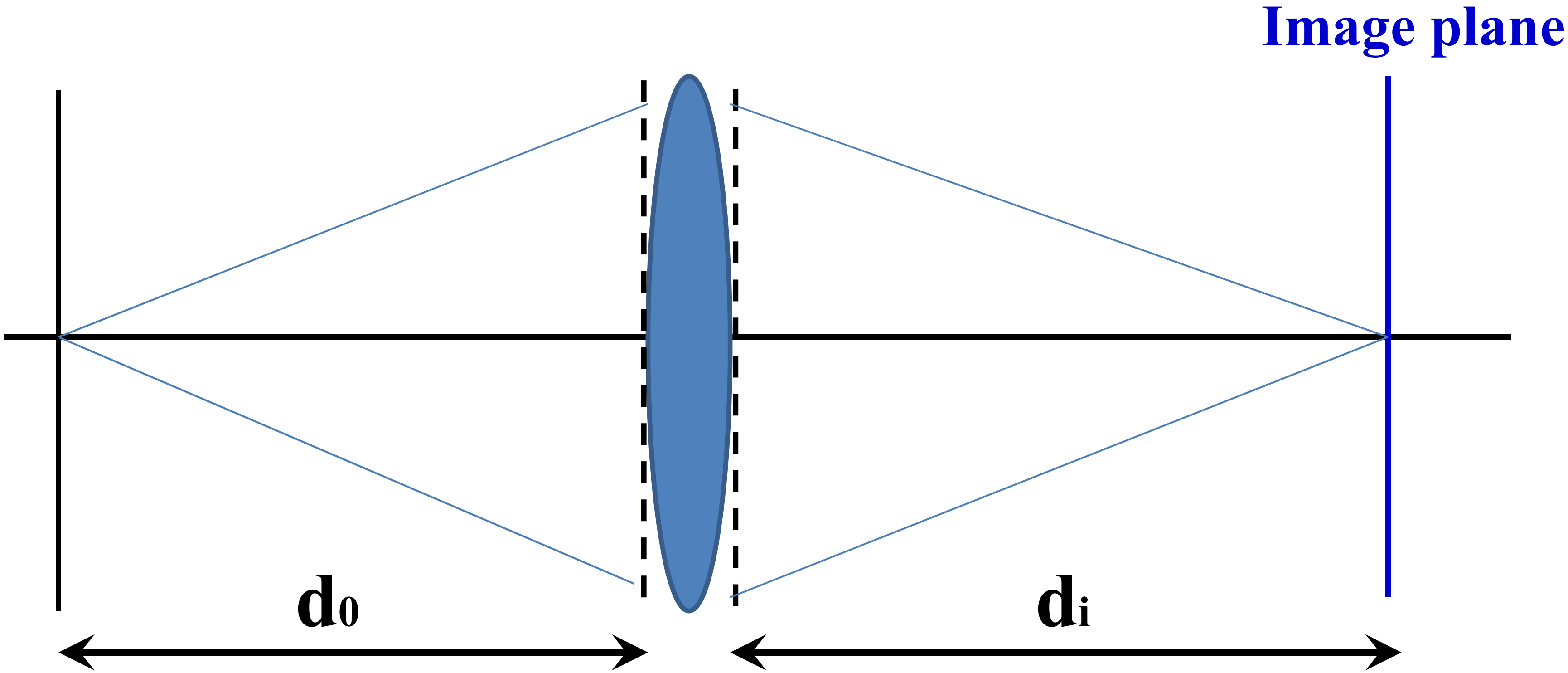

$$\frac{1}{d_0}+\frac{1}{d_i}-\frac{1}{f}=0$$

Lens equation !

Then phase factor $\exp\left[i\frac{k}{2}\left(\frac{1}{d_0}+\frac{1}{d_i}-\frac{1}{f}\right)\left(x^2+y^2\right)\right]$ **be 1**

Then, h becomes

$$\mathbf{h}\left(x_0, y_0 : x_i, y_i\right) = \iint \mathbf{P}(x, y) \exp\left[-ik\left(\left(\frac{x_0}{d_0}+\frac{x_i}{d_i}\right)x + \left(\frac{y_0}{d_0}+\frac{y_i}{d_i}\right)y\right)\right]dxdy$$

Introducing magnification M; $M \equiv \frac{d_i}{d_0}$

$$\mathbf{h}\left(x_0, y_0 : x_i, y_i\right) \cong \iint \mathbf{P}(x, y) \exp\left[-\frac{ik}{d_i}\left(\left(x_i + Mx_0\right)x + \left(y_i + My_0\right)y\right)\right]dxdy$$

The Fraunhofer diffraction will be appear on image plane with magnification in geometrical optics!

Let us introduce very important parameter, Spatial frequency f_x, f_y by

$$f_x = \frac{2\pi x}{\lambda d_i}$$

$$f_y = \frac{2\pi y}{\lambda d_i}$$

$$\mathbf{h}\left(x_0, y_0 : x_i, y_i\right) = \iint \mathbf{P}(x, y) \exp\left[-\frac{ik}{d_i}\left(\left(x_i + Mx_0\right)x + \left(y_i + My_0\right)y\right)\right] dx dy$$

$$= M \iint \mathbf{P}(f_x, f_y) \exp\left[-i\left(\left(x_i + Mx_0\right)f_x + \left(y_i + My_0\right)f_y\right)\right] df_x df_y$$

Then, we introduce the spatial invariant response function by;

$$\tilde{\mathbf{h}} = \frac{1}{M}\mathbf{h}$$

$$\tilde{\mathbf{h}}\left(x_0, y_0 : x_i, y_i\right) = \iint \mathbf{P}(f_x, f_y) \exp\left[-i\left(\left(x_i + Mx_0\right)f_x + \left(y_i + My_0\right)f_y\right)\right] df_x df_y$$

Now we stand in front of entrance for the inverse space!

Impulsive response function in inverse space and CTF, OTF, MTF

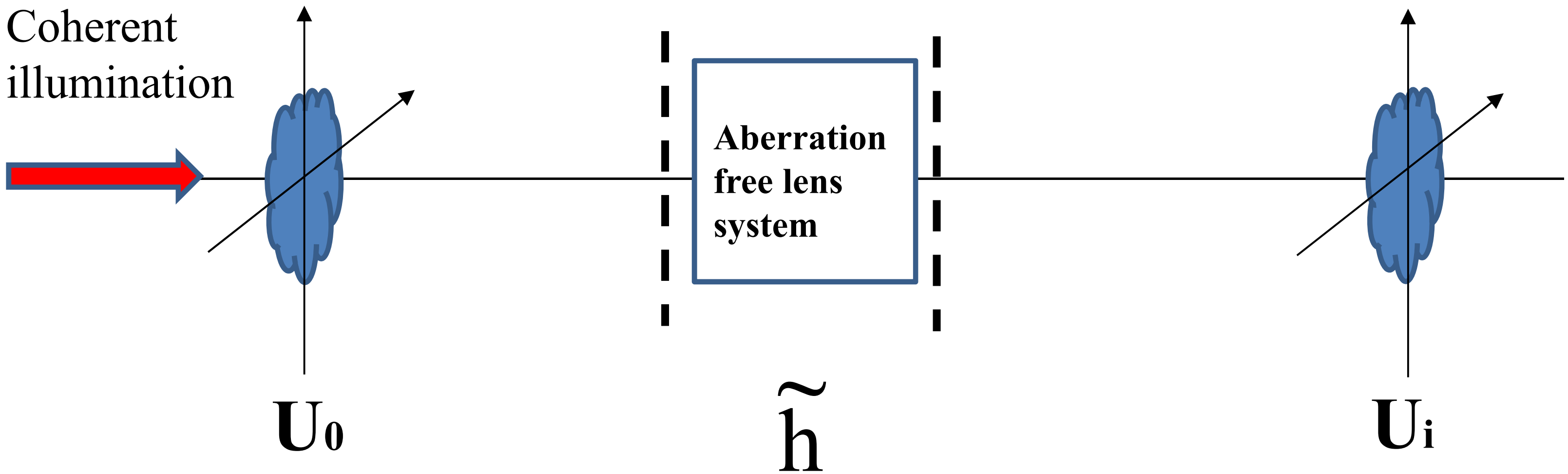

Let us consider in inverse space

Coherent transfer function, CTF

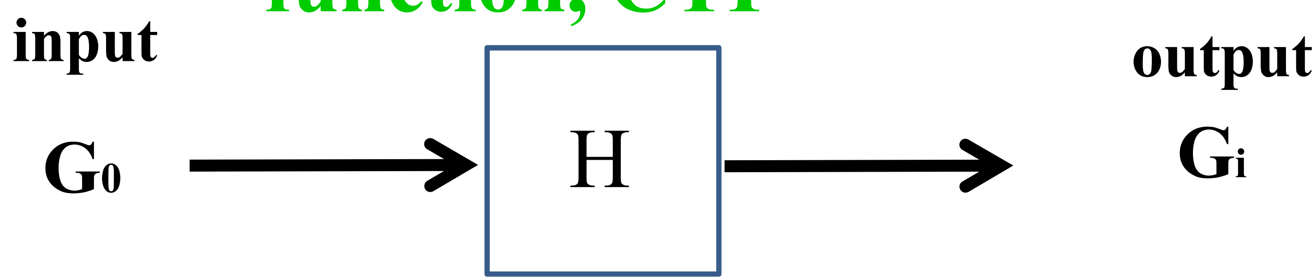

What is coherent illumination?

Disturbance of illumination U_c is represented by:

$$U_c = \frac{A\,\mathbf{exp}(ikz)}{i\lambda z}\,\mathbf{exp}\left[i\frac{k}{2z}\left(x^2 + y^2\right)\right]$$

if z becomes very large, U_c becomes plane wave.

Example: CW Laser such as He-Ne Laser

$G_0 = \mathscr{F}(U_0)$ $\mathscr{F}(\quad)$: Fourier transform

$G_i = \mathscr{F}(U_i)$

$H = \mathscr{F}(\tilde{h})$

Then

$G_i = HG_0$

$$\tilde{h} = \mathscr{F}(P(f_x,f_y))$$

Then,

$$H=\mathscr{F}(\mathscr{F}(P(f_x,f_y)))=P(f_x,f_y)$$

Coherent transfer function (CTF) is pupil function it self !

Properties of CTF

Lens has pupil of radius r and focal length d_i

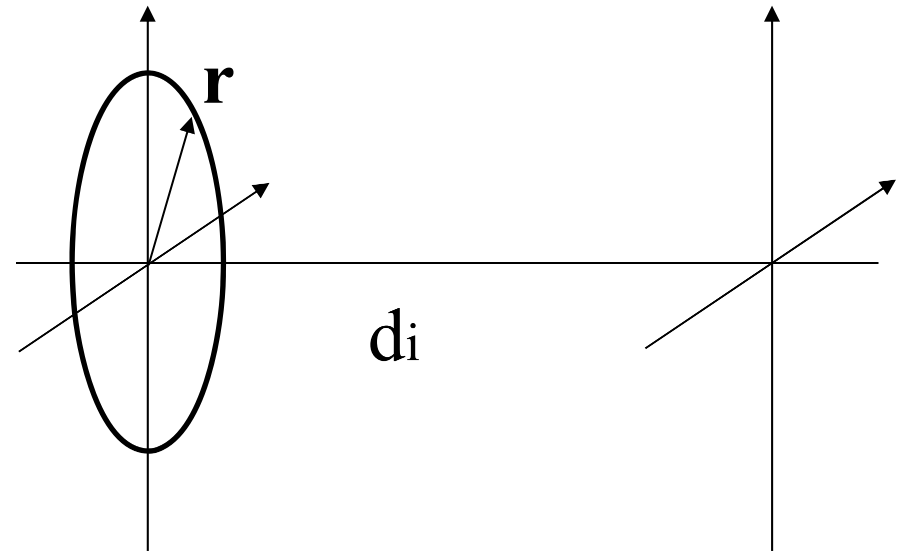

1. **Cut off frequency:** $f_0 = \dfrac{2\pi r}{\lambda d_i}$
2. **Inside of cut off frequency, information of amplitude, phase will transfer without distortion**

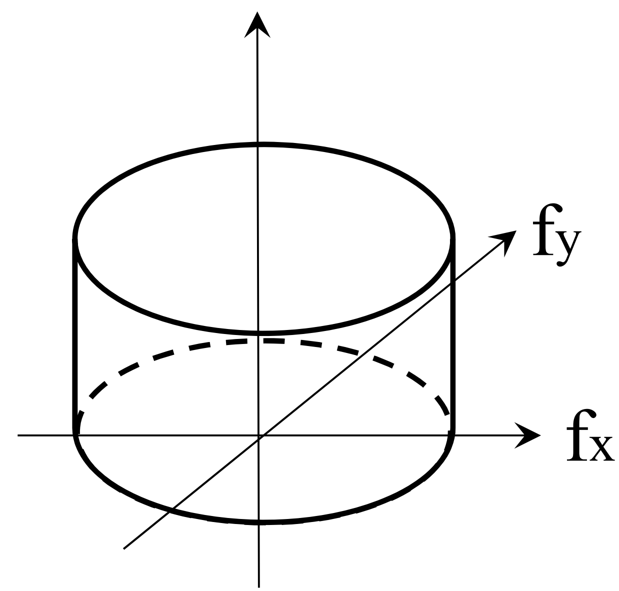

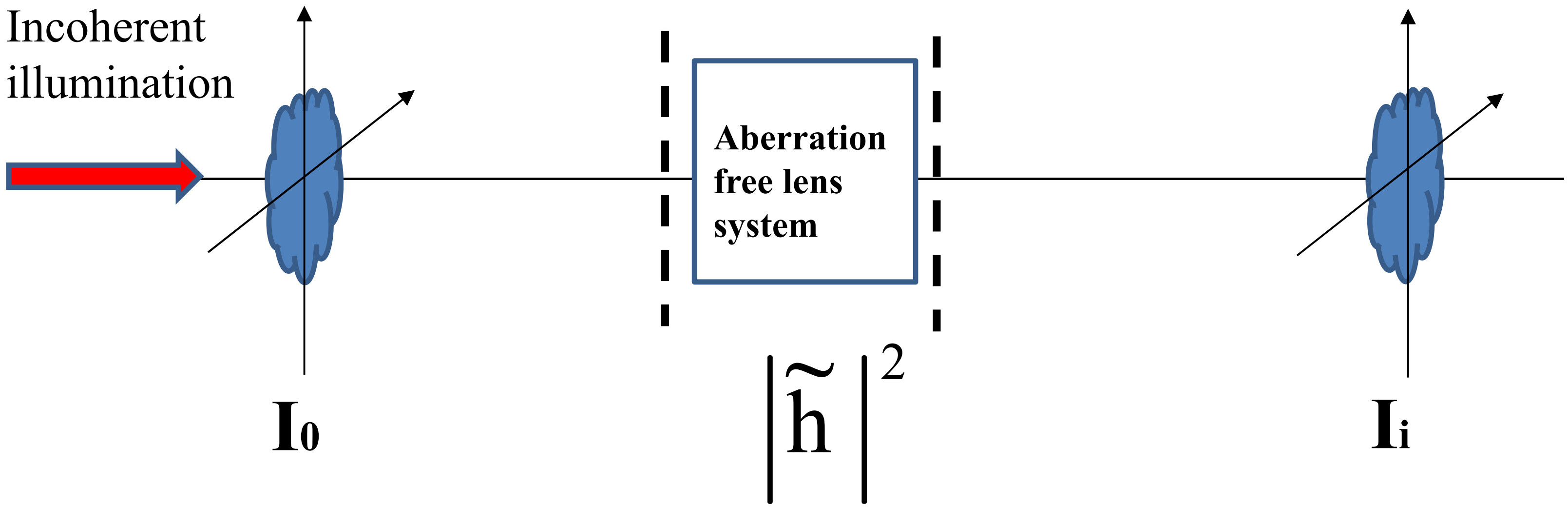

Optical transfer function, OTF

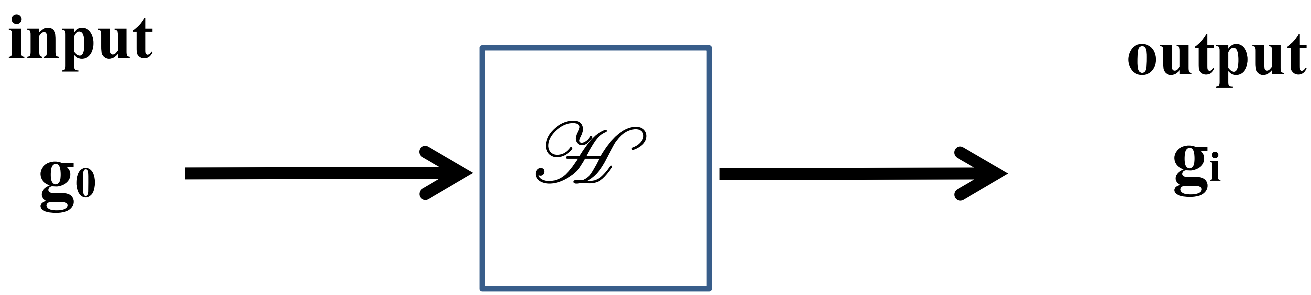

$\mathbf{g_0} = \mathscr{F}(\mathbf{I_0})$ $\mathscr{F}(\quad)$: **Fourier transform normalized by it's value at $f_x, f_y = 0$**

$\mathbf{g_i} = \mathscr{F}(\mathbf{I_i})$

$\mathscr{H} = \mathscr{F}\left(\left|\tilde{h}\right|^2\right)$

Then

$\mathbf{g_i} = \mathscr{H}\,\mathbf{g_0}$

OTF is given by autocorrelation of CTF

$$\mathscr{H}\,(\mathbf{f_x,f_y}) = \frac{\iint H(\xi,\eta)H(\xi-f_x,\eta-f_y)d\xi d\eta}{\iint |H(\xi,\eta)|^2 d\xi d\eta}$$

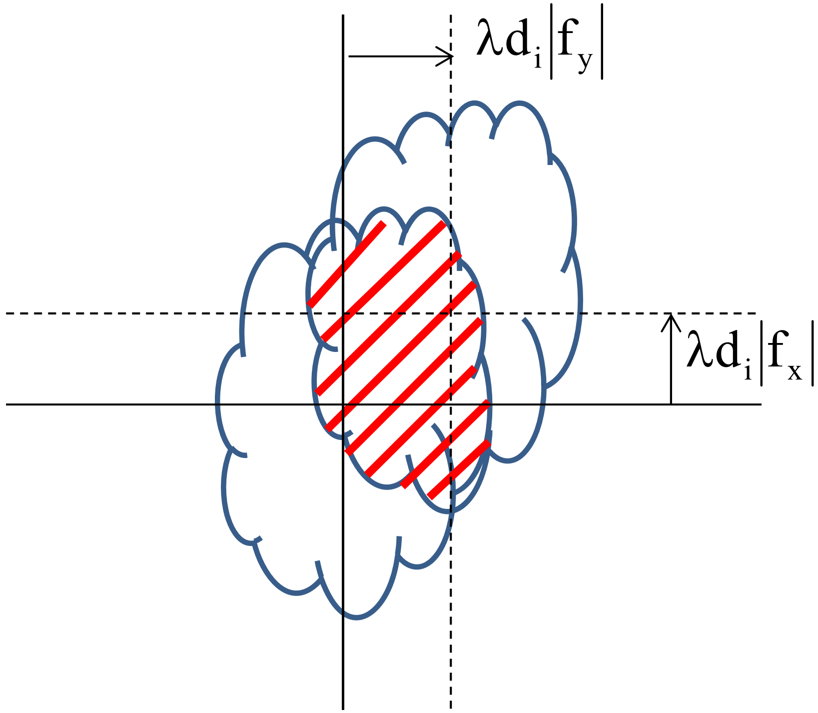

Geometrical meaning of OTR

$$\mathscr{H}\,(\mathbf{f_x,f_y}) = \frac{\text{area of overlap}\left(f_x,f_y\right)}{\text{total area}}$$

Example of OTR

Lens has pupil of radius r and focal length d_i

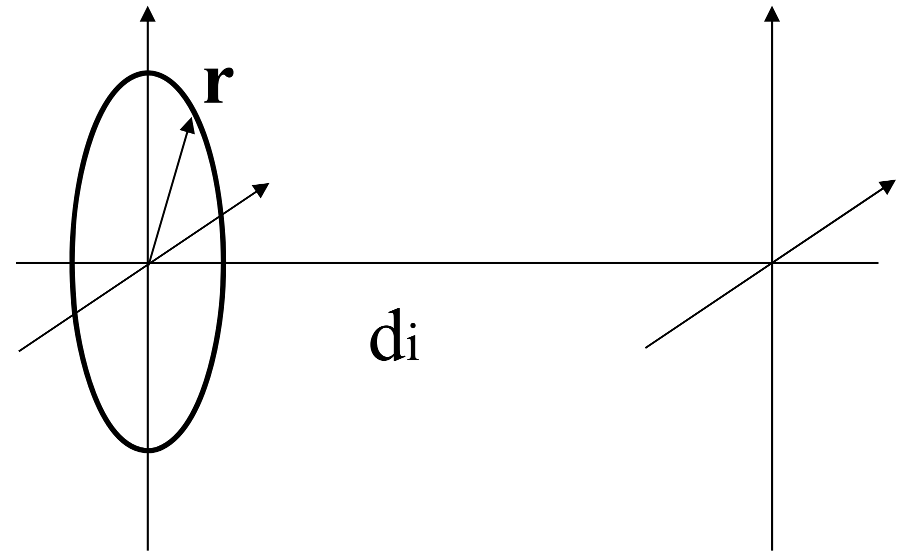

Cut off frequency of OTR

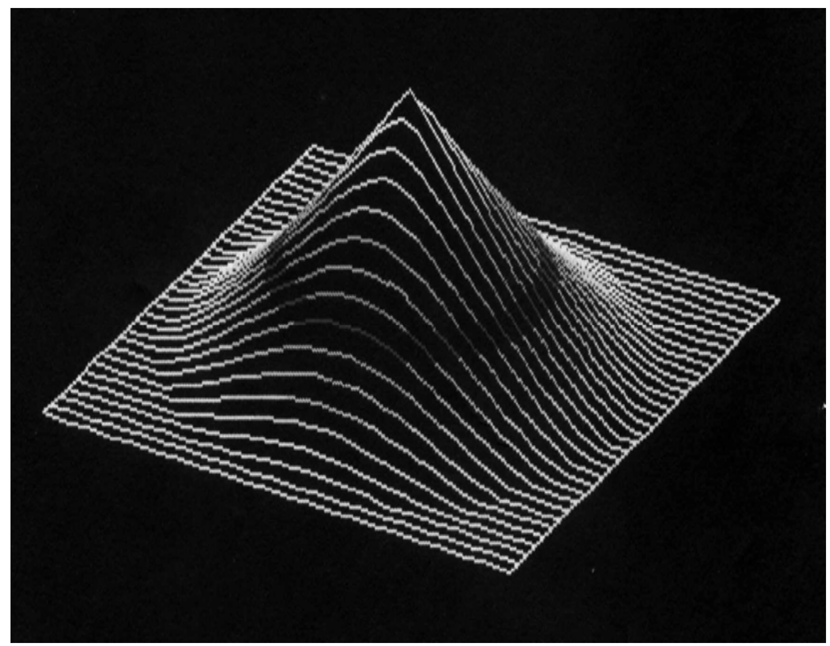

twice of CTF cut off frequency

$$f_0 = 2 \times \frac{2\pi r}{\lambda d_i}$$

Influence of aberration

Influence of aberration to frequency response

Phase transmittance

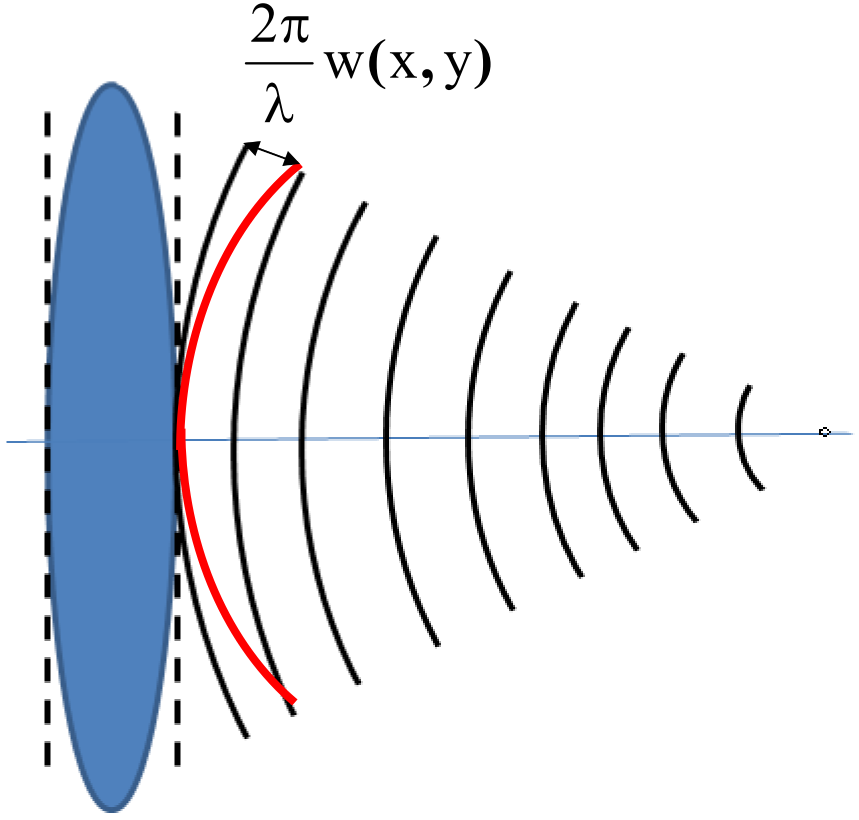

Amplitude transmittance: A(x,y)

Generalized pupil function

$$p(x,y) = A(x,y)P(x,y)\,\mathbf{exp}\left(i\frac{2\pi}{\lambda}w(x,y)\right)$$

CTF is given by

$$H(f_x,f_y) = A\left(\frac{\lambda d_i}{2\pi}f_x,\frac{\lambda d_i}{2\pi}f_y\right)P\left(\frac{\lambda d_i}{2\pi}f_x,\frac{\lambda d_i}{2\pi}f_y\right)\mathbf{exp}\left(i\frac{2\pi}{\lambda}w\left(\frac{\lambda d_i}{2\pi}f_x,\frac{\lambda d_i}{2\pi}f_y\right)\right)$$

OTF is again given by autocorrelation of CTF

OTF with aberration is sometimes complex, so we use absolute value of OTF, It is called Modulation Transfer Function, MTF

Important general properties of MTF:

1. **MTF having aberration is always smaller than aberration-free MTF (diffraction limited MTF)**

2. **Cut-off frequency is not changed by aberration**

3. **Zero cross of MTF corresponding to inverse of contrast.**

Singlet D=80mm f=1000mm

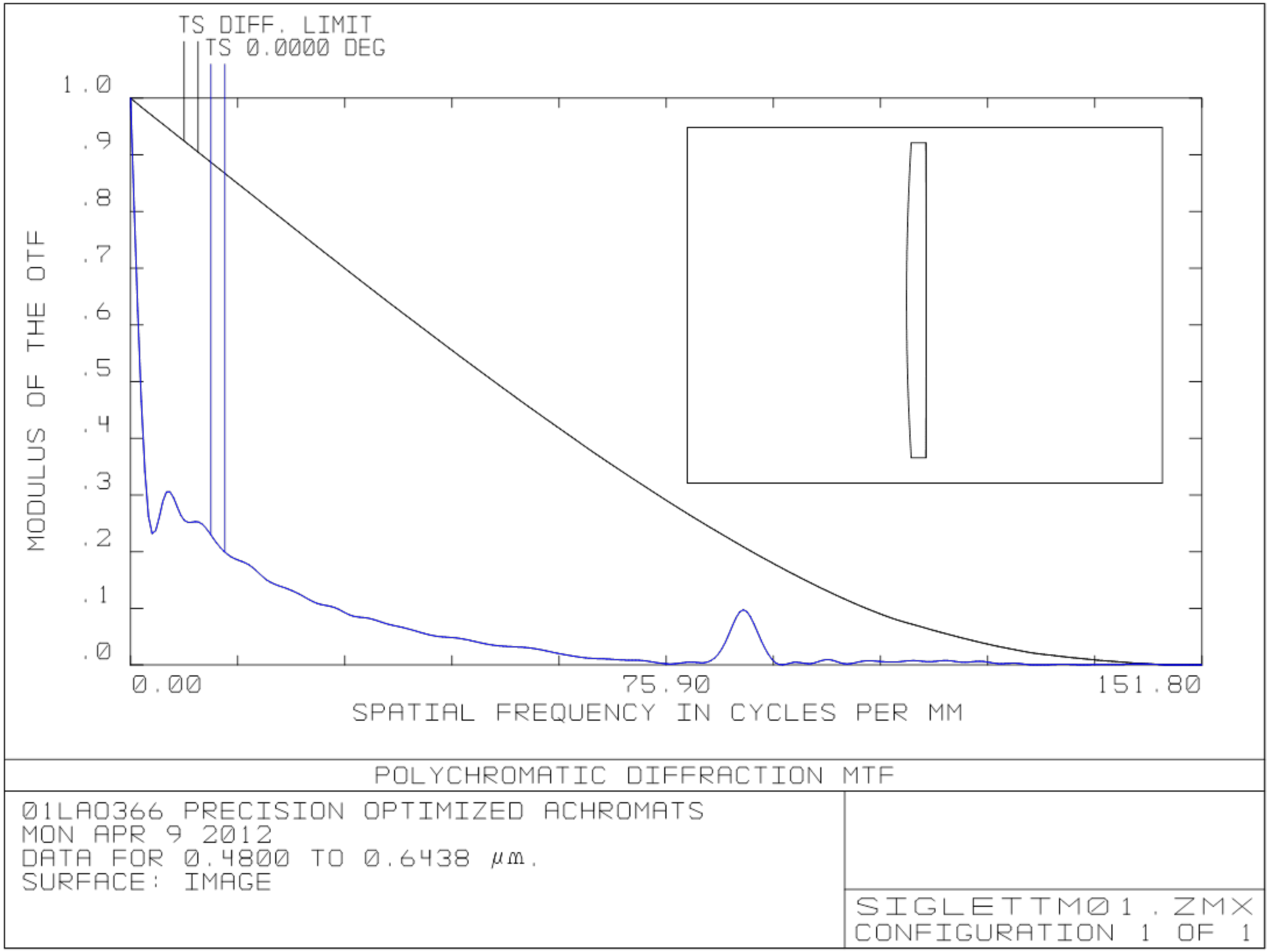

Doublet D=80mm f=1000mm

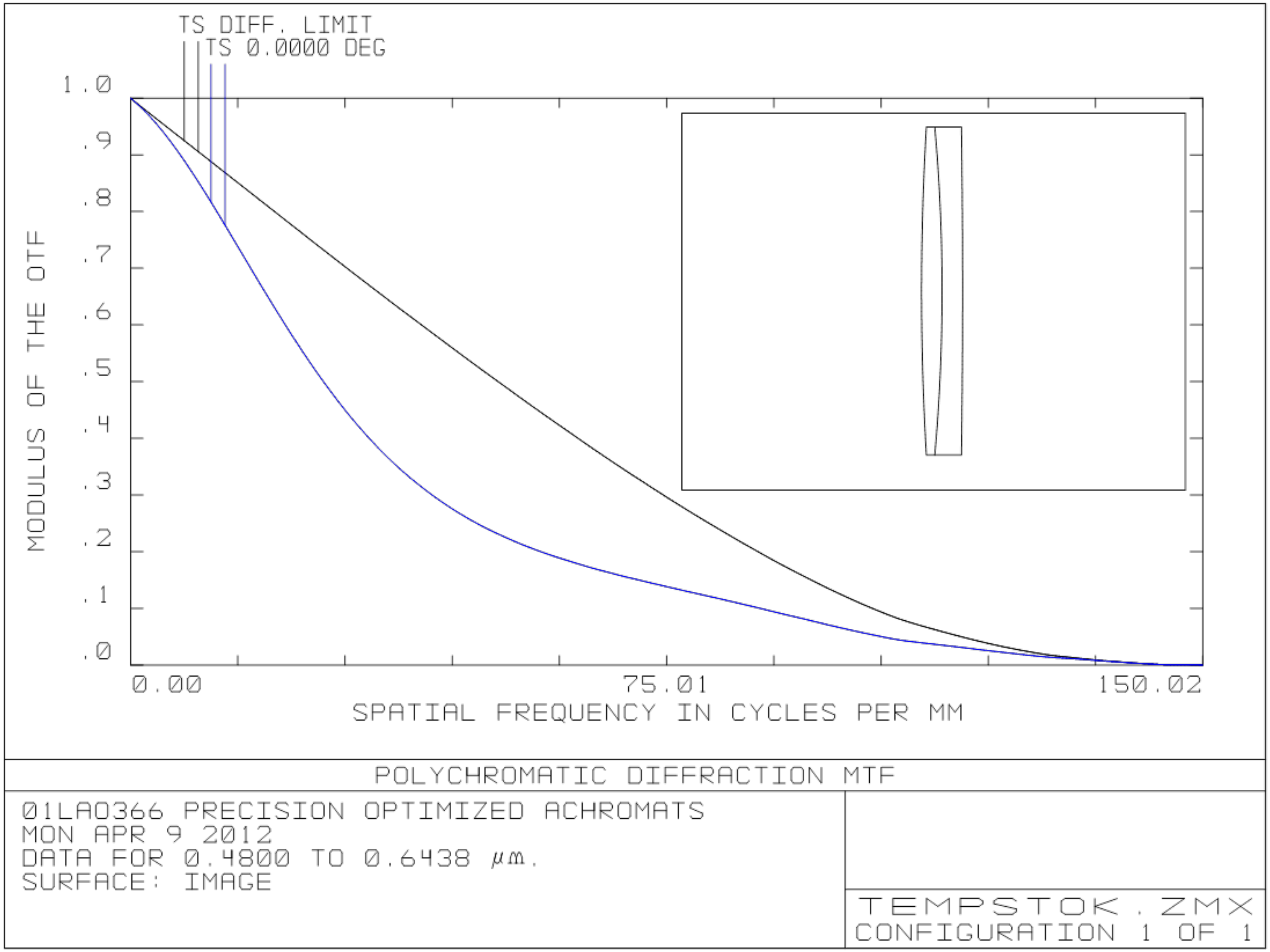

Singlet D=80mm f=1000mm
λ=0.55μm

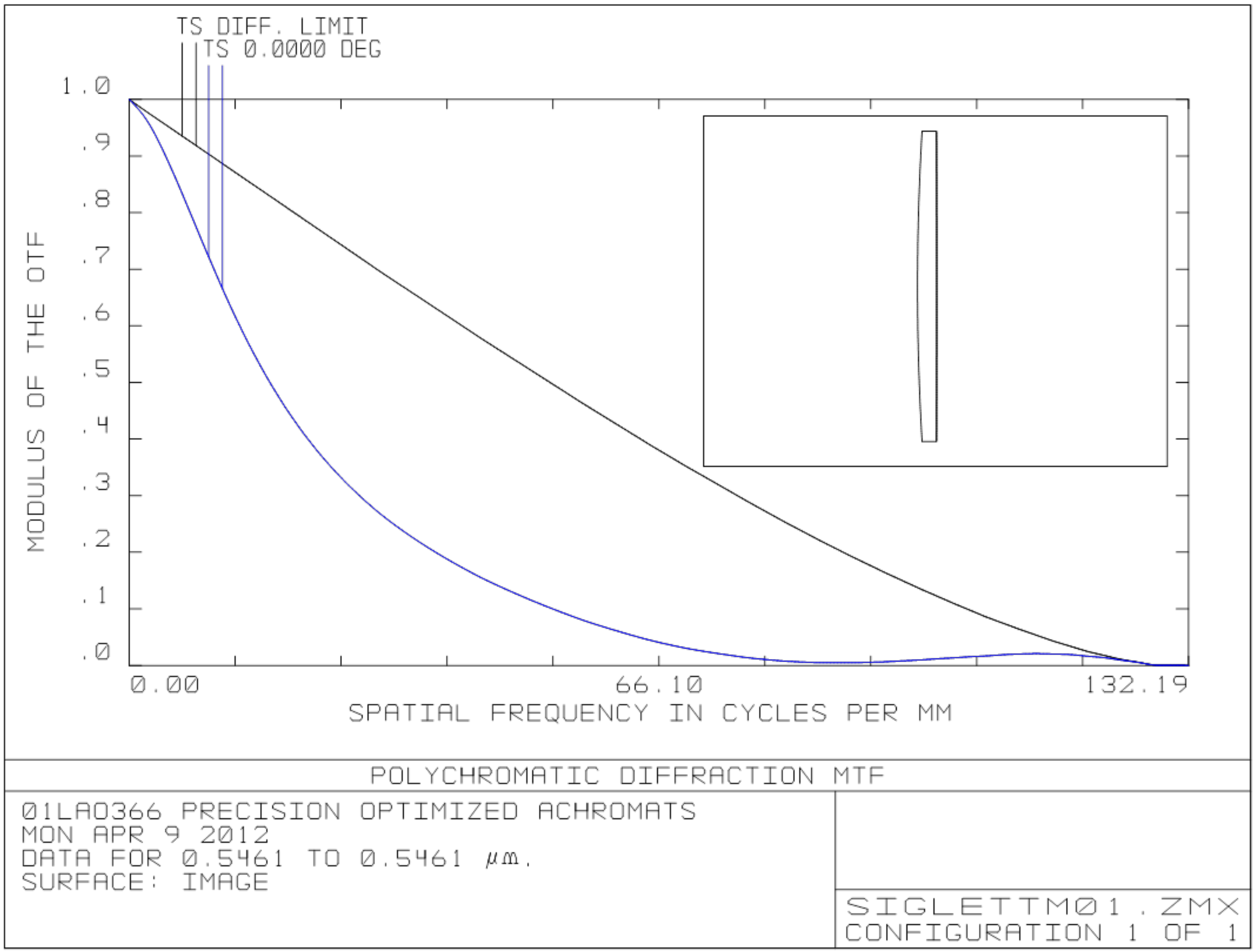

Doublet D=80mm f=1000mm
λ=0.55μm

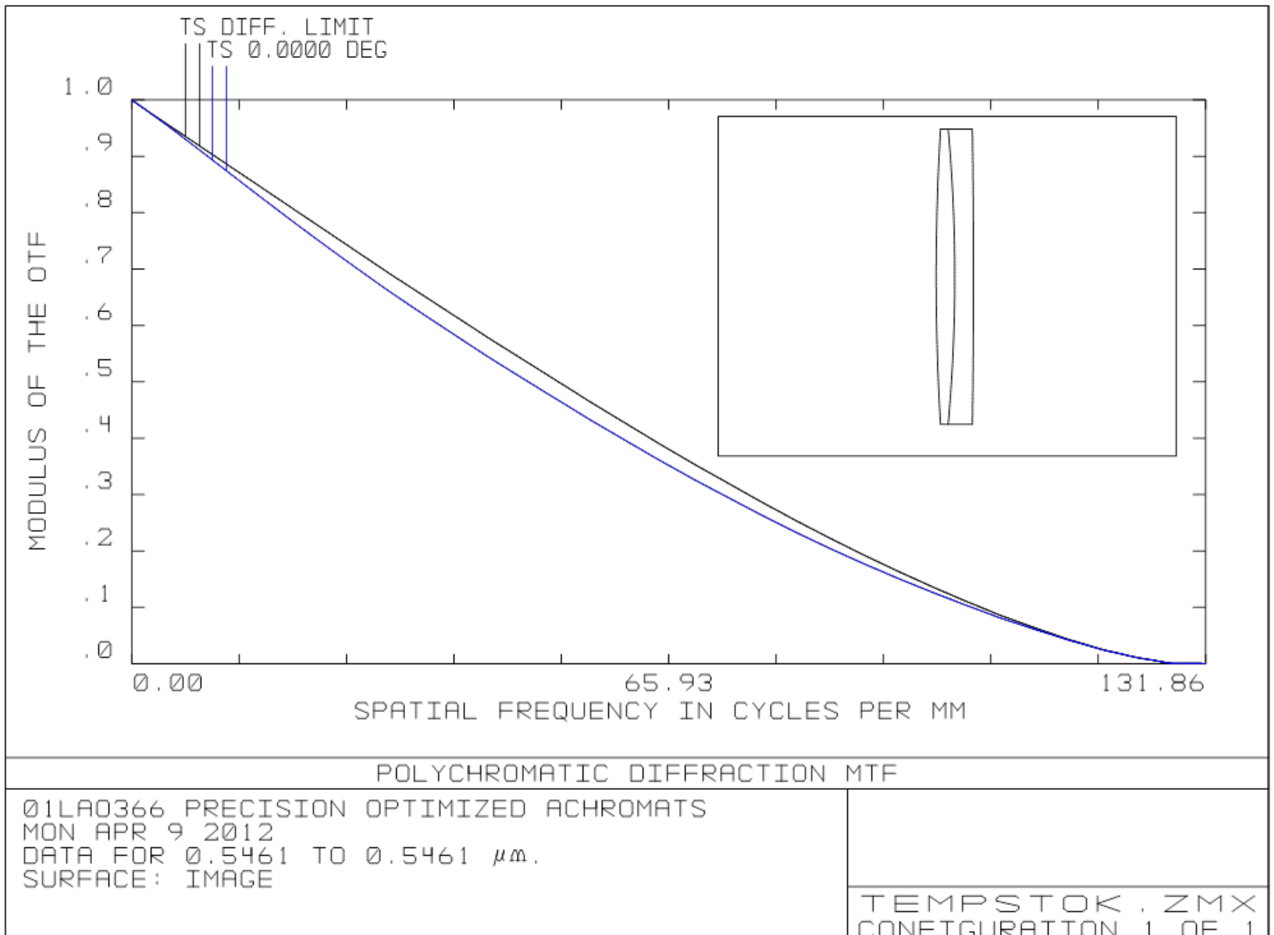

Appodization or super resolution

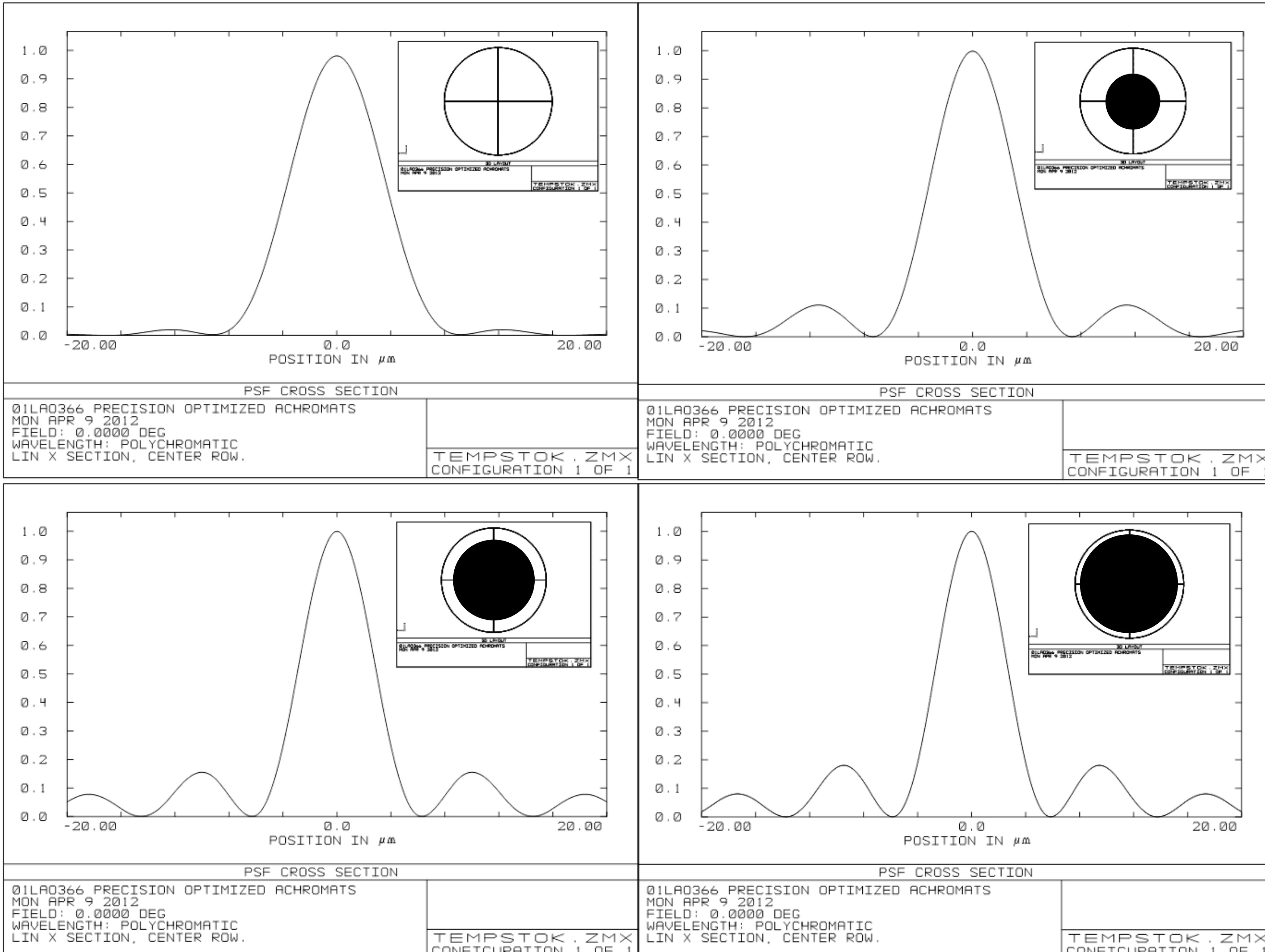

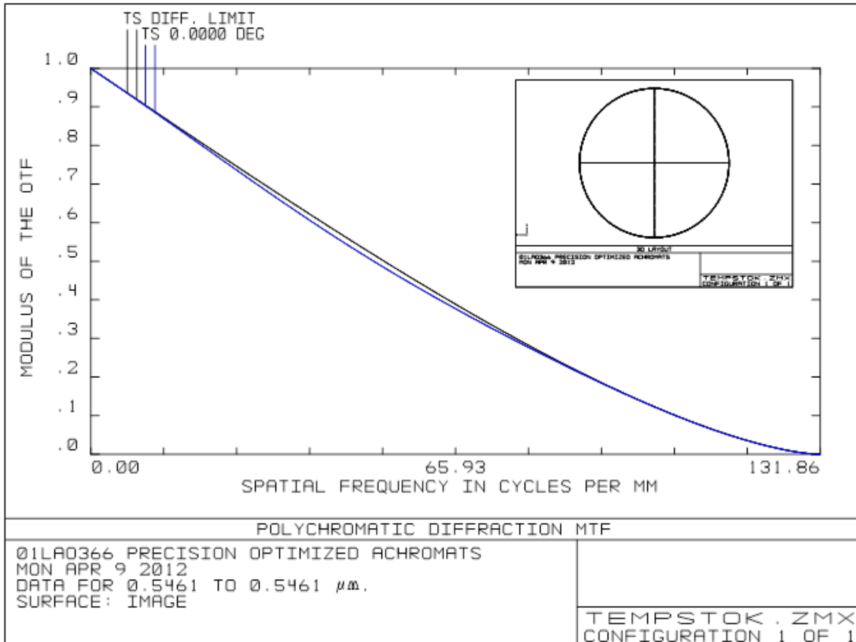
TS DIFF. LIMIT
TS 0.0000 DEG
MODULUS OF THE OTF
1.0
.9
.8
.7
.6
.5
.4
.3
.2
.1
.0
0.00
65.93
131.86
SPATIAL FREQUENCY IN CYCLES PER MM
POLYCHROMATIC DIFFRACTION MTF
01LAO366 PRECISION OPTIMIZED ACHROMATS
MON APR 9 2012
DATA FOR 0.5461 TO 0.5461 µm.
SURFACE: IMAGE
TEMPSTOK.ZMX
CONFIGURATION 1 OF 1

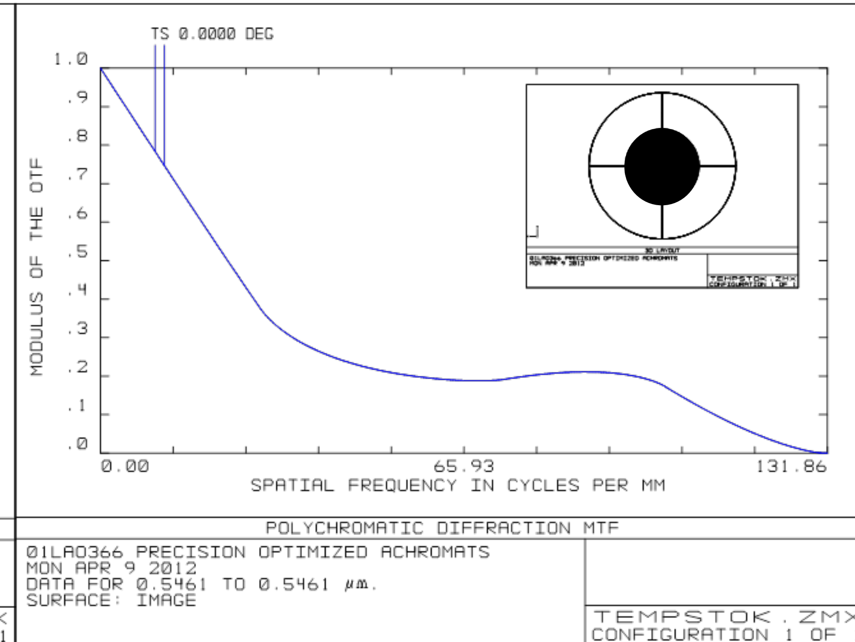
TS 0.0000 DEG
MODULUS OF THE OTF
1.0
.9
.8
.7
.6
.5
.4
.3
.2
.1
.0
0.00
65.93
131.86
SPATIAL FREQUENCY IN CYCLES PER MM
POLYCHROMATIC DIFFRACTION MTF
01LAO366 PRECISION OPTIMIZED ACHROMATS
MON APR 9 2012
DATA FOR 0.5461 TO 0.5461 µm.
SURFACE: IMAGE
TEMPSTOK.ZMX
CONFIGURATION 1 OF 1

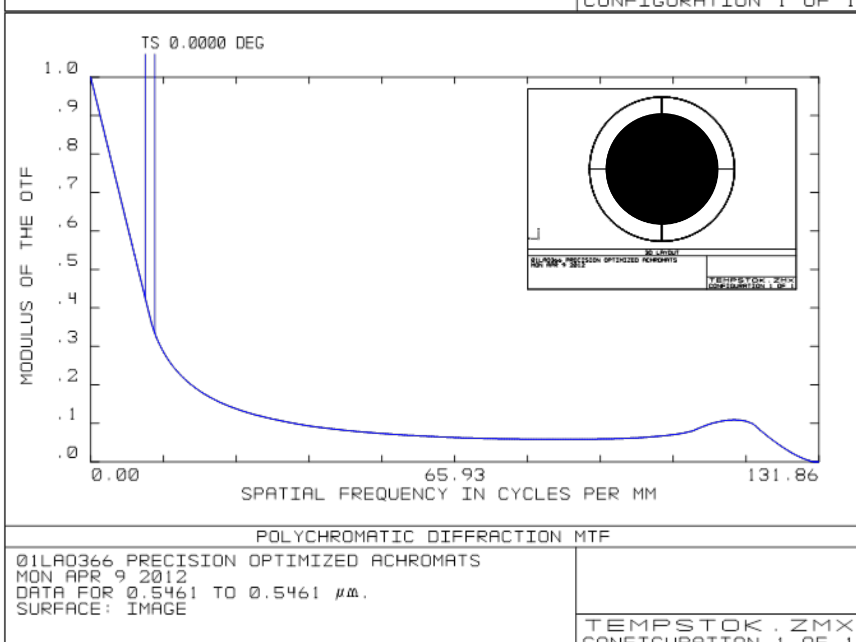
TS 0.0000 DEG
MODULUS OF THE OTF
1.0
.9
.8
.7
.6
.5
.4
.3
.2
.1
.0
0.00
65.93
131.86
SPATIAL FREQUENCY IN CYCLES PER MM
POLYCHROMATIC DIFFRACTION MTF
01LAO366 PRECISION OPTIMIZED ACHROMATS
MON APR 9 2012
DATA FOR 0.5461 TO 0.5461 µm.
SURFACE: IMAGE
TEMPSTOK.ZMX
CONFIGURATION 1 OF 1

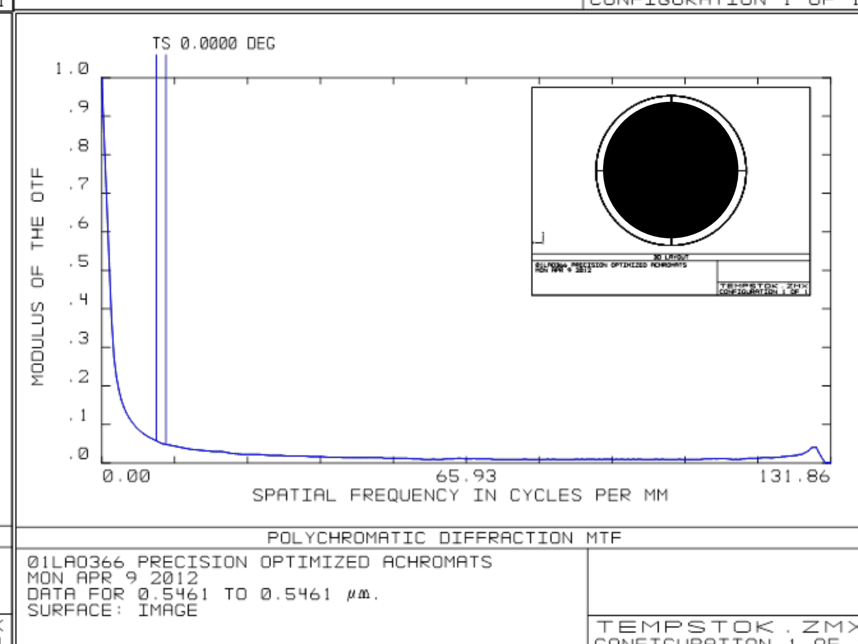
TS 0.0000 DEG
MODULUS OF THE OTF
1.0
.9
.8
.7
.6
.5
.4
.3
.2
.1
.0
0.00
65.93
131.86
SPATIAL FREQUENCY IN CYCLES PER MM
POLYCHROMATIC DIFFRACTION MTF
01LAO366 PRECISION OPTIMIZED ACHROMATS
MON APR 9 2012
DATA FOR 0.5461 TO 0.5461 µm.
SURFACE: IMAGE
TEMPSTOK.ZMX
CONFIGURATION 1 OF 1

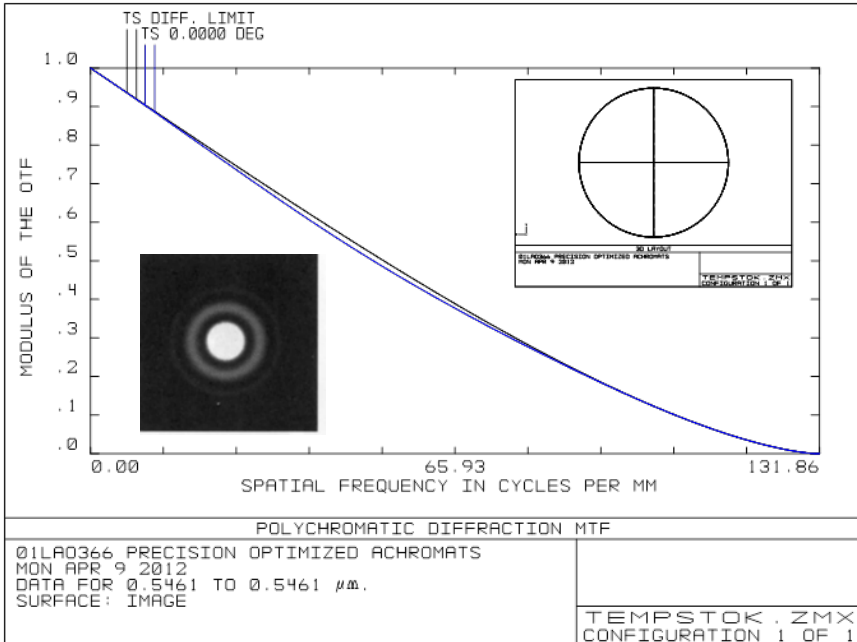
TS DIFF. LIMIT
TS 0.0000 DEG
MODULUS OF THE OTF
SPATIAL FREQUENCY IN CYCLES PER MM
0.00
65.93
131.86
POLYCHROMATIC DIFFRACTION MTF
01LAO366 PRECISION OPTIMIZED ACHROMATS
MON APR 9 2012
DATA FOR 0.5461 TO 0.5461 µm.
SURFACE: IMAGE
TEMPSTOK.ZMX
CONFIGURATION 1 OF 1

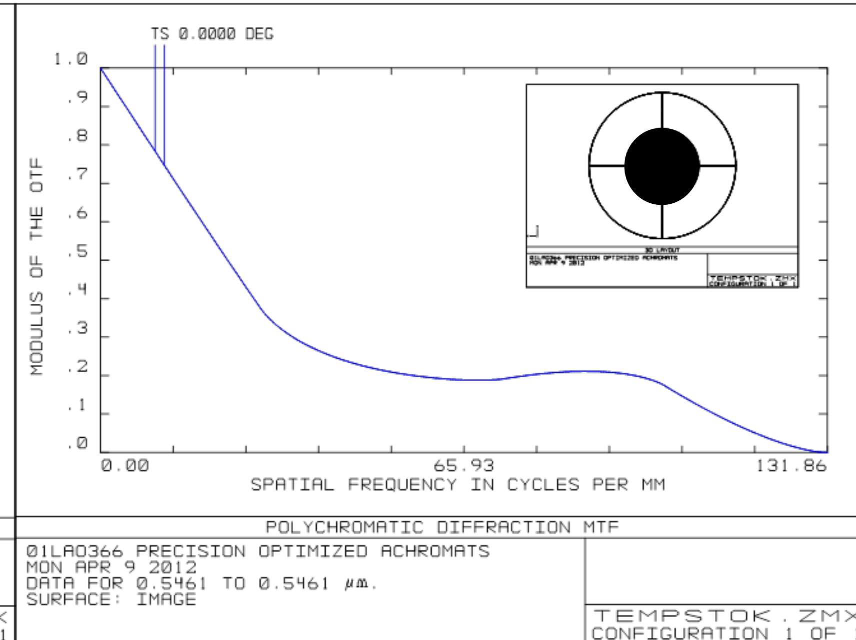
TS 0.0000 DEG
MODULUS OF THE OTF
SPATIAL FREQUENCY IN CYCLES PER MM
0.00
65.93
131.86
POLYCHROMATIC DIFFRACTION MTF
01LAO366 PRECISION OPTIMIZED ACHROMATS
MON APR 9 2012
DATA FOR 0.5461 TO 0.5461 µm.
SURFACE: IMAGE
TEMPSTOK.ZMX
CONFIGURATION 1 OF 1

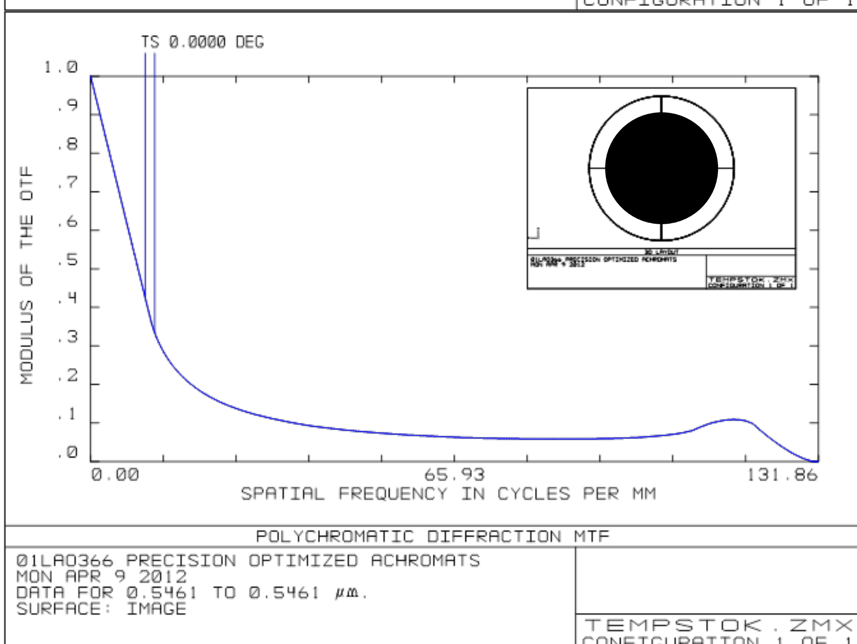
TS 0.0000 DEG
MODULUS OF THE OTF
SPATIAL FREQUENCY IN CYCLES PER MM
0.00
65.93
131.86
POLYCHROMATIC DIFFRACTION MTF
01LAO366 PRECISION OPTIMIZED ACHROMATS
MON APR 9 2012
DATA FOR 0.5461 TO 0.5461 µm.
SURFACE: IMAGE
TEMPSTOK.ZMX
CONFIGURATION 1 OF 1

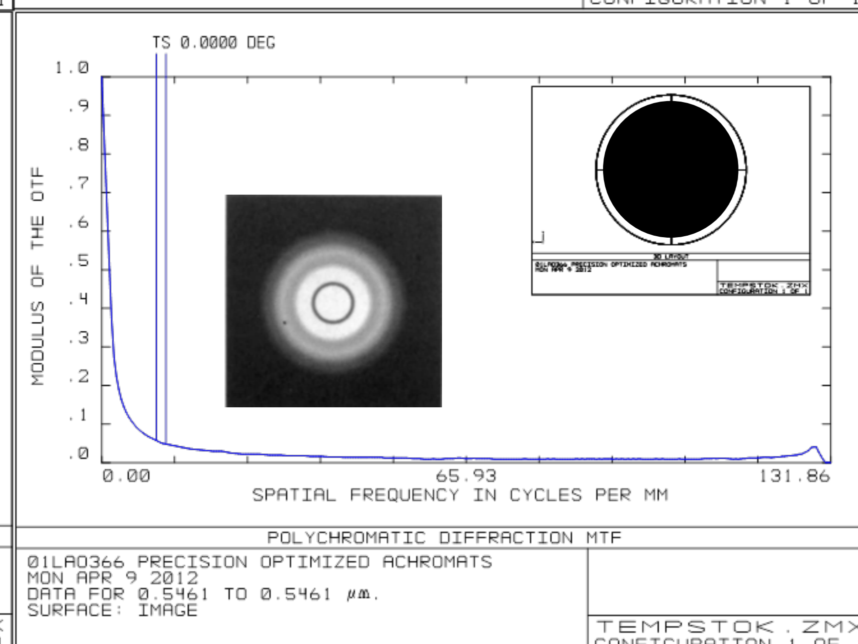
TS 0.0000 DEG
MODULUS OF THE OTF
SPATIAL FREQUENCY IN CYCLES PER MM
0.00
65.93
131.86
POLYCHROMATIC DIFFRACTION MTF
01LAO366 PRECISION OPTIMIZED ACHROMATS
MON APR 9 2012
DATA FOR 0.5461 TO 0.5461 µm.
SURFACE: IMAGE
TEMPSTOK.ZMX
CONFIGURATION 1 OF 1

Diffraction without wavefront error

Surface plot of MTF

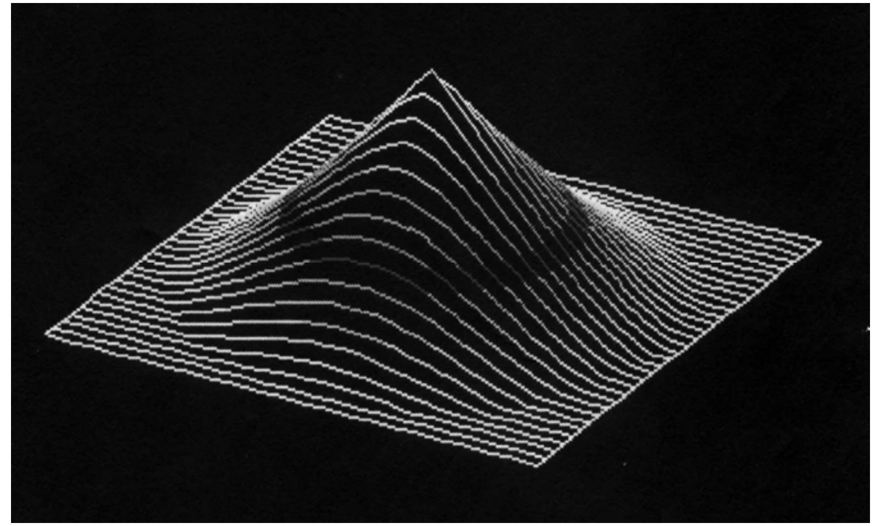

PSF plot

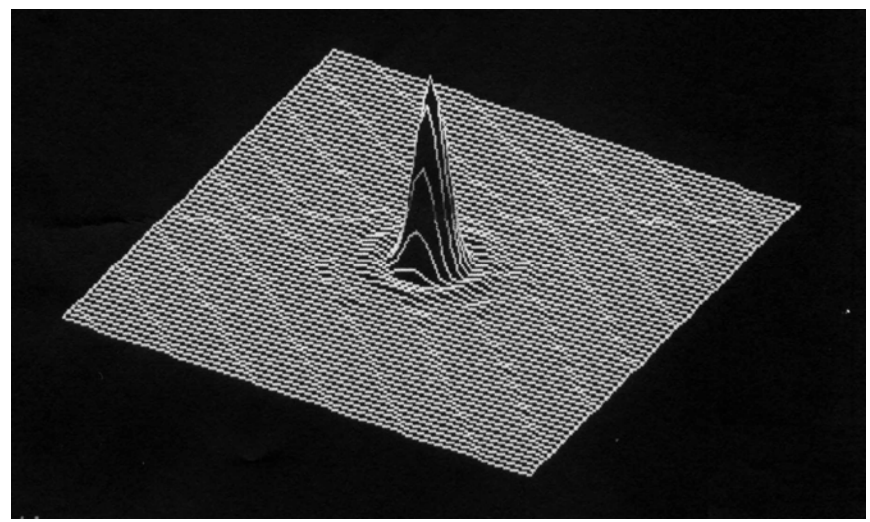

Diffraction with wavefront error

p-v: 0.82λ,   RMS : 0.092λ

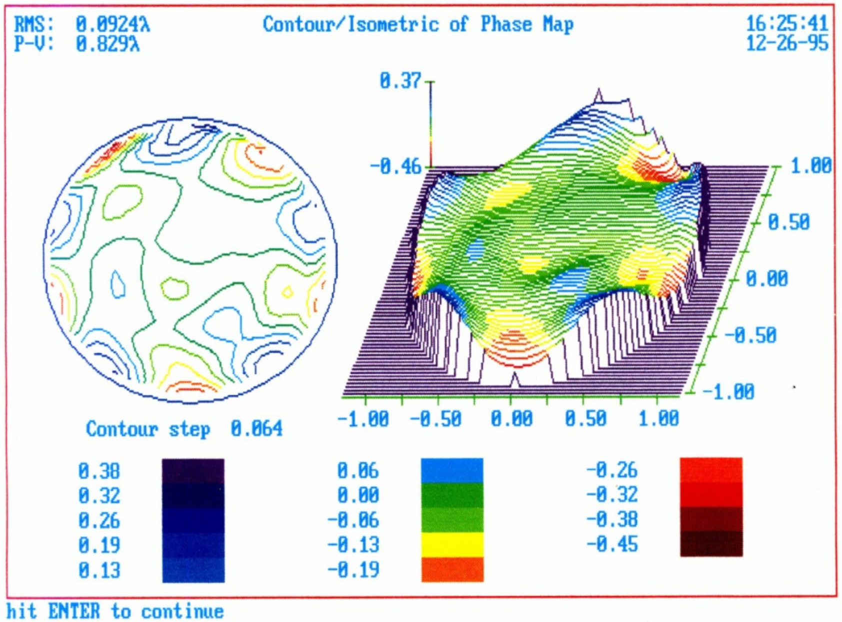

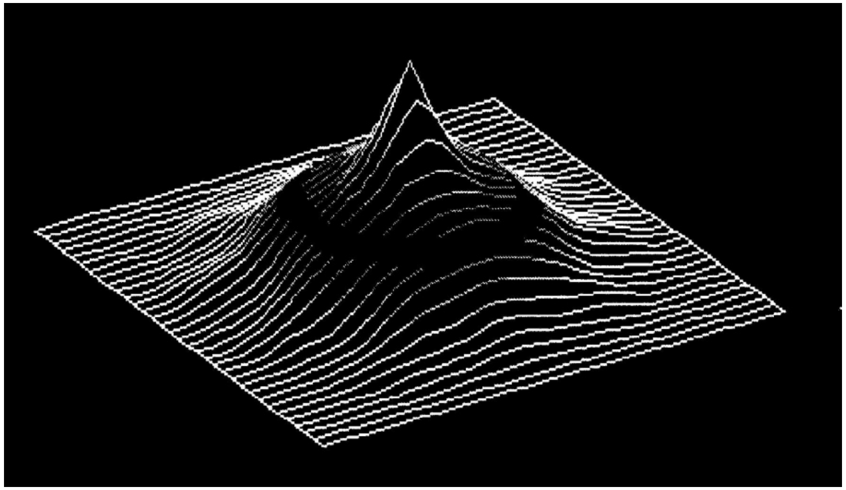

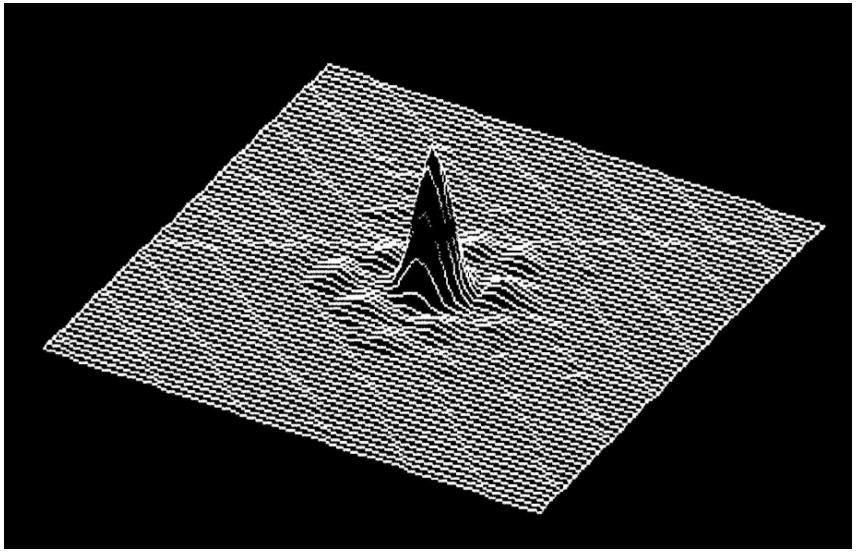

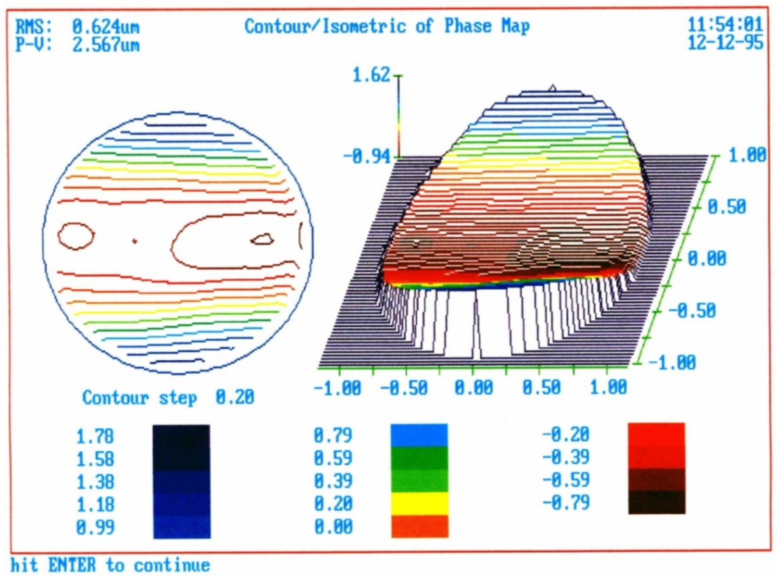
RMS: 0.624um
P-V: 2.567um
Contour/Isometric of Phase Map
11:54:01
12-12-95
1.62
-0.94
1.00
0.50
0.00
-0.50
-1.00
-1.00 -0.50 0.00 0.50 1.00
Contour step 0.20
1.78
1.58
1.38
1.18
0.99
0.79
0.59
0.39
0.20
0.00
-0.20
-0.39
-0.59
-0.79
hit ENTER to continue

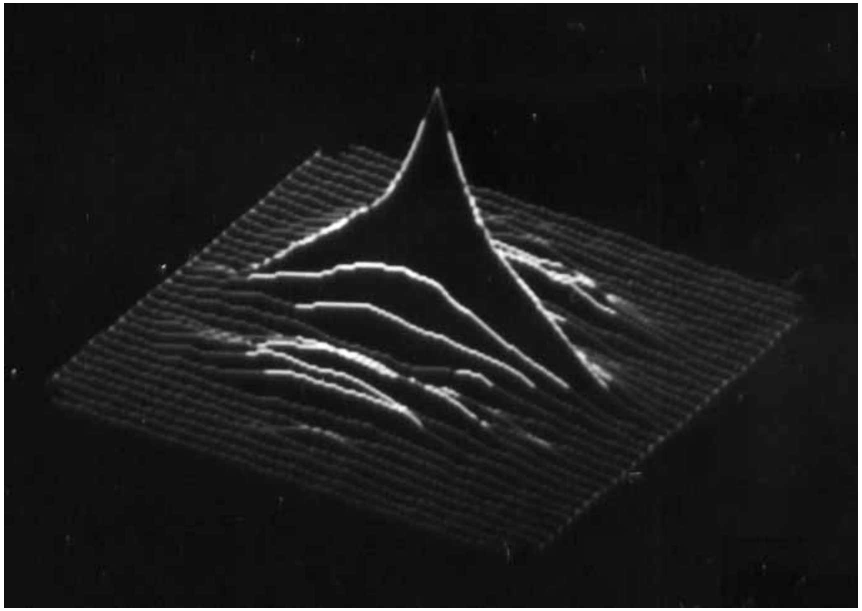

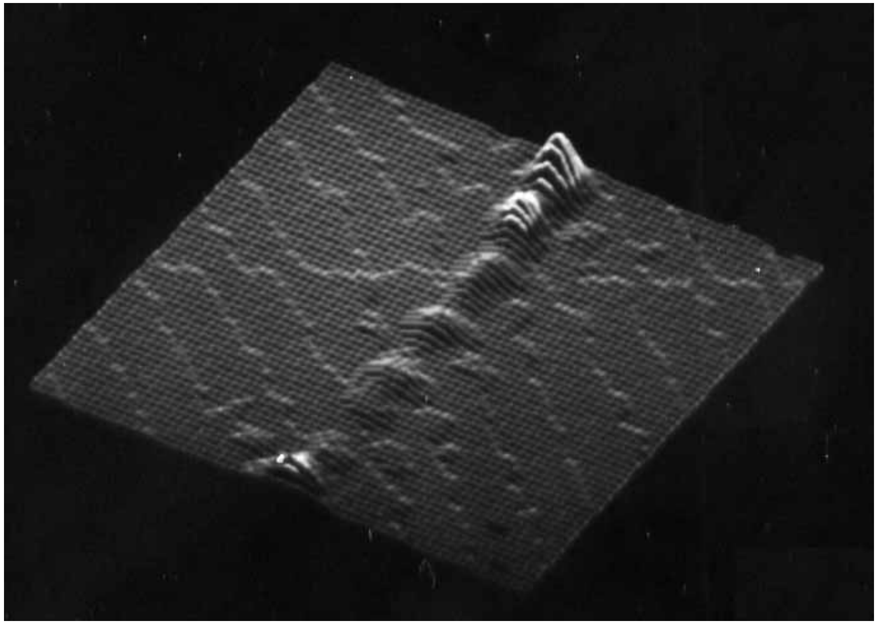

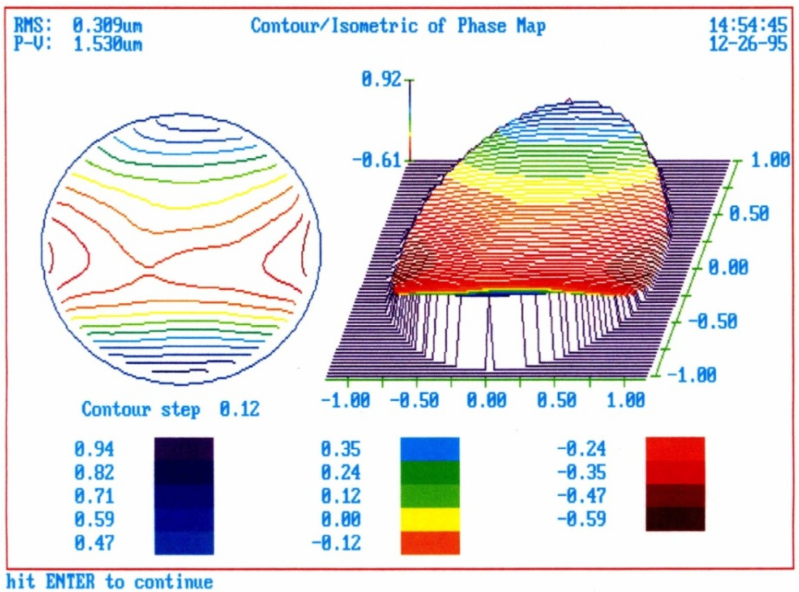
RMS: 0.309um
P-V: 1.530um
Contour/Isometric of Phase Map
14:54:45
12-26-95
0.92
-0.61
1.00
0.50
0.00
-0.50
-1.00
-1.00 -0.50 0.00 0.50 1.00
Contour step 0.12
0.94
0.82
0.71
0.59
0.47
0.35
0.24
0.12
0.00
-0.12
-0.24
-0.35
-0.47
-0.59
hit ENTER to continue

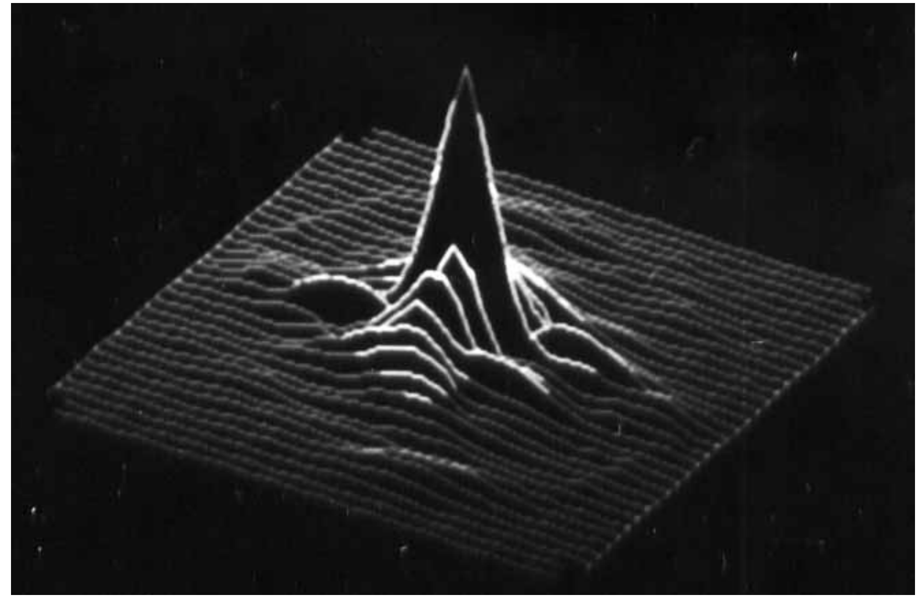

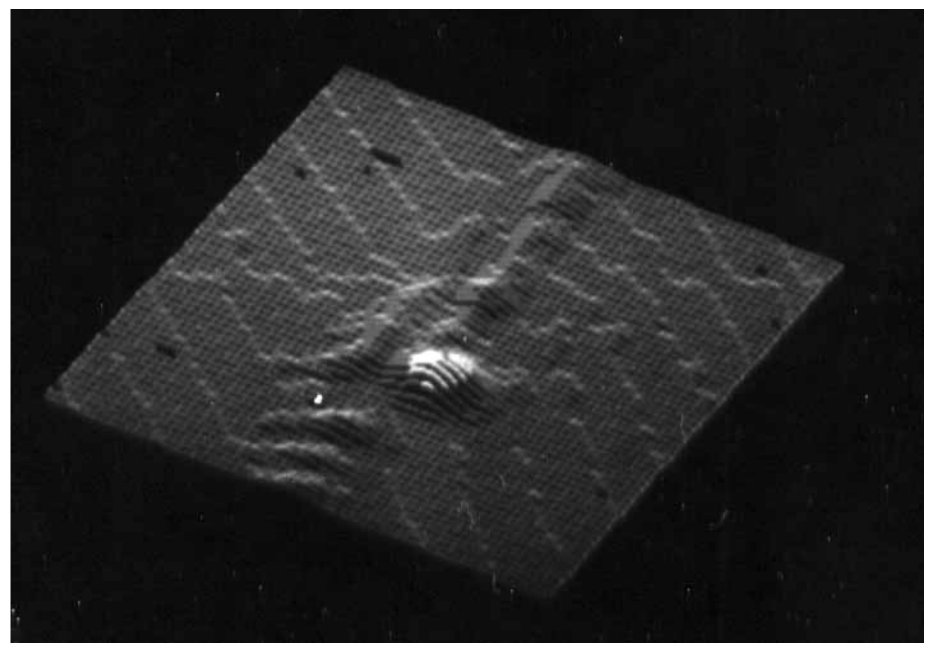

MTF measurement

Test pattern

Spoke chart

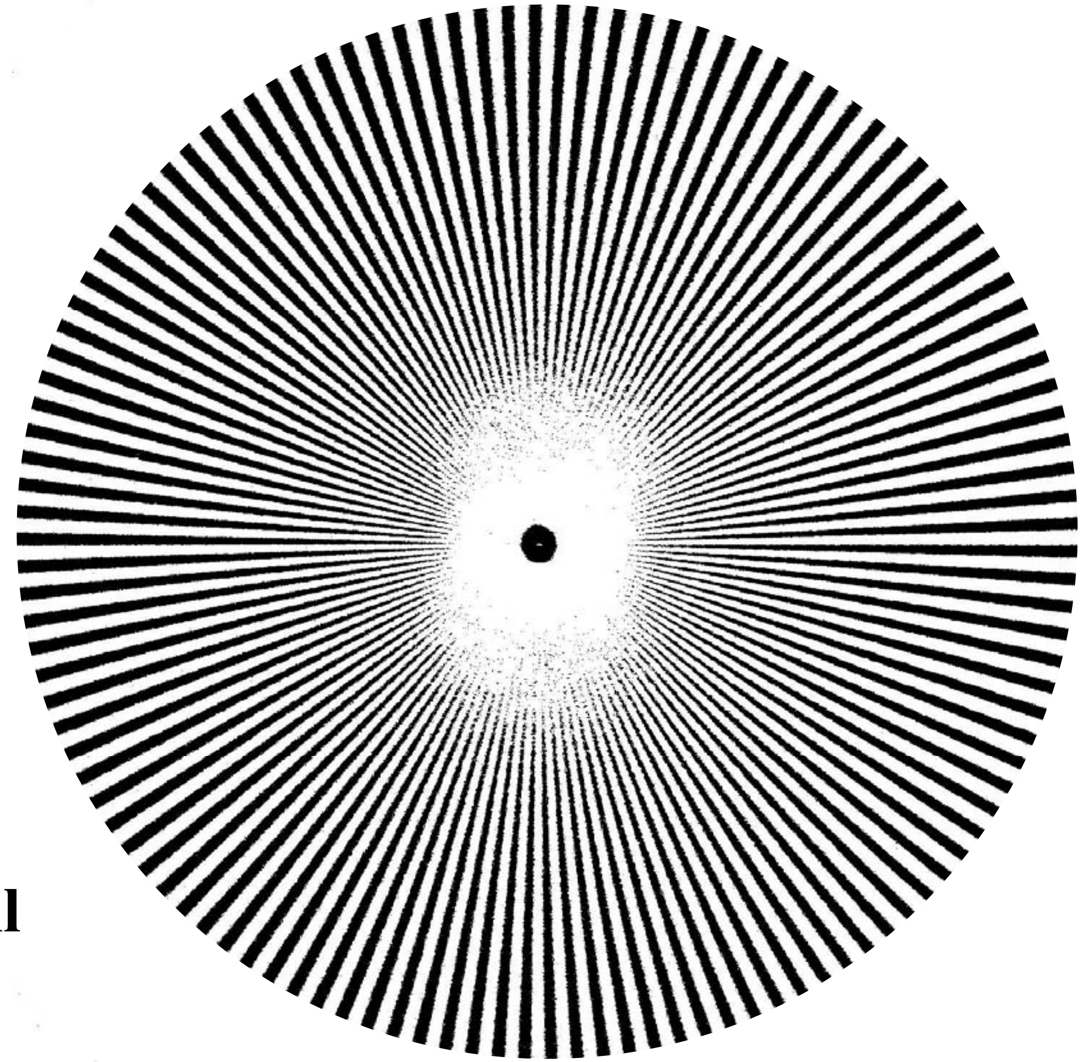

From center to edge, spatial frequency will change higher to lower

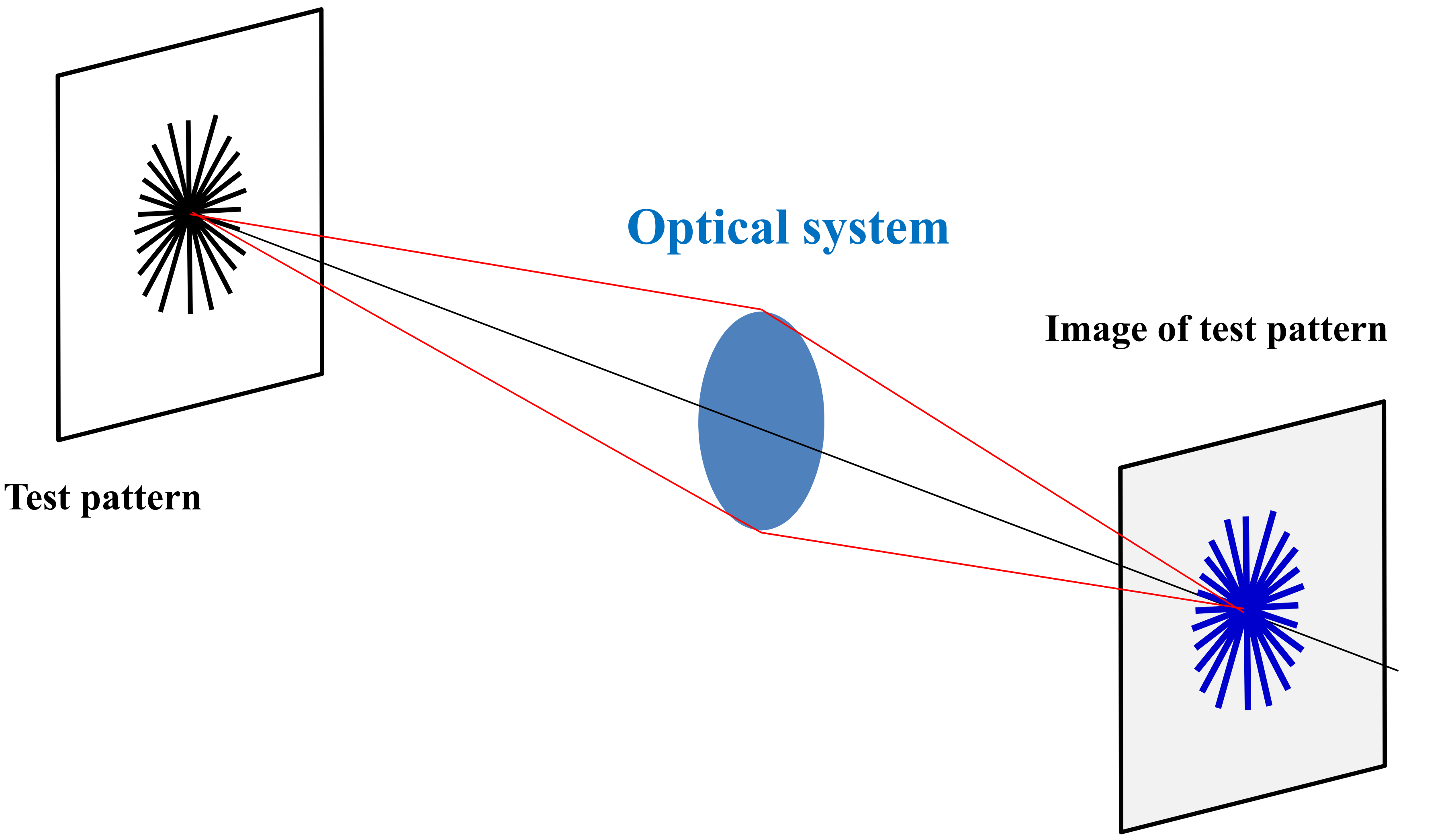
Optical system
Image of test pattern
Test pattern

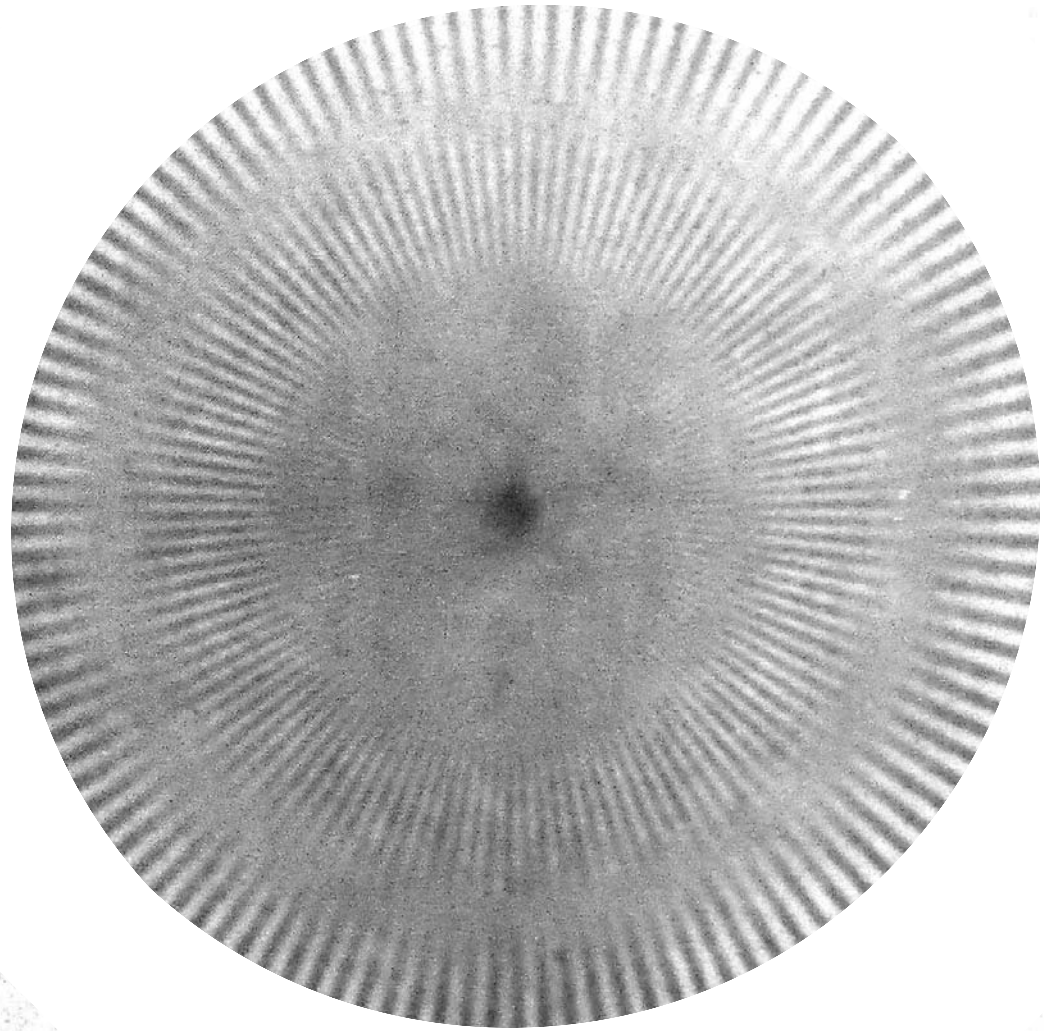

Corresponding MTF

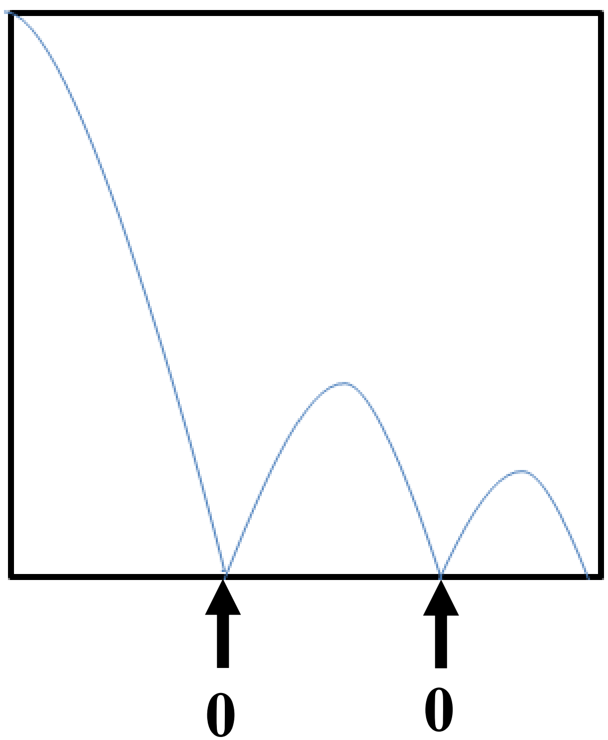

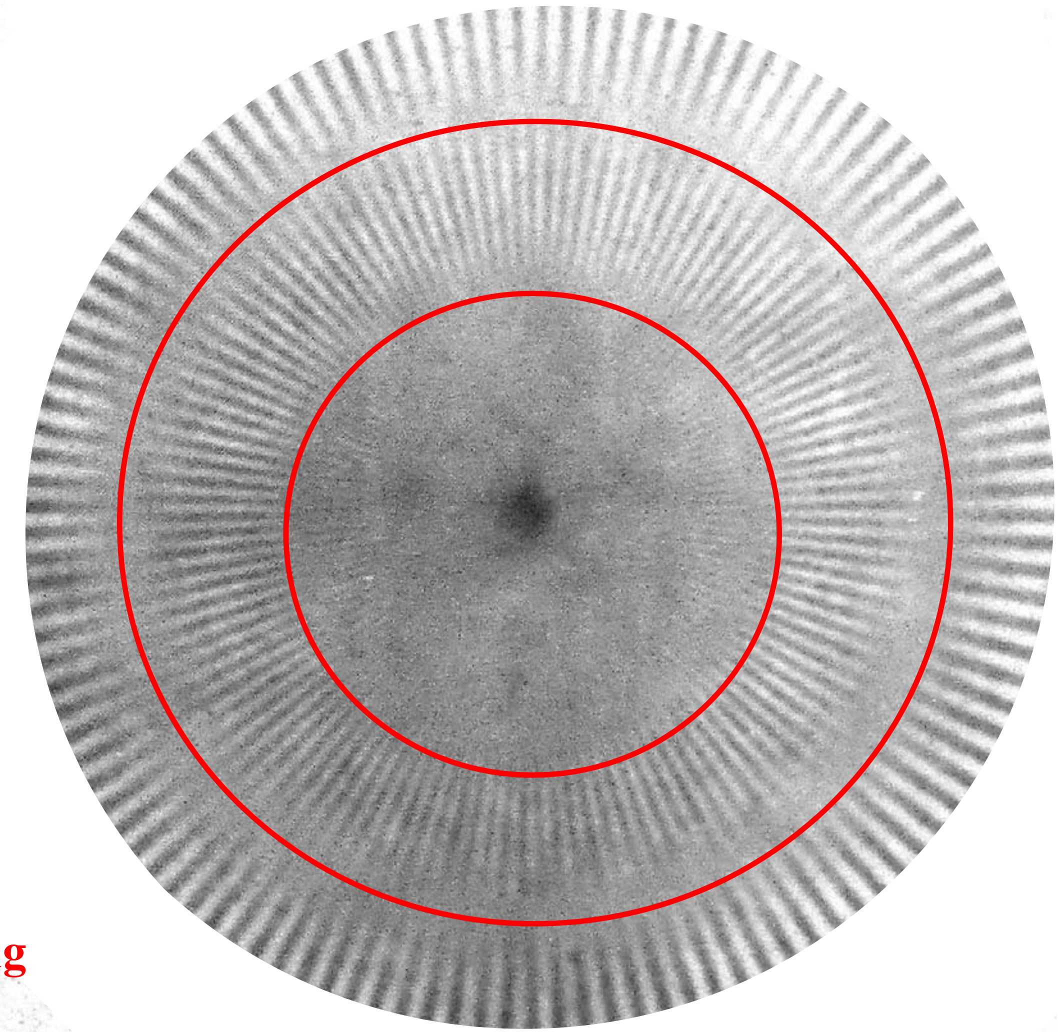

Information at corresponding spatial frequencies are not transmitted

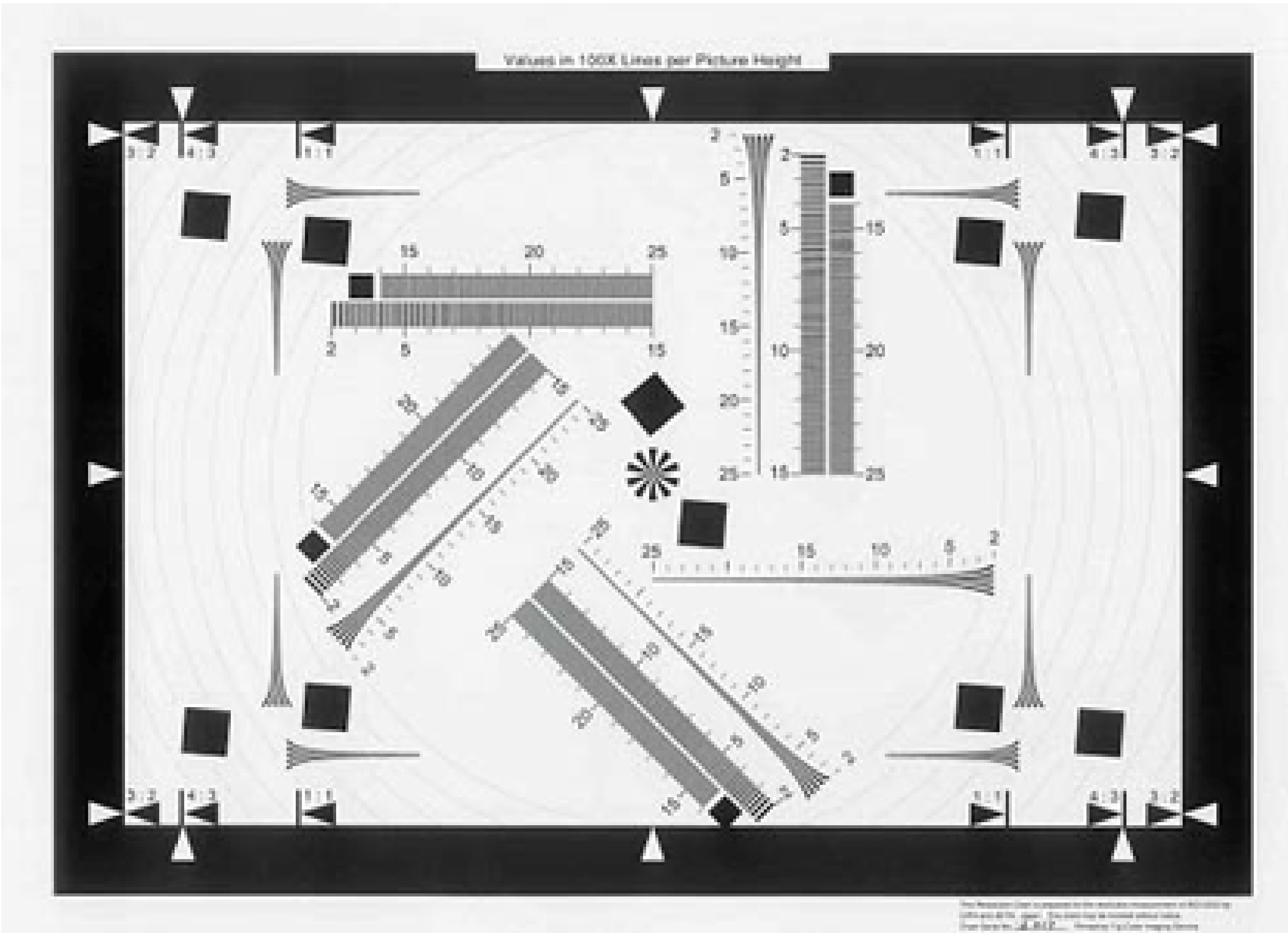
Values in 100X Lines per Picture Height
3 : 2
4 : 3
1 : 1

Streak camera reflective input optics

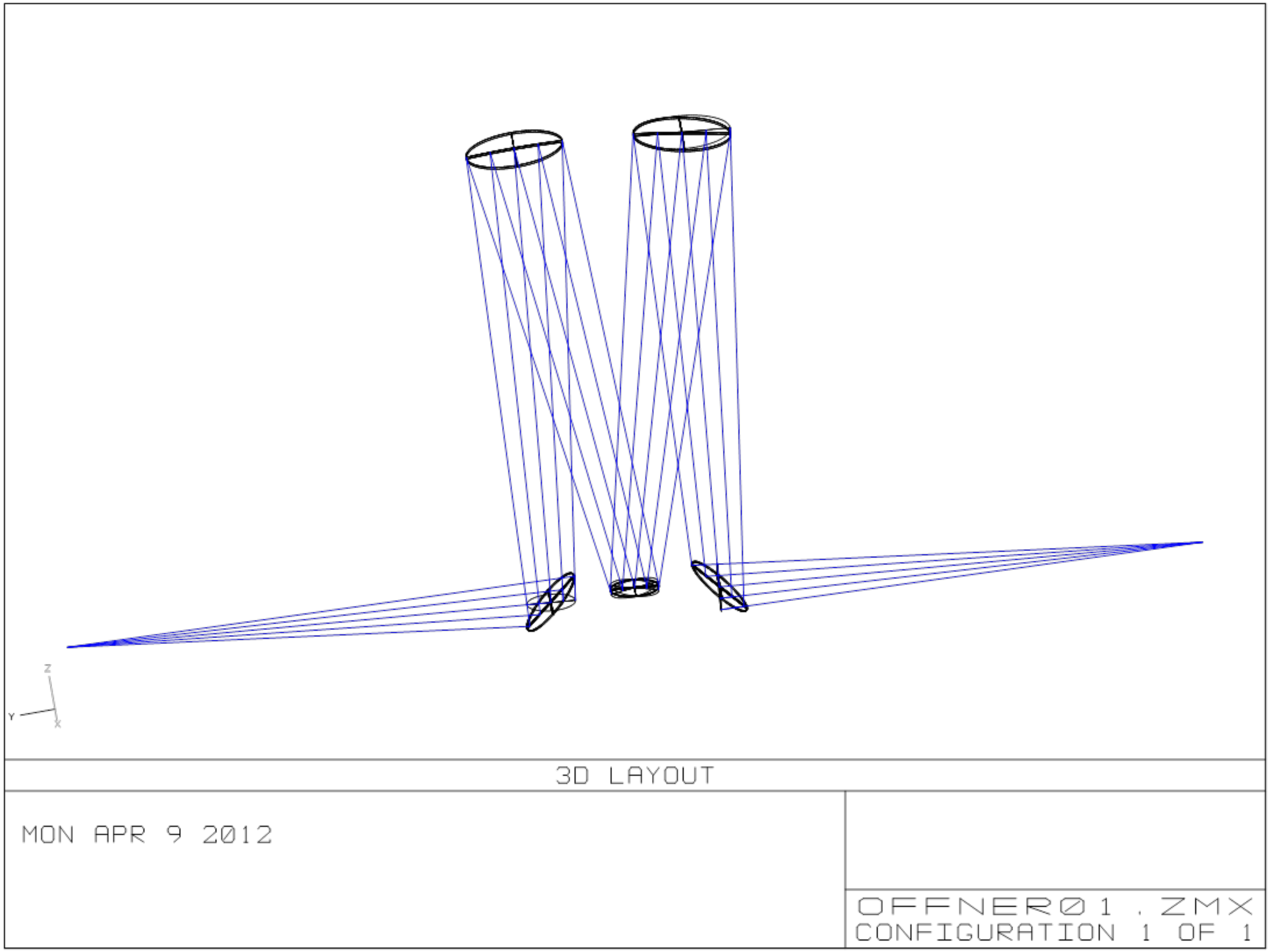

Optical performance of reflective relay

OPD<0.055μm

2σ PSF width   5.06μm

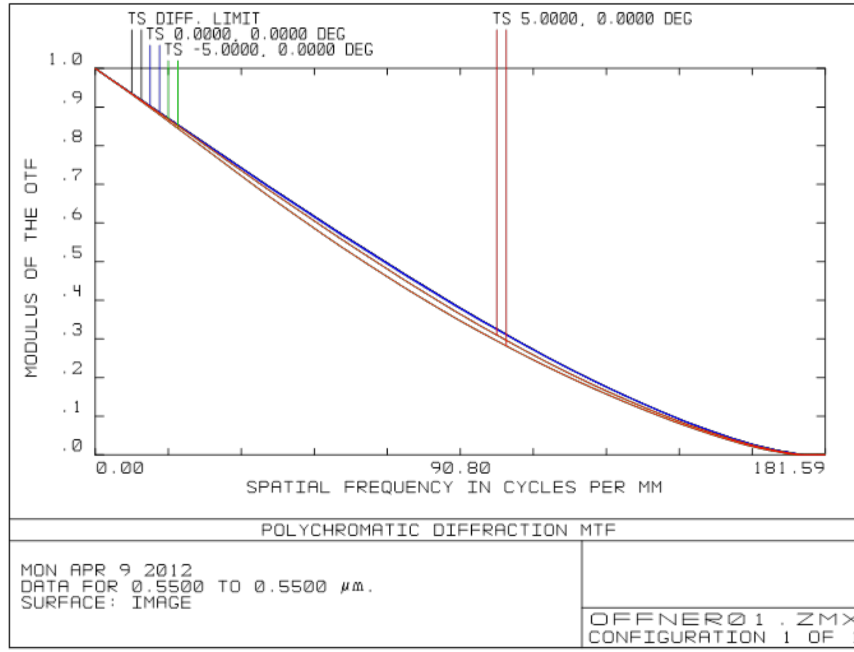

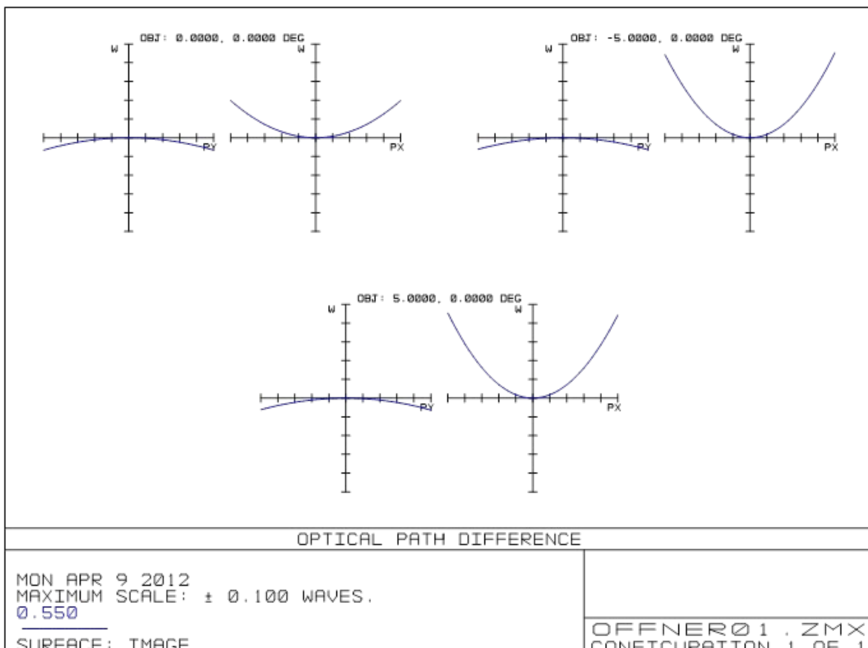

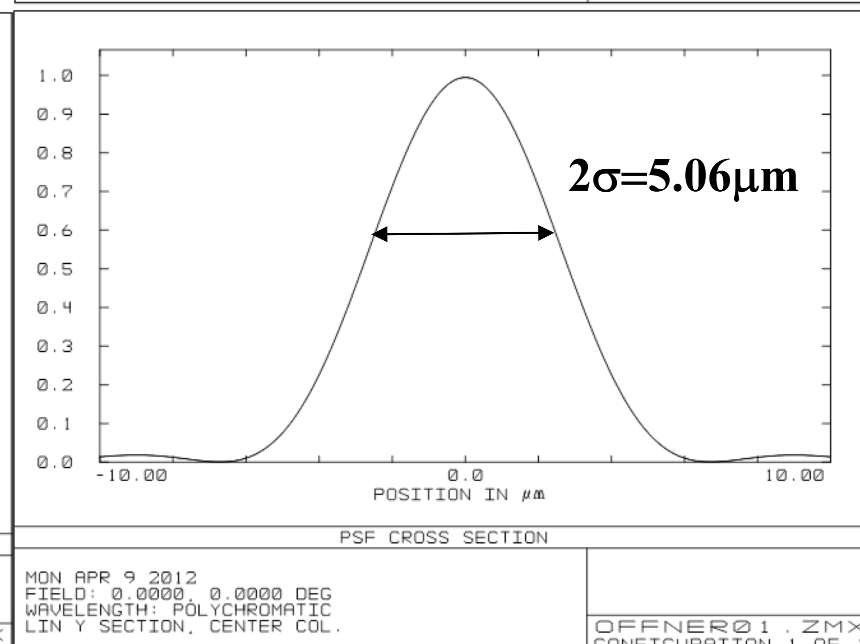

Interesting property of double aperture

Interesting property of double aperture

Extraction mirror with cold finger

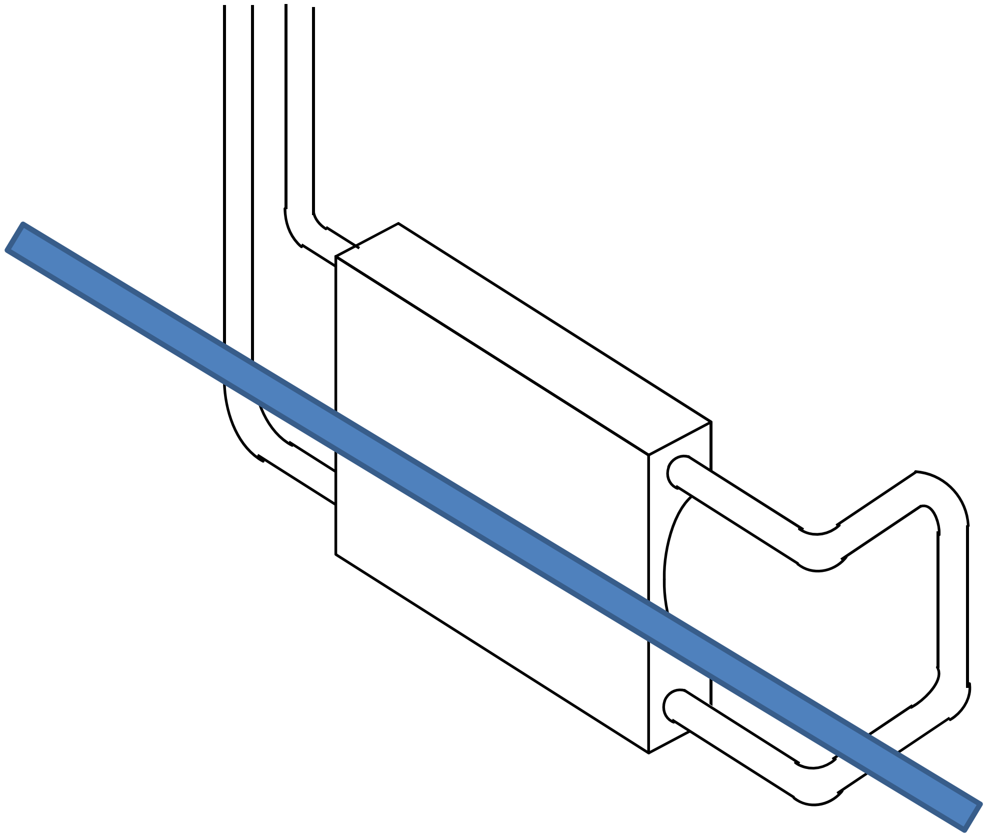

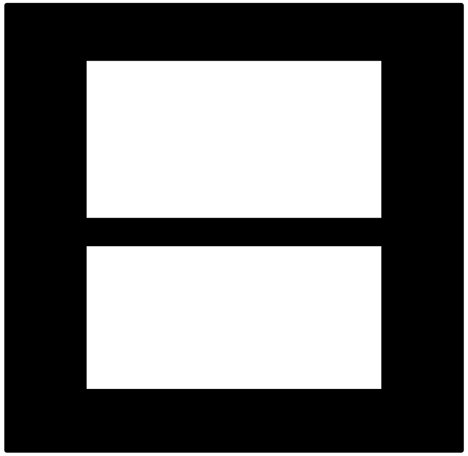

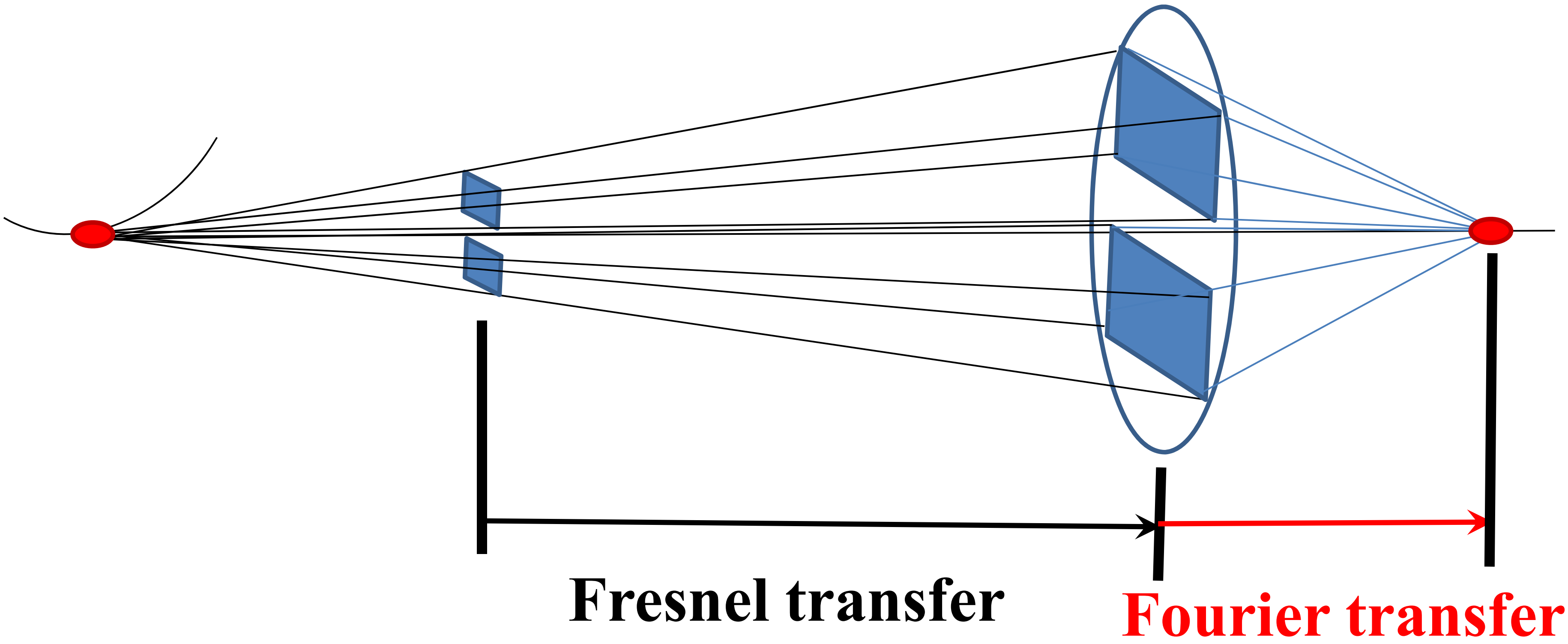
Fresnel transfer
Fourier transfer

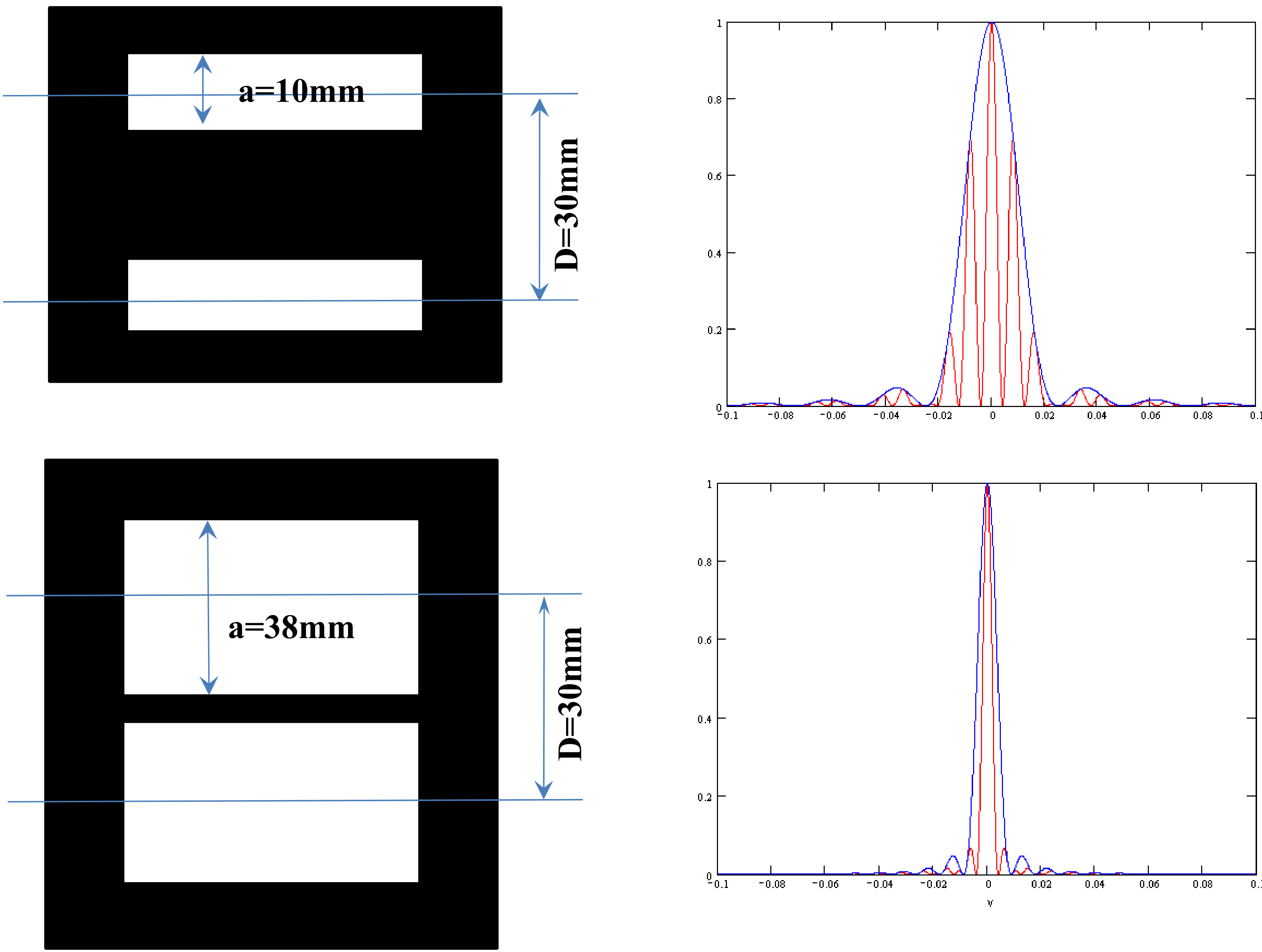
a=10mm
D=30mm
a=38mm
D=30mm
1
0.8
0.6
0.4
0.2
0
-0.1
-0.08
-0.06
-0.04
-0.02
0
0.02
0.04
0.06
0.08
0.1
v

1. **Width of Diffraction envelope is dominated by single aperture height.**

2. **Inside diffraction envelope is modulated by interference of double aperture.**

3. **PSF including interference is almost same width of diffraction with full aperture, but contrast is more worth the single aperture case due to surrounding fringes.**
   Seems still better than large thermal deformation of mirror.

Conclusions

1. **Good extraction mirror**
   Identification of extraction mirror deformation is important
2. **Good optical path design**
   Optical path having no focusing components or double optical path
3. **Good lens or reflector for focusing system**
   Do not use singlet lens even monochromatic light!
4. **Good alignment**

MTF measurement is very helpful to know performance of your optical system!

Thank you for your attention!

Decomvolution with OTF

Decomvolution using the Wiener inverse filter

Fourier transform of blurred image $G(f_x,f_y)$ in spatial frequency domain (f_x,f_y) is given by,

$$G(f_x,f_y)=\mathscr{H}(f_x,f_y)F(f_x,f_y) + N(f_x,f_y)$$

where $\mathscr{H}(f_x,f_y)$ is thought as a inverse filter (Fourier transform of PSF), $F(f_x,f_y)$ is a Fourier transform of geometric image, and $N(f_x,f_y)$ is a Fourier transform of noise in the image). So, inverse problem can be written by,

$$F(f_x,f_y)=\frac{G(f_x,f_y)-N(f_x,f_y)}{\mathscr{H}(f_x,f_y)}$$

Winner introduce so-called winner's inverse filter;

$$H_w(f_x, f_y) = \frac{\mathscr{H}^*(f_x, f_y)}{\left| \mathscr{H}(f_x, f_y) \right|^2 + \dfrac{\phi_n(f_x, f_y)}{\phi_f(f_x, f_y)}}$$

where asterisk indicates the complex conjugate of $\mathscr{H}$, and ϕ_n is a power spectra of the noise, and ϕ_f is a power spectra of the signal.

PSF to evaluate inverse filter for decomvolution

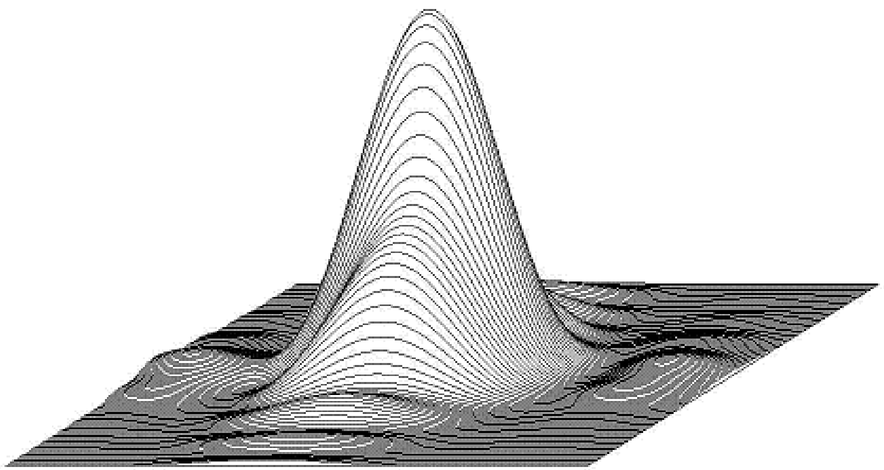

Original image of beam

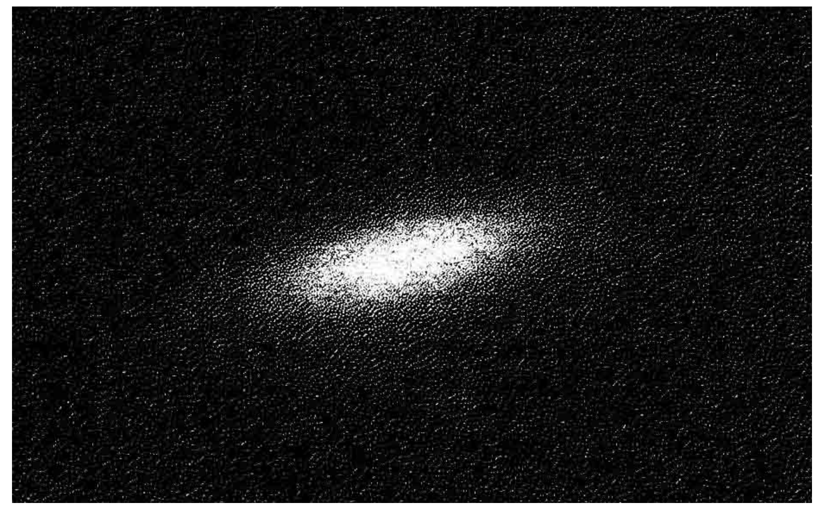

Original image

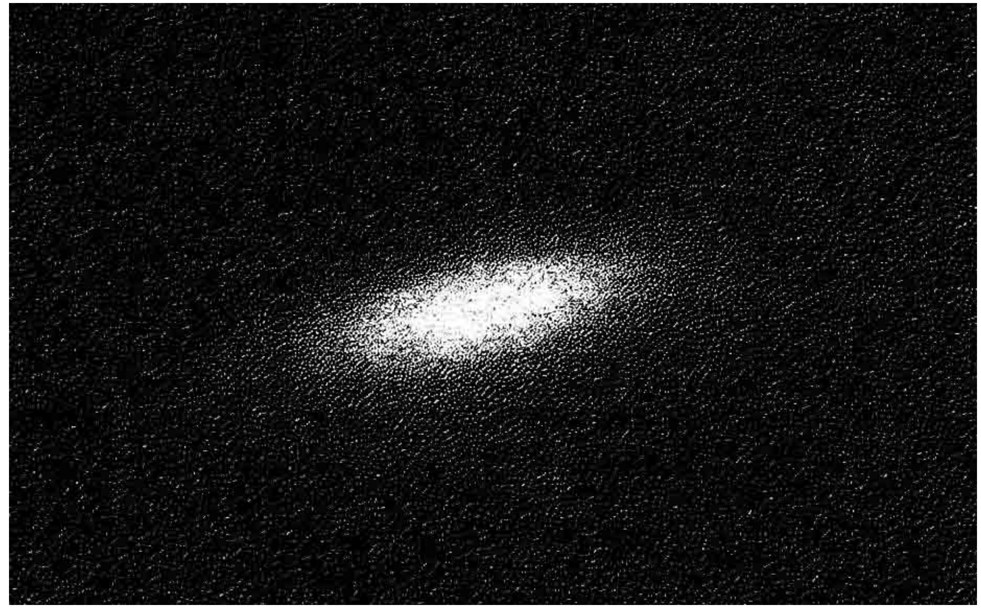

Image after decomvolution

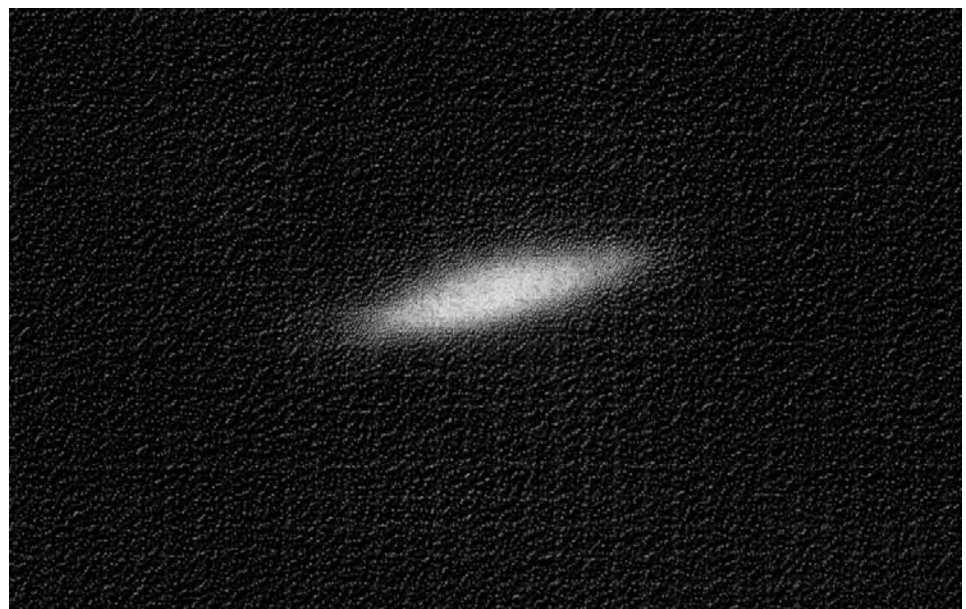

Application of Adaptive optics to correct thermal deformation of extraction mirror

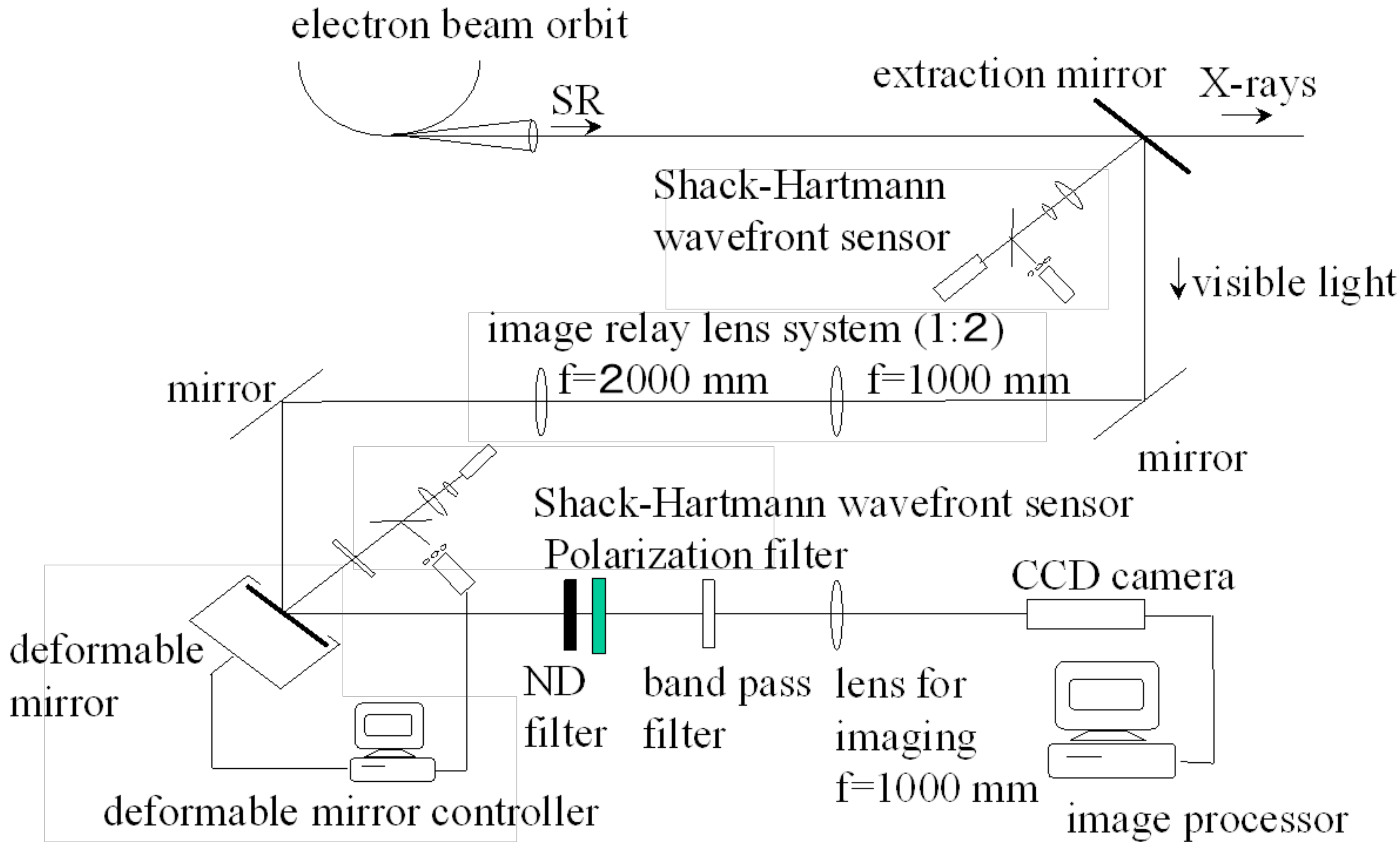

electron beam orbit
SR
extraction mirror
X-rays
Shack-Hartmann
wavefront sensor
visible light
image relay lens system (1:2)
f=2000 mm
f=1000 mm
mirror
mirror
Shack-Hartmann wavefront sensor
Polarization filter
CCD camera
deformable
mirror
ND
filter
band pass
filter
lens for
imaging
f=1000 mm
image processor
deformable mirror controller

Deformable mirror

Bimorph corrector mirror

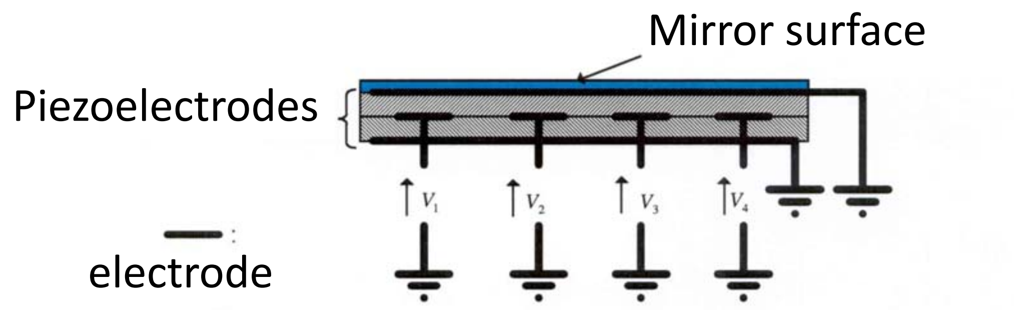

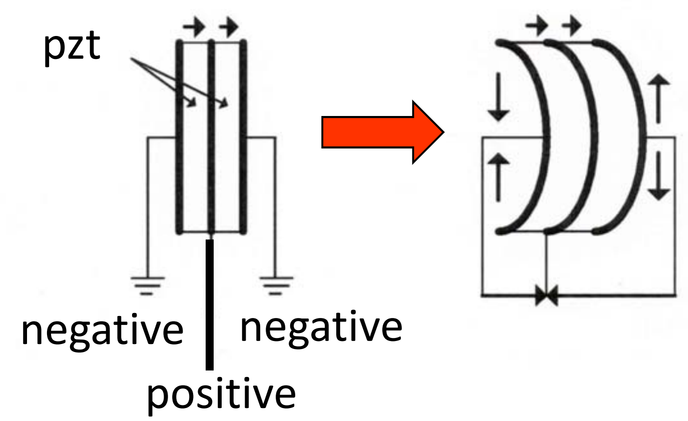

Arrangement of pzt

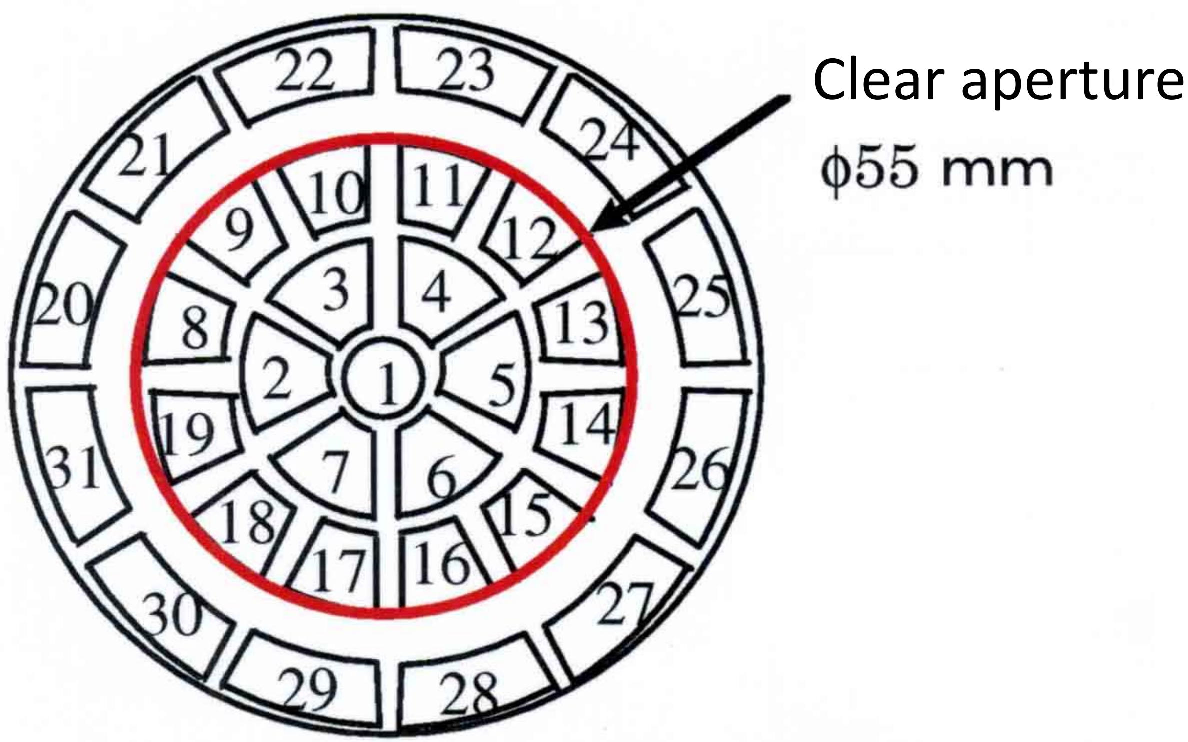

Response of deformation

Electrode No.1

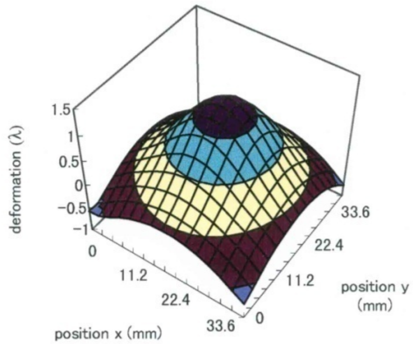

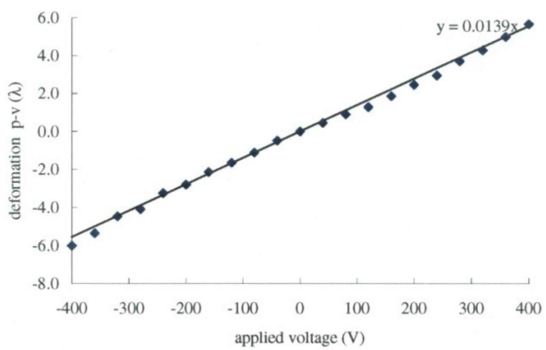

Electrode No.2

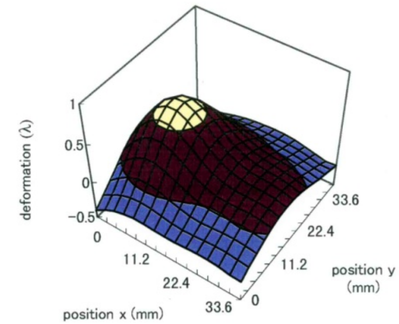

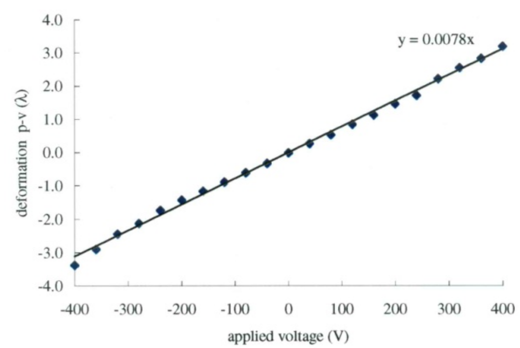

example of wavefront correction at beam current 92mA.

A: wavefront by SR extraction mirror,

B: wavefront by deformable mirror,

C: summation of A and B.

A

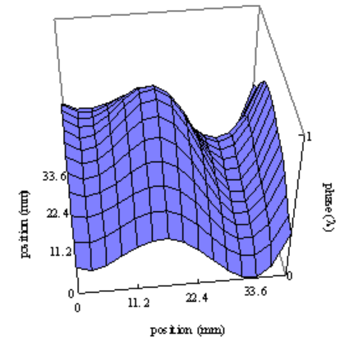

p-v : 0.911
rms. : 0.211

B

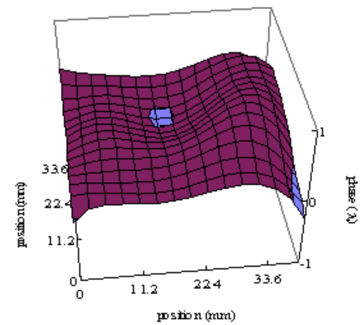

p-v : 0.921
rms. : 0.171

C

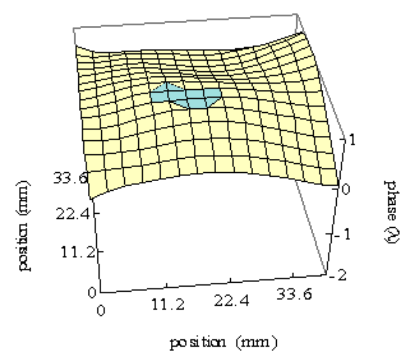

p-v : 1.01
rms. : $\lambda/5.0$

Result of wavefront correction at 12.6mA

uncorrected image σ_x=430μm
σ_y=240μm

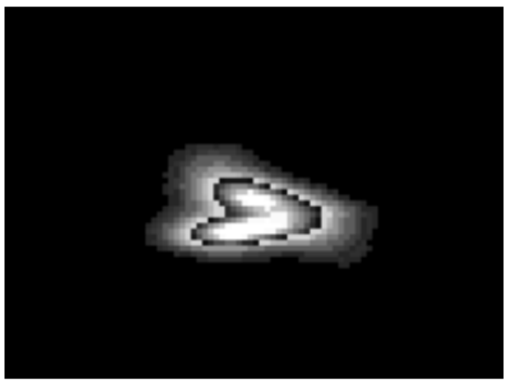

corrected image σ_x=255μm
σ_y=139μm

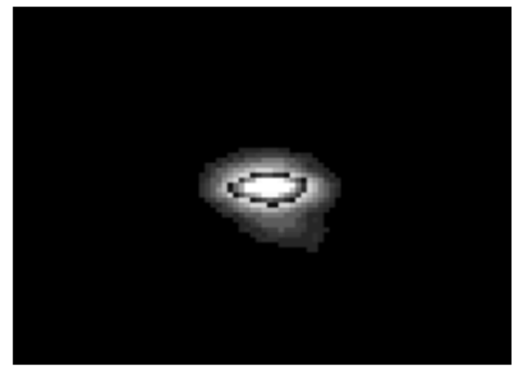

remaining wavefront error p-v : λ/2.7,
rms. : λ/12.5

Result of wavefront correction at 92.0mA

uncorrected image σ_x=250μm σ_y=237μm

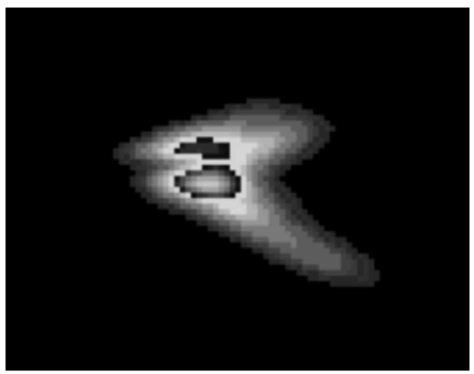

corrected image σ_x=254μm σ_y=139μm

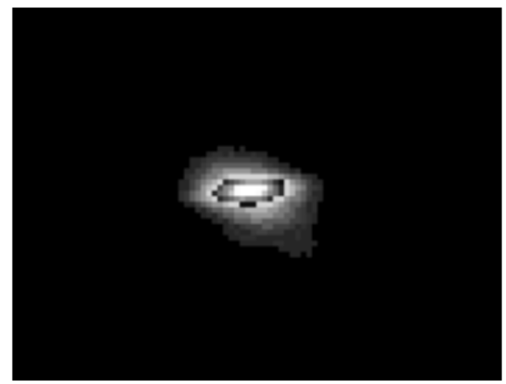

remaining wavefront error p-v : λ/2.7,
rms. : λ/5.0

Dynamical observation of beam profile with high-speed gated camera

Function of high-speed gated camera

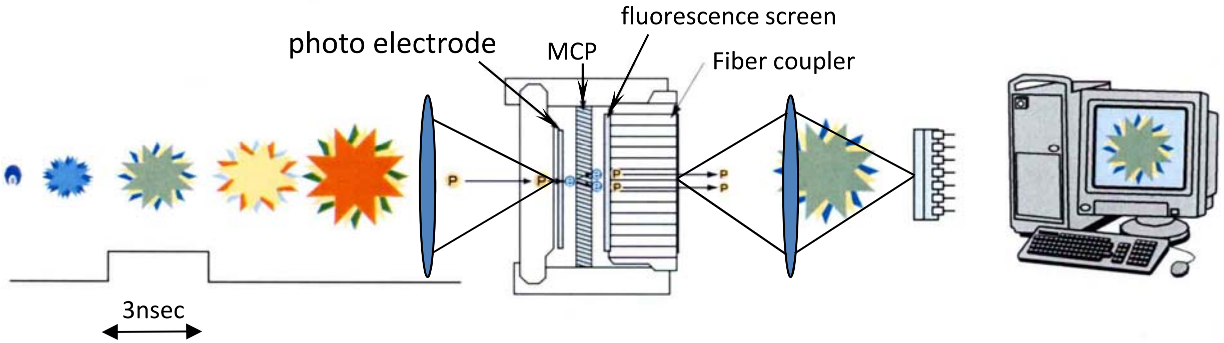

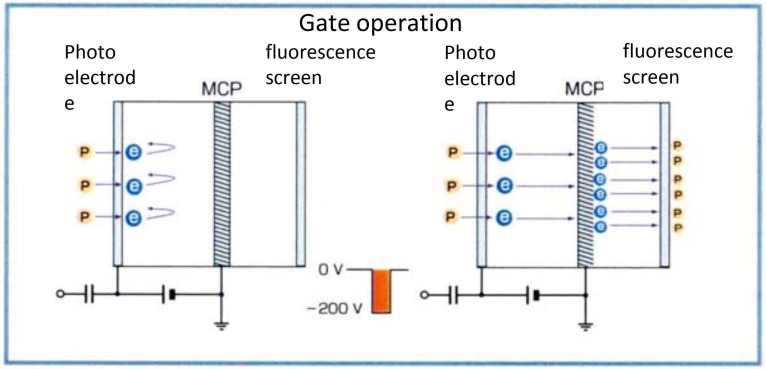

Results of bunch by bunch beam size measurement at KEK B-factory

Blowup of the beam size
 in bunch train due to
photoelectron instability
was observed.

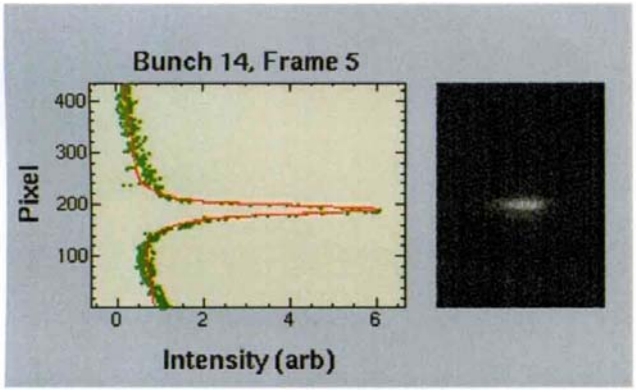

Typical bunch profile with two-component Gaussian fit profile superimposed.

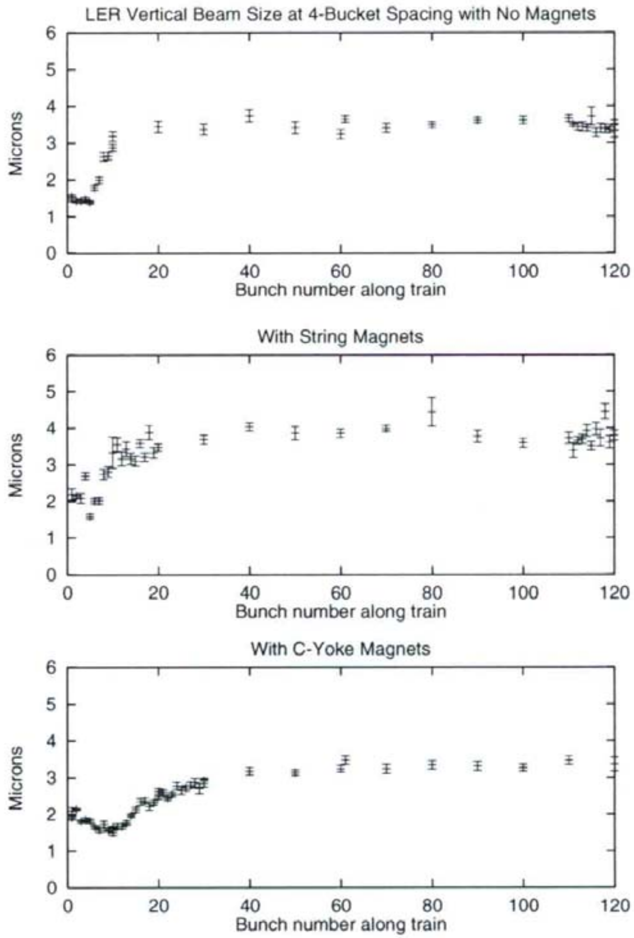

Bunch train profiles for the cases of a) no permanent magnets, b) "string" permanent magnets and c) C-yoke permanent magnets.

Dynamical observation of injected beam profile by high-speed gated camera at the Photon factory.

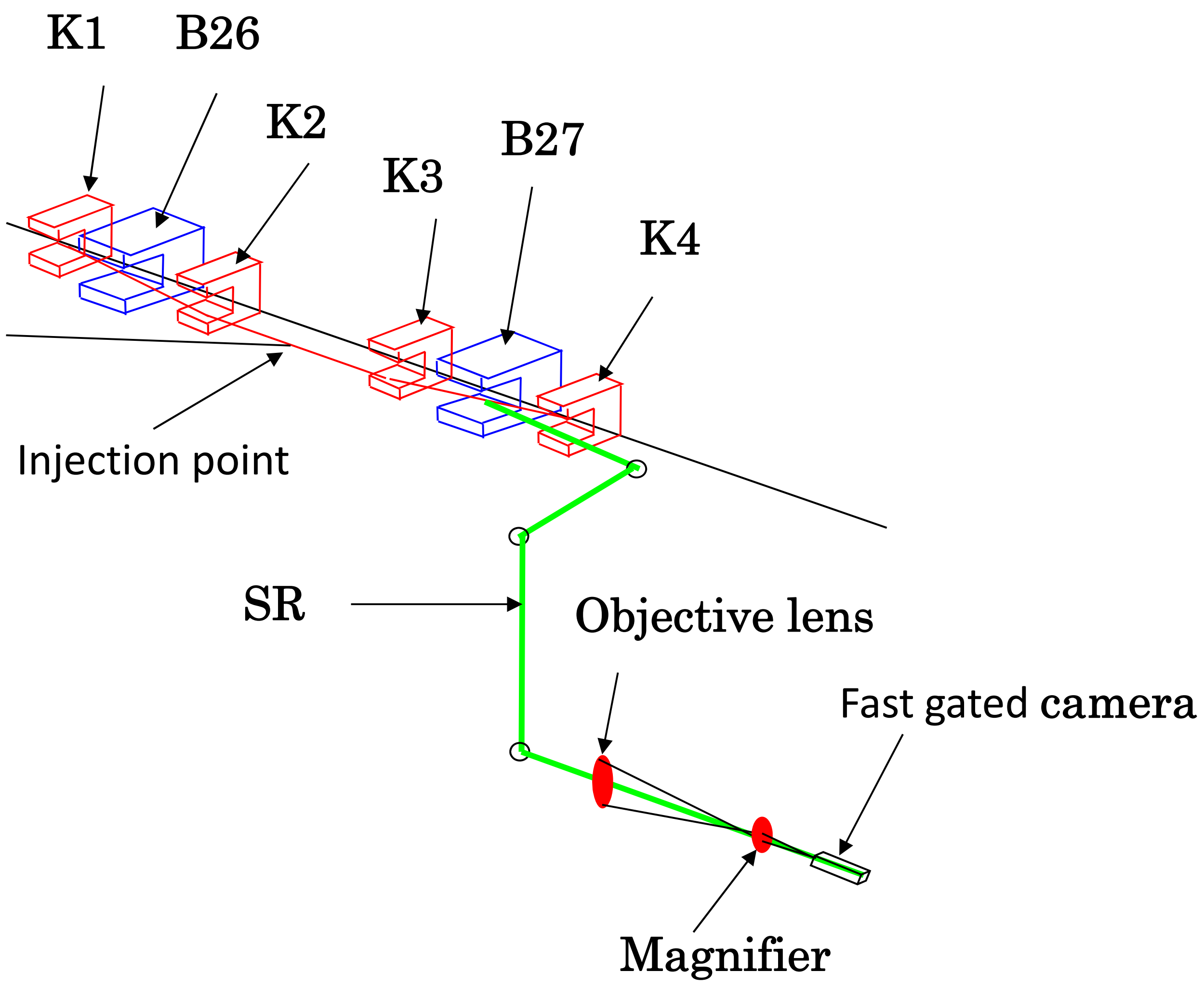

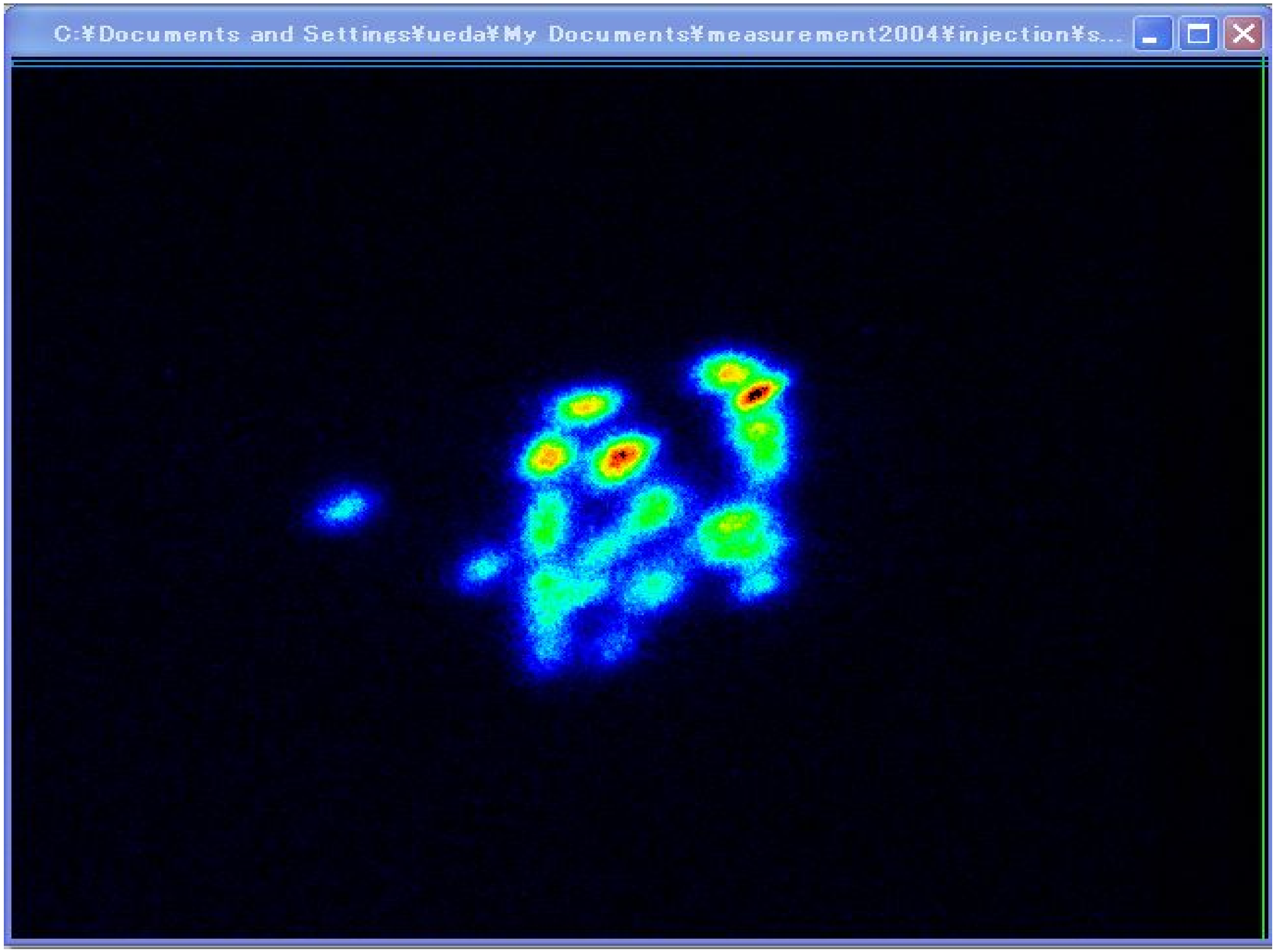
C:¥Documents and Settings¥ueda¥My Documents¥measurement2004¥injection¥s...

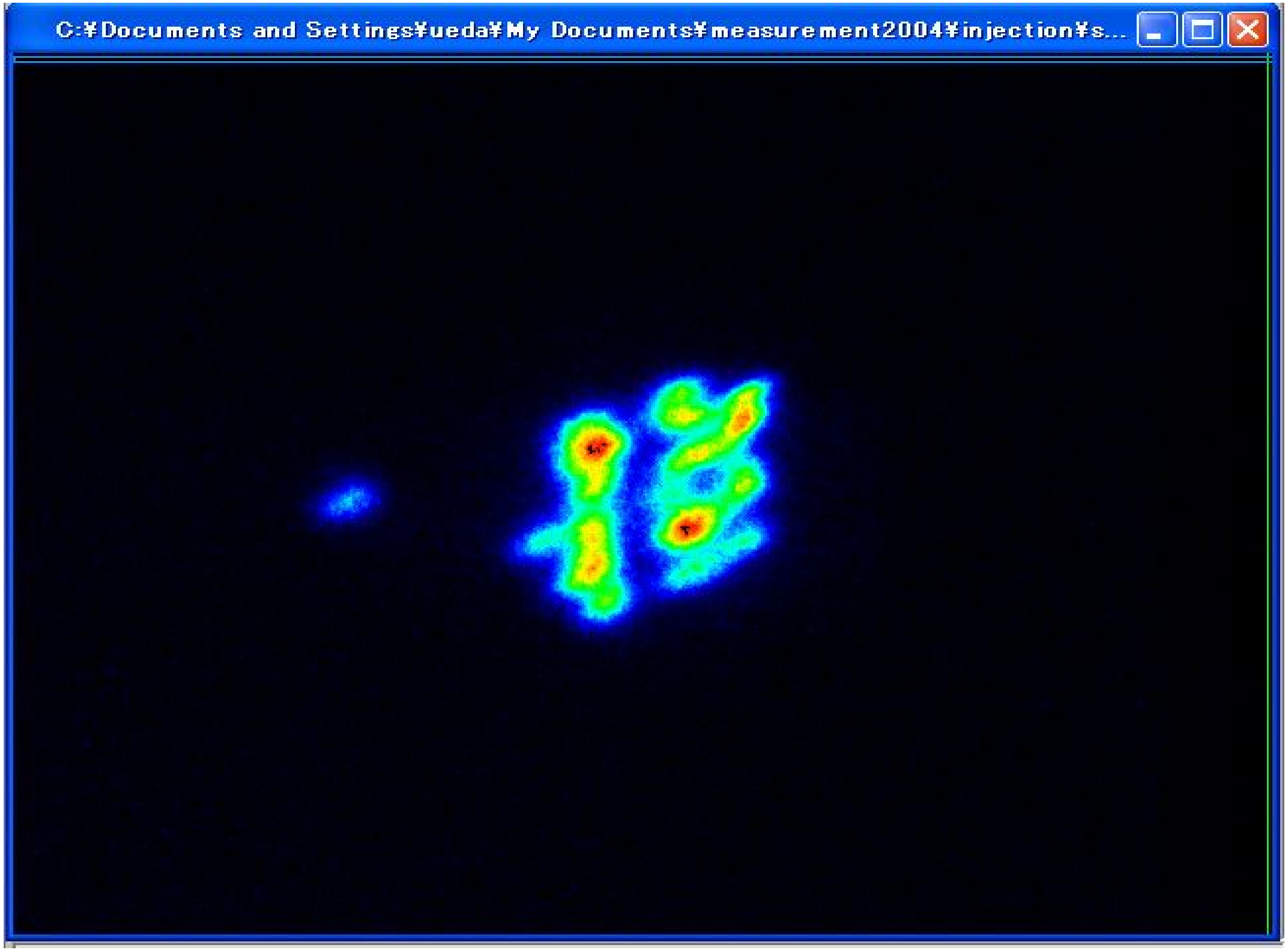
C:¥Documents and Settings¥ueda¥My Documents¥measurement2004¥injection¥s...

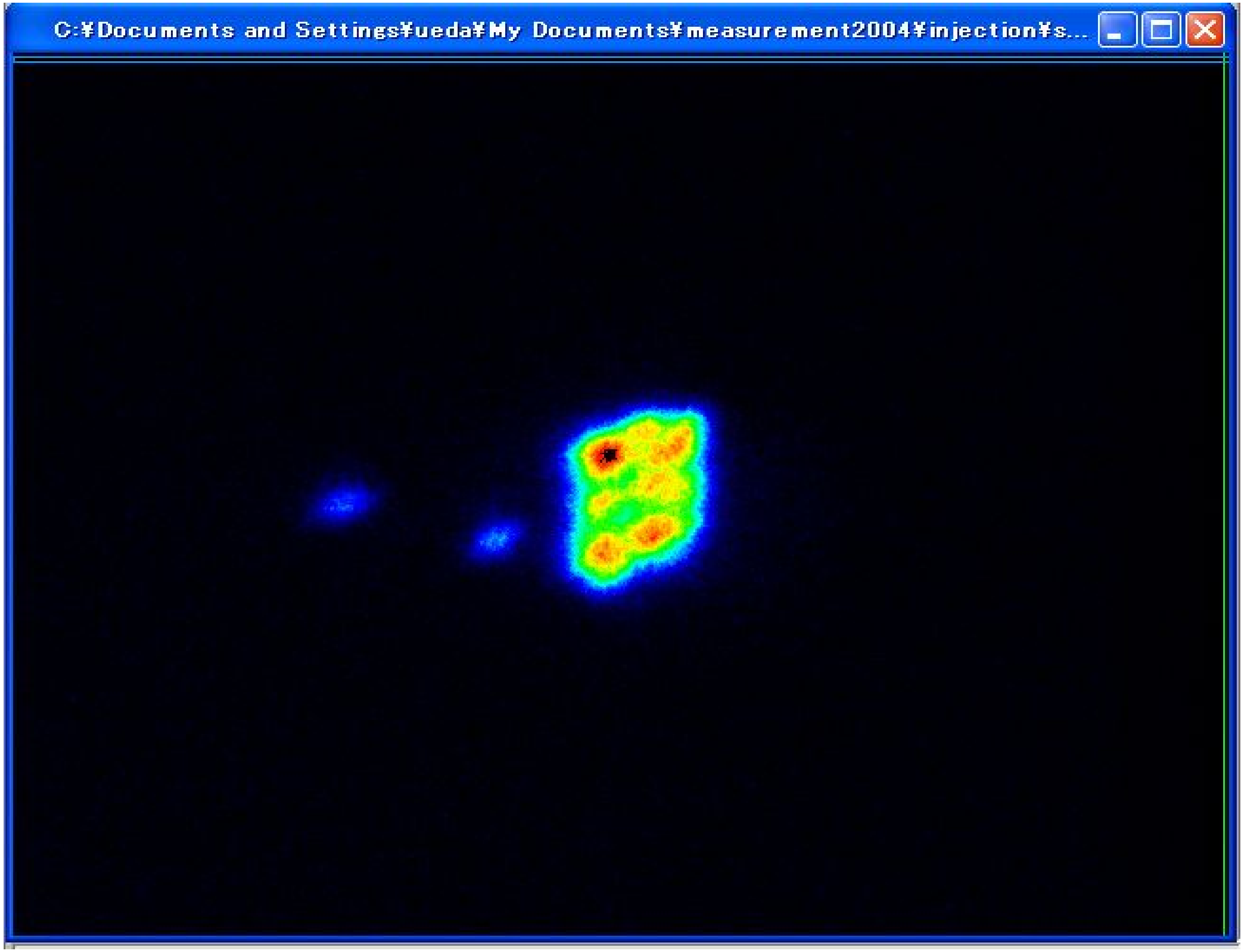
C:¥Documents and Settings¥ueda¥My Documents¥measurement2004¥injection¥s...

This kind of dynamical observation of the injected beam is very helpful to regulate Top-up injection!

Streak camera technique for longitudinal profile measurement

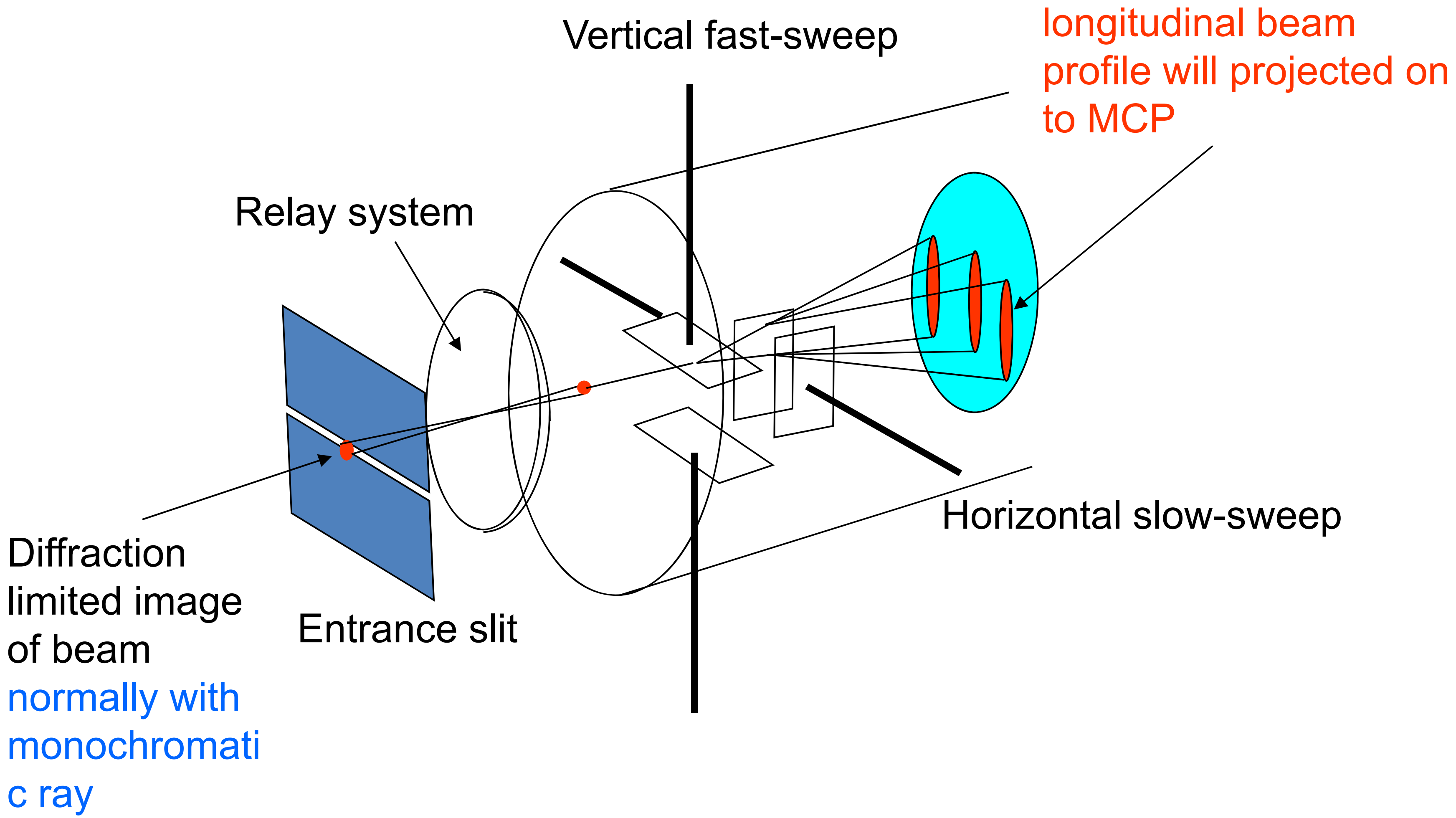
Vertical fast-sweep
longitudinal beam profile will projected on to MCP
Relay system
Horizontal slow-sweep
Diffraction limited image of beam normally with monochromati c ray
Entrance slit

Error in bunch length measurement due to chromatic aberration

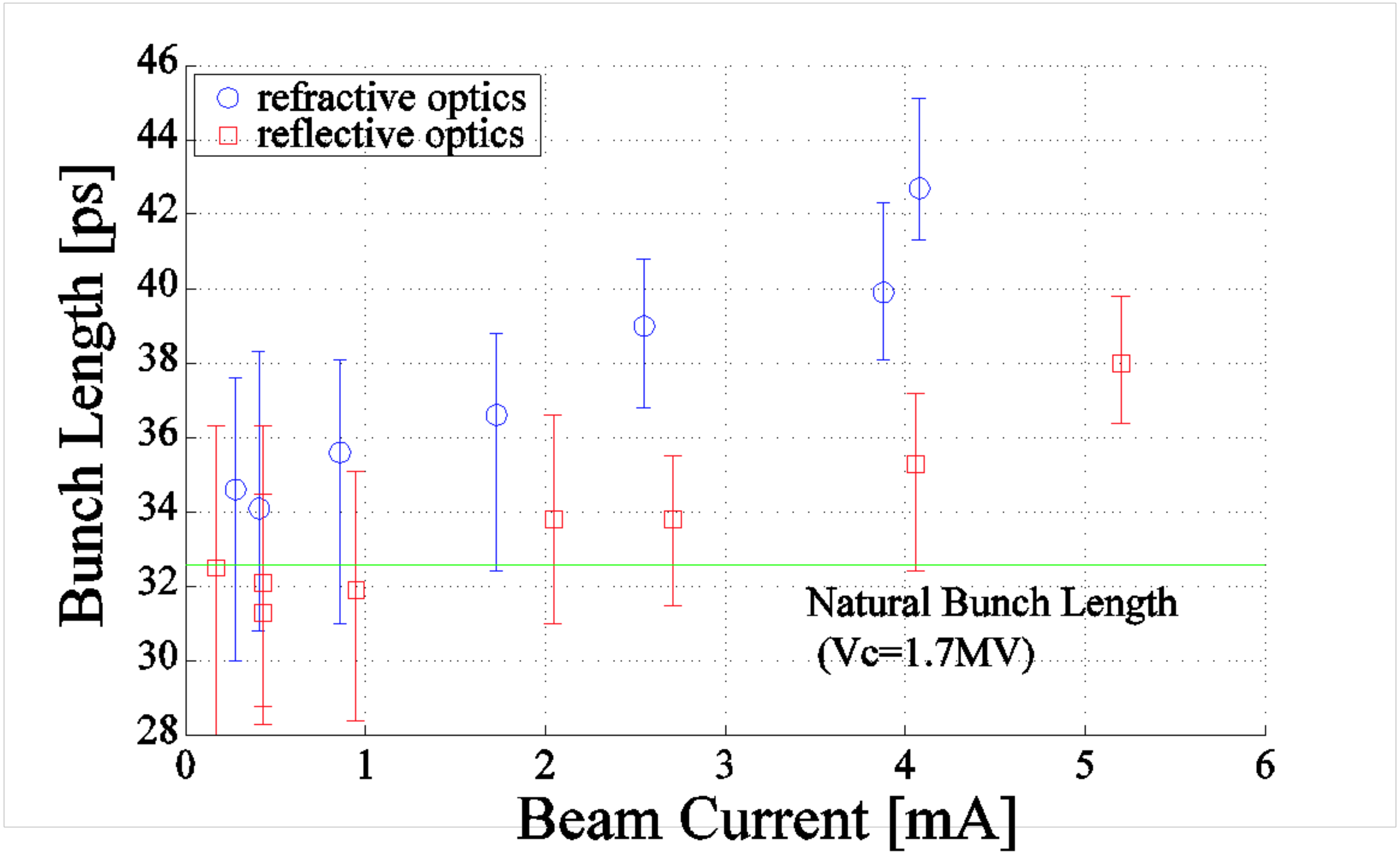

Result of bunch length measurement at the Photon Factory by white ray (non-monochromatic)

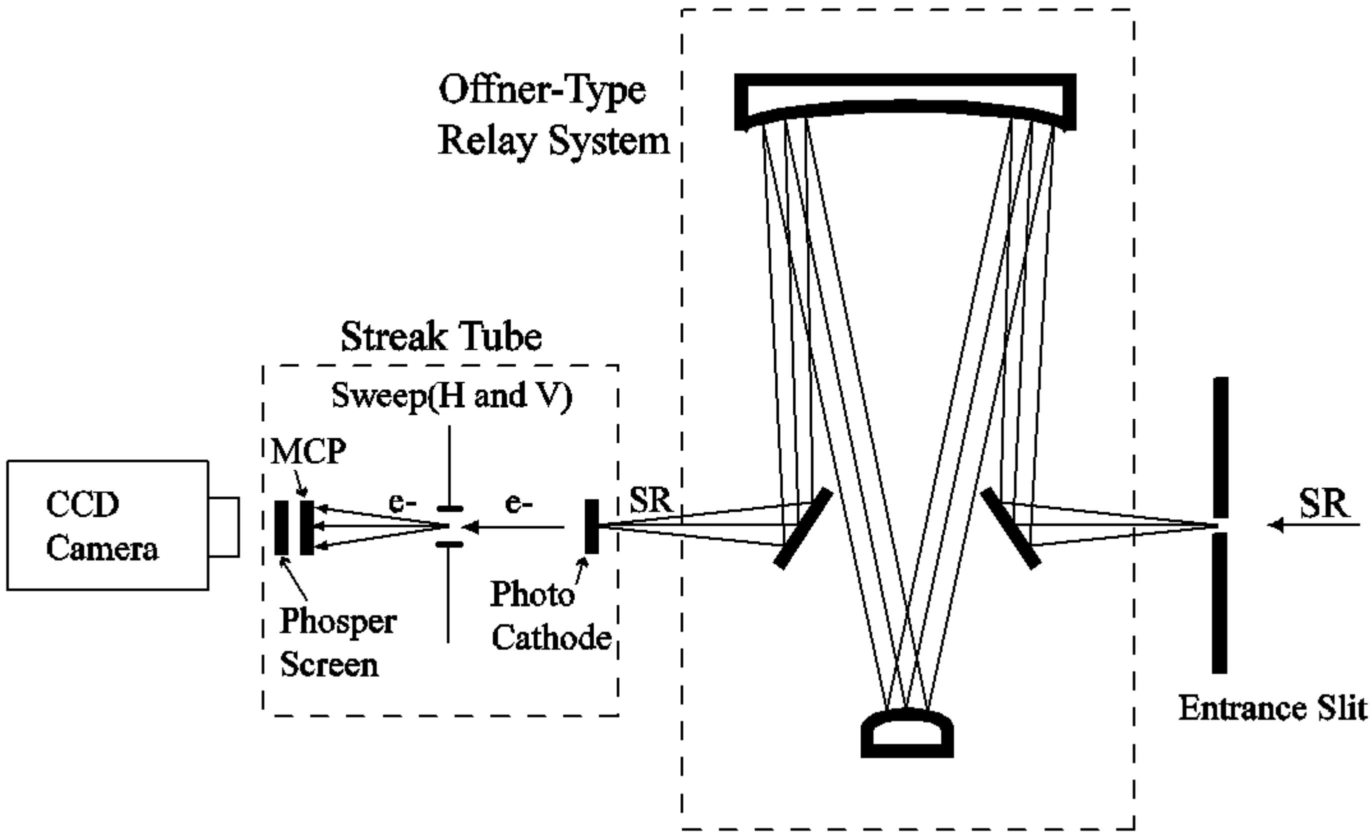
Offner-Type
Relay System
Streak Tube
Sweep(H and V)
MCP
CCD
Camera
e-
e-
SR
SR
Phosper
Screen
Photo
Cathode
Entrance Slit

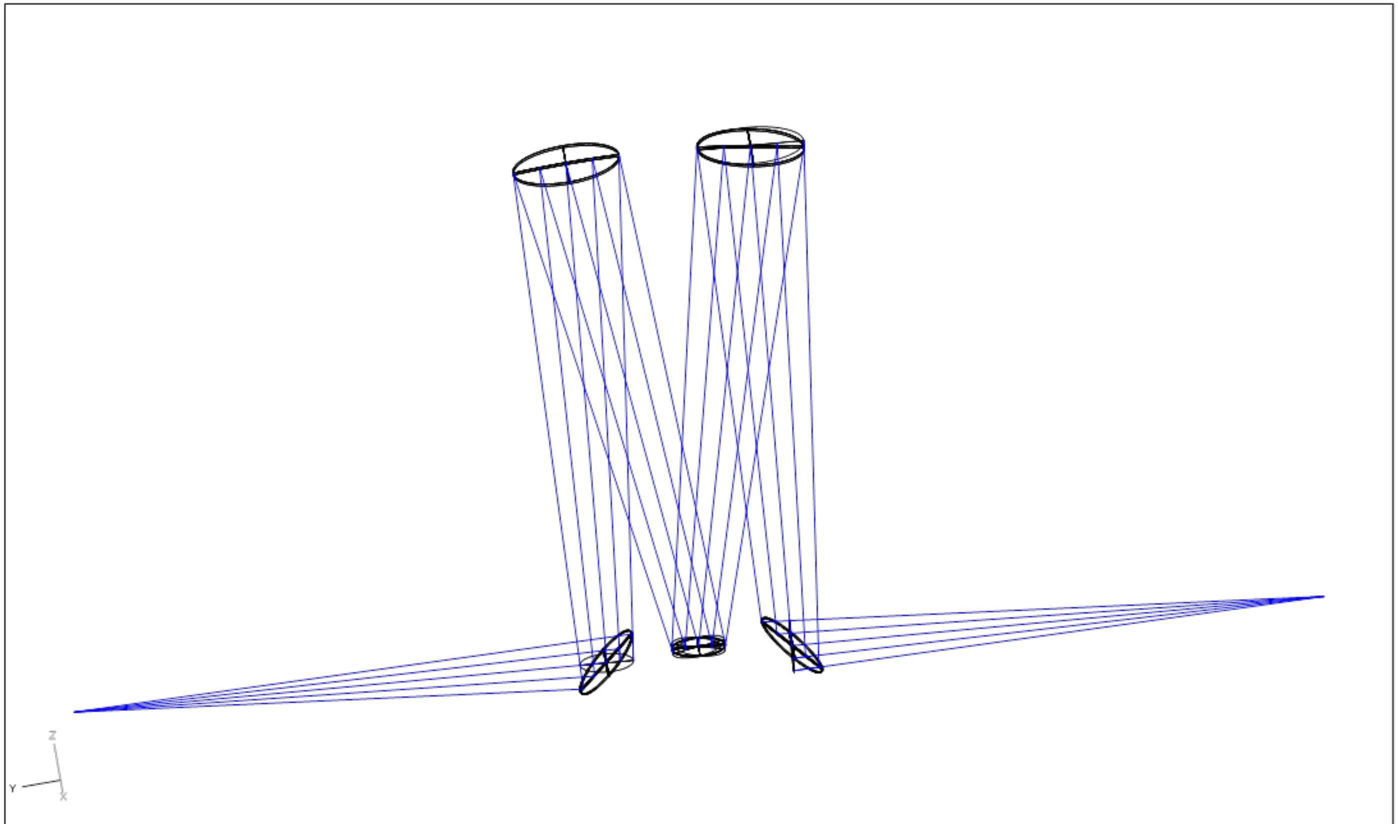

3D LAYOUT

MON APR 9 2012

OFFNER01.ZMX
CONFIGURATION 1 OF 1

Optical performance of reflective relay

OPD<0.055μm

2σ PSF width 5.06μm

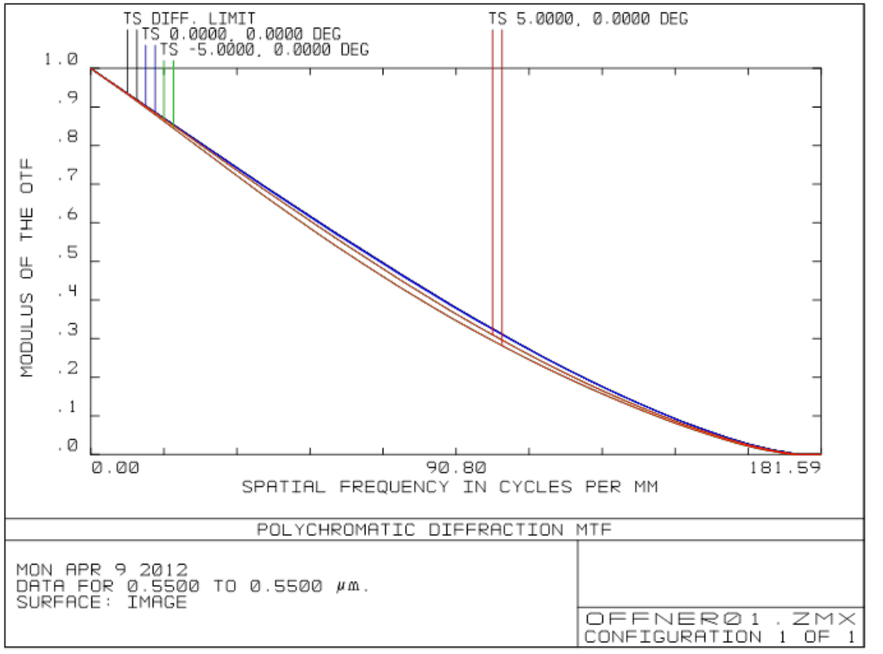

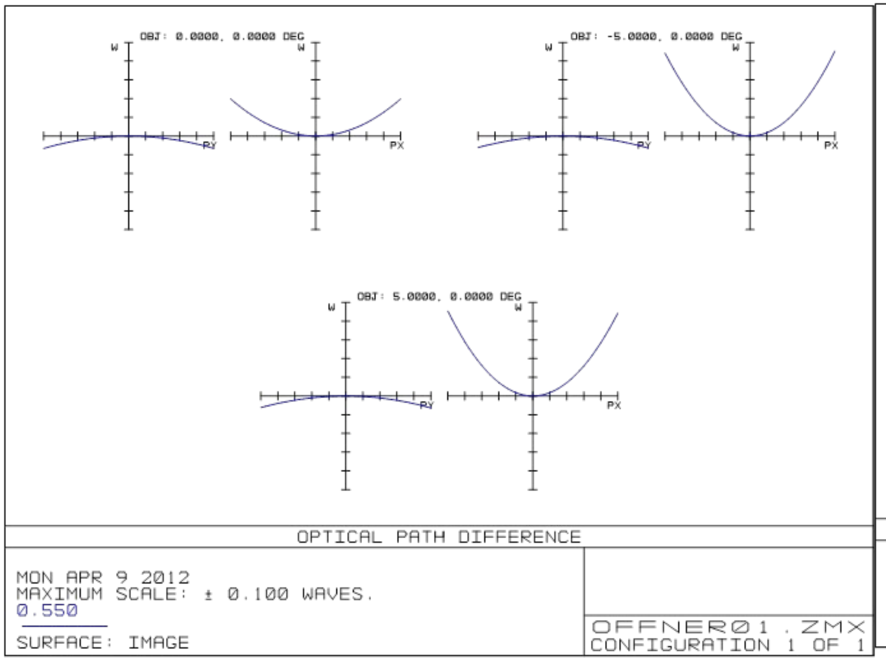

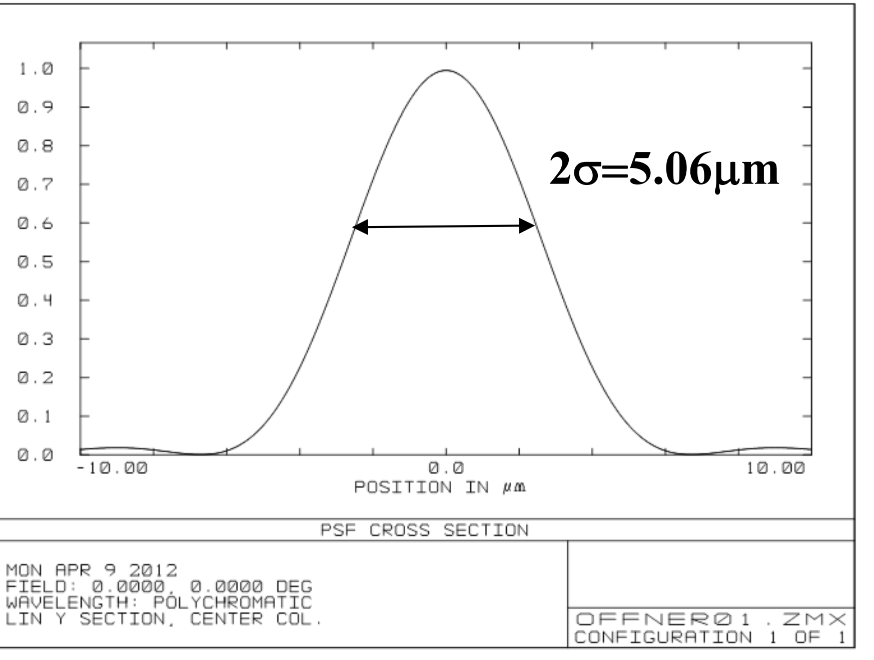

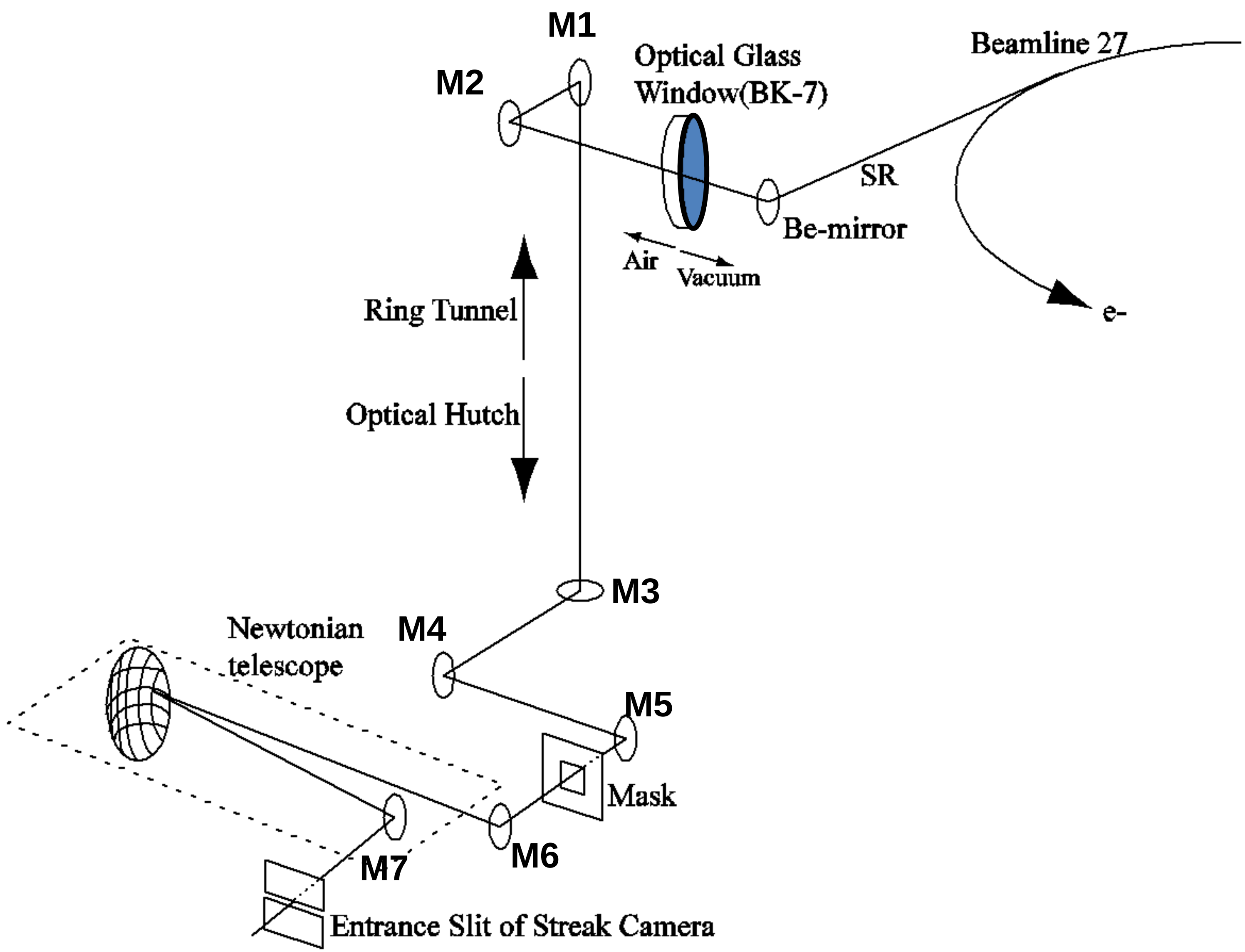
M1
M2
Optical Glass
Window(BK-7)
Beamline 27
SR
Be-mirror
Air
Vacuum
e-
Ring Tunnel
Optical Hutch
M3
M4
Newtonian
telescope
M5
Mask
M6
M7
Entrance Slit of Streak Camera

Result of bunch length at rage between 0.2mA to 70mA

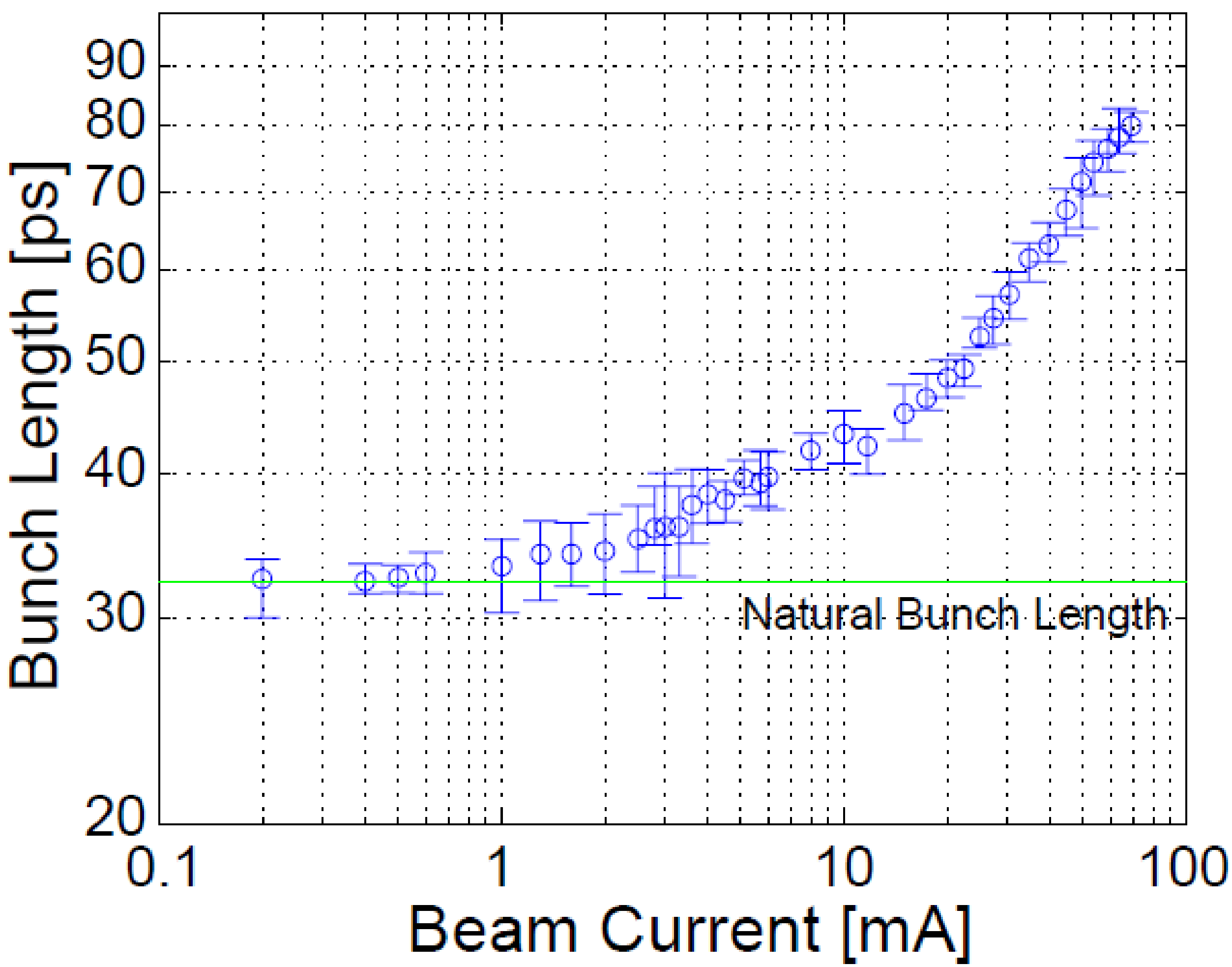

Spatial-temporal observation of bunch motion

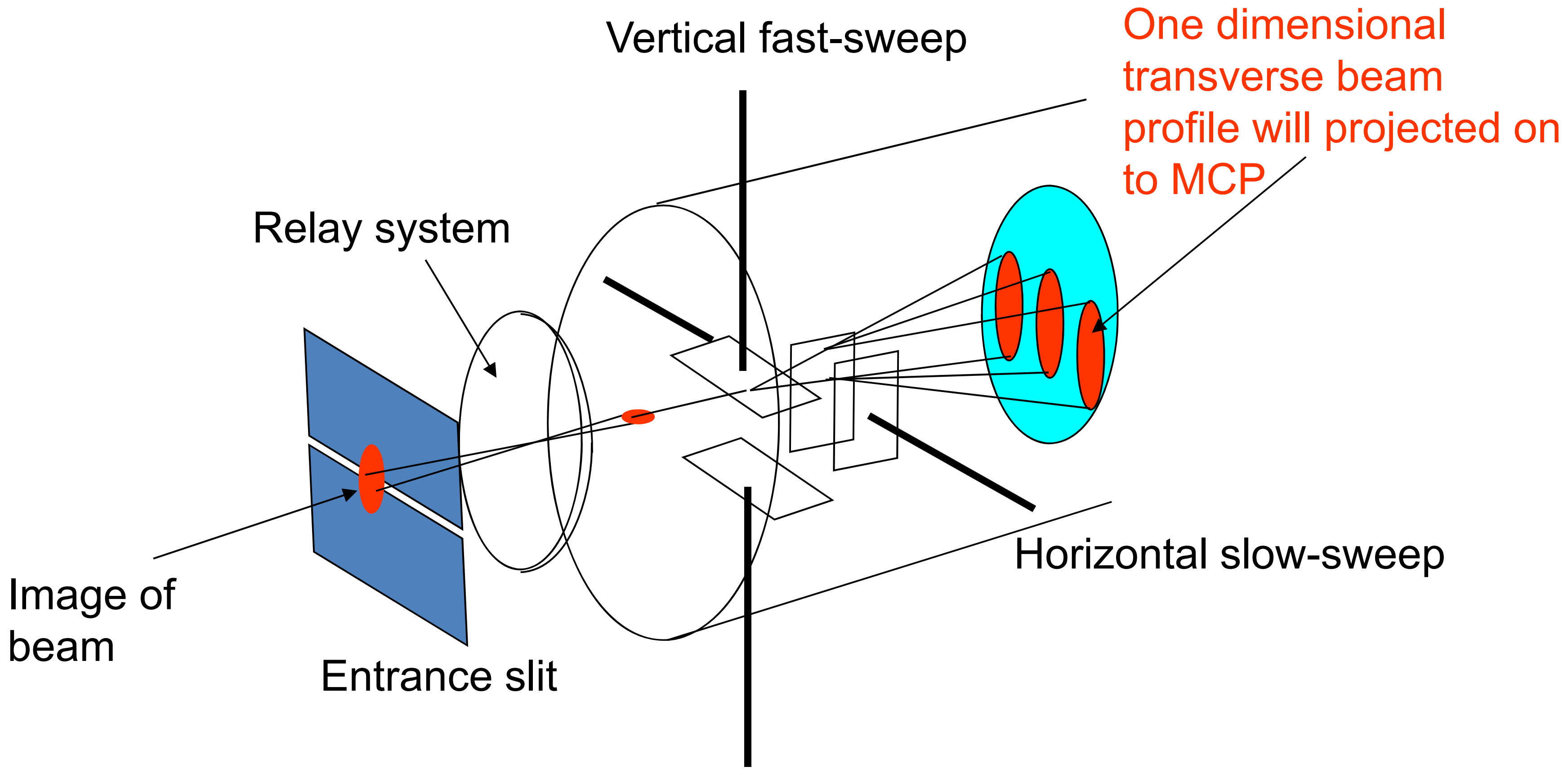
Vertical fast-sweep
One dimensional transverse beam profile will projected on to MCP
Relay system
Horizontal slow-sweep
Image of beam
Entrance slit

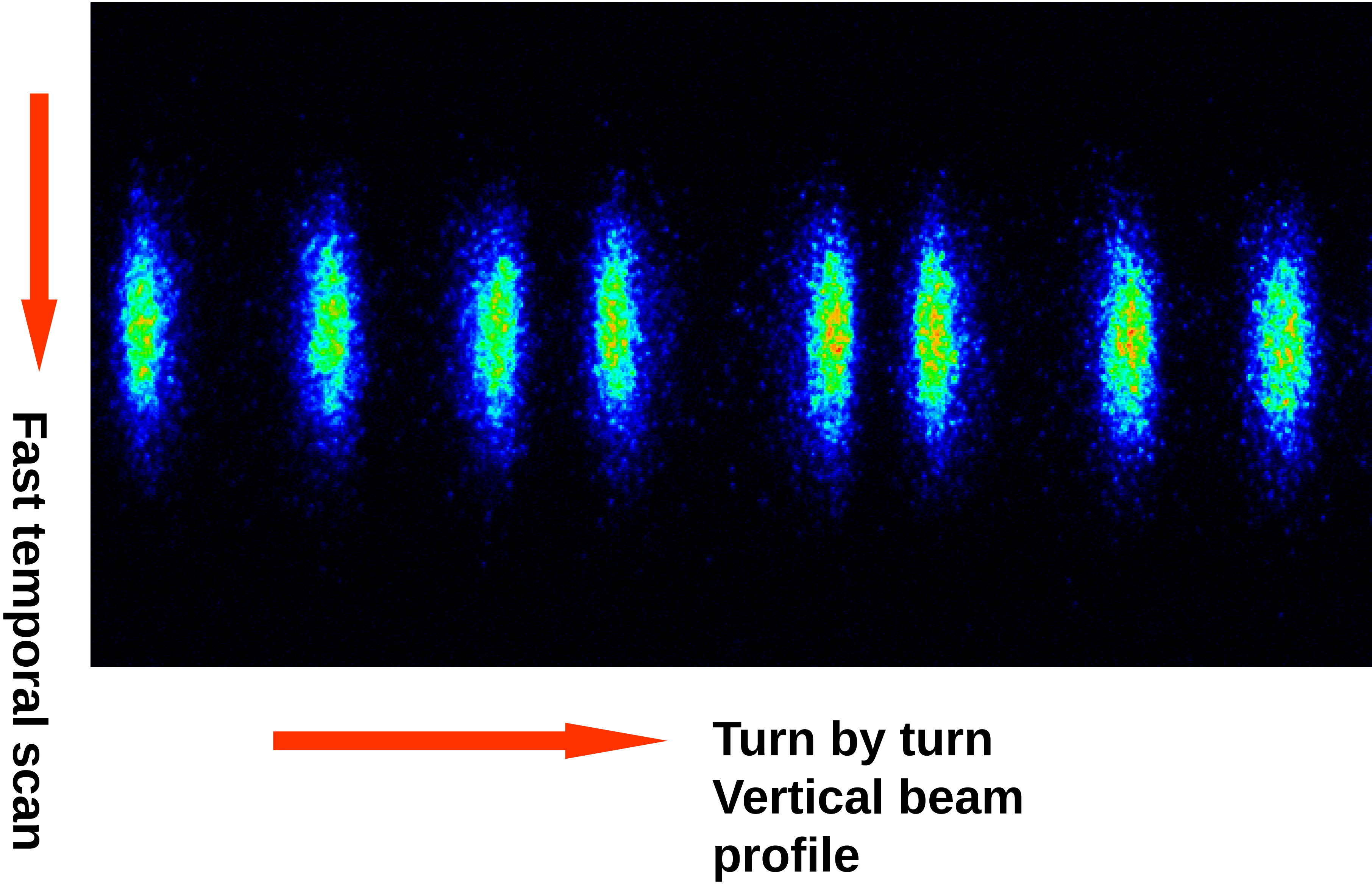
Fast temporal scan
Turn by turn
Vertical beam
profile

Observation of transverse quadruple motion in the vertical beam profile

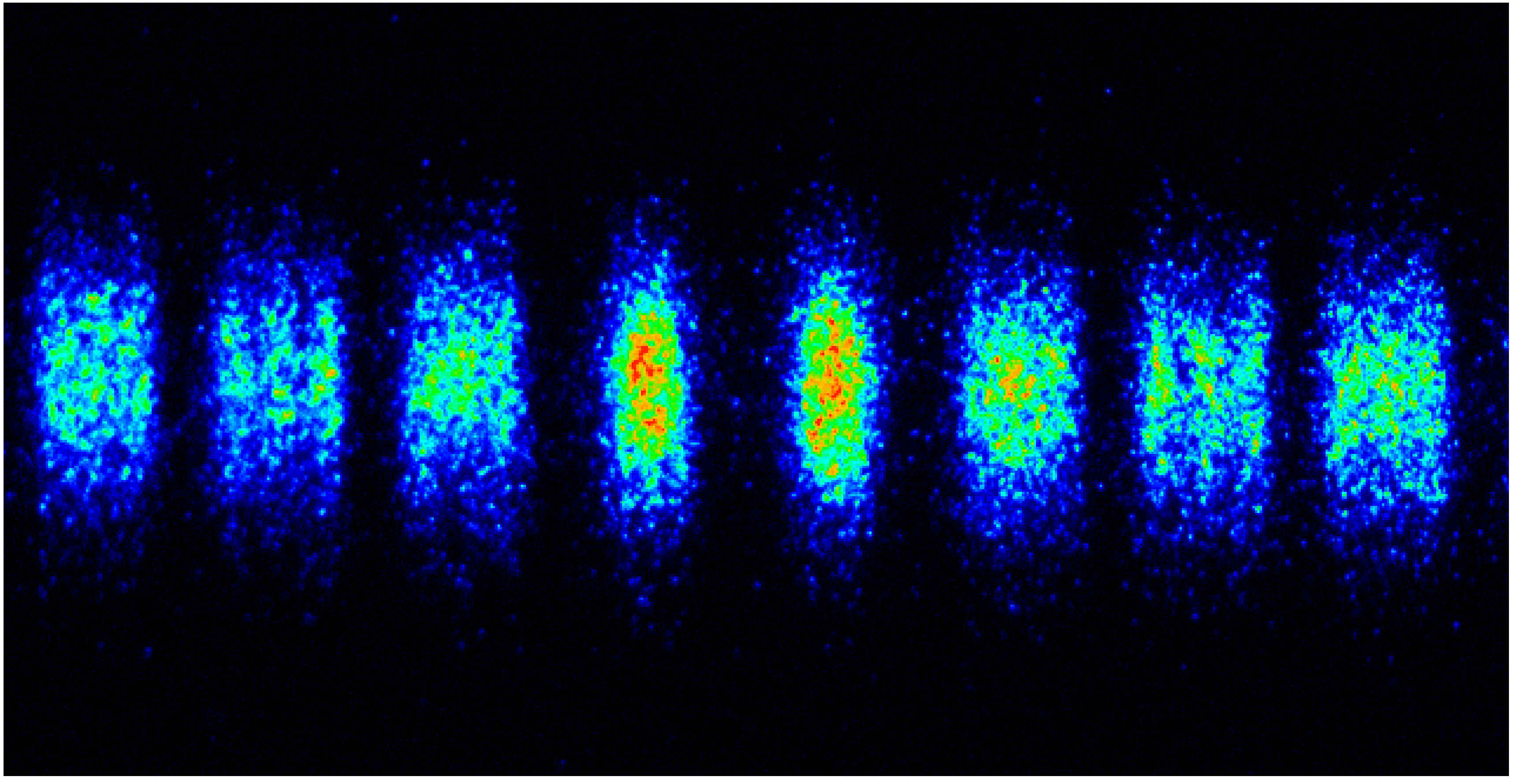

Optical phase space monitor (position and angle of the electron beam) by focusl system and afocal system

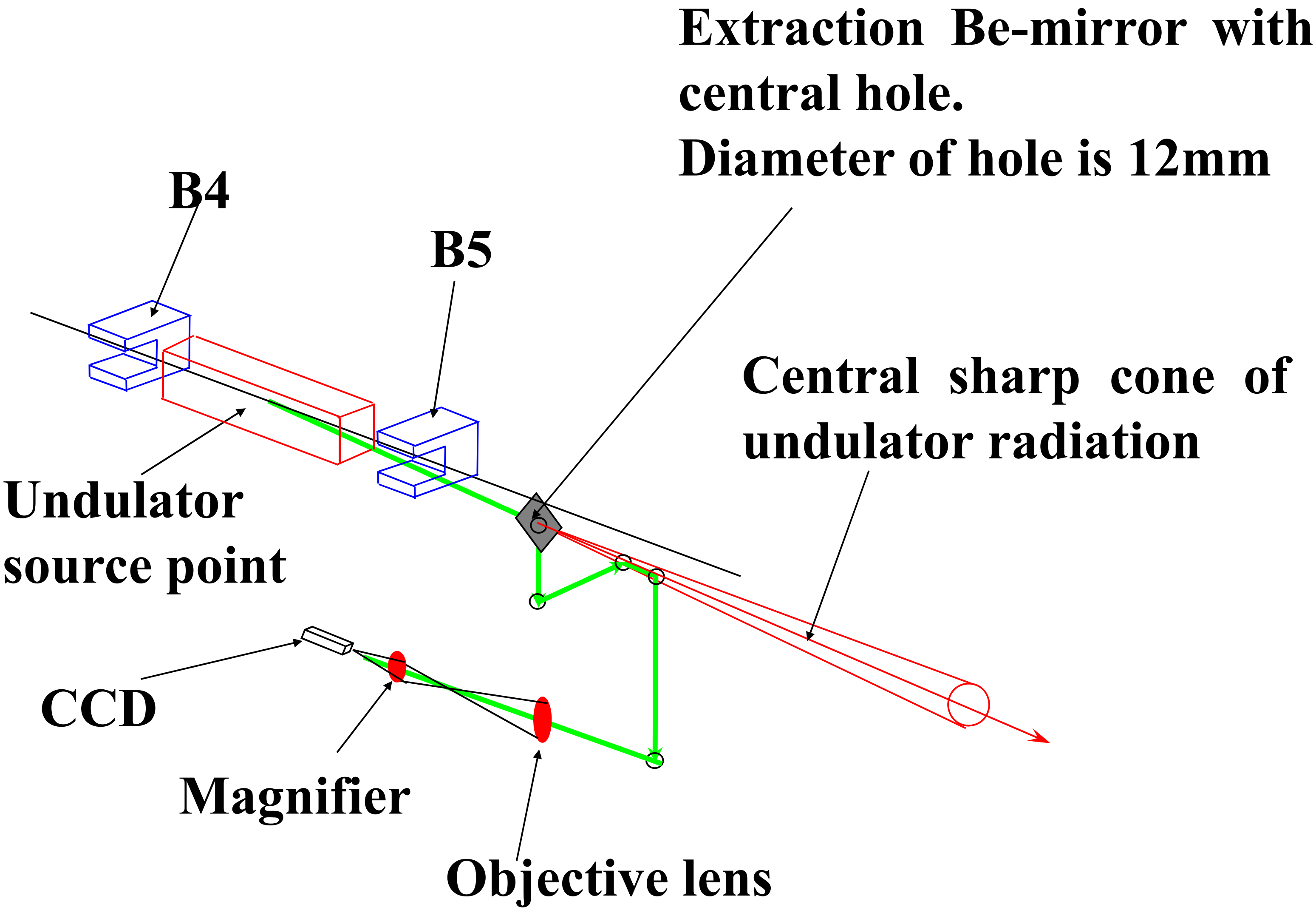

Extraction Be-mirror with central hole.
Diameter of hole is 12mm
B4
B5
Central sharp cone of undulator radiation
Undulator source point
CCD
Magnifier
Objective lens

Power density of BL5 Undulation

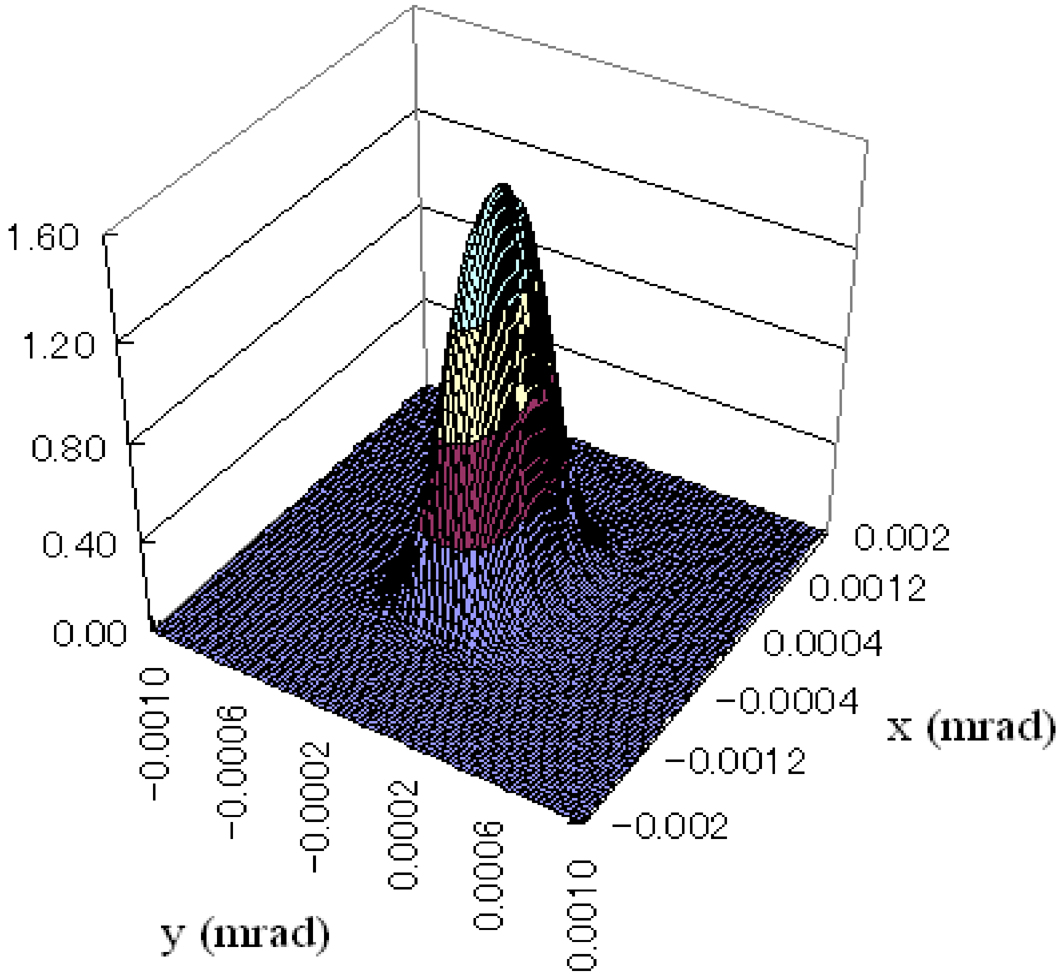

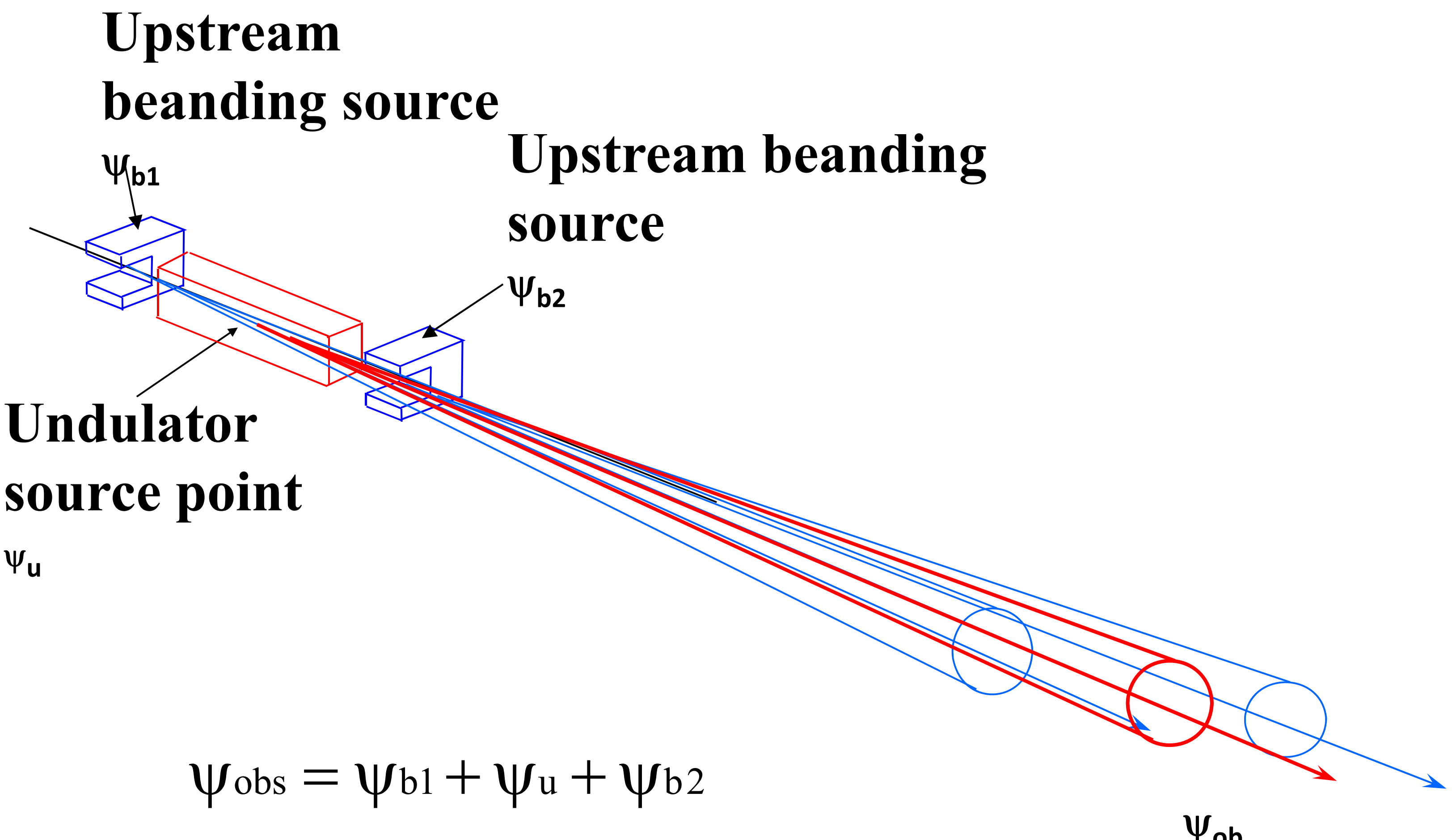

$$\psi_{obs} = \psi_{b1} + \psi_u + \psi_{b2}$$

$$\psi^2_{obs} = \psi^2_{b1} + \psi^2_u + \psi^2_{b2}$$

Focused onto the undulator

Radiation from undulator

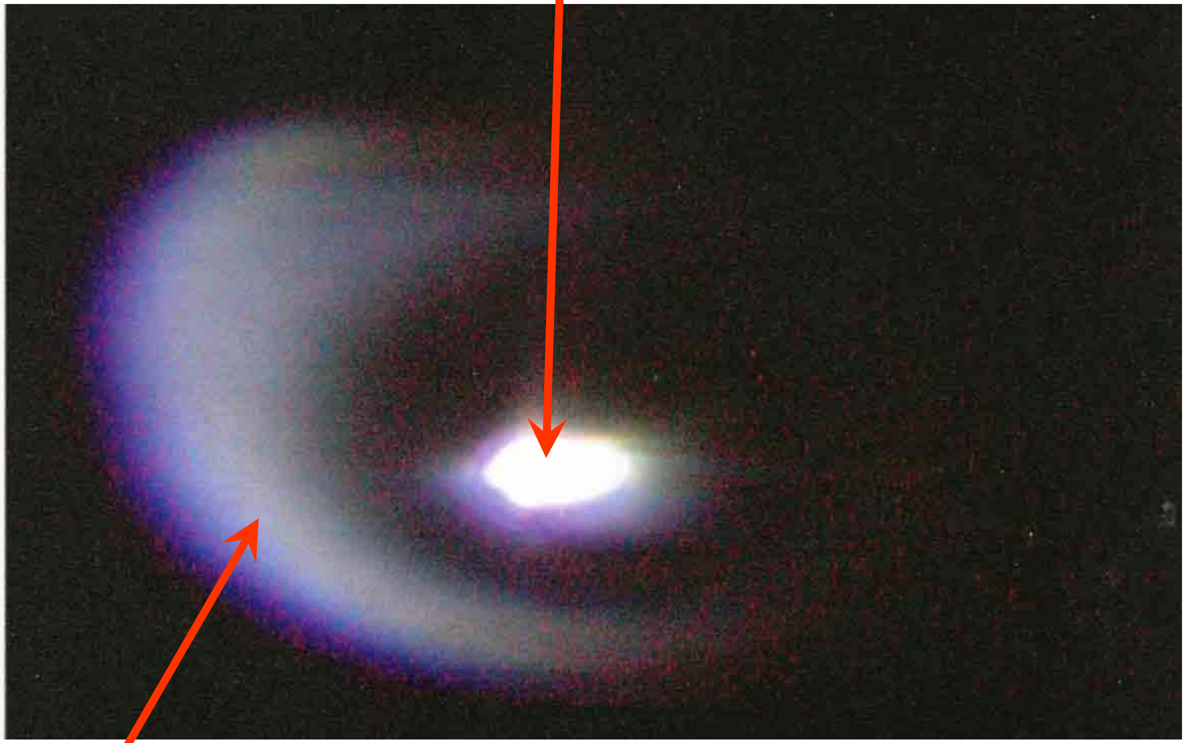

Radiation from downstream bend

image of electron beam in downstream bend

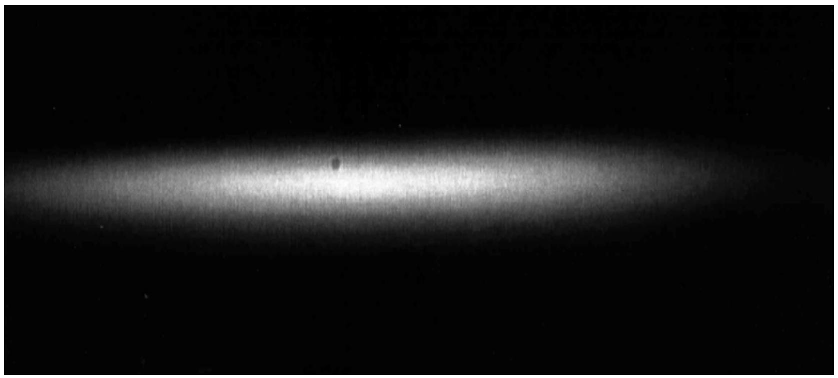

image of electron beam in undulator

x $\psi_{obs} = \psi_{b1} + \psi_u + \psi_{b2}$

o $\psi^2{}_{obs} = \psi^2{}_{b1} + \psi^2{}_u + \psi^2{}_{b2}$

Focusing system (a) for the observation of the beam position and afocal system (b) for the observation of beam angle.

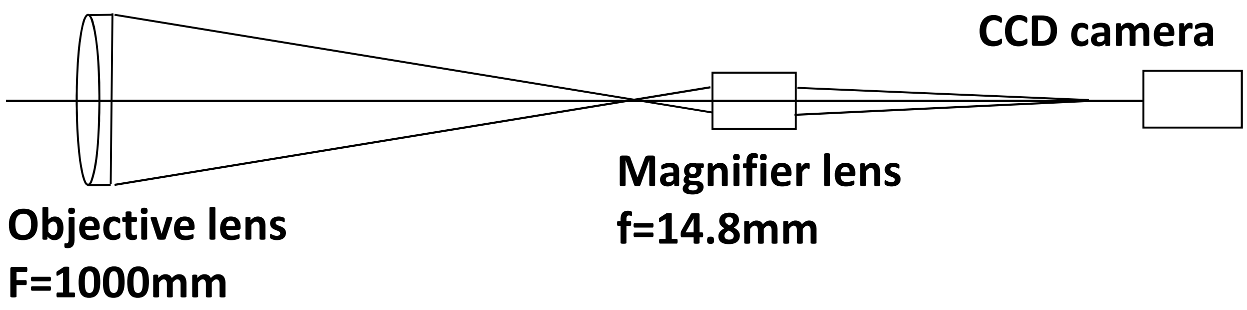

(a)

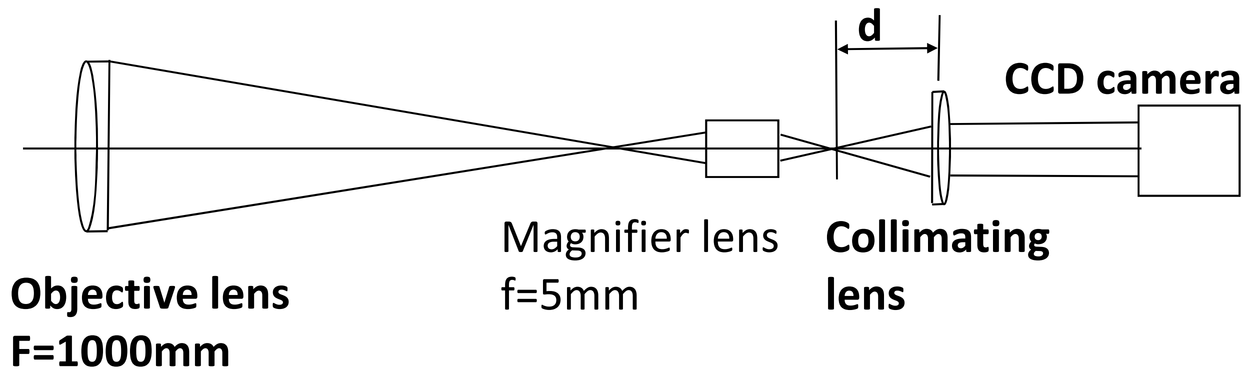

(b)

Collimating section in the afocal system.

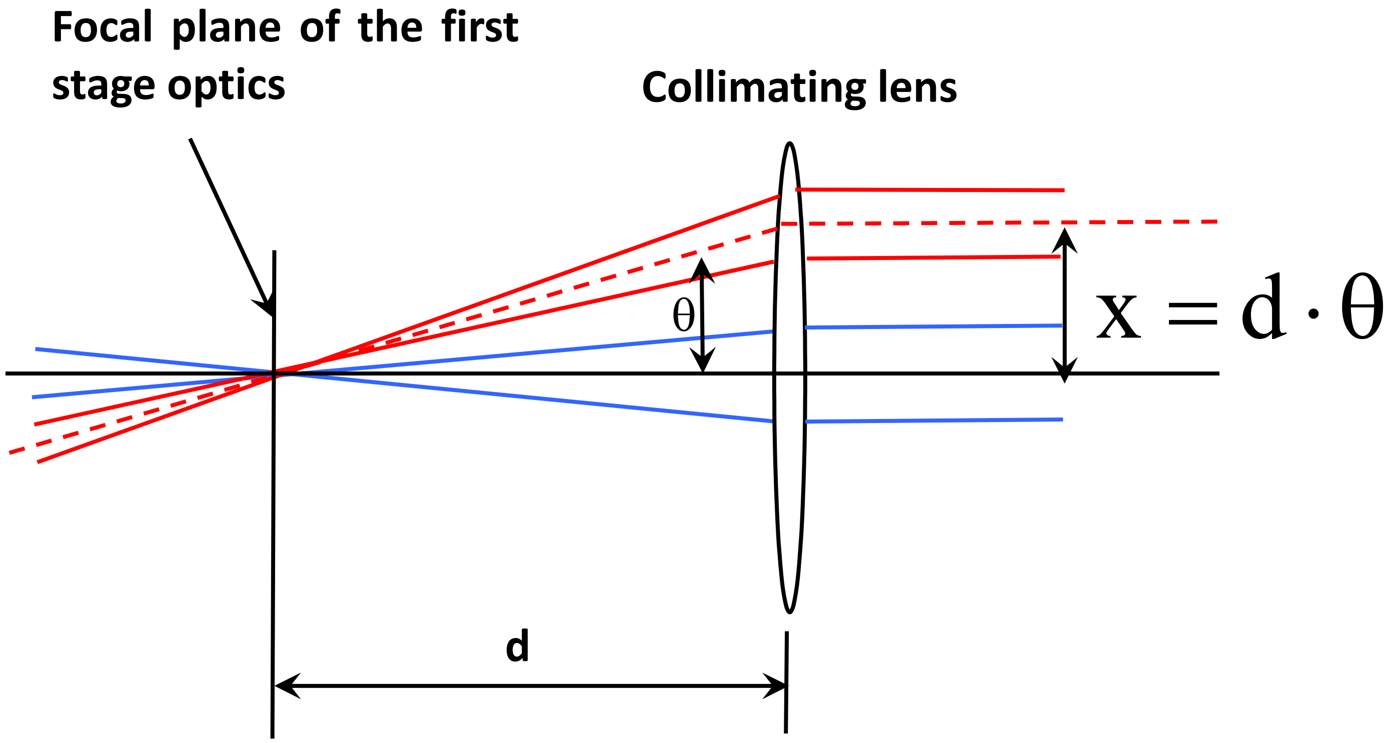

Electron beam image produced by the focusing system.

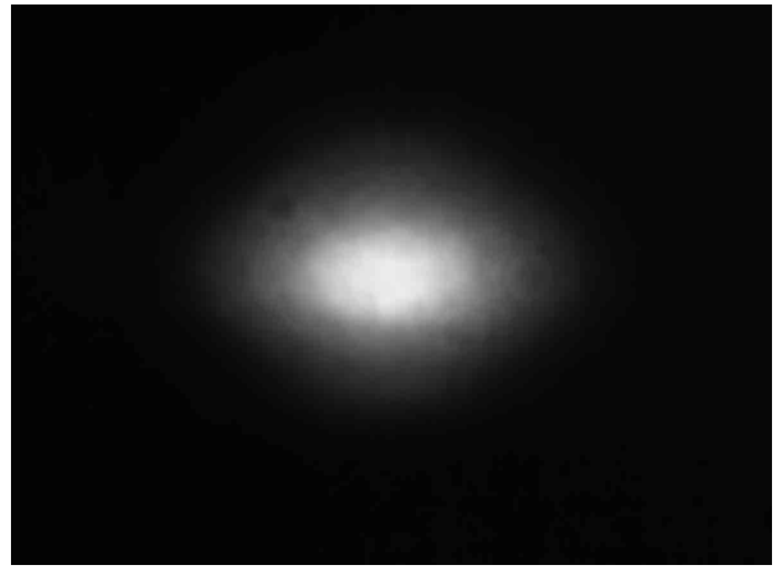

Intensity distribution of the light beam at the afocal system.

Due to a large floor motion at BL5, the calibration and phase space observation were performed at BL21.

Results of calibrations

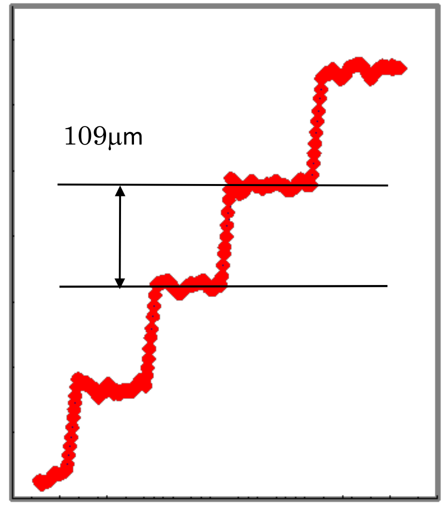

(a) Horizontal position

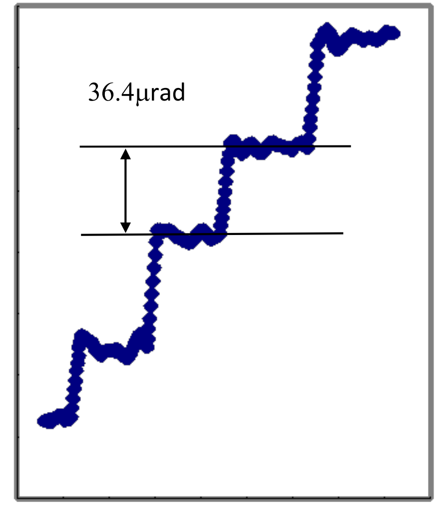

(b) Horizontal angle

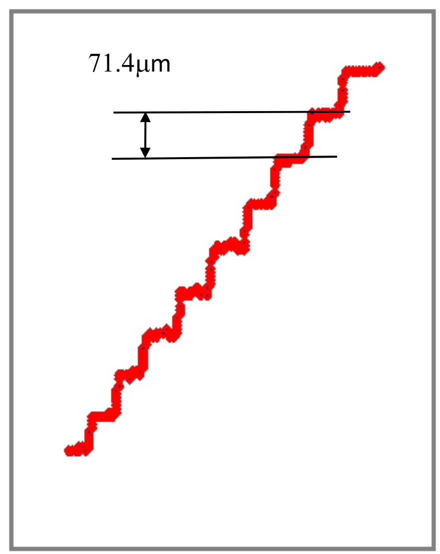

(c) Vertical position

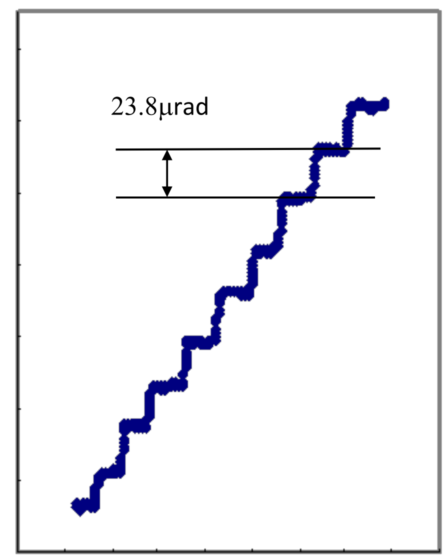

(d) Vertical angle

Result of phase space motion of electron beam at BL21

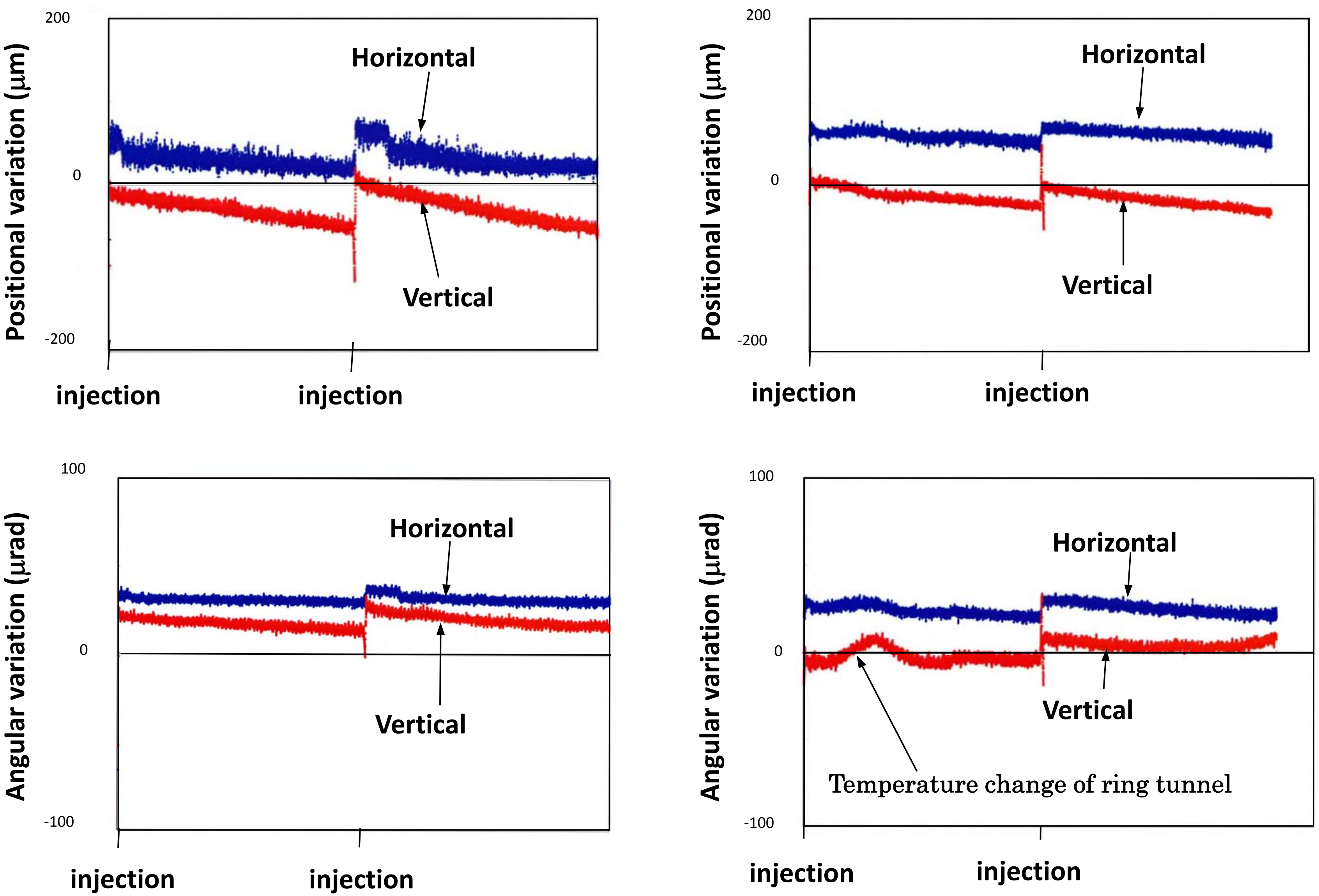

A result of measurements beam positions during moving the gap from 140mm to 70mm atBL5.

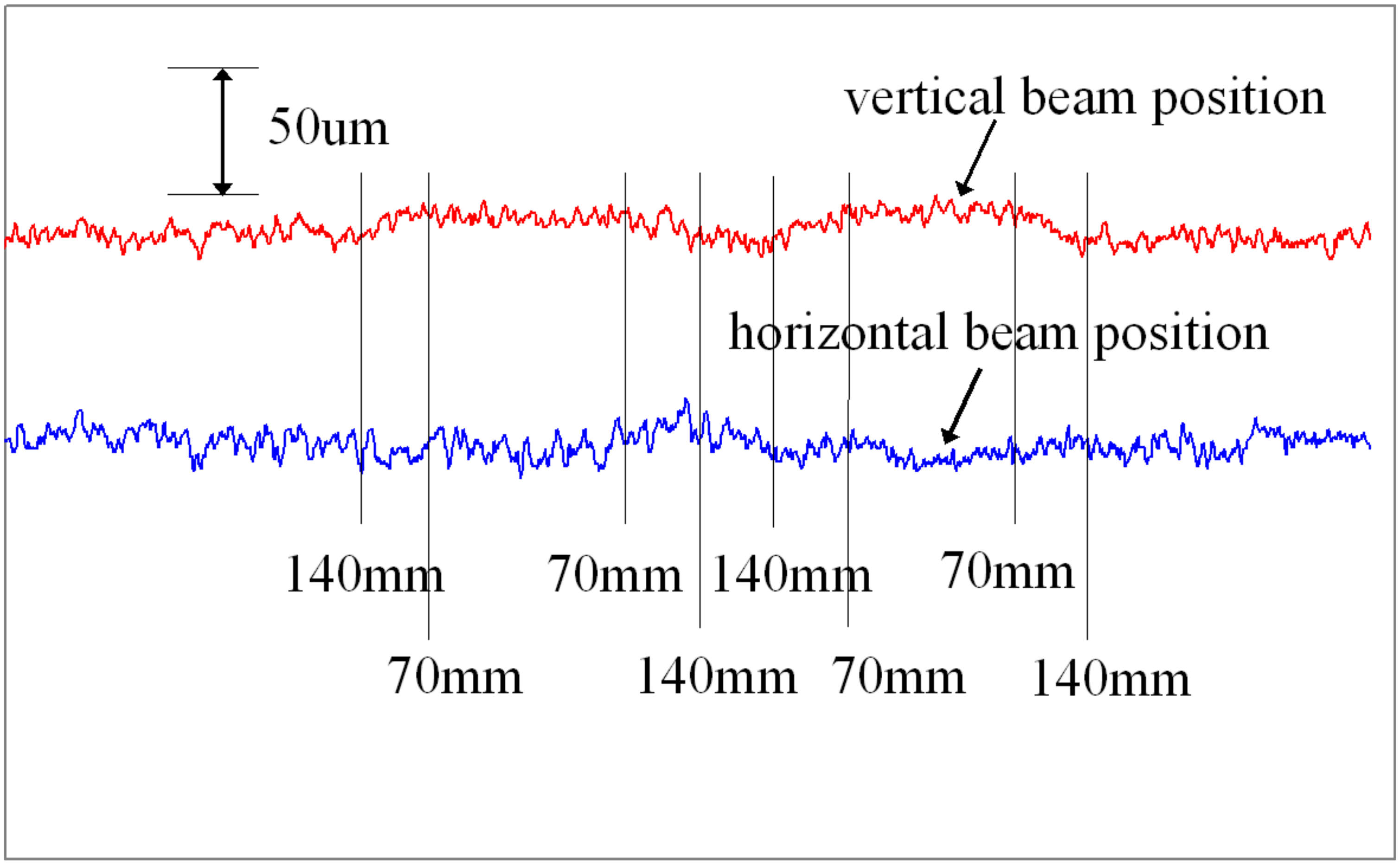

1st order spatial Interferometry Beam size measurement

To measure a size of object by means of spatial coherence of light (interferometry) was first proposed by H. Fizeau in 1868!

This method was realized by A.A. Michelson as the measurement of apparent diameter of star with his stellar interferometer in 1921.

This principle was now known as " Van Cittert-Zernike theorem" because of their works;

1934 Van Cittert

1938 Zernike.

Simple understanding of van Cittert-Zernike theorem

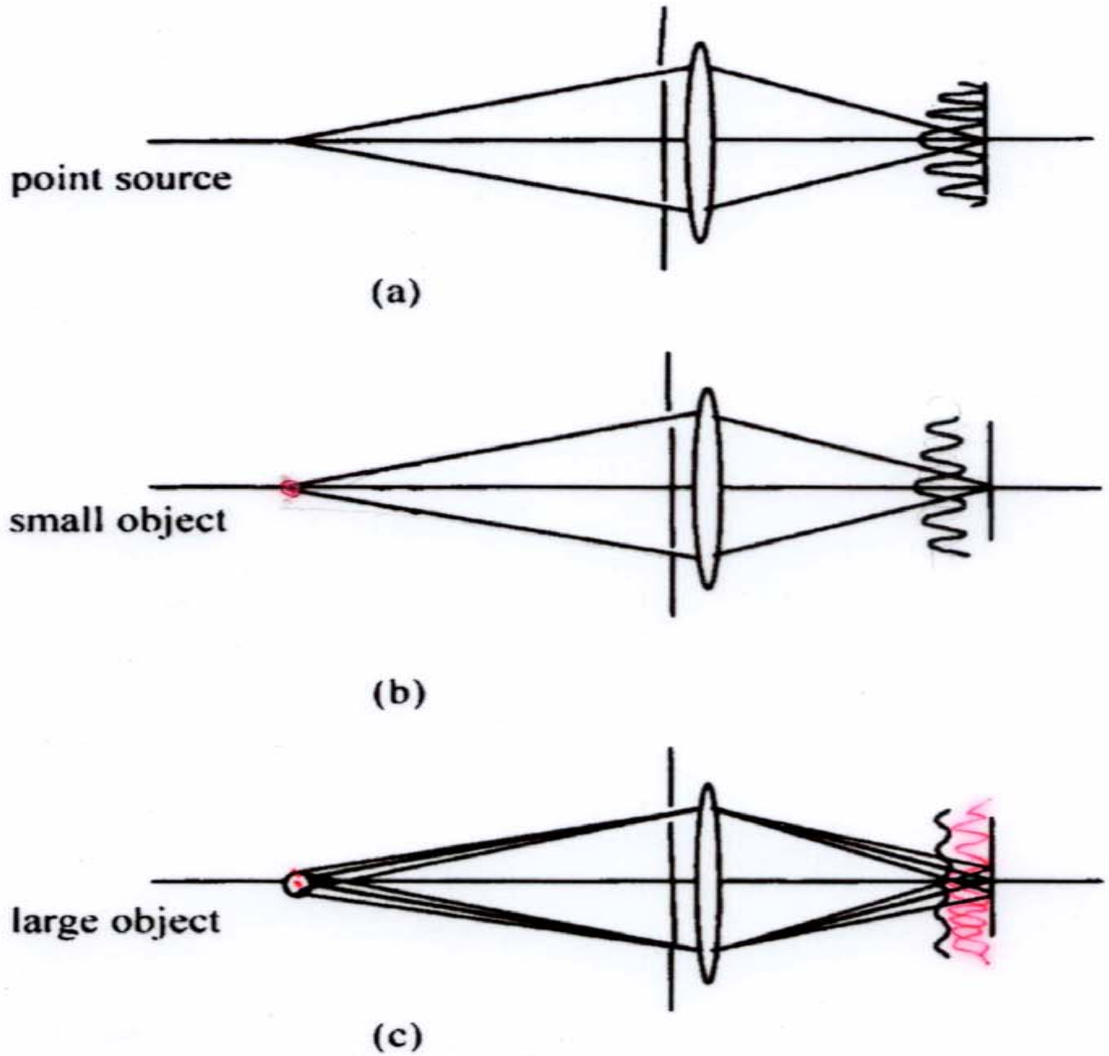

Spatial coherence and profile of the object Van Cittert-Zernike theorem

According to van Cittert-Zernike theorem, with the condition of light is temporal incoherent (no phase correlation), the complex degree of spatial coherence $\gamma(\upsilon_x,\upsilon_y)$ is given by the Fourier Transform of the spatial profile f(x,y) of the object (beam) at longer wavelengths such as visible light.

$$\gamma(\upsilon_x,\upsilon_y)=\int\int f(x,y)\exp\{-i\cdot 2\cdot\pi(\upsilon_x\cdot x+\upsilon_y\cdot y)\}dxdy$$

where υ_x,υ_y are spatial frequencies given by;

$$\upsilon_x=\frac{D_x}{\lambda\cdot R_0}\;,\quad \upsilon_y=\frac{D_y}{\lambda\cdot R_0}$$

Theoretical resolution of interferometry

Uncertainty principle in phase of light

Function of the 1st order interferometer

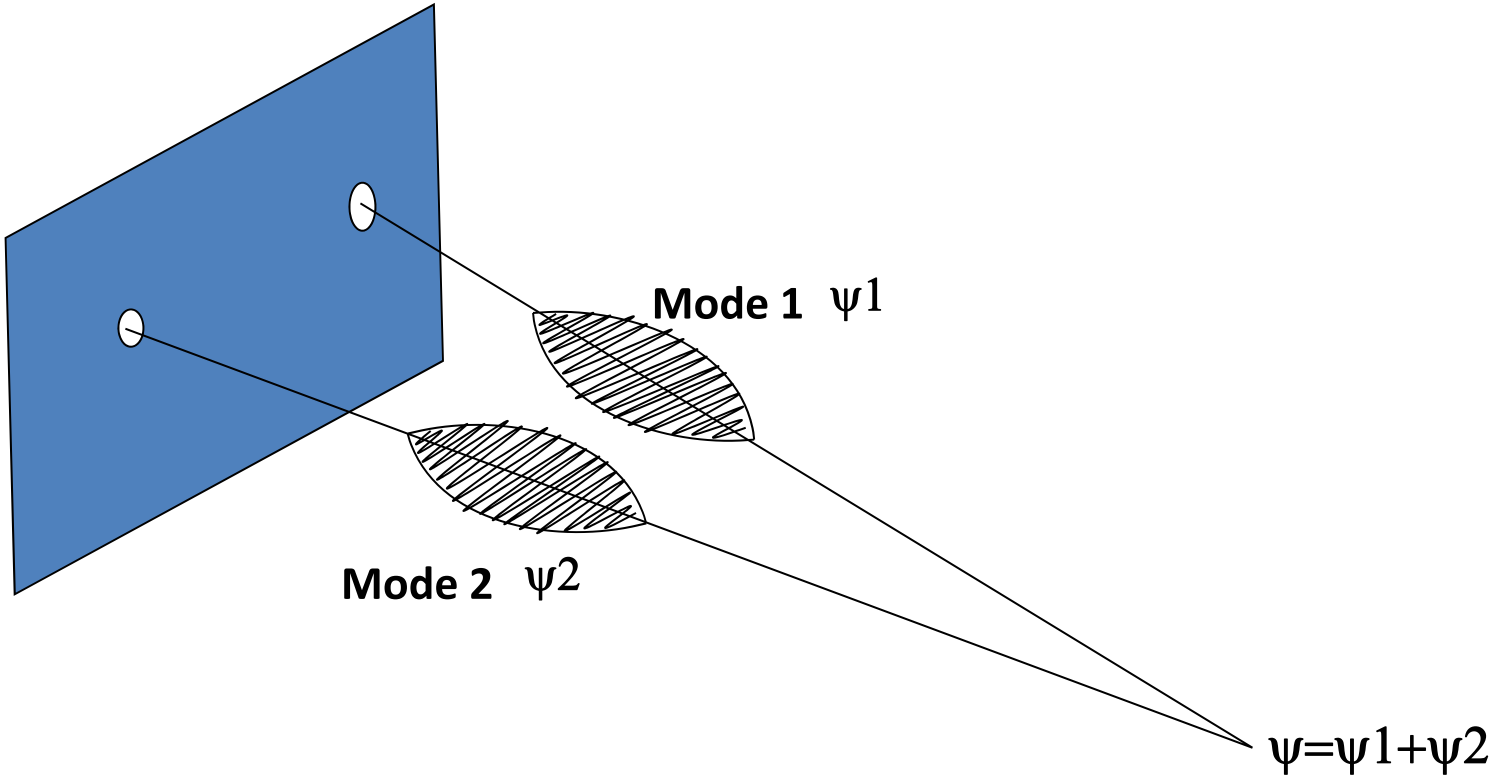

Measure the correlation of light phase in two modes

Uncertainty principal between photon number and phase
$2\cdot\Delta\phi\cdot\Delta N\geq1$

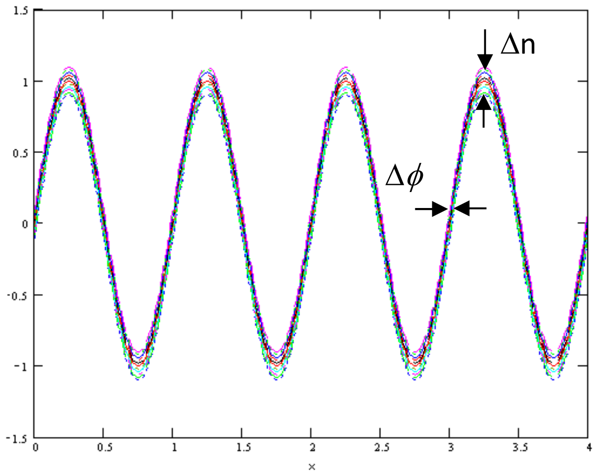

$|n|^2=5$
0

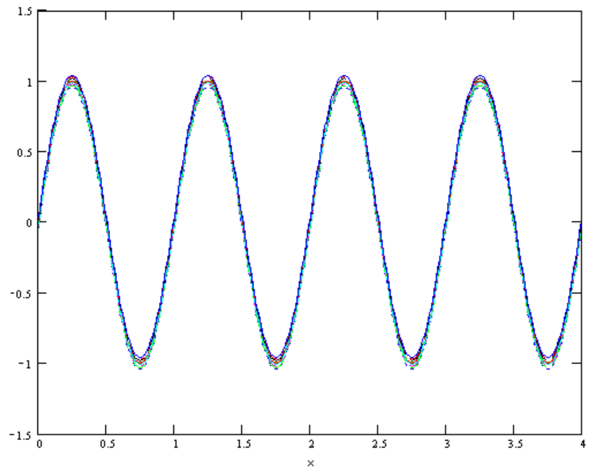

$|n|^2=100$

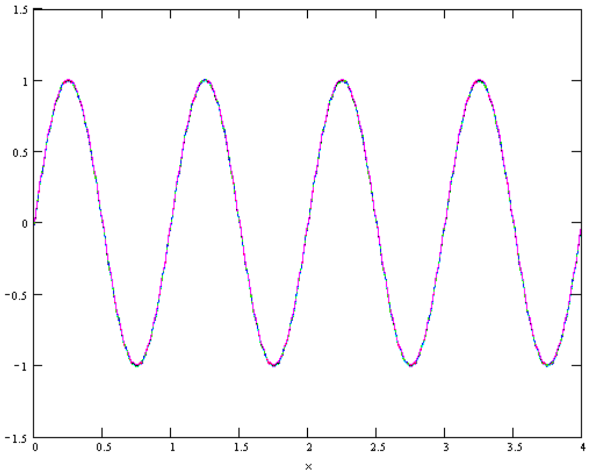

$|n|^2=500$

Provability distribution of light phase

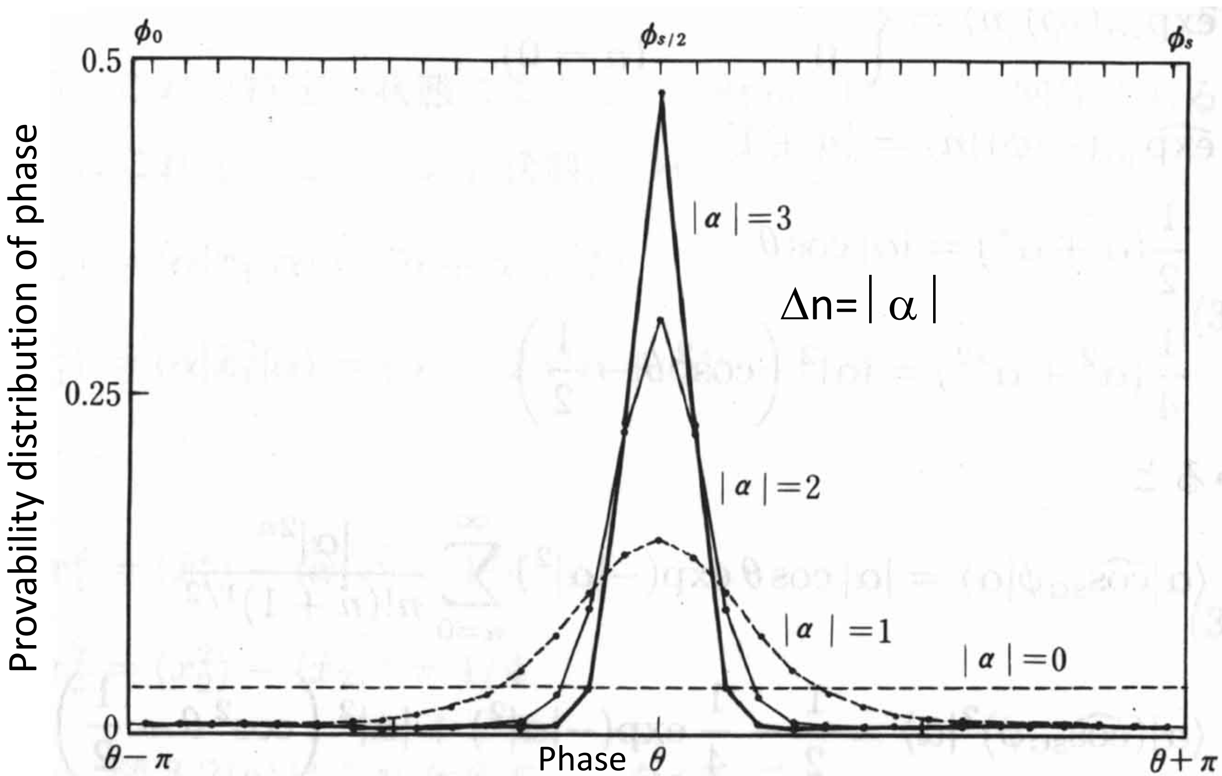

Using the wavy aspect of photon in small number of photons, Forcibly ;
From uncertainty principal
$\Delta\phi \cdot \Delta N \geq 1/2$,
Even in the case of coherent mode, interference fringe will be smeared by the uncertainty of phase.

$$I(y,D) = \int_{\Delta\phi} (I_1 + I_2) \cdot \left\{ \sin c\left(\frac{\pi \cdot a \cdot y}{\lambda \cdot f} \right) \right\}^2 \left\{ 1 + \cos\left(k \cdot D \frac{y}{f} + \phi \right) \right\} d\phi$$

Interference fringe with no phase fluctuation

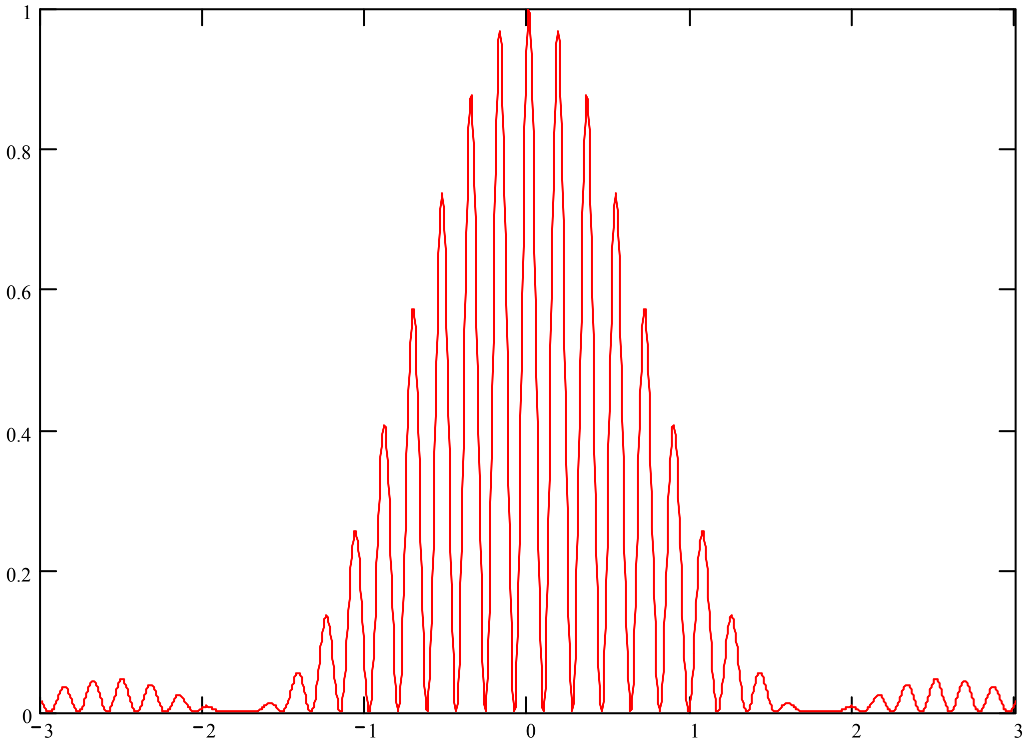

Interference fringe with uncertainty of phase $\pi/2$

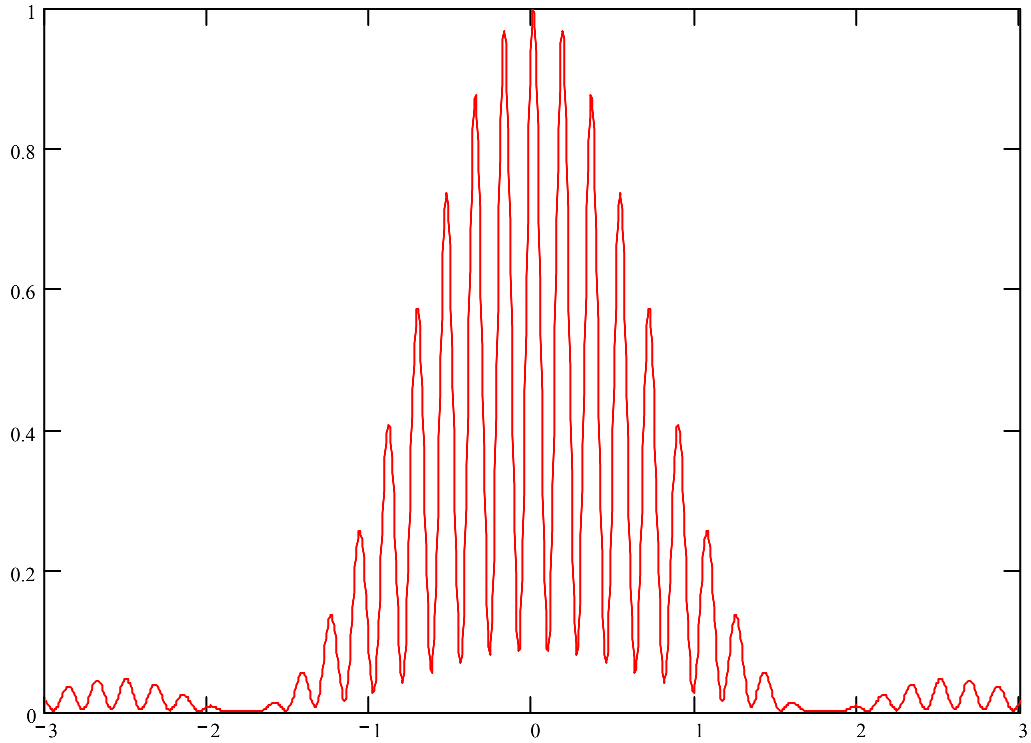

We can feel the visibility of interference fringe will reduced by uncertainty of phase under the small number of photons.
But actually, under the small number of photons, photons are more particle like, and difficult to see wave-phenomena.

In actual case, we cannot observe interference fringe with small number of photons!

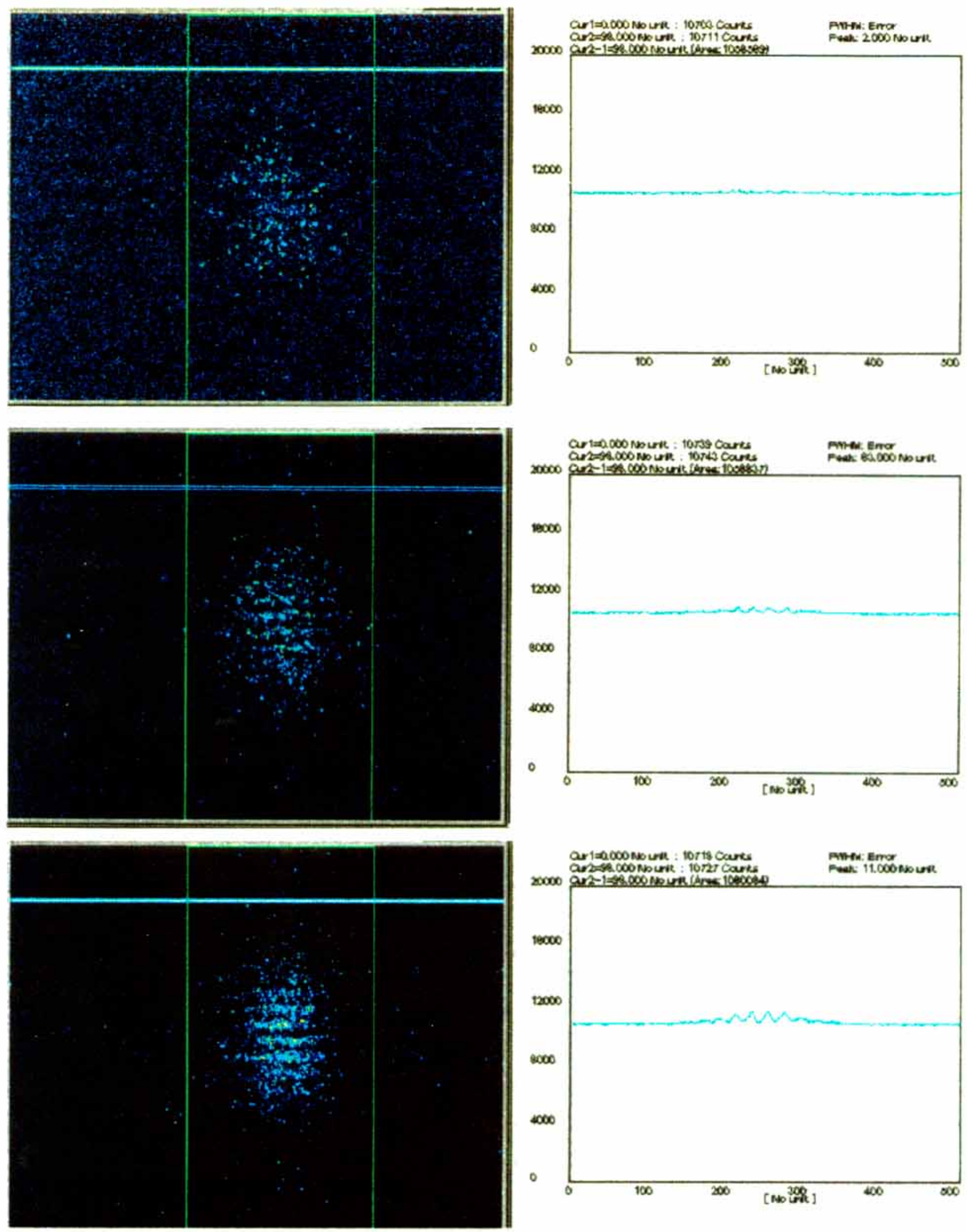

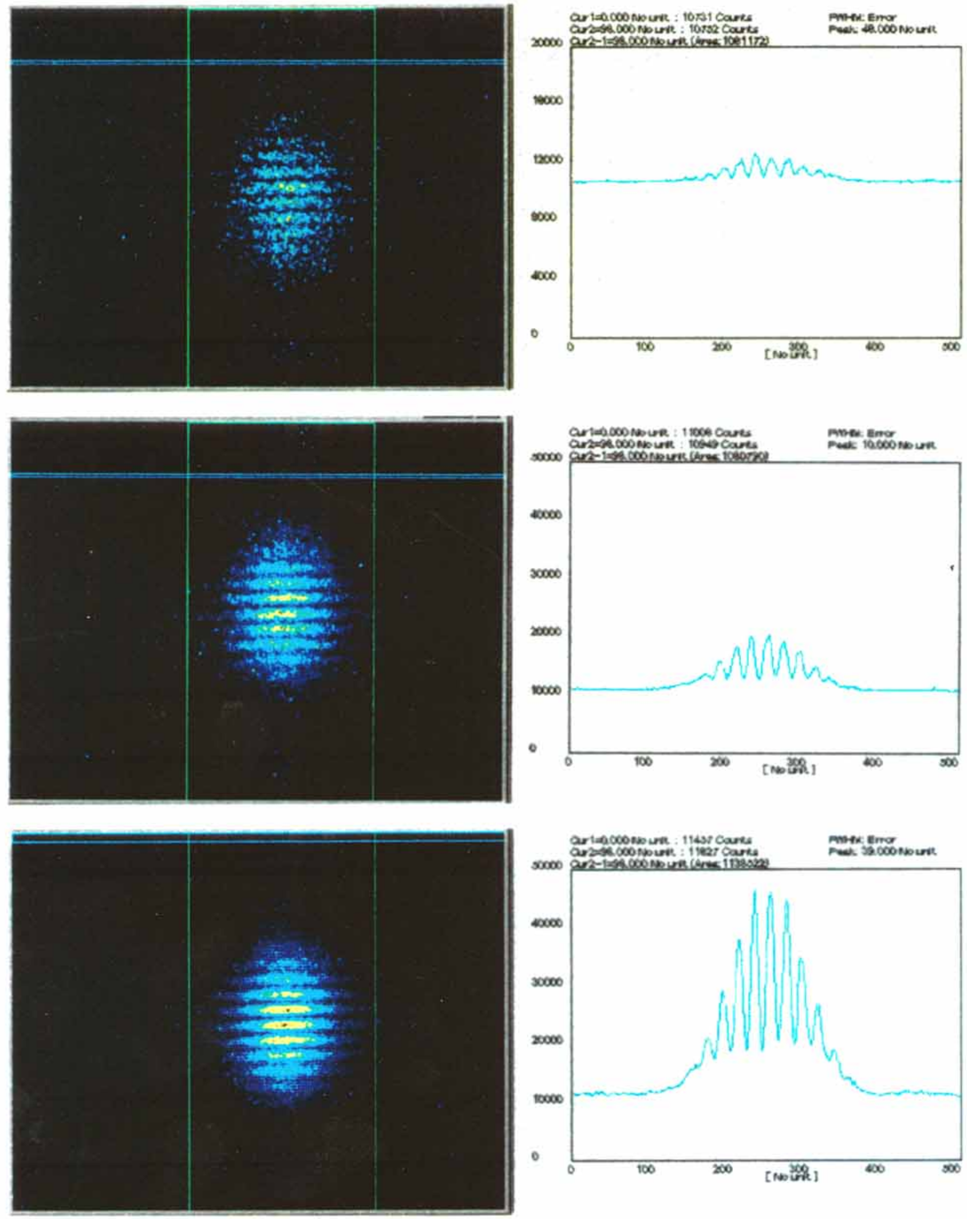

FWHM: Error
Peak: 48.000 No unit
[No unit]
FWHM: Error
[No unit]
FWHM: Error
[No unit]

Design of interferometer

Sommerfeldt type refractive two slit interferometer with quasi monochromatic rays

Dimensions are those used at the Photon Factory

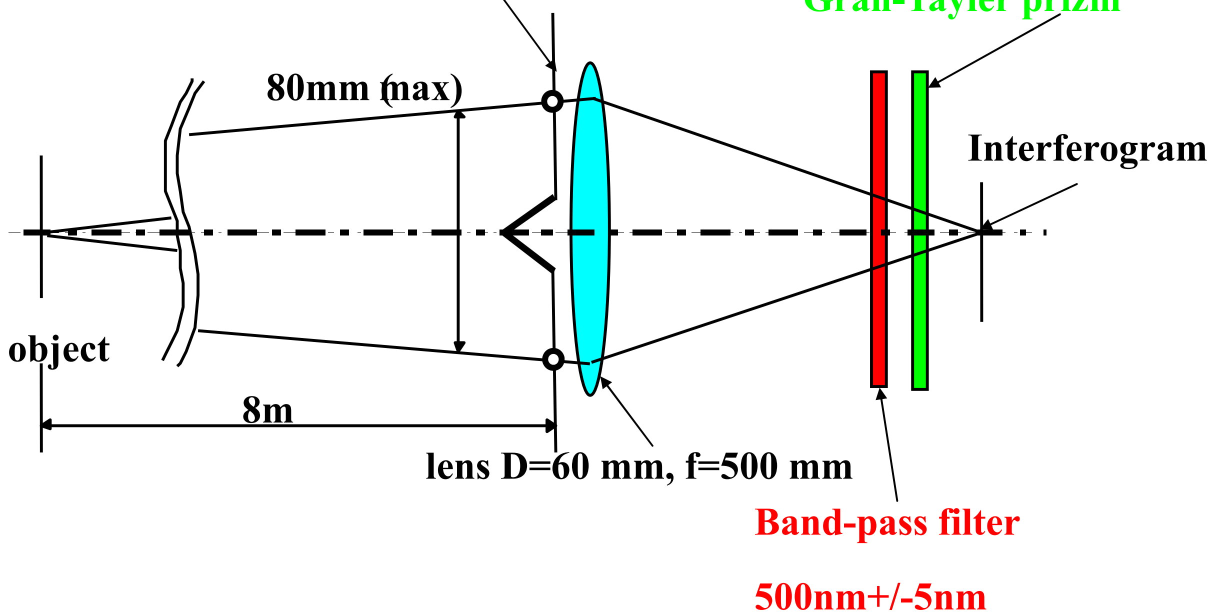

Important function of the objective lens ;

1. Localize the interfering volume to make the interferometer bright.

2. Elimination of parasitic modes coming into the interfering volume.

Depth of interfering volume is given by

$$\Delta z \cong \frac{3.2\lambda}{\pi}\left(\frac{f}{a}\right)^2$$

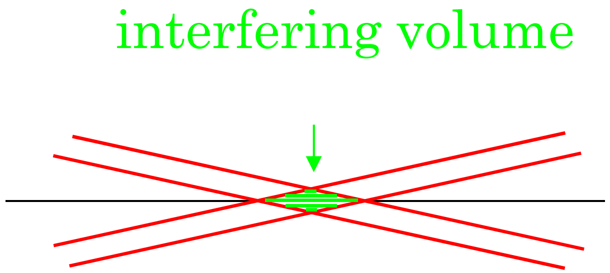

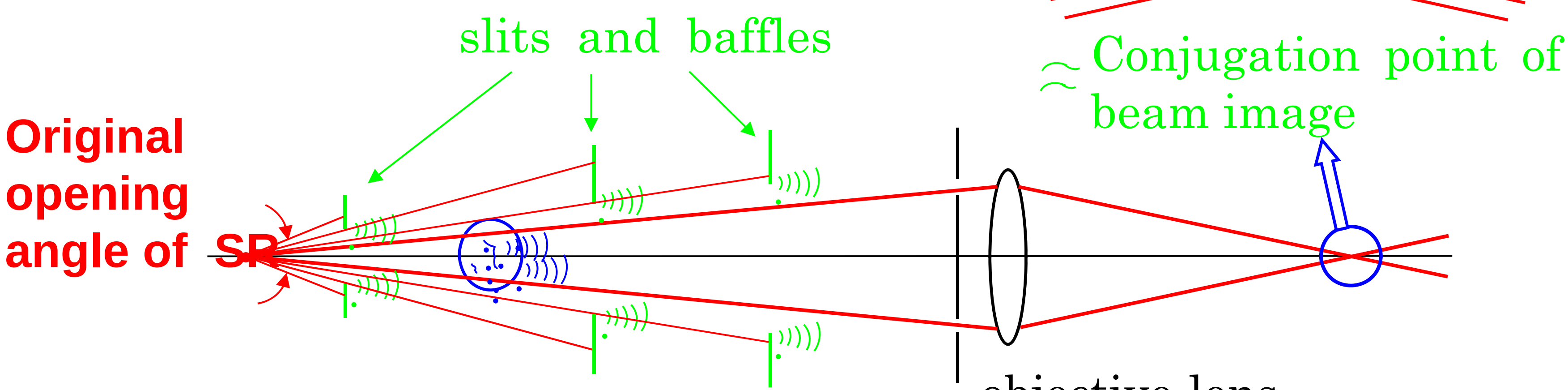

parasitic modes < 0.1% into the interfering volume

The intensity of the interferogram is given by;

$$I(y,D)=\int (I_1+I_2)\cdot\left\{\mathrm{sinc}\left(\frac{\pi\cdot a\cdot y\cdot\chi(D)}{\lambda\cdot f}\right)\right\}^2\cdot\left\{1+\gamma\cdot\cos\left(k\cdot D\cdot\left(\frac{y}{f}+\psi\right)\right)\right\}d\lambda$$

$$\gamma=\left(\frac{2\cdot\sqrt{I_1\cdot I_2}}{I_1+I_2}\right)\cdot\left(\frac{I_{\max}-I_{\min}}{I_{\max}+I_{\min}}\right)\quad,\quad \psi=\tan^{-1}\frac{S(D)}{C(D)}$$

y **: position in the interferogram**

a **: half-height of a slit**

f **: distance between secondary principal point of lens and interfrogram**

S(D),C(D)**: sine and cosine component of Fourier transformation of the distribution function of the SR source**

χ**(*****D*****) : an instrumental function of the interferometer.**

This term has a cosine-like dependence, and comes mainly from two sources:

1) a cosine term in the Fresnel-Kirchhoff diffraction formula which represents the angular dependence between the incident and diffracted light of a single slit
2) reduction of effective slit height as double slit separation D increases.

This term χ is normally neglected in diffraction theory under the paraxial approximation, but we cannot neglect this term in the practical use of the interferometer.

Typical interferogram in vertical direction at the Photon Factory.
D=10mm

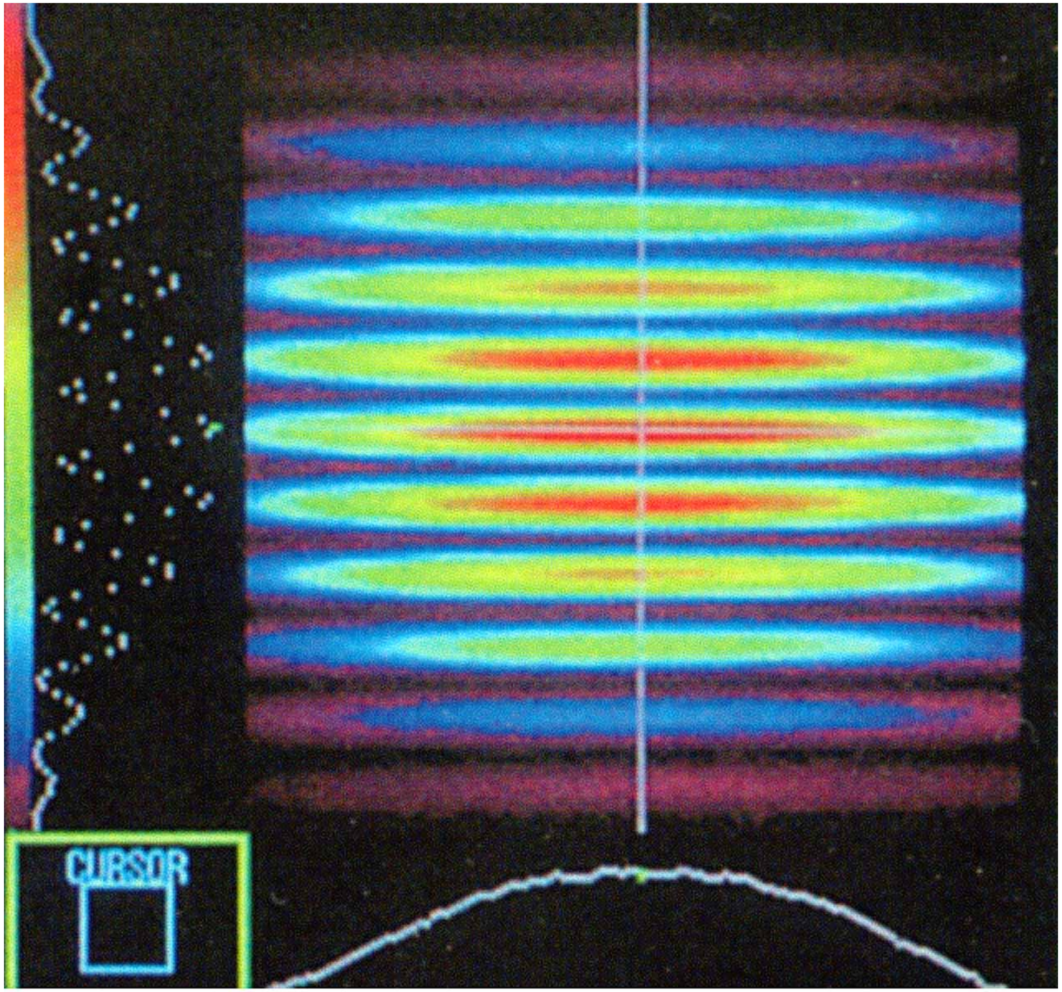

Absolute value of the complex degree of spatial coherence me asured at the Photon Factory KEK.

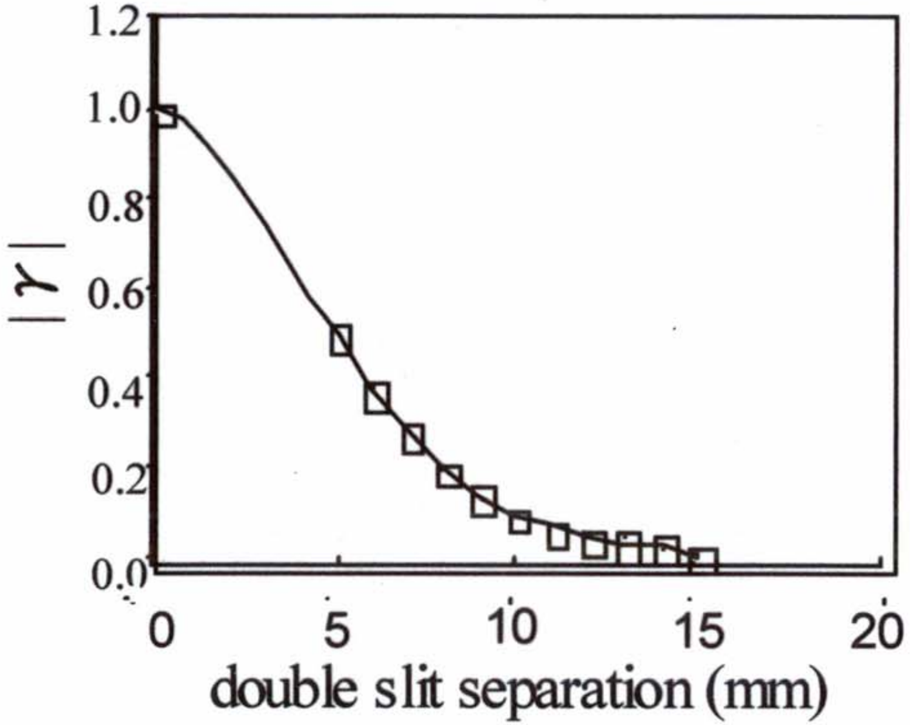

Phase of the complex degree of spatial coherence
vertical axis is phase in radian

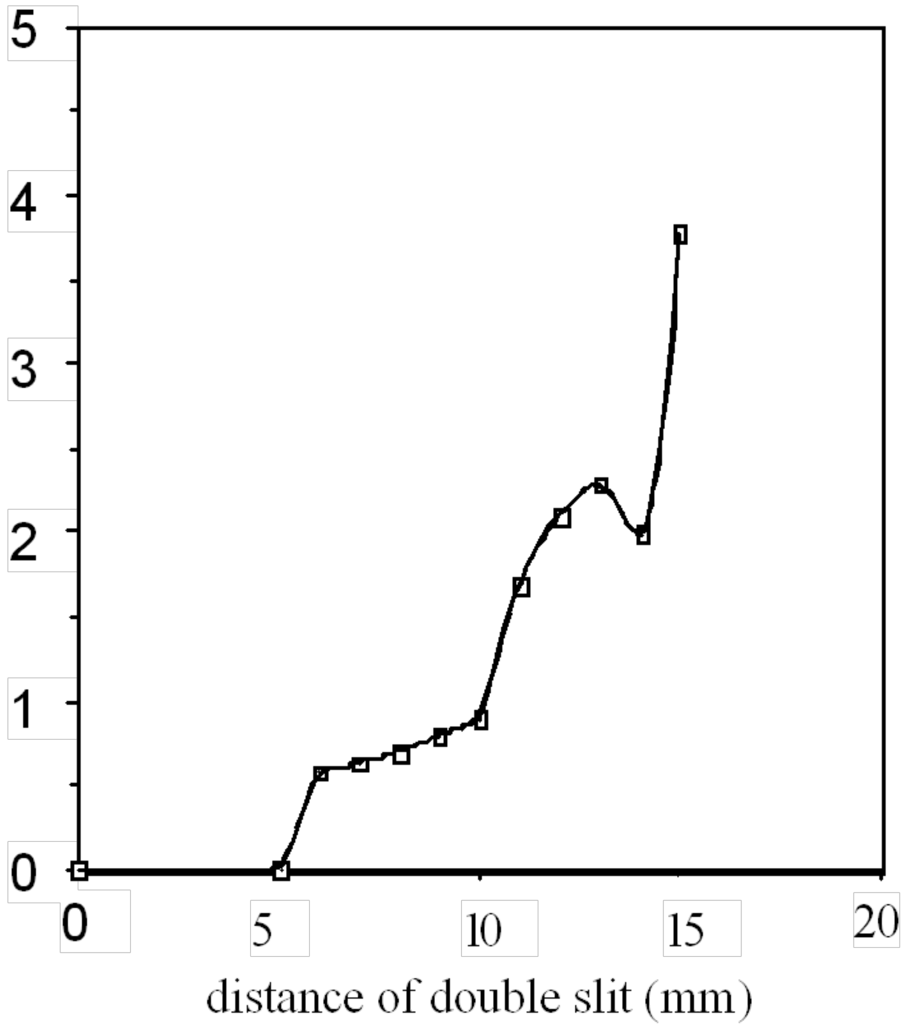

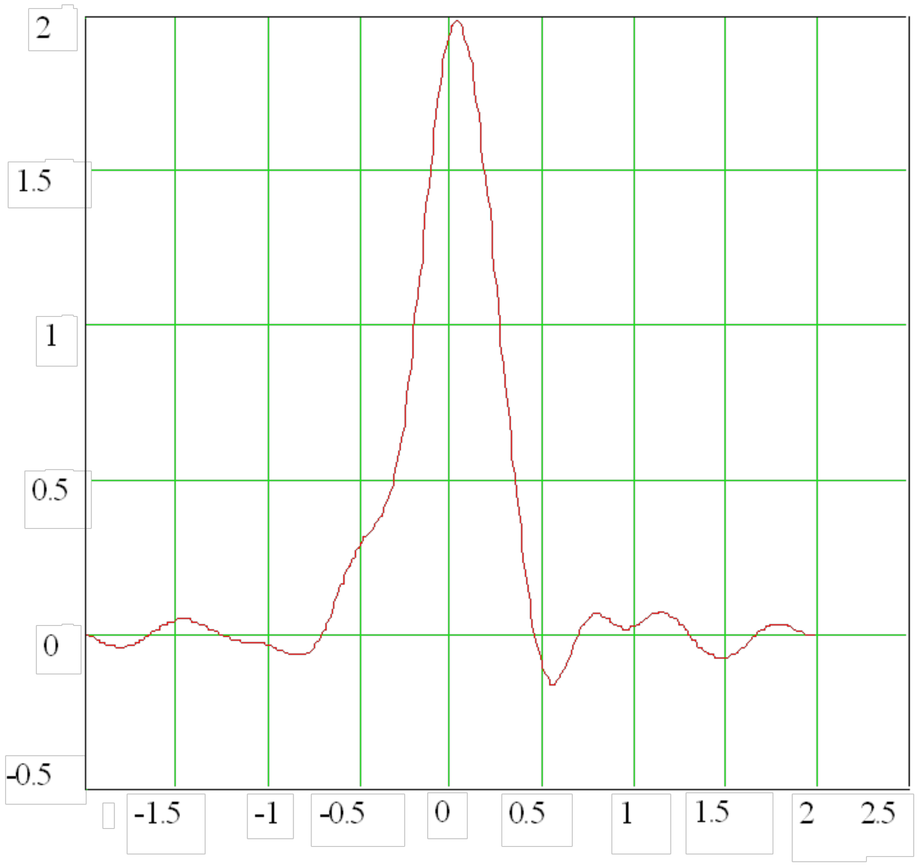

Vertical beam profile obtained by a Fourier transform of the complex degree of coherence.

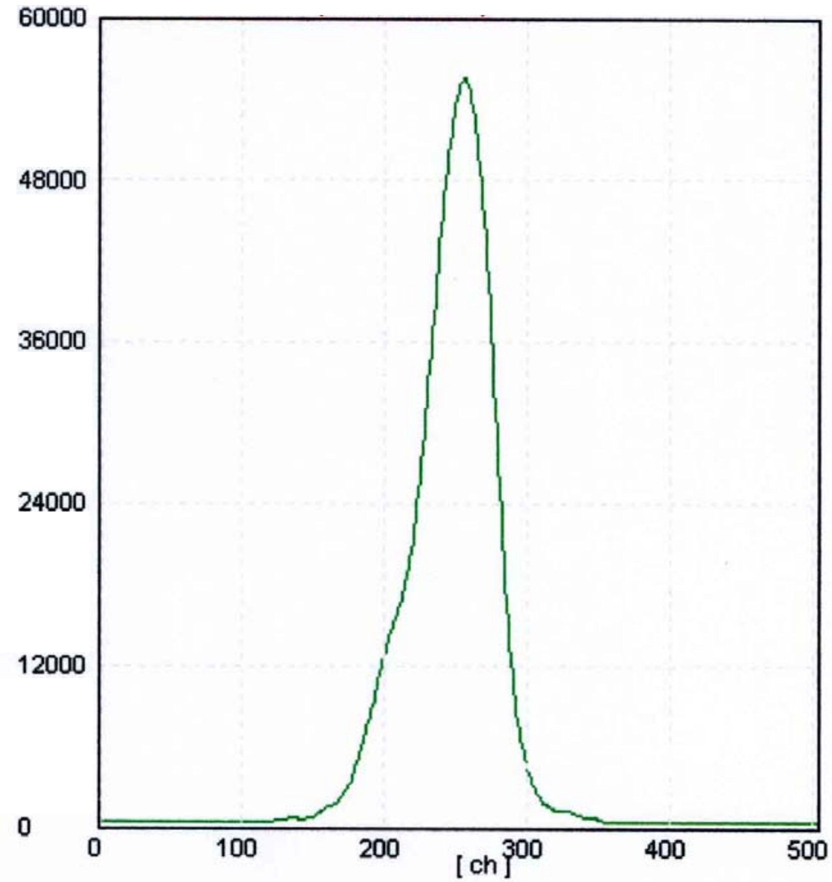

Beam profile taken with an imaging system

Vertical beam profile obtained by Fourier Cosine transform

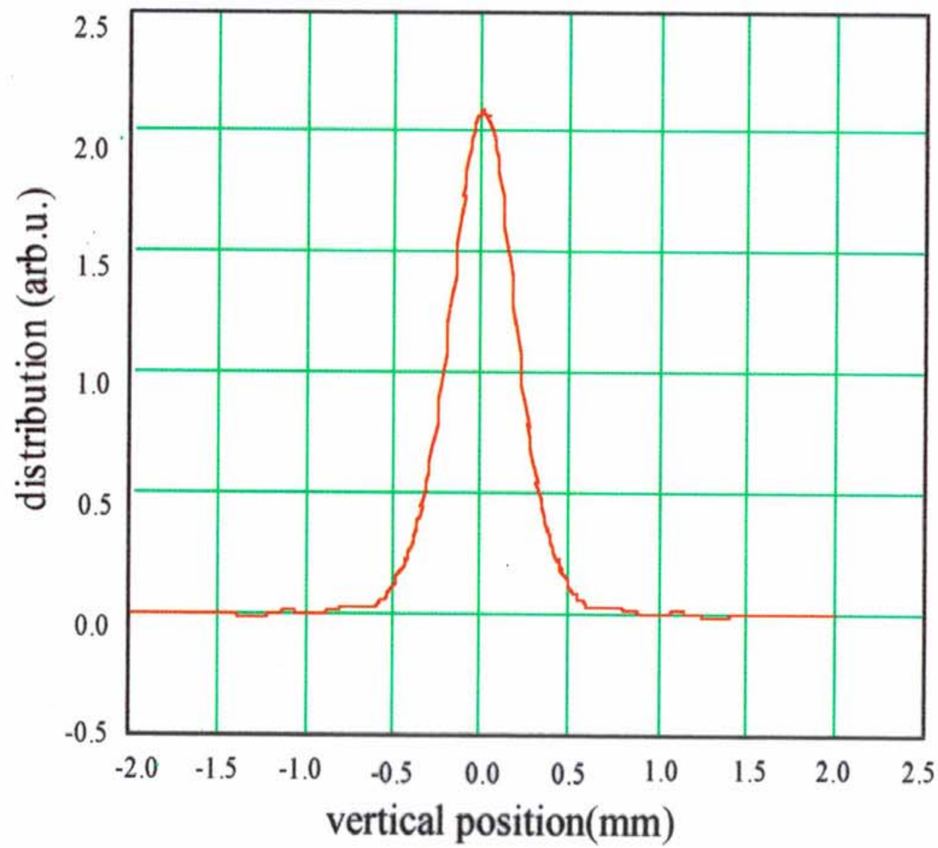

Result of beam size is 214μm

Result by imaging is 228μm

Application of interferometry

Small beam size measurement using Gaussian beam profile approximation

SMALL BEAM SIZE MEASUREMENT

We often approximate the beam profile with a Gaussian shape. A spatial coherence is also given by a Gauss function. We can evaluate a RMS width of spatial coherence by using q least-squares analysis. The RMS beam size σ_{beam} is given by the RMS width of the spatial coherence curve σ_γ as follows:

$$\sigma_{beam} = \frac{\lambda \cdot R}{2 \cdot \pi \cdot \sigma_\gamma}$$

where R : distance between the beam and the double slit.

λ : wave length

Vertical and horizontal beam size in low emittance lattice at the Photon Factory

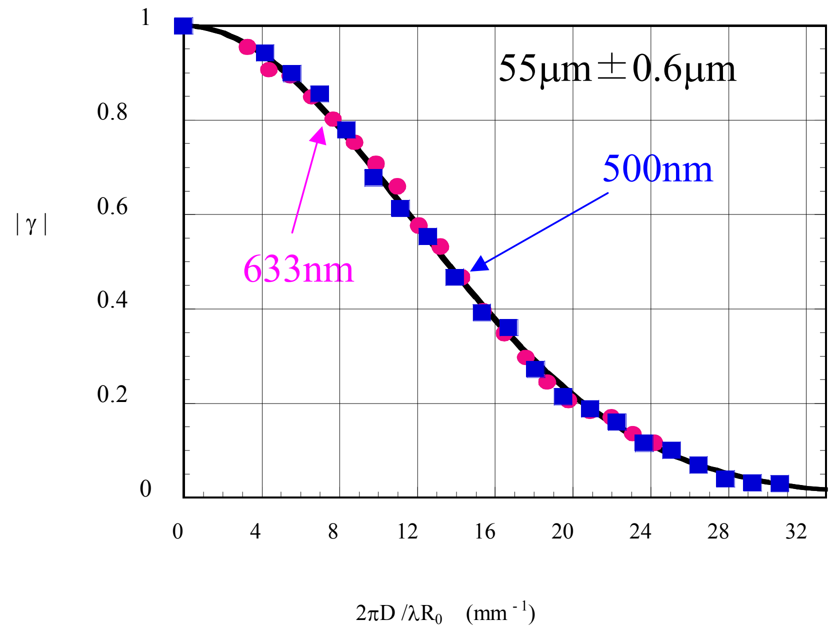

(a) vertical

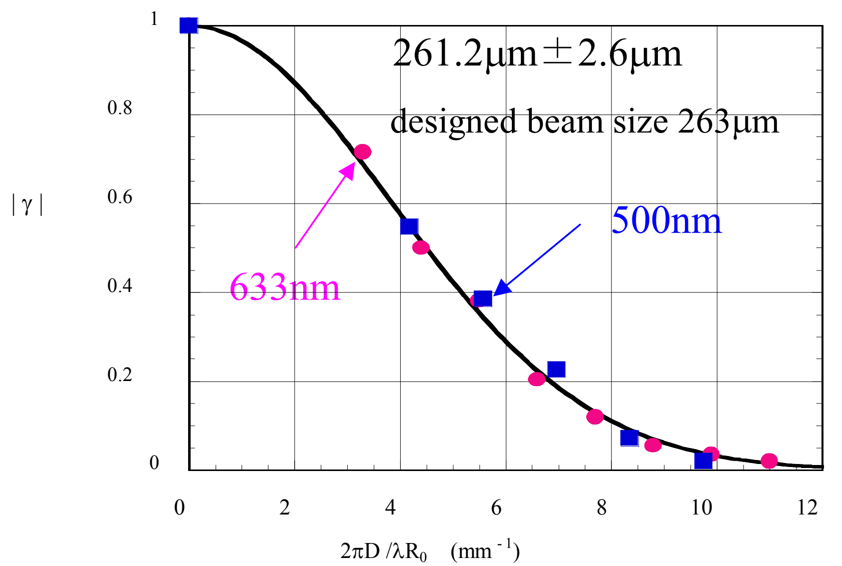

(b) horizontal

Vertical beam size at the SR center of Ritsumeikan university AURORA.

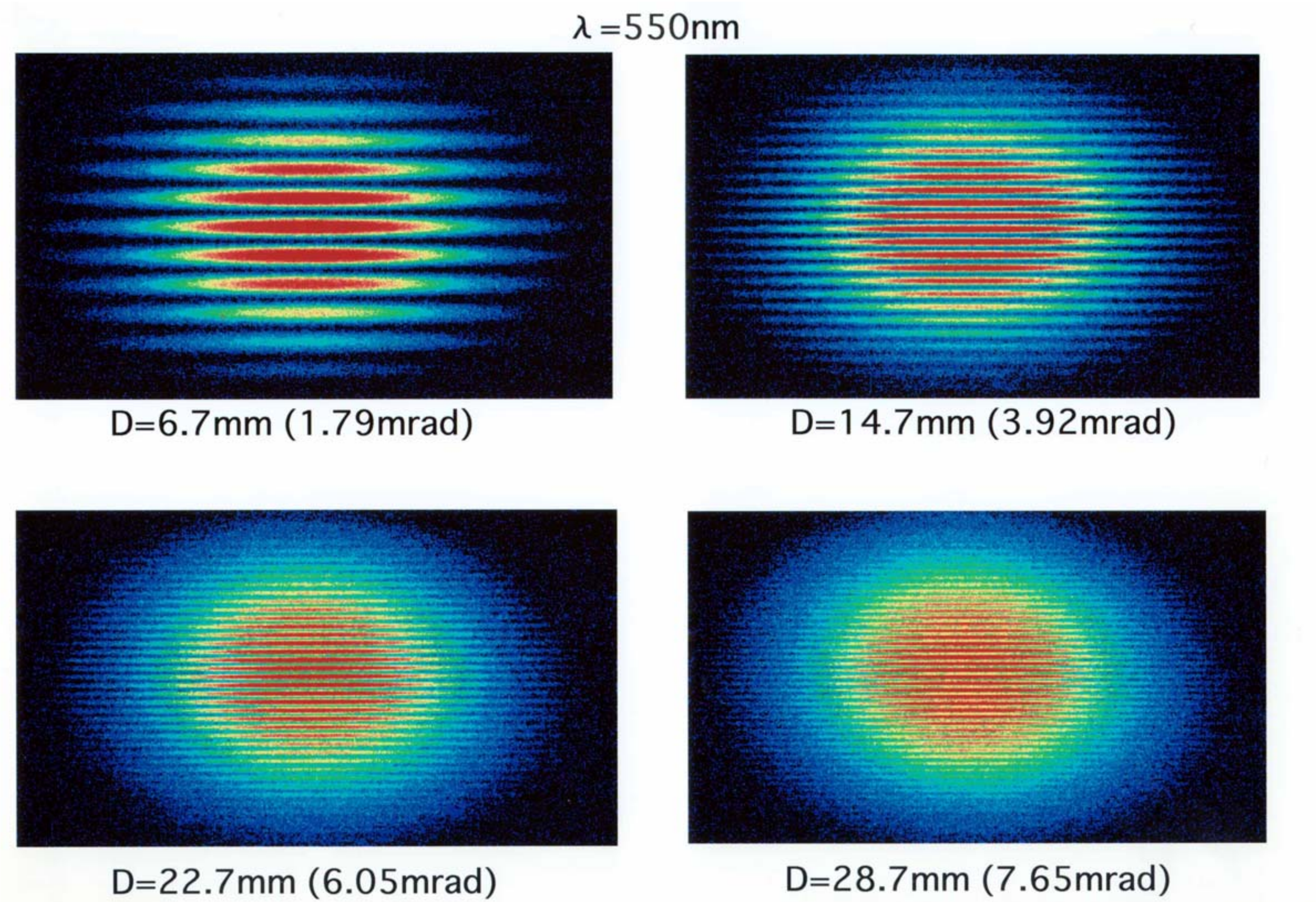

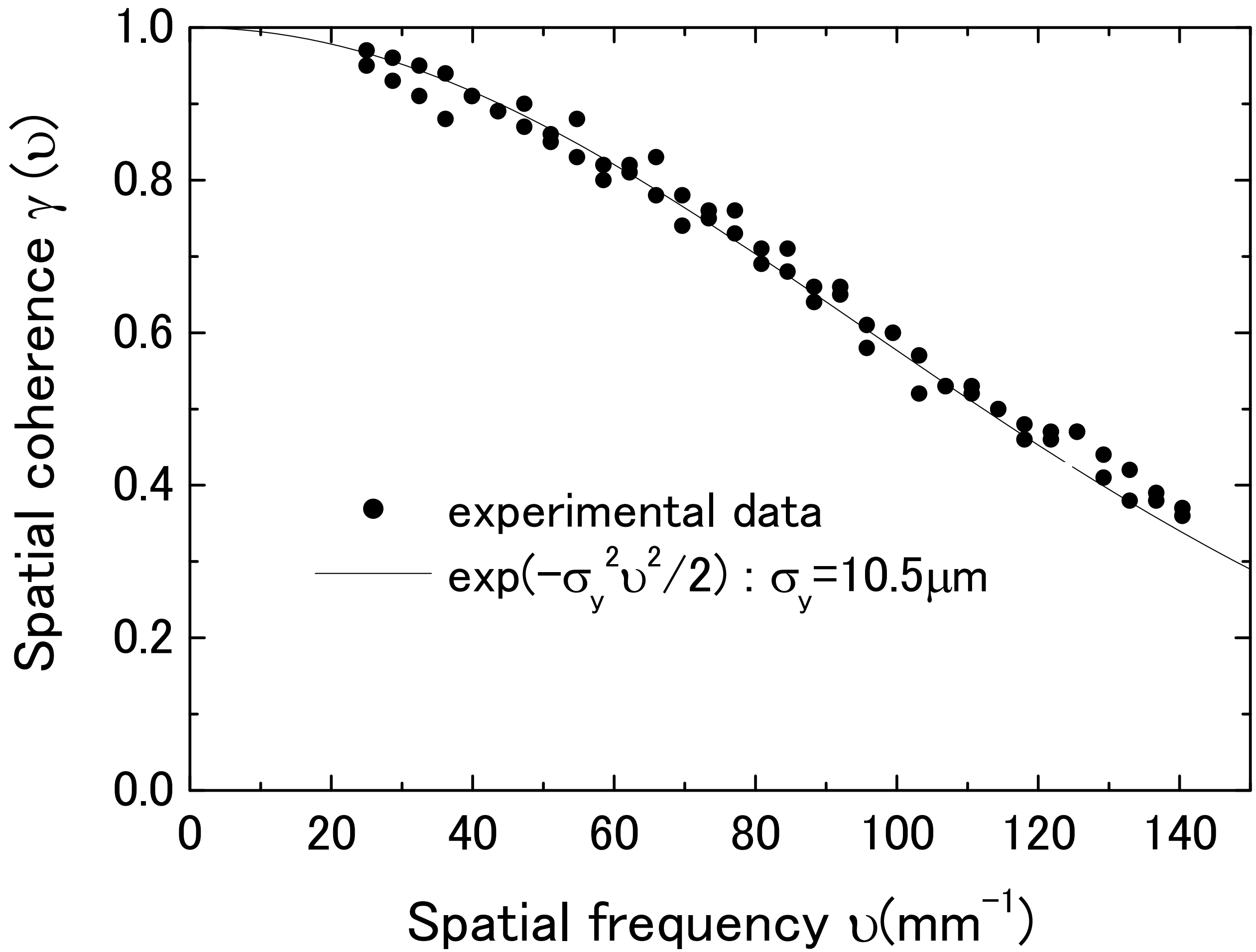

1.0
0.8
0.6
0.4
0.2
0.0
0
20
40
60
80
100
120
140
Spatial coherence γ (υ)
Spatial frequency υ(mm^{-1})
experimental data
$\exp(-\sigma_y^2\upsilon^2/2)$: σ_y=10.5μm

SR interferometer as a daily beam size monitor

We can also evaluate the RMS. beam size from one data of visibility, which is measured at a fixed separation of double slit. The RMS beam size σ_{beam} is given by ,

$$\sigma_{beam} = \frac{\lambda \cdot R_0}{\pi \cdot D} \cdot \sqrt{\frac{1}{2} \cdot \ln\left(\frac{1}{\gamma}\right)}$$

where γ denotes the visibility, which is measured at a double slit separation of D.

To consider that in the case to make an image, the resolution is limited by diffraction which is a Fourier transform using a given region of spatial frequency space (measurement in the real space).

In the case of interferometry, we can measure a small beam size with limited region of spatial frequency space by means of these two methods (measurement in the inverse space).

Assuming to use ATF conditions;

1. 500nm and 400nm
2. double slit separation 50mm 6.7mrad
3. distance between source point and double slit is 7.4m.

How small beam can we measure?

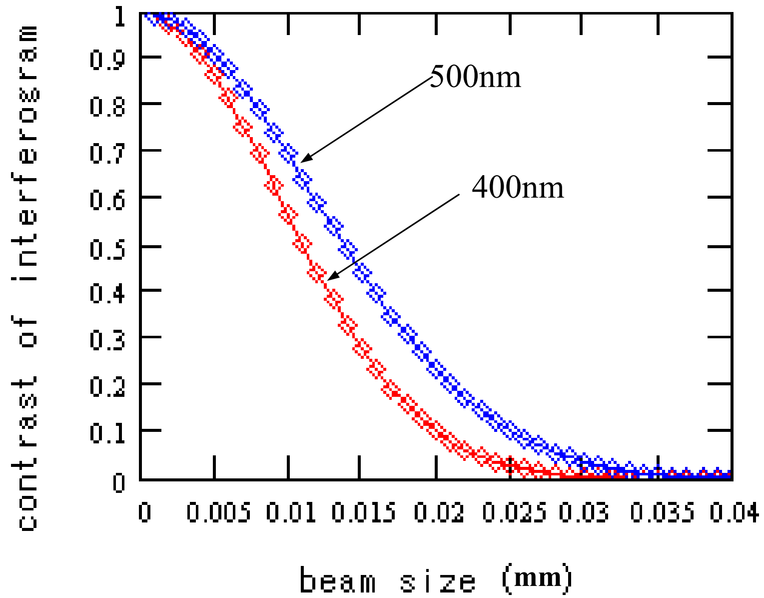

With 500nm;

beam size 3.0μm → contrast : 0.97

beam size 4.0μm → contrast : 0.94

If we measure contrast of the interferomgram in 1%, we can measure difference between 3μm and 4μm with a resolution less than 1μm

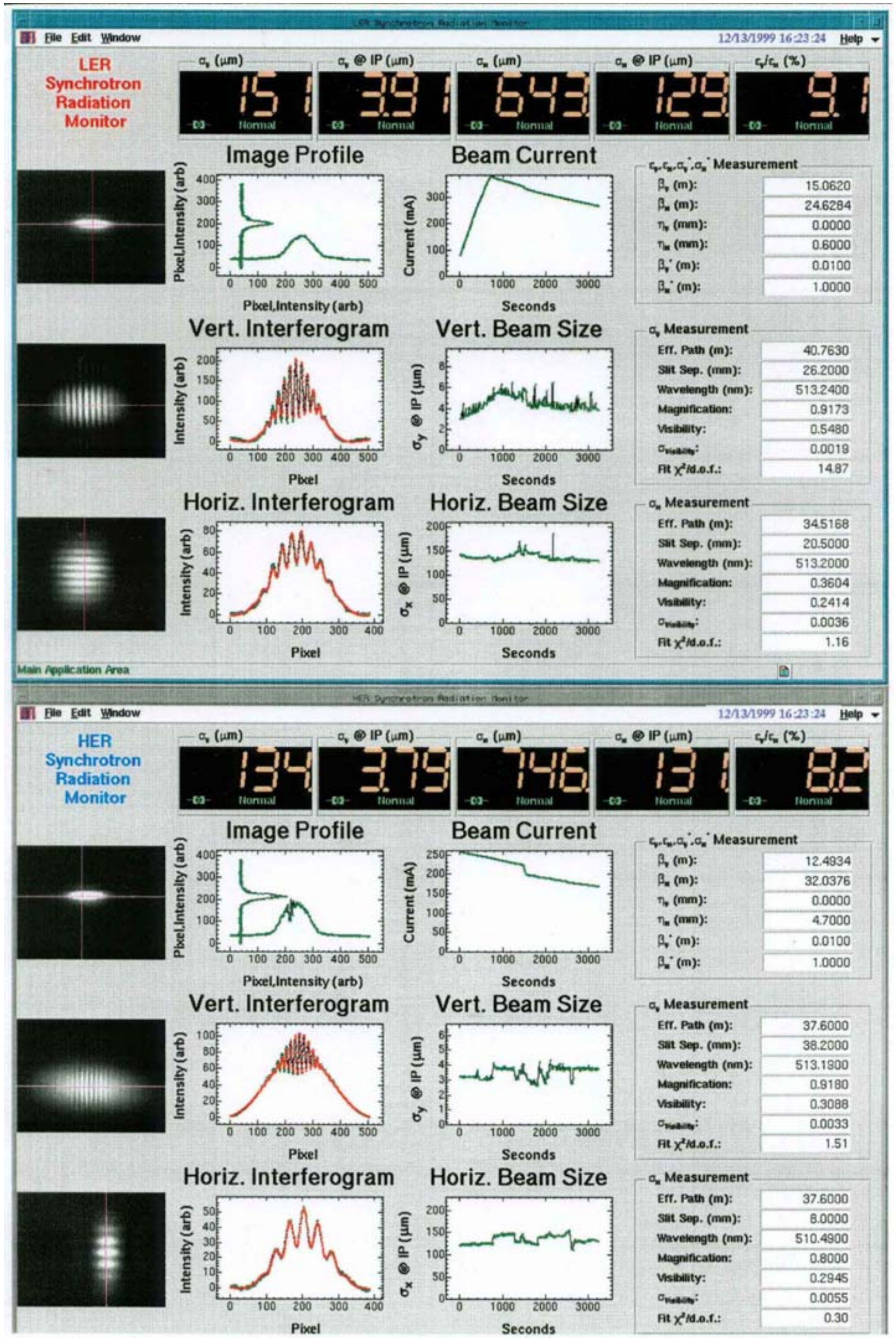

File Edit Window
12/13/1999 16:23:24
Help
LER Synchrotron Radiation Monitor
σy (μm) 151
σy @ IP (μm) 3.91
σx (μm) 643
σx @ IP (μm) 129
εy/εx (%) 9.1
Normal
Image Profile
Pixel,Intensity (arb)
Beam Current
Current (mA)
Seconds
εy,εx,σy*,σx* Measurement
βy (m): 15.0620
βx (m): 24.6284
ηy (mm): 0.0000
ηx (mm): 0.6000
βy* (m): 0.0100
βx* (m): 1.0000
Vert. Interferogram
Intensity (arb)
Pixel
Vert. Beam Size
σy @ IP (μm)
σy Measurement
Eff. Path (m): 40.7630
Slit Sep. (mm): 26.2000
Wavelength (nm): 513.2400
Magnification: 0.9173
Visibility: 0.5480
σVisibility: 0.0019
Fit χ²/d.o.f.: 14.87
Horiz. Interferogram
Horiz. Beam Size
σx @ IP (μm)
σx Measurement
Eff. Path (m): 34.5168
Slit Sep. (mm): 20.5000
Wavelength (nm): 513.2000
Magnification: 0.3604
Visibility: 0.2414
σVisibility: 0.0036
Fit χ²/d.o.f.: 1.16
Main Application Area
File Edit Window
12/13/1999 16:23:24
Help
HER Synchrotron Radiation Monitor
σy (μm) 134
σy @ IP (μm) 3.79
σx (μm) 746
σx @ IP (μm) 131
εy/εx (%) 8.2
Normal
Image Profile
Pixel,Intensity (arb)
Beam Current
Current (mA)
Seconds
εy,εx,σy*,σx* Measurement
βy (m): 12.4934
βx (m): 32.0376
ηy (mm): 0.0000
ηx (mm): 4.7000
βy* (m): 0.0100
βx* (m): 1.0000
Vert. Interferogram
Intensity (arb)
Pixel
Vert. Beam Size
σy @ IP (μm)
σy Measurement
Eff. Path (m): 37.6000
Slit Sep. (mm): 38.2000
Wavelength (nm): 513.1900
Magnification: 0.9180
Visibility: 0.3088
σVisibility: 0.0033
Fit χ²/d.o.f.: 1.51
Horiz. Interferogram
Horiz. Beam Size
σx @ IP (μm)
σx Measurement
Eff. Path (m): 37.6000
Slit Sep. (mm): 8.0000
Wavelength (nm): 510.4900
Magnification: 0.8000
Visibility: 0.2945
σVisibility: 0.0055
Fit χ²/d.o.f.: 0.30

Horizontal beam size measurement

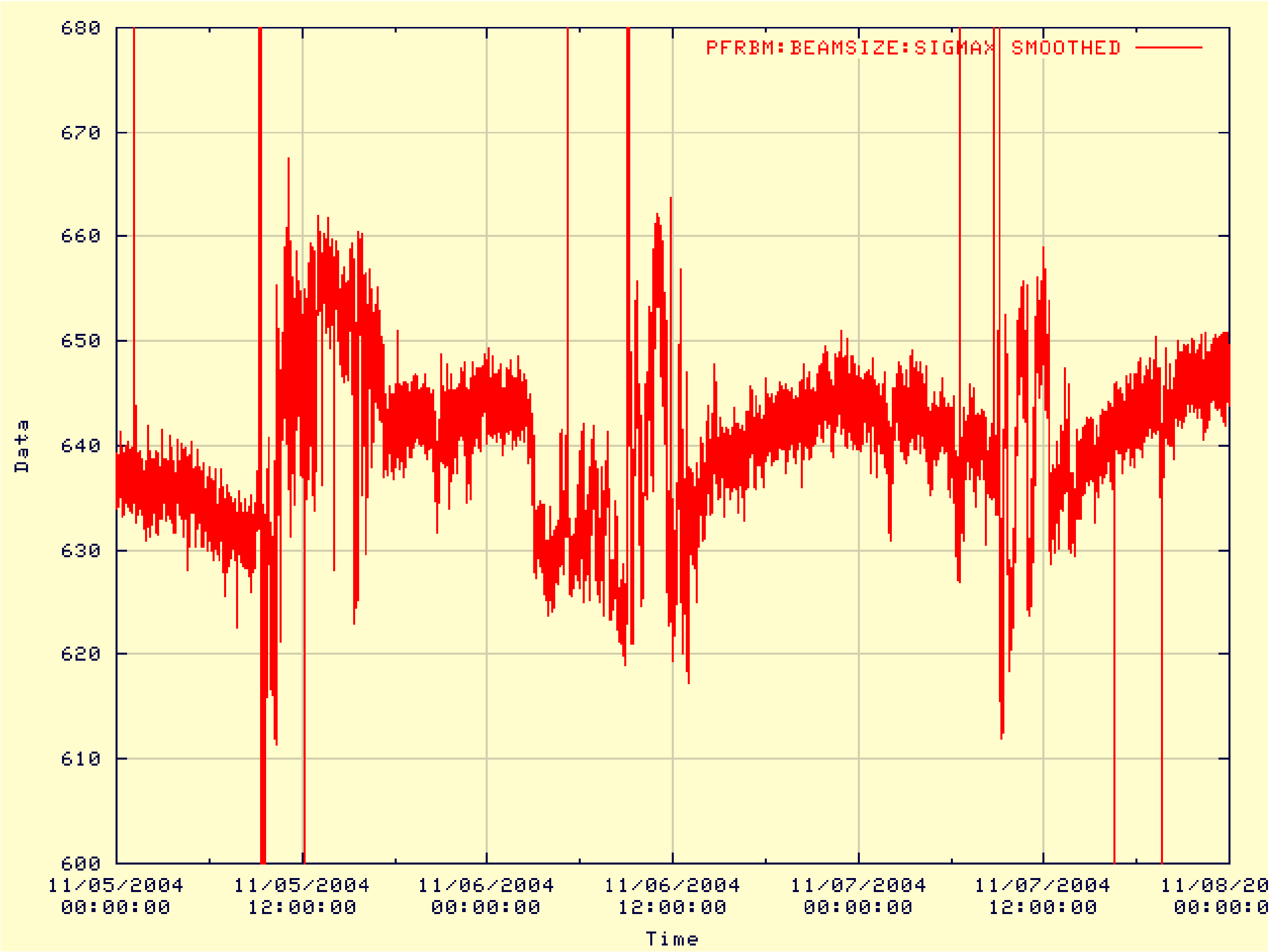

±3μm

Vertical beam size measurement

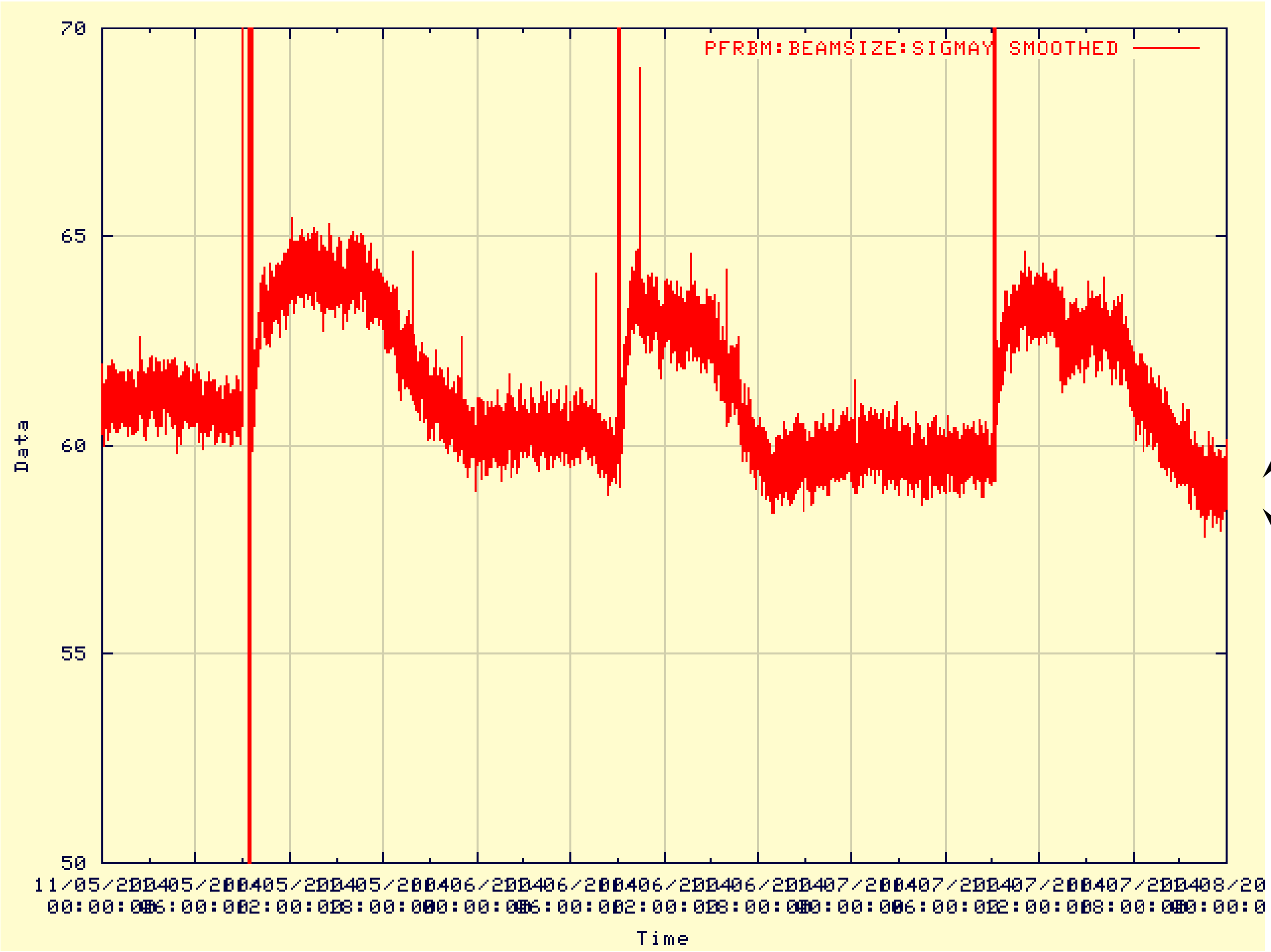

$\pm 1\mu m$

Few μm range very small beam size measurement at the ATF

Newtonian arrengement of optics

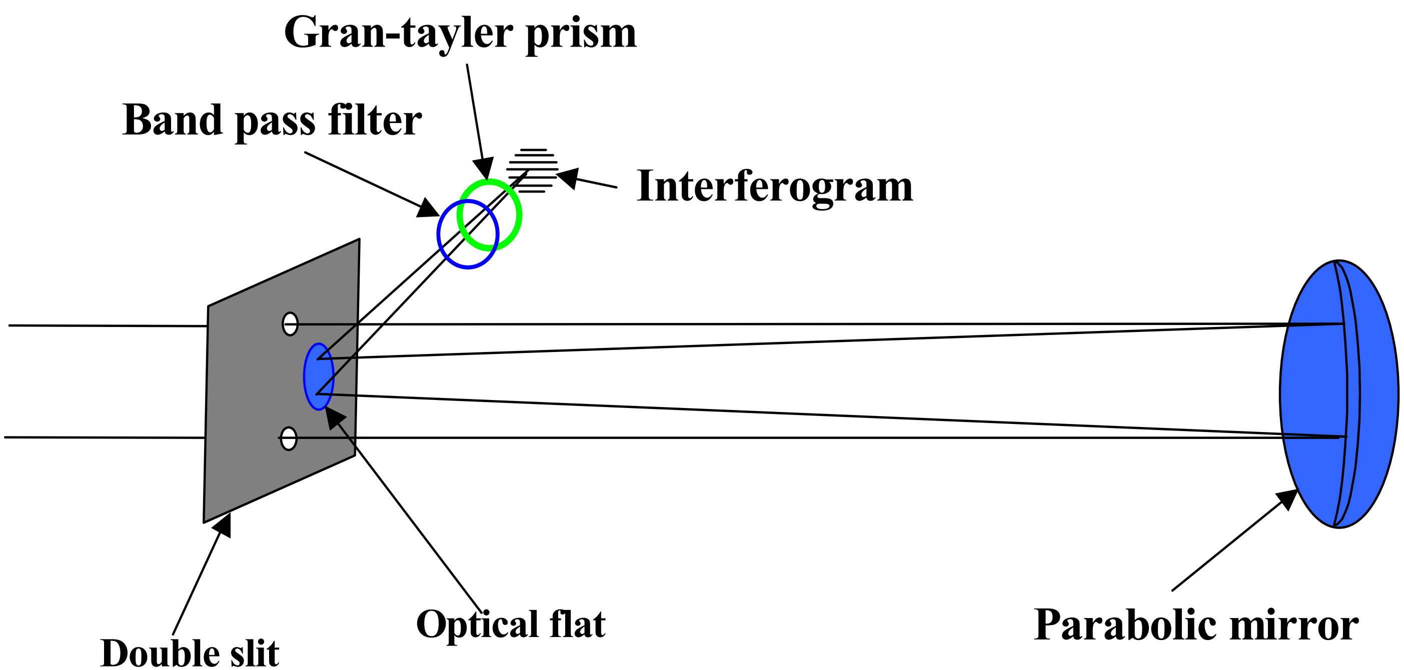

Measured interferogram

Result of beam size is 4.73μm±0.55μm
Corresponding emittance is 9.7pmrad

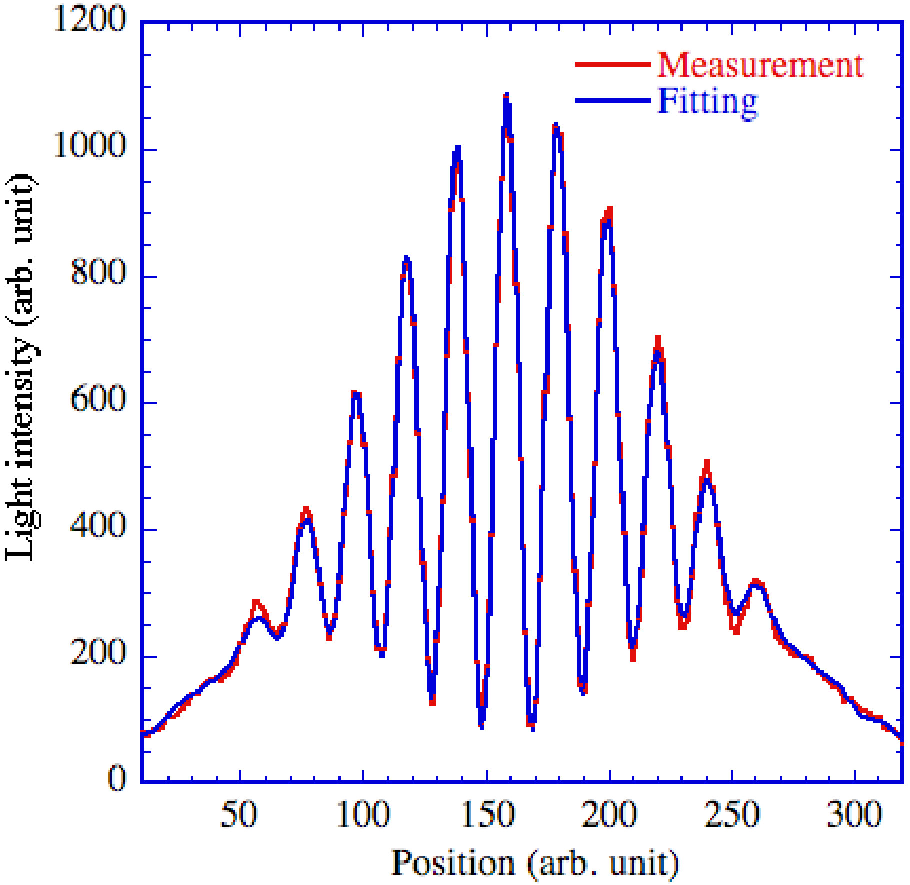

The x-y coupling is controlled by the strength of the skew winding of sextupole magnets(SD, SF) at ATF

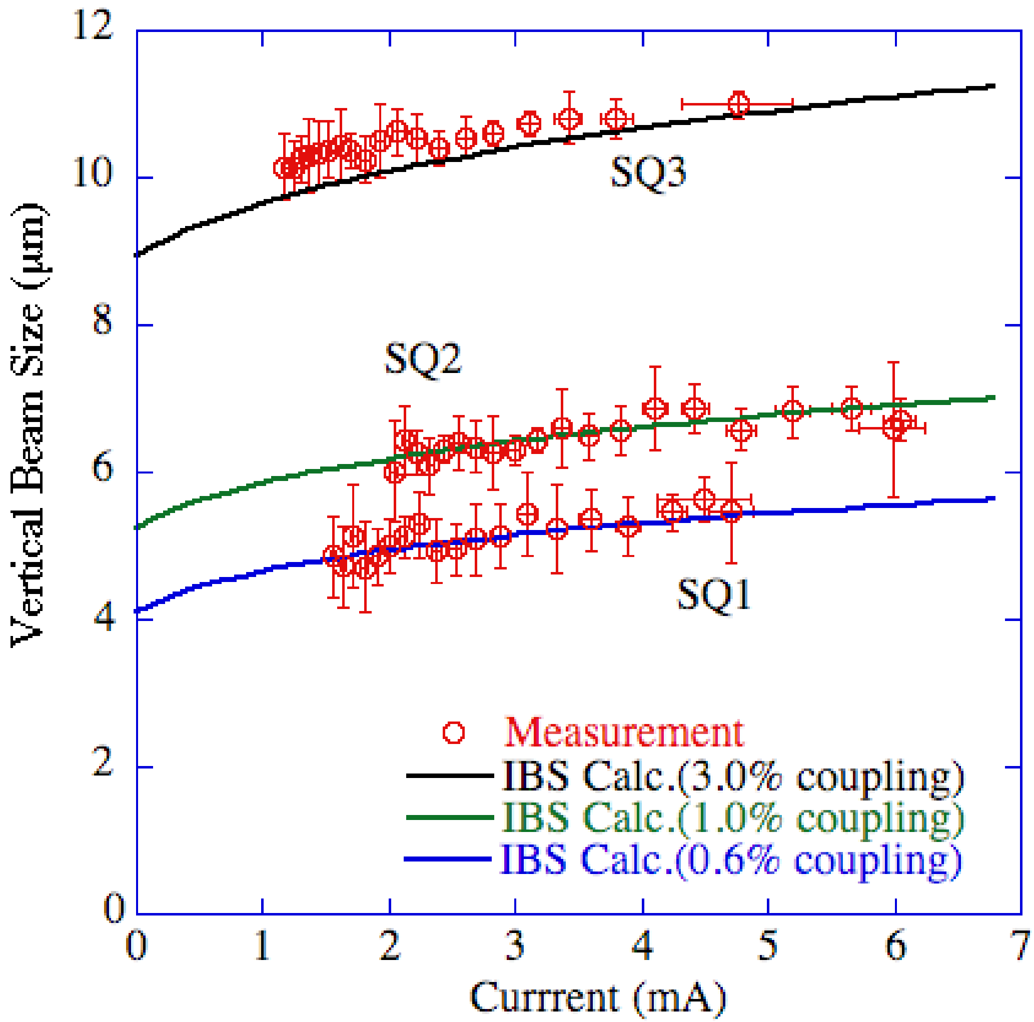

Two dimensional interferometer

Single photon four modes

Choice 1

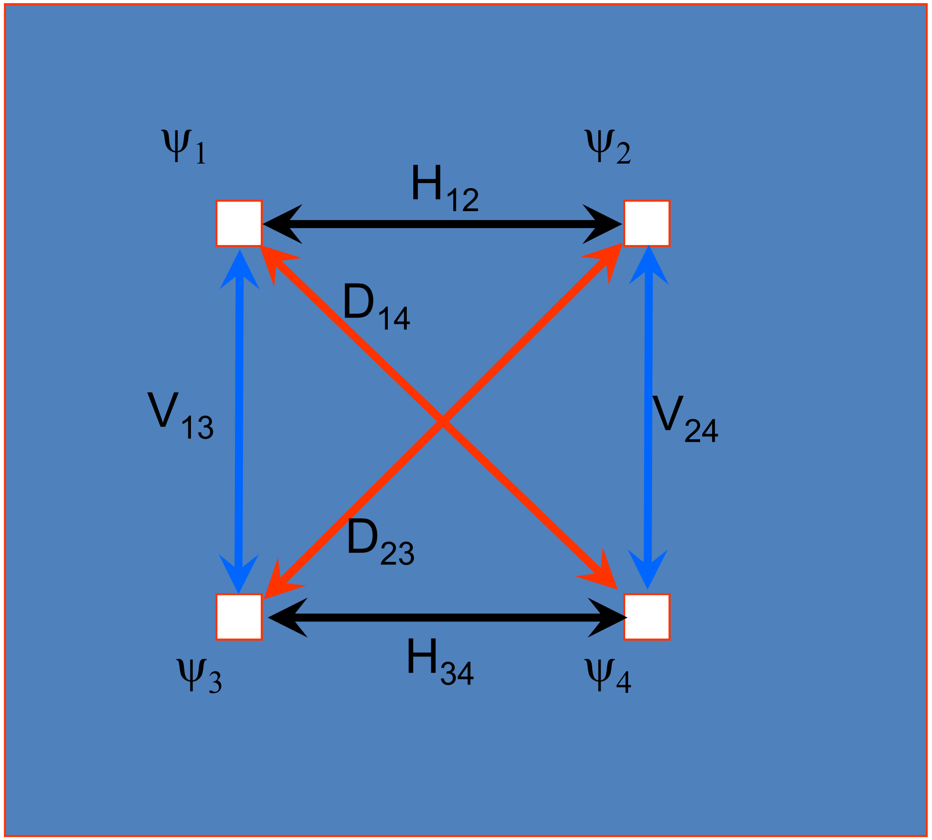

$$I = \psi_1^2 + \psi_2^2 + \psi_3^2 + \psi_4^2$$
$$+ H_{12} + H_{34} + V_{13} + V_{24} + D_{14} + D_{23}$$

In here,

$\psi_2=\psi_1^*$

$\psi_3=\psi_1^*$

$\psi_4=\psi_3^*=\psi_1$

$H12= |\psi_1 \cdot \psi_1^*|_{D1}$

$H34= |\psi_1^* \cdot \psi_1 |_{D1}$

$V13=|\psi_1 \cdot \psi_1^* |_{D2}$

$V24= |\psi_1^* \cdot \psi_1 |_{D2}$

$D14= \psi_1 \cdot \psi_1|_{D3}$ unobservable

$D23= \psi_1^* \cdot \psi_1^*|_{D3}$ unobservable

2-D interferometer experiment April,1998

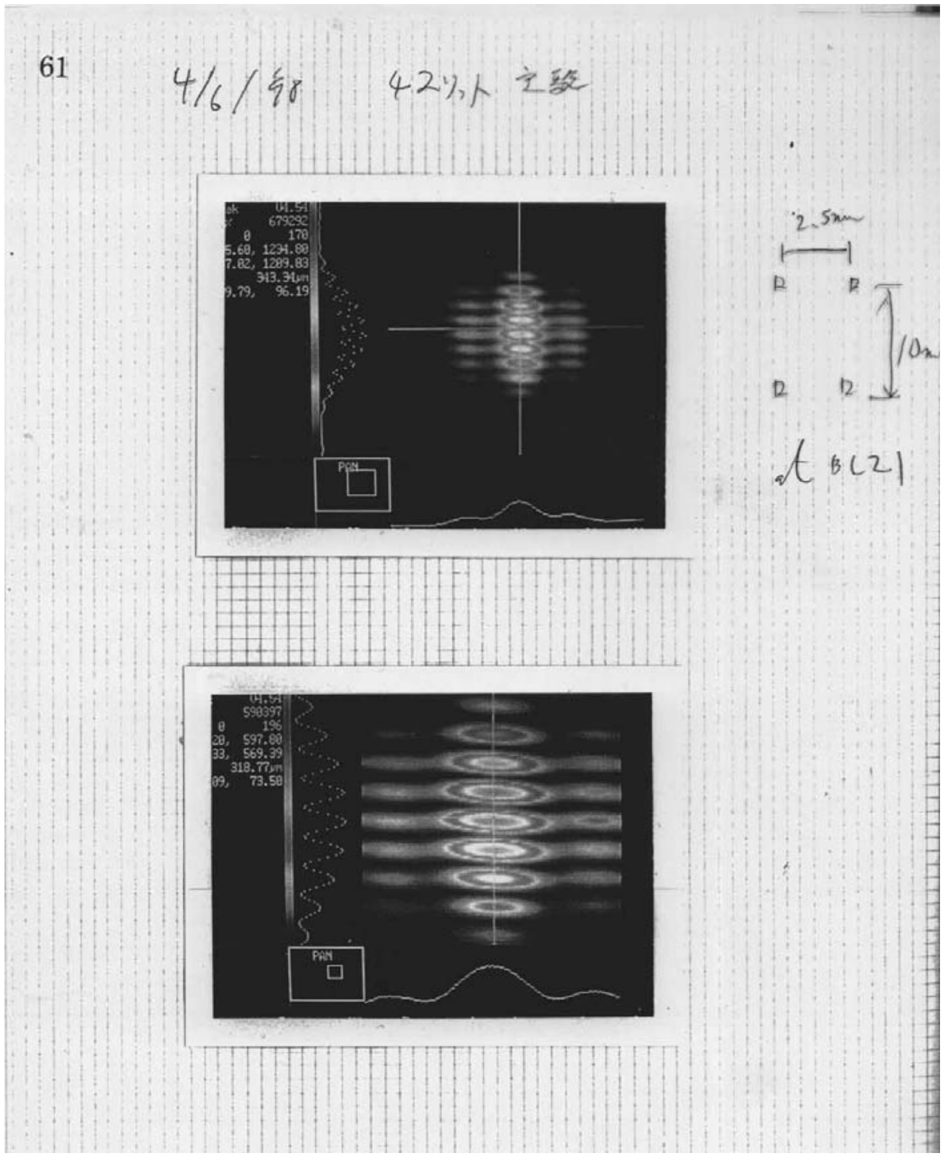

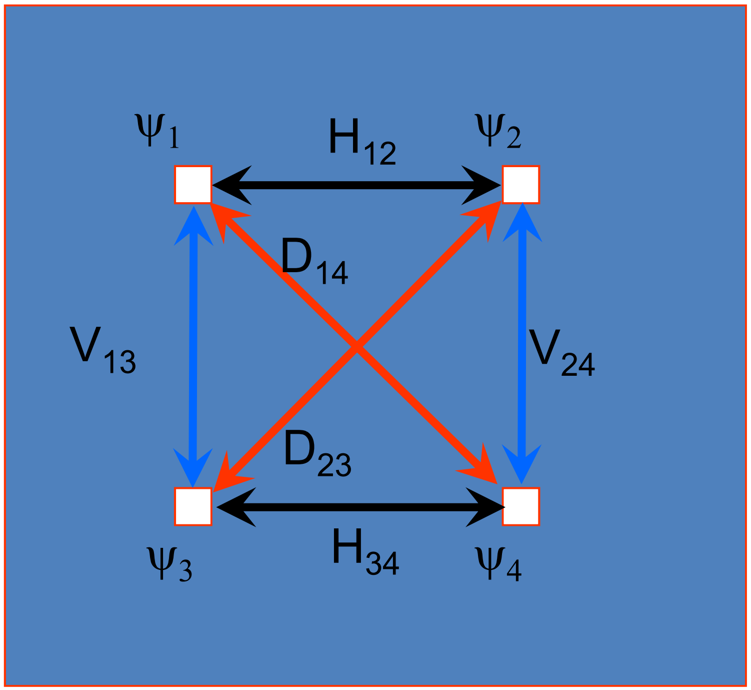

Using this scheme, If, wavefront error will existing (actually, it will be happen very often) between 1-2 and 2-4, or (and) 1-3 and 2-4, H_{12}will not equal to H_{34}, or (and) V_{13} will not equal to V_{24}.

In this situation, we cannot measure beam size correctly.

Choice 2

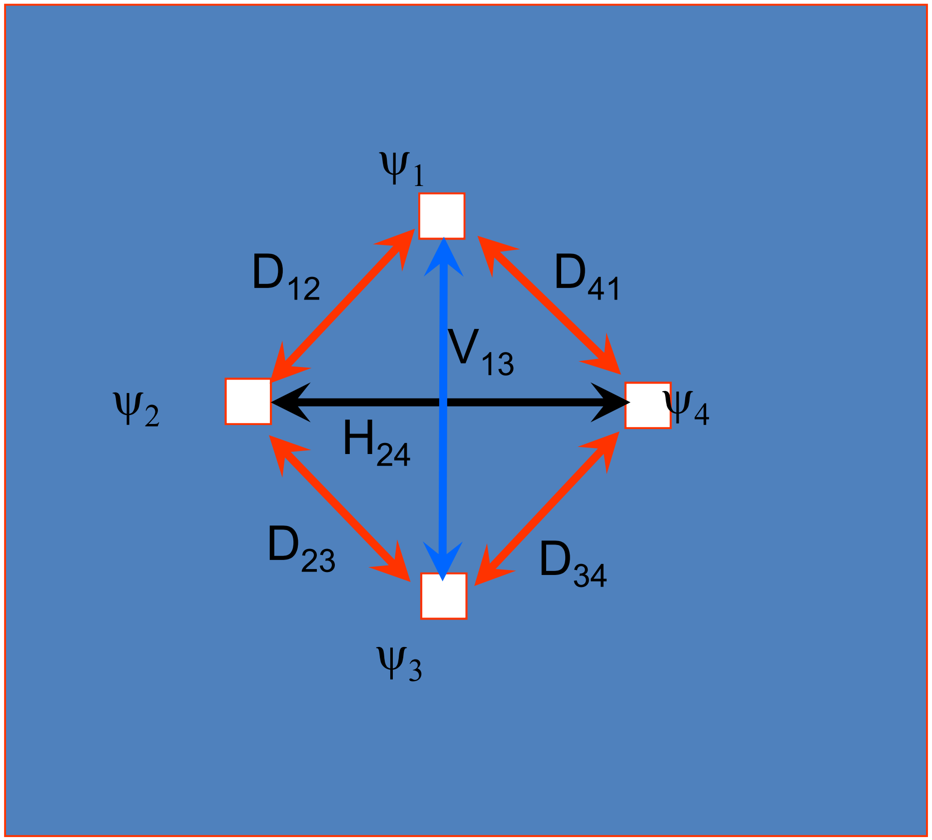

This choice seems decisively better than choice 1 from the view point of wavefront error, because vertical and horizontal cross term is only V_{13} and H_{24}. Oppositely, askew correlation terms D_{ij} will be double, but these terms are not observable, of the optics will no aberrations.

Merit and demerit in 2D interferometer

Merit

1) We can measure vertical and horizontal beam sizes simultaneously.

Demerit

1) We cannot change the conditions of interferometer such as slit separation independently.
2) It seems very difficult to perform the slit scanning.
3) If vertical beam size and horizontal beam size are something different, other configuration of the interferometer will necessary(for example retro-focus type interferometer).

Conclusion

It seems convenient to use two independent interferometers!

Beam halo measurement with the Coronagraph

The coronagraph to observe sun corona

Developed by B.F.Lyot in 1934 for a observation of sun corona by artificial eclipse.

Special telescope having a
re-diffraction system to eliminate a diffraction fringe.

Everything was start with astronomer's dream……

Eclipse is rare phenomena, and only few second is available for observation of sun corona, prominence etc.

Artificial eclipse was dream of astronomers, but……..

Diffraction fringes vs. beam halo

Observation with normal telescope

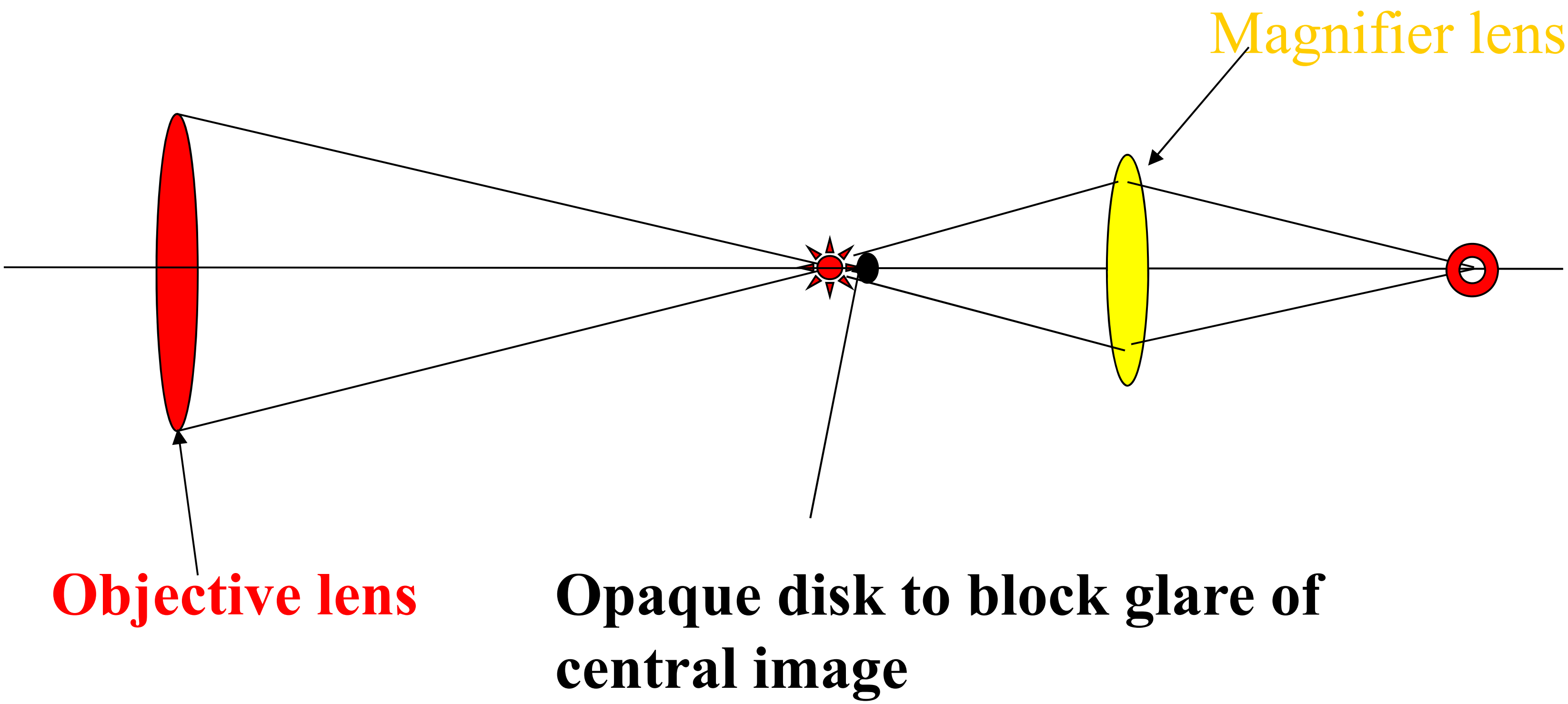

Diffraction fringes makes tail surrounding from the central beam image.

Intensity of diffraction tail is in the range of 10^{-2} -10^{-3} of the peak intensity.

↓

The diffraction tail disturb an observation of week object surrounding from bright central beam

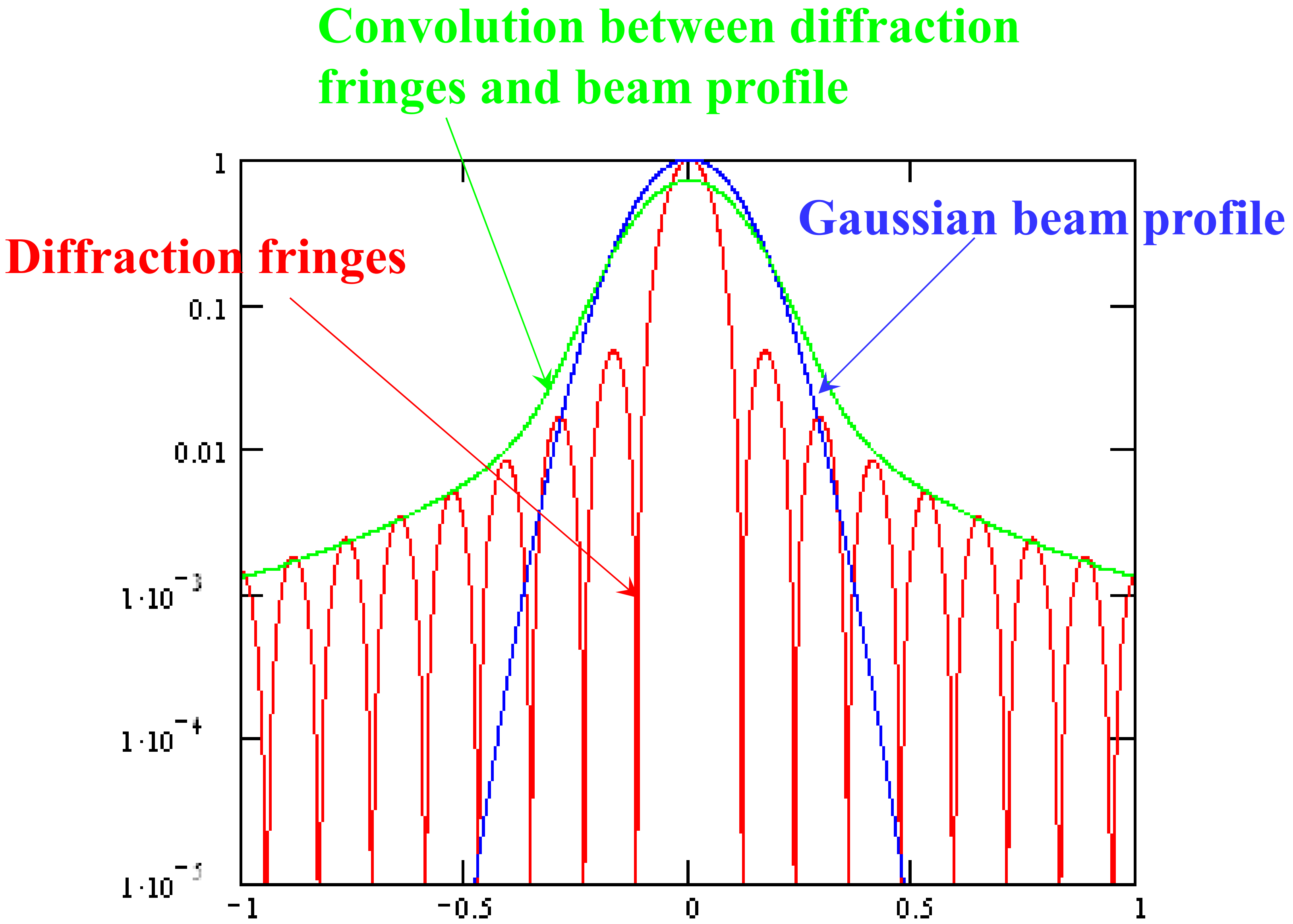

Convolution between diffraction fringes and beam profile
Gaussian beam profile
Diffraction fringes
1
0.1
0.01
1·10⁻³
1·10⁻⁴
1·10⁻⁵
−1
−0.5
0
0.5
1

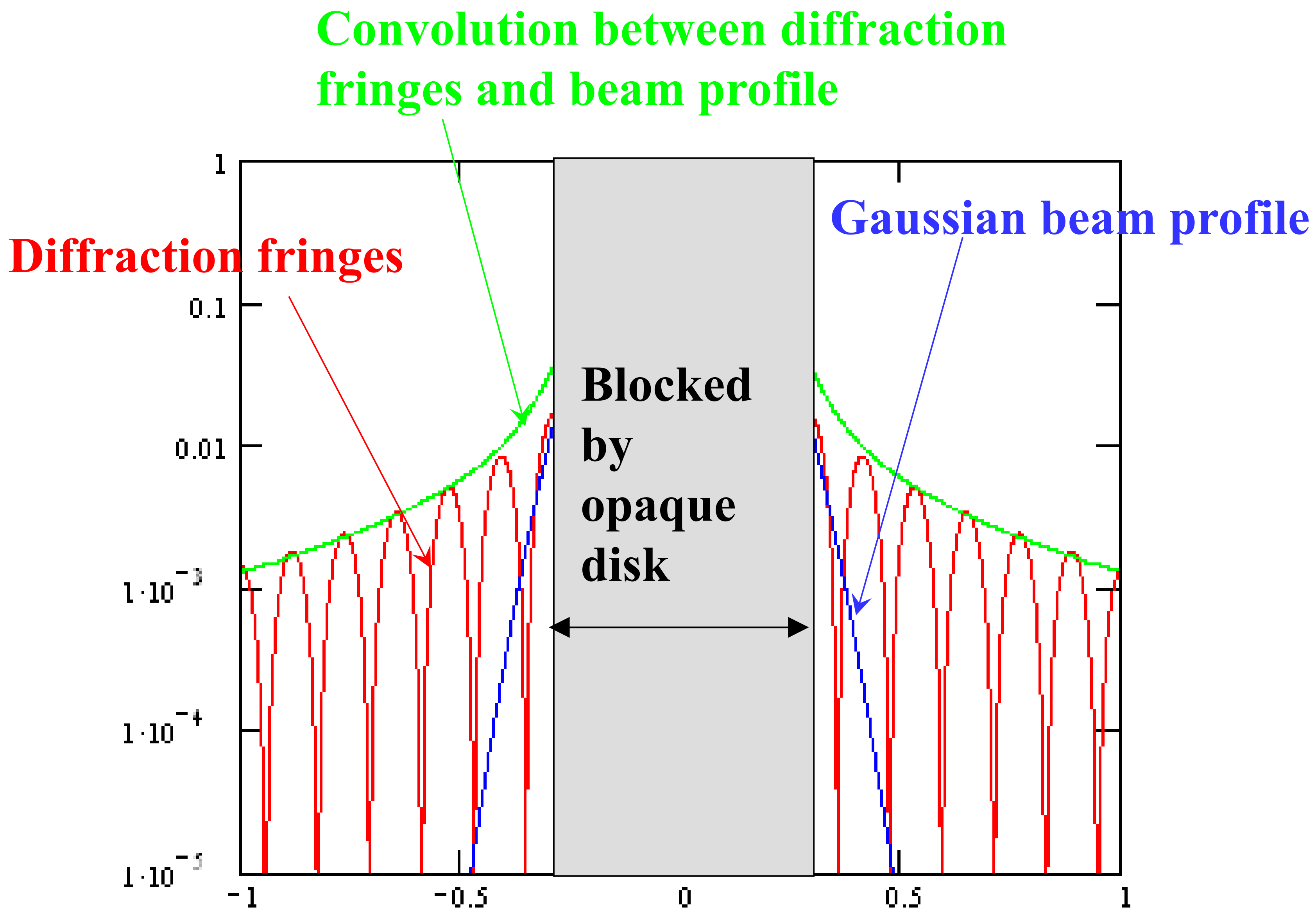

Convolution between diffraction fringes and beam profile
Gaussian beam profile
Diffraction fringes
Blocked by opaque disk
1
0.1
0.01
1·10⁻³
1·10⁻⁴
1·10⁻⁵
−1
−0.5
0
0.5
1

2004 Observation of beam halo with corona graph

Optical system of Lyott's corona graph

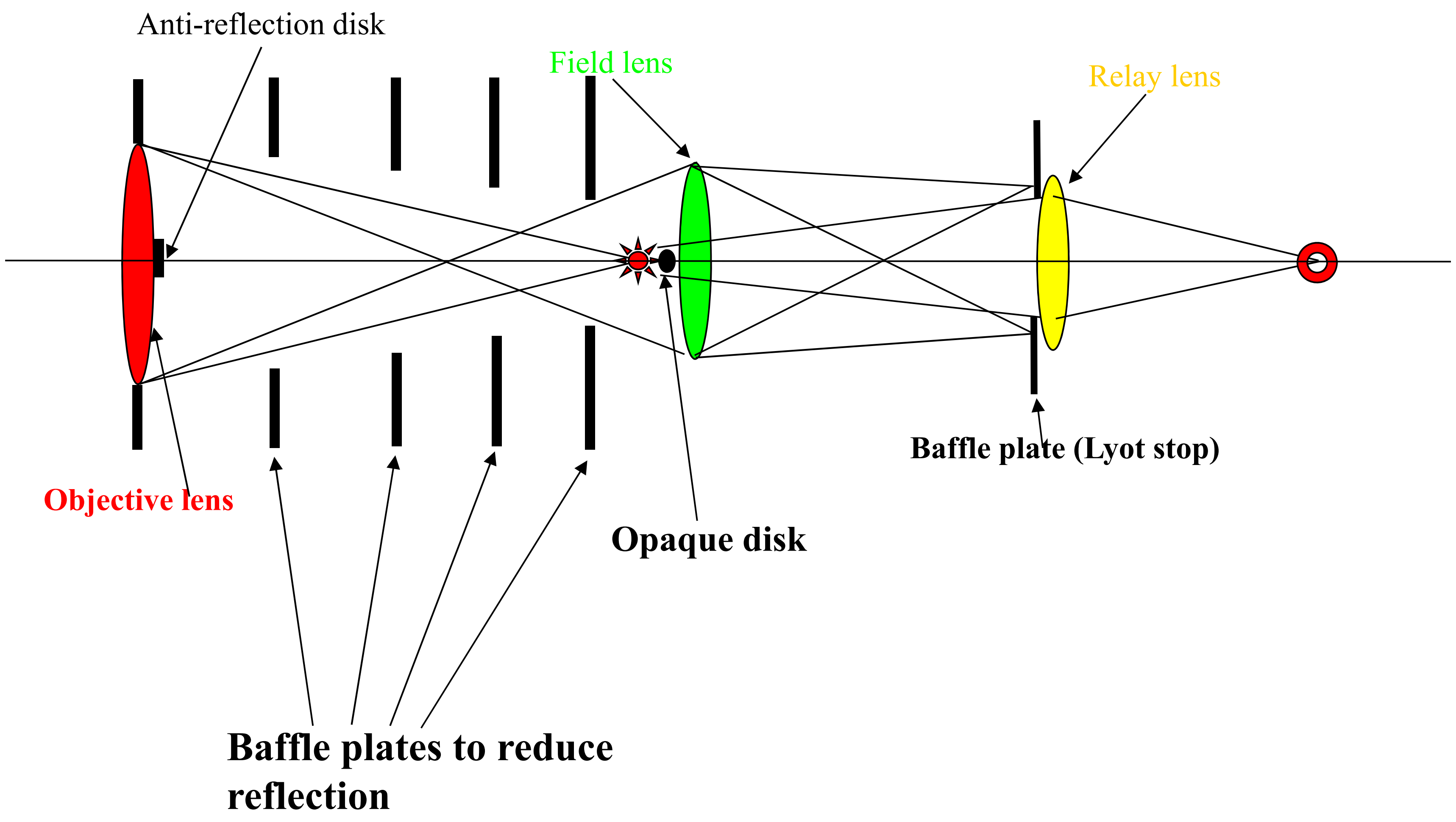

Image of beam profile without the opaque disk. Exposure time of CCD camera is 10msec.

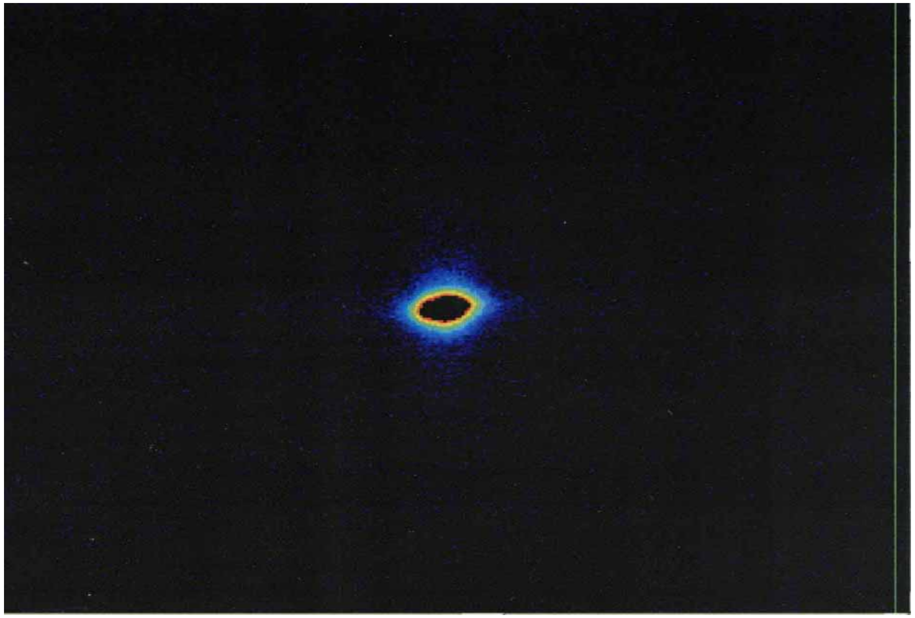

Image of beam tail with the opaque disk. Transverse magnification is same as in Fig.6. Exposure time of CCD camera is 10msec.

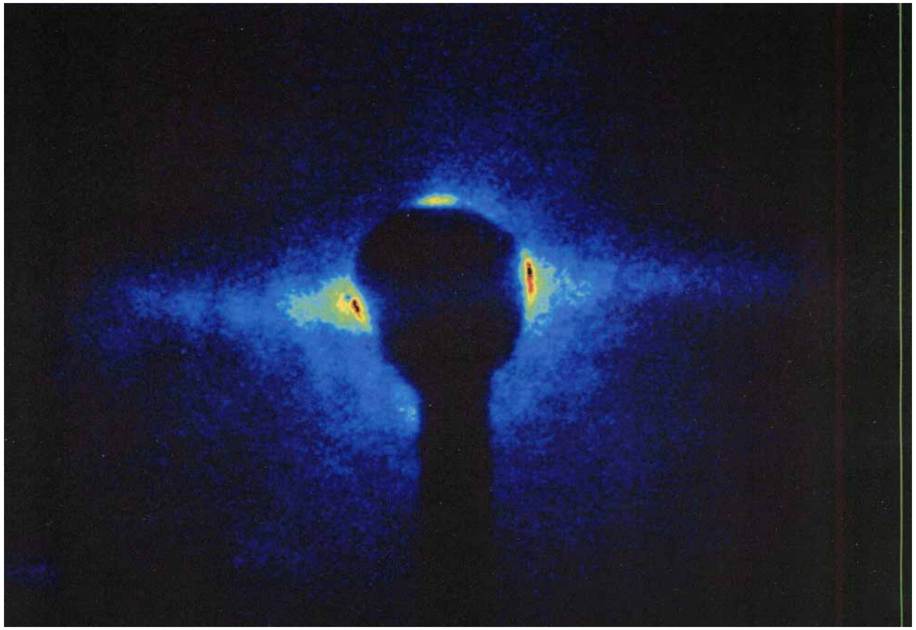

Beam tail images in the single bunch operation at the KEK PF measured at different current

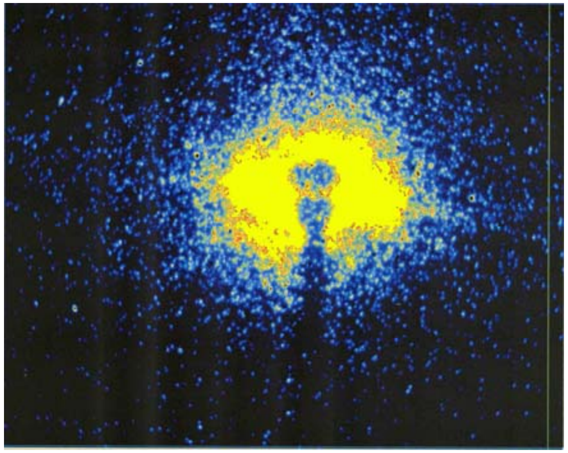

65.8mA

61.4mA

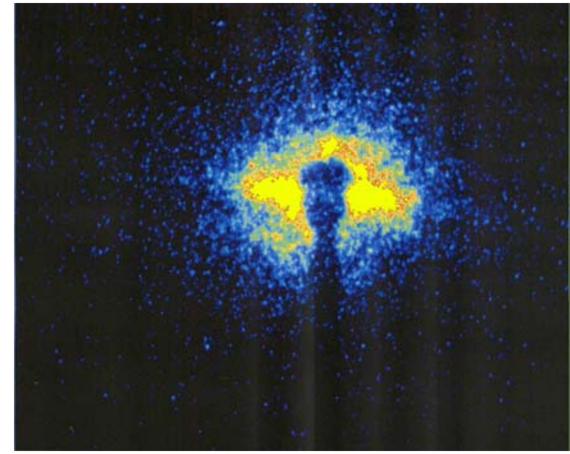

54.3mA

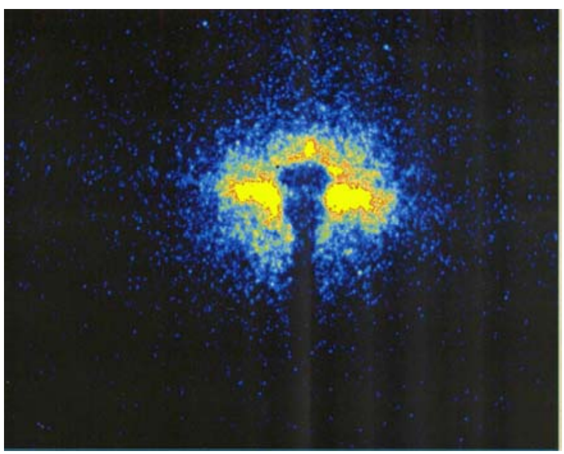

45.5mA

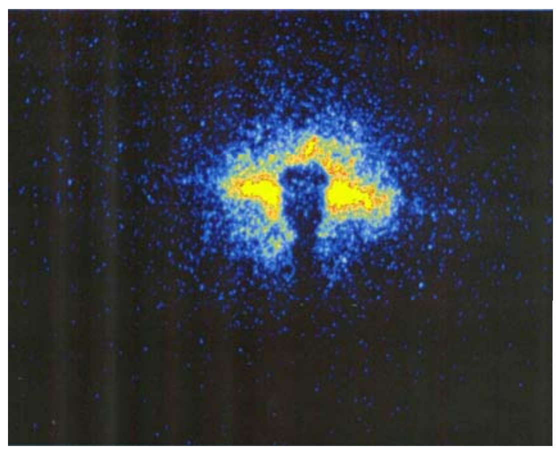

35.5mA

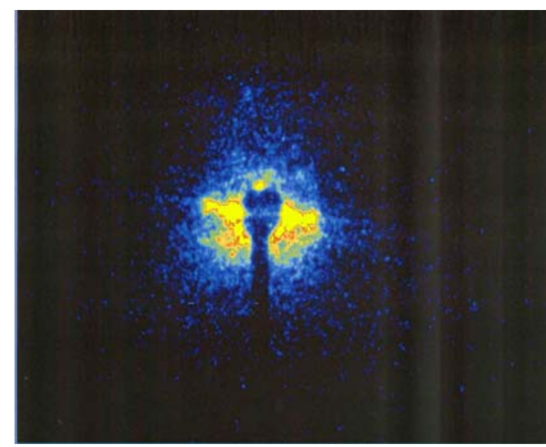

396.8mA
Multi-bunch
bunch current 1.42mA

Observation for the deep out side

Single bunch
65.8mA
Exposure time of CCD : 3msec

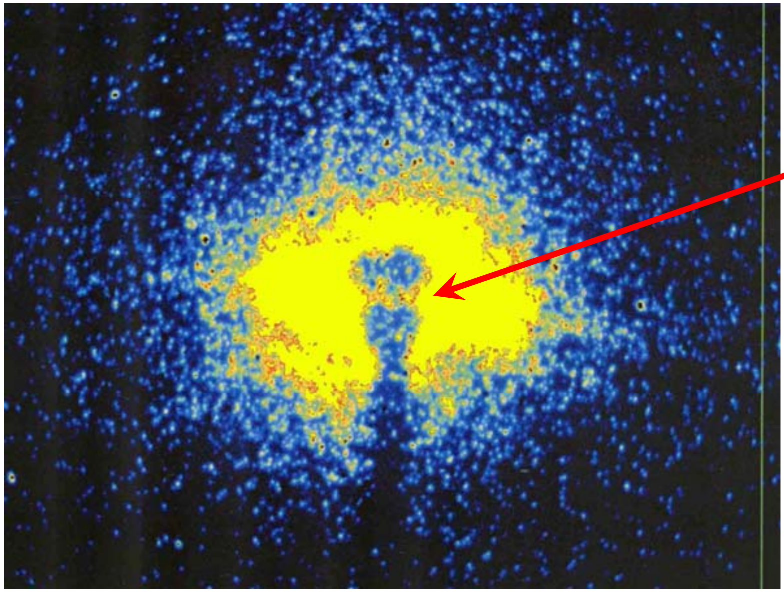

Intensity in here : 2.05×10^{-4} of peak intensity

Deep outside

Exposure time of CCD : 100msec

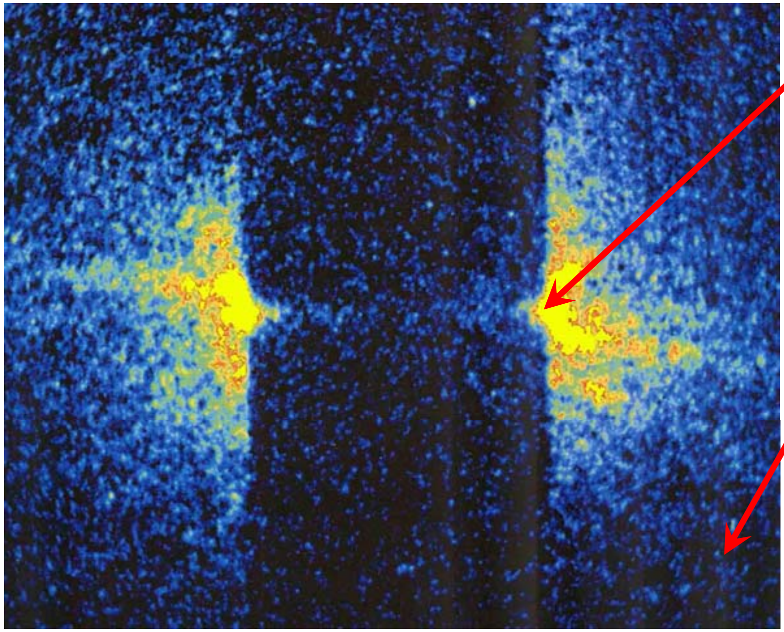

2.55×10^{-6}

Background leavel : about 6×10^{-7}

5. Project now started

Visible and X-ray synchrotron radiation monitor for ATF2

Two dimensional beam halo diagnostics with coronagraph.

X-ray imaging system aiming for 100nm spatial resolution.

X-ray interferometer for 1nm spatial resolution

5. SR monitor based on X-ray

X-ray pin-hole camera

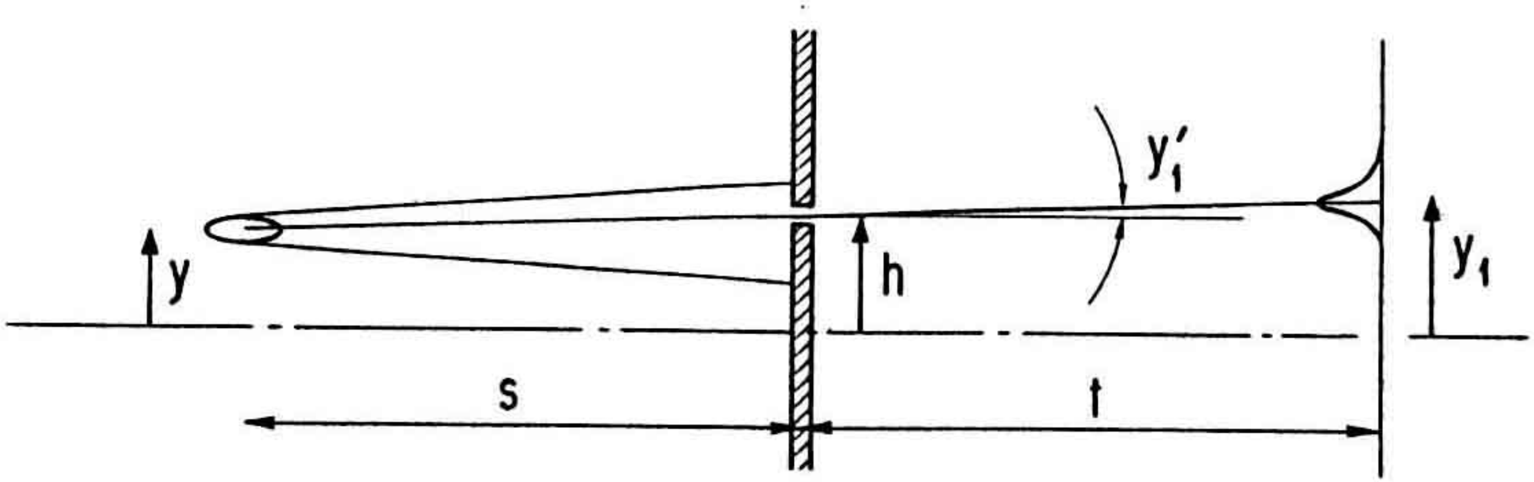

$$\begin{pmatrix} y_1 \\ y_1' \end{pmatrix} = \begin{pmatrix} 1 & s+t \\ 0 & 1 \end{pmatrix} \begin{pmatrix} y \\ y' \end{pmatrix}.$$

Representation in the phase space

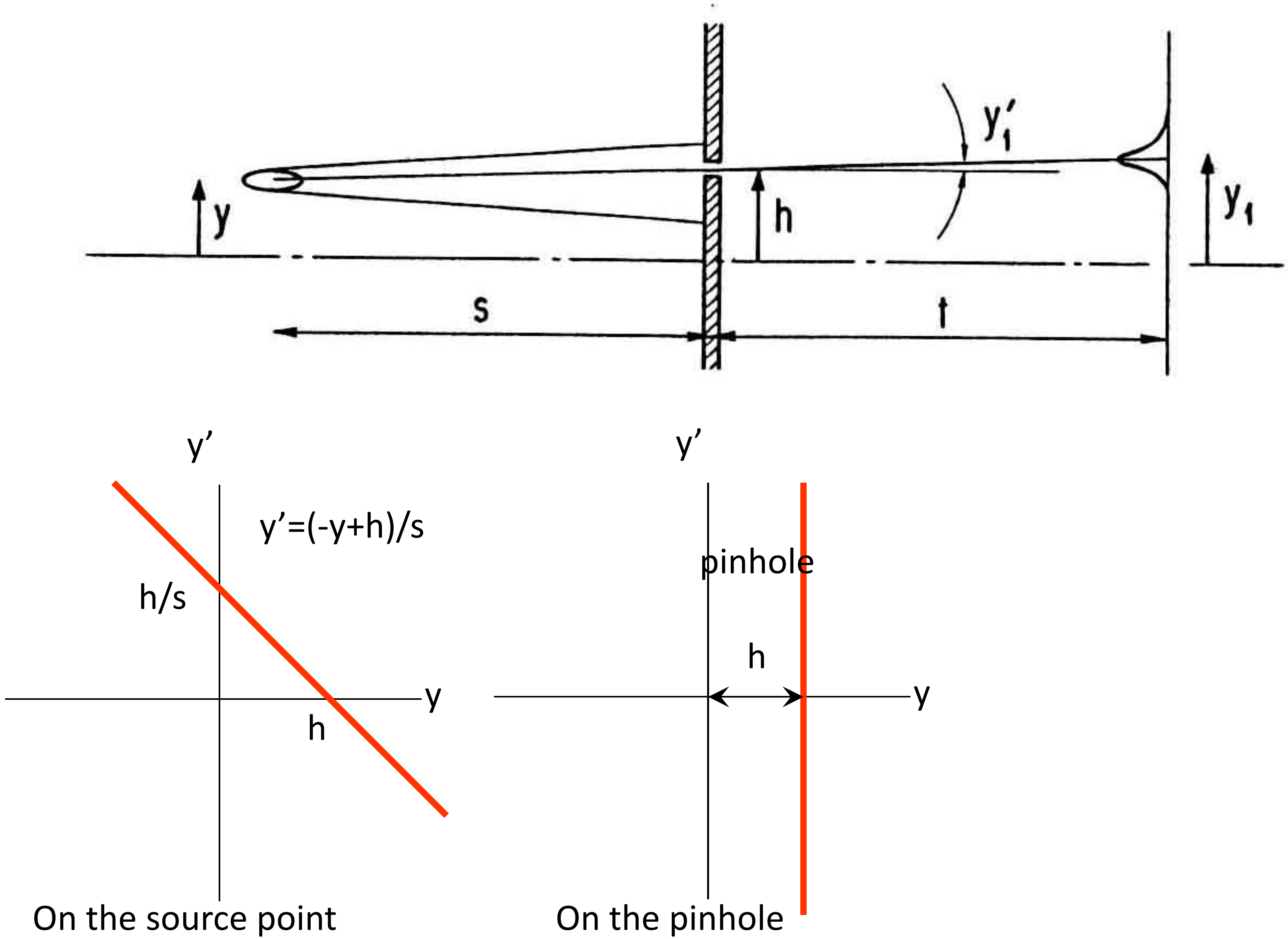

Pinhole in phase space on source point

$$\begin{pmatrix} h \\ y'_p \end{pmatrix} = \begin{pmatrix} 1 & s \\ 0 & 1 \end{pmatrix} \begin{pmatrix} y \\ y' \end{pmatrix}$$

h=y+sy’

y’=(-y+h)/s

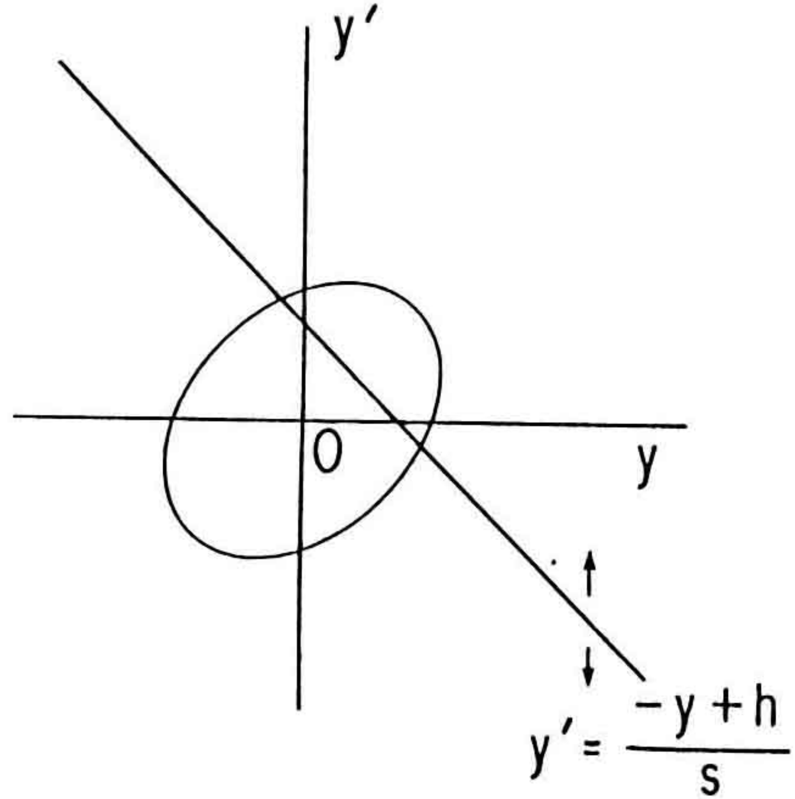

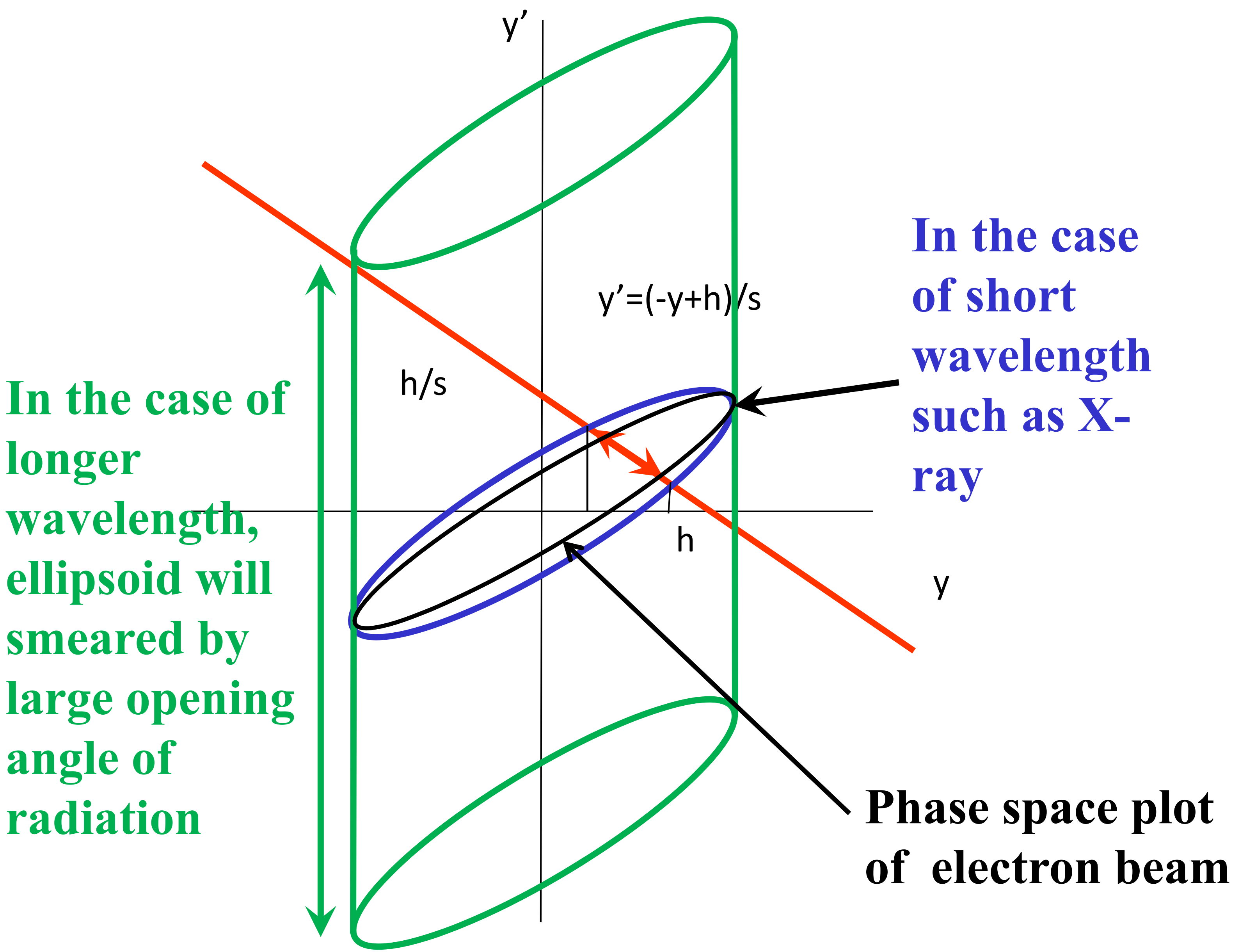

y'
y'=(-y+h)/s
h/s
h
y
In the case of longer wavelength, ellipsoid will smeared by large opening angle of radiation
In the case of short wavelength such as X-ray
Phase space plot of electron beam

Optimization between emittance ellipsoid and distance s will necessary!

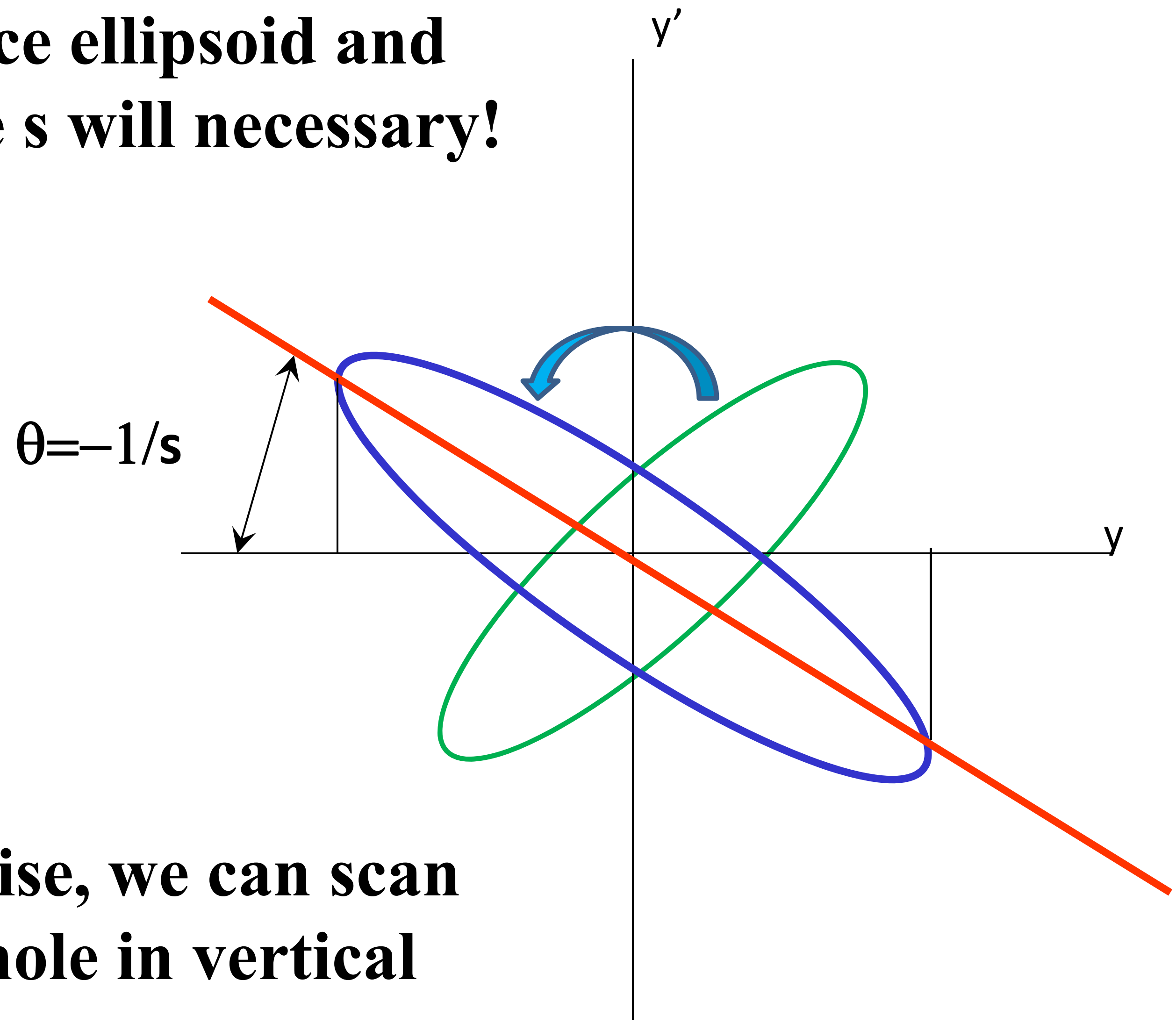

Otherwise, we can scan the pinhole in vertical

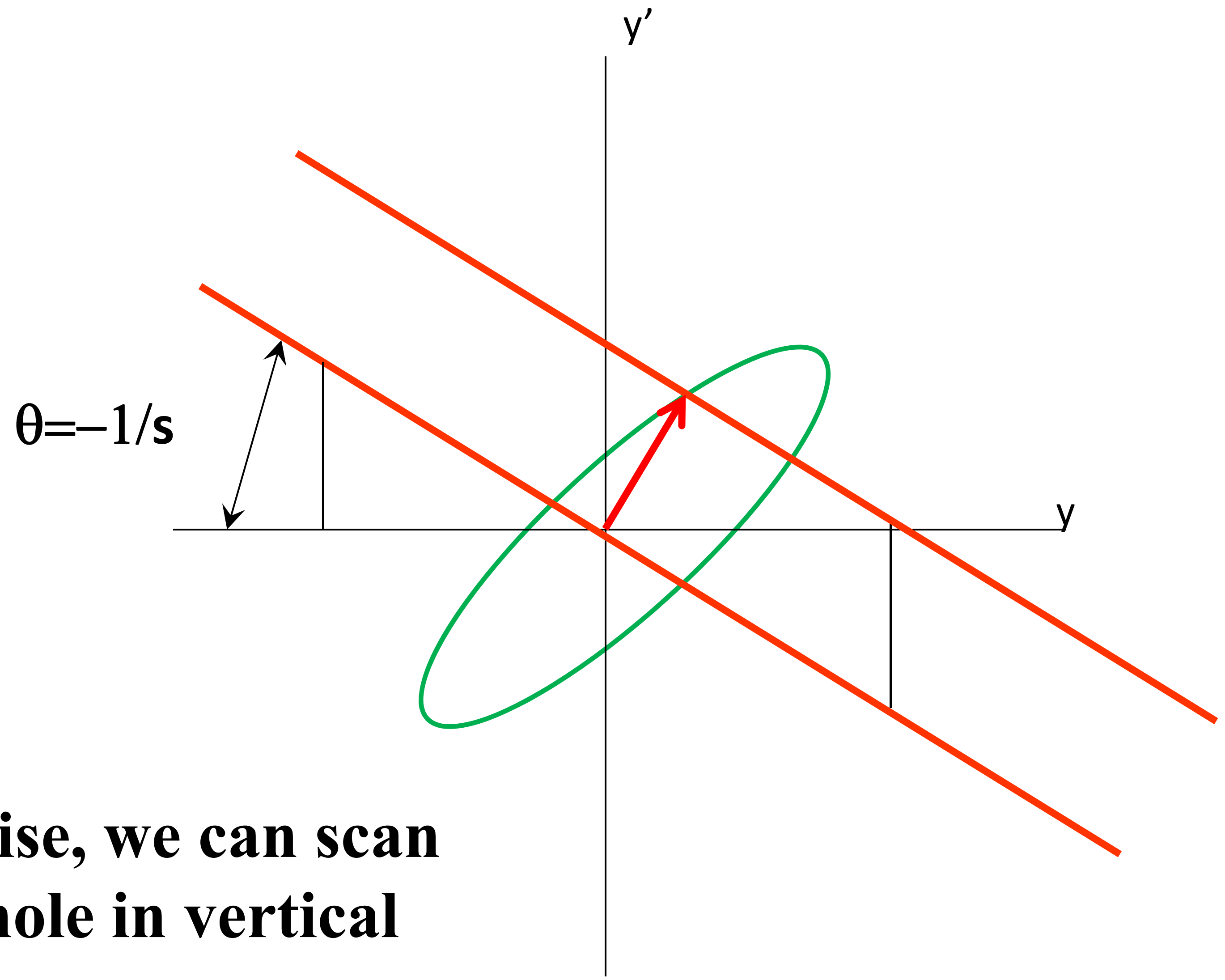

Otherwise, we can scan the pinhole in vertical

Vertical histogram taken at a scan of pinhole height.

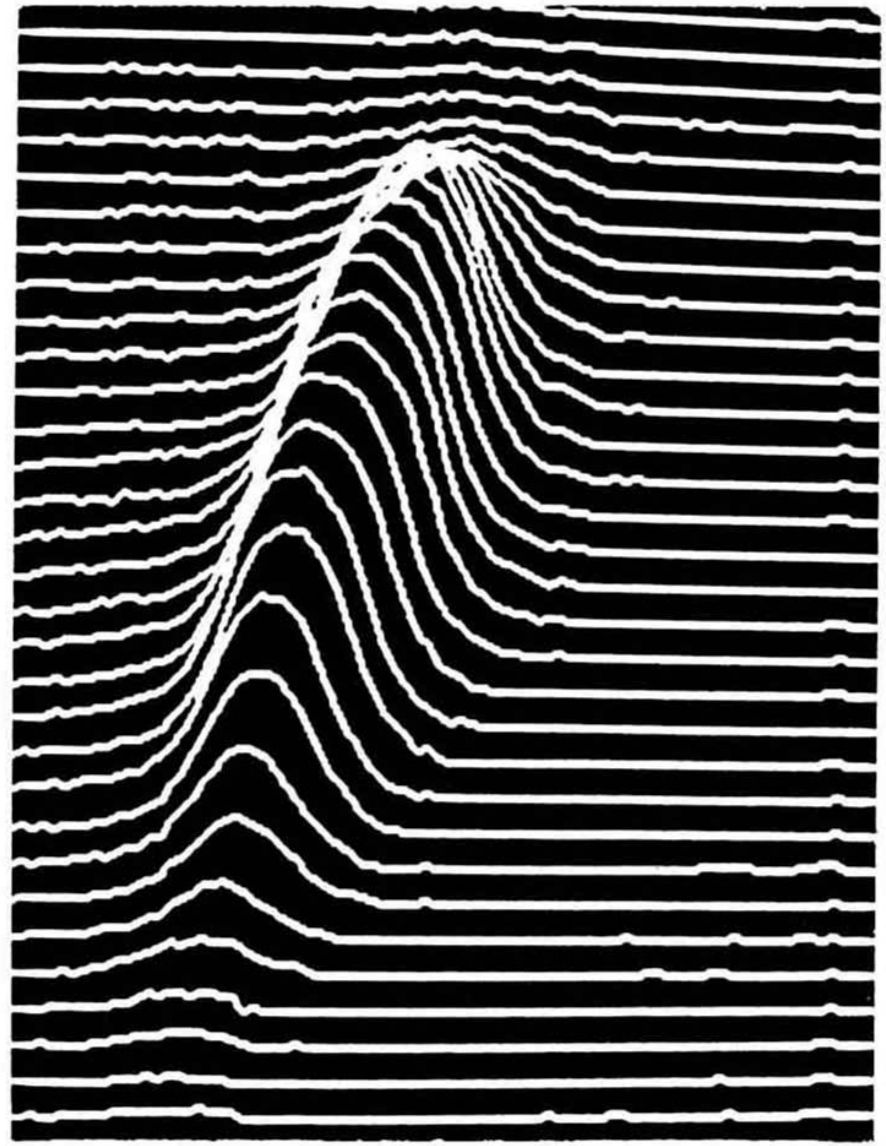

Vertical phase space profile reconstructed from vertical histogram.

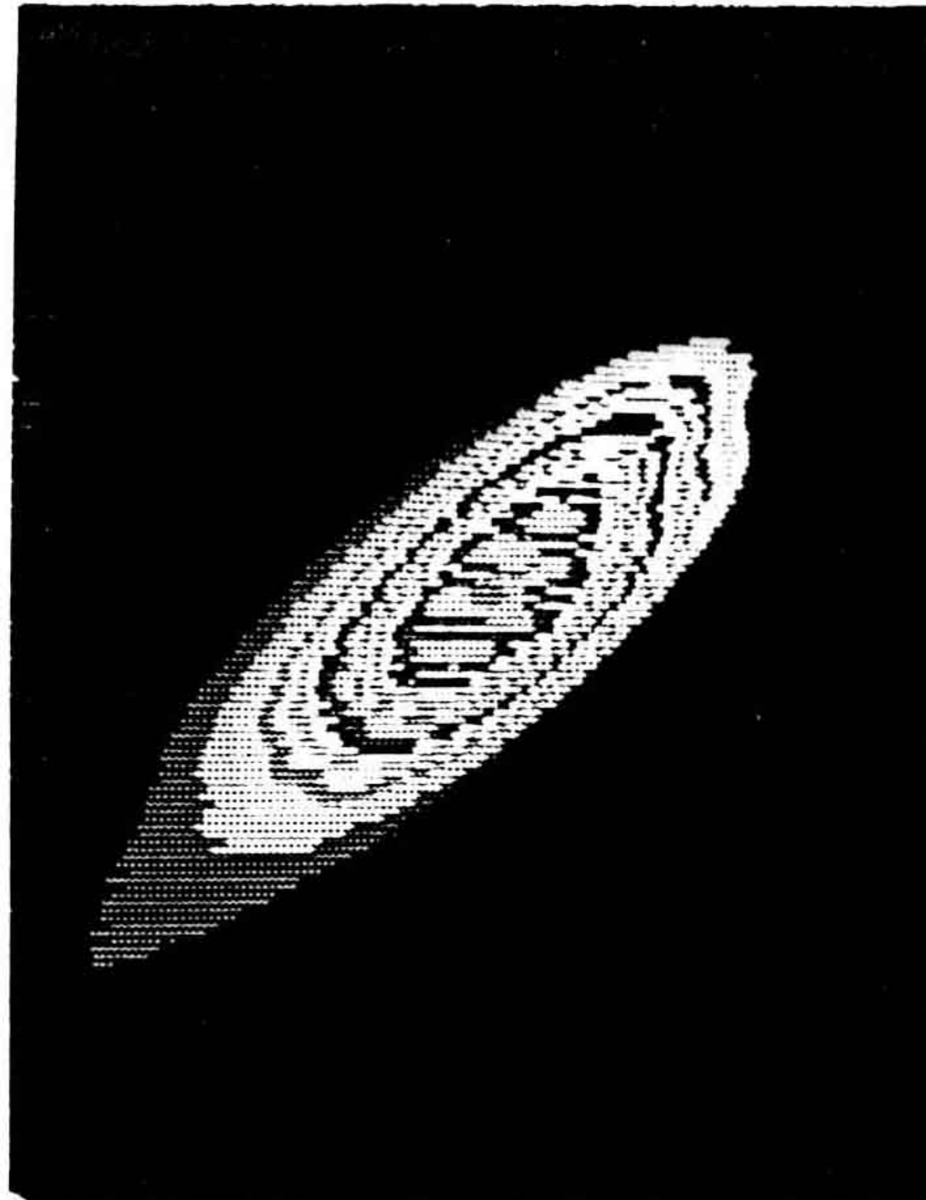

Diffraction in the pinhole

The pinhole camera treated with wave optics

Intensity of diffraction is given by Fresnel transform of pupil function F of the pinhole

$$I(x,y) = \left| \iint F(x_0, y_0) \exp\left\{ \frac{ik}{2z} \left[(x_0 - x)^2 + (y_0 - y)^2 \right] \right\} d\xi d\eta \right|^2$$

Thus, in the case of simple circular hole

$$I(x,y) = \left| 2\pi \int \exp\left\{ izr^2 \right\} \cdot J_0(Rr) dr \right|^2$$

$\tau = f/(a^2/\lambda) < 1$

Fresnel like region

$\tau = f/(a^2/\lambda) > 3$

Franhofer like region

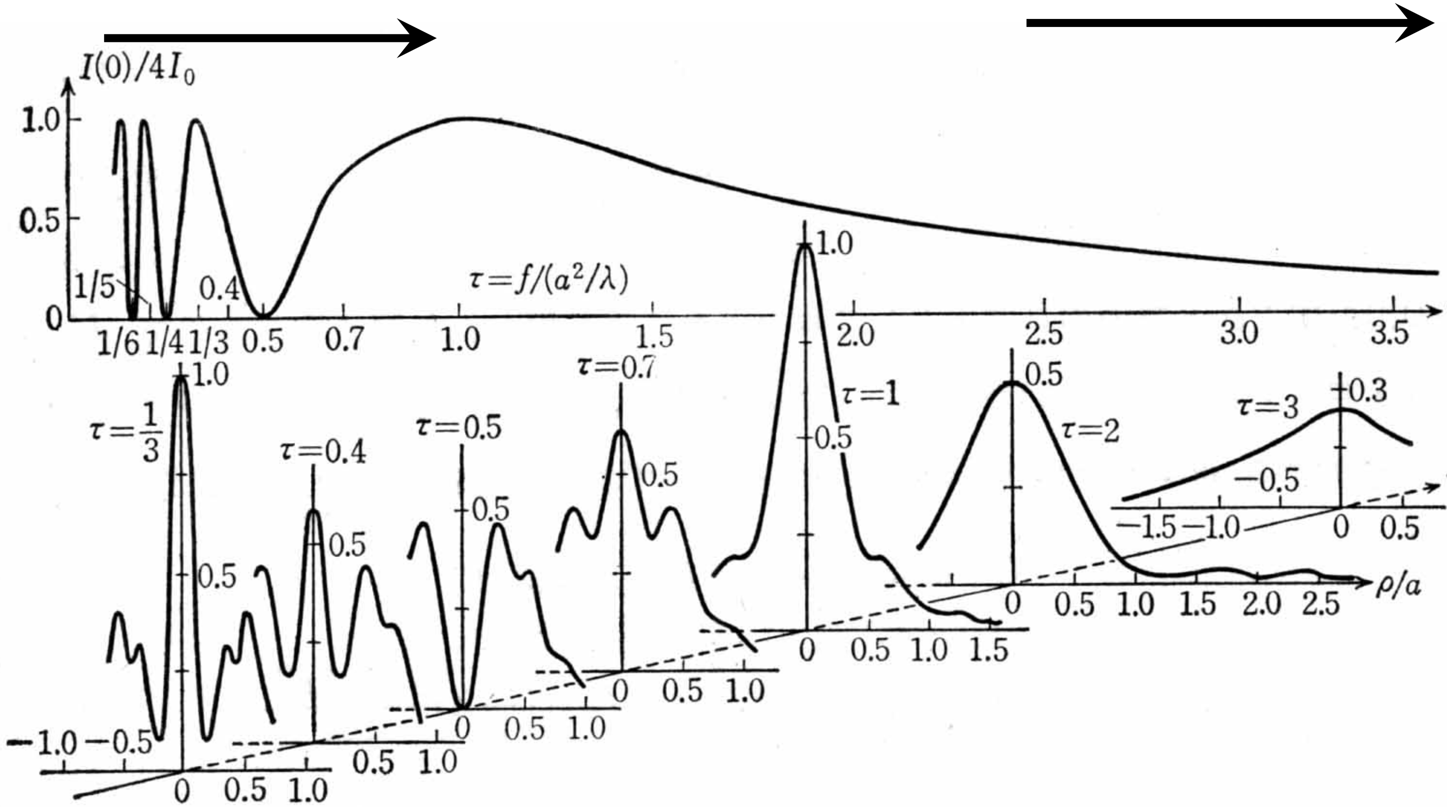

For example, λ=0.1nm, a=2μm

Franhofer region > 0.12m

In most case, pinhole with x-rays should be Franhofer region.

λ=0.1nm
a=2μm
(D=4μm)
F=10m

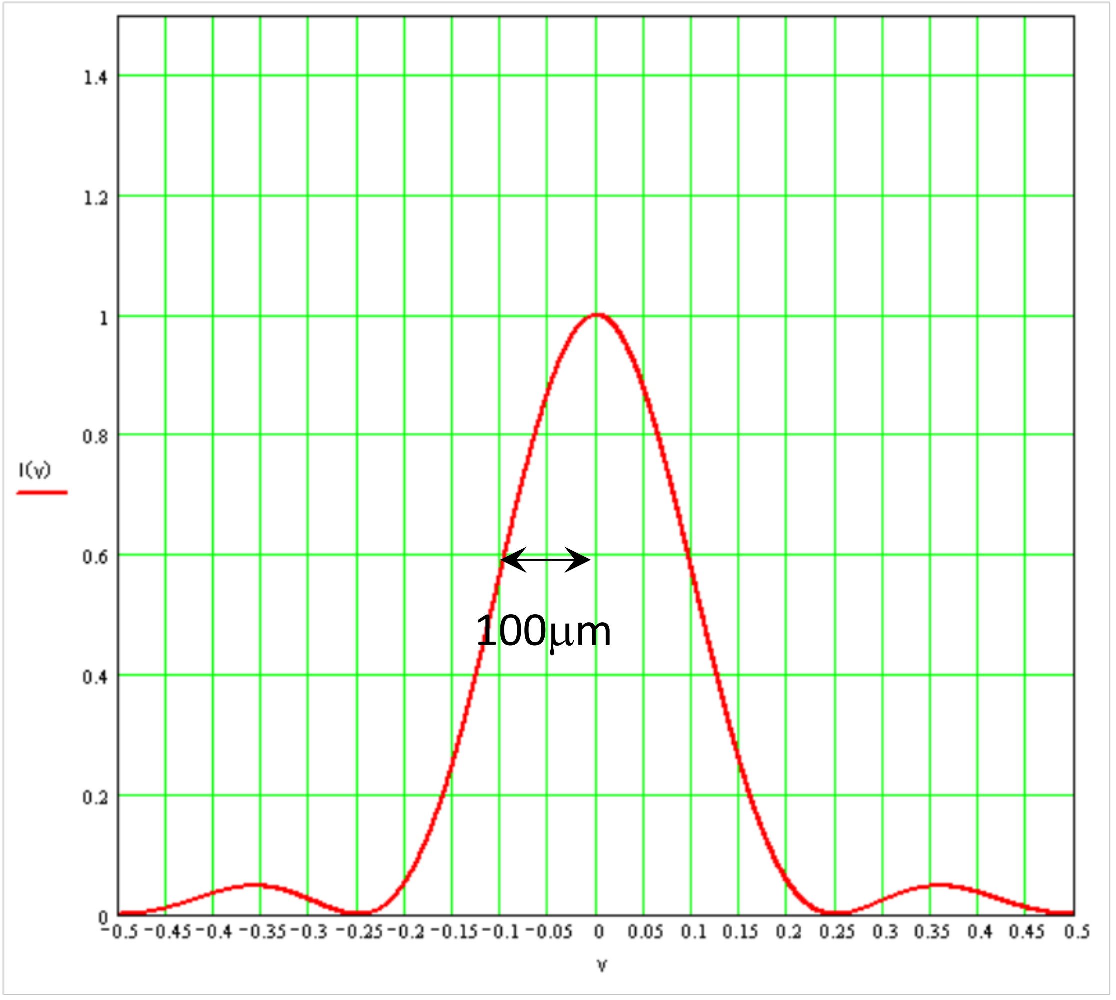

Diffraction patterns for several wave lengths

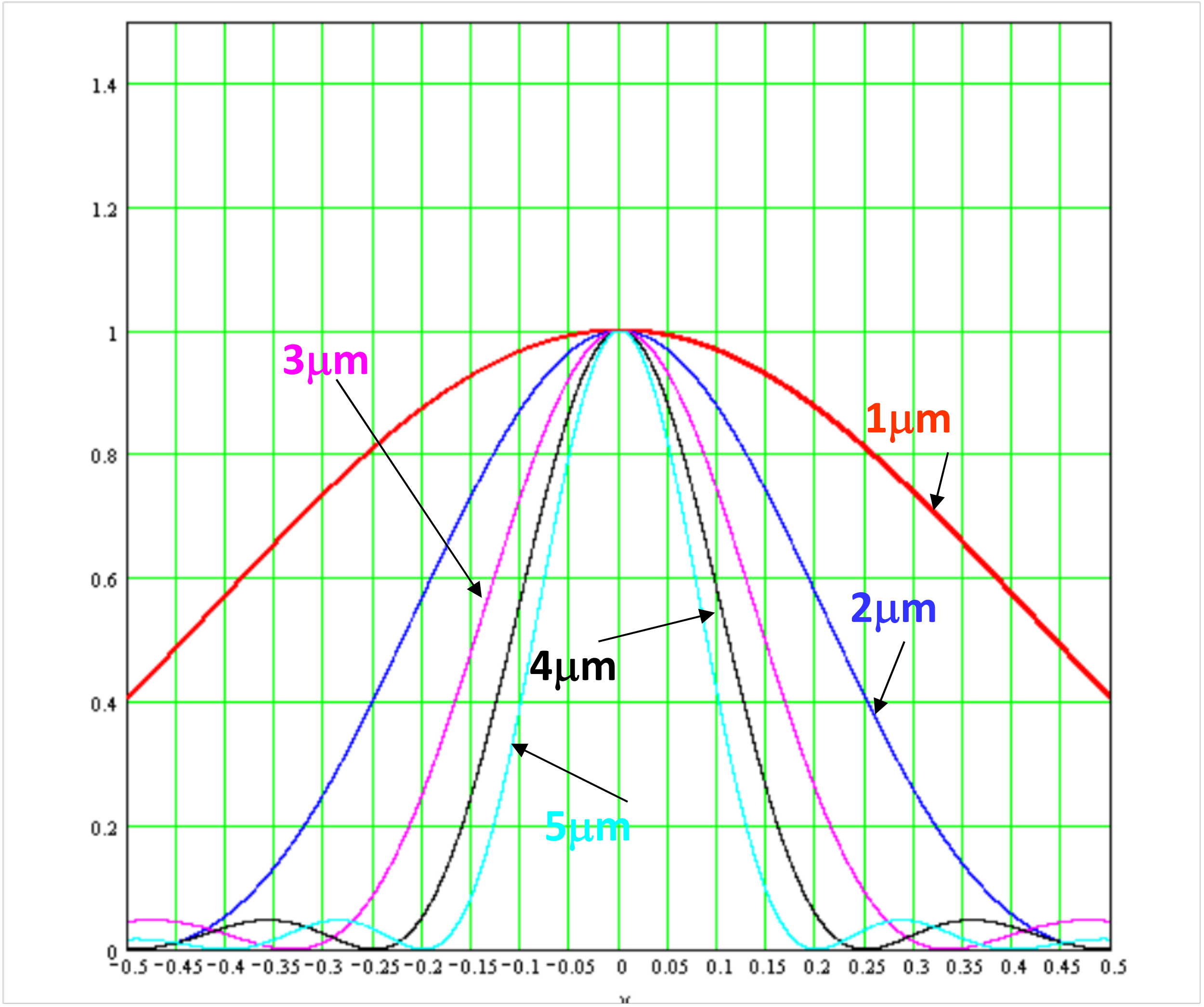

Diffraction width as a function of pinhole diameter
λ=0.1nm, F=10m

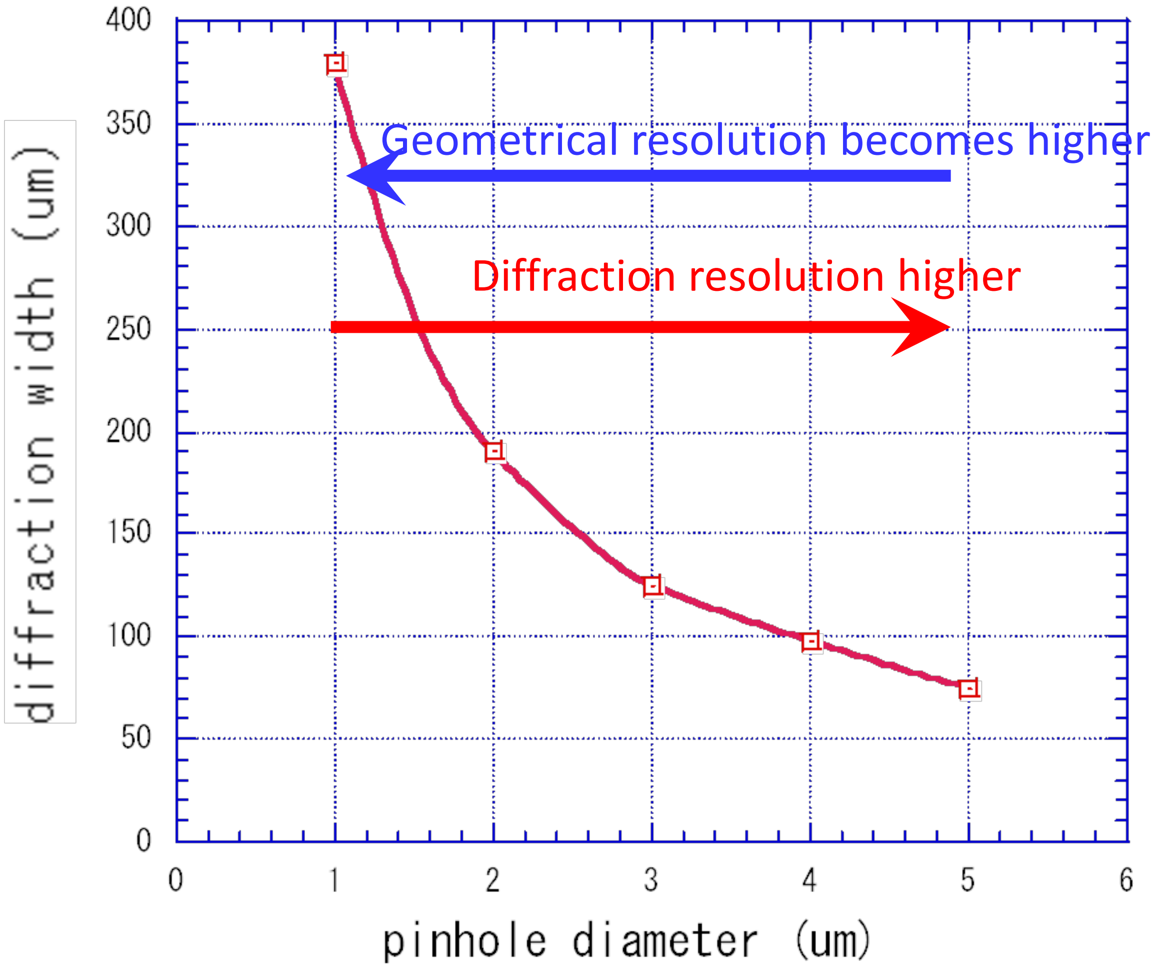

An example of pinhole camera measurement setup

Pinhole D=4μm

Beam
1σ=10μm

Diffraction size should be 100μm

Observation plane at 10m

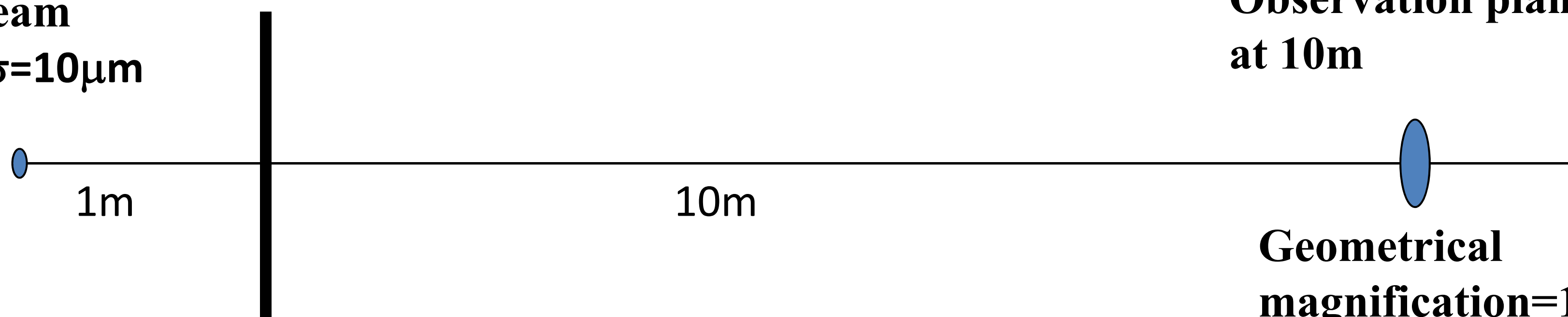

Geometrical magnification=10

Geometrical image size should be 100μm Without convolution between pinhole diameter

Result of beam size should be 14μm without convolution of pinhole diameter

Total reflection by surface of pinhole blocks

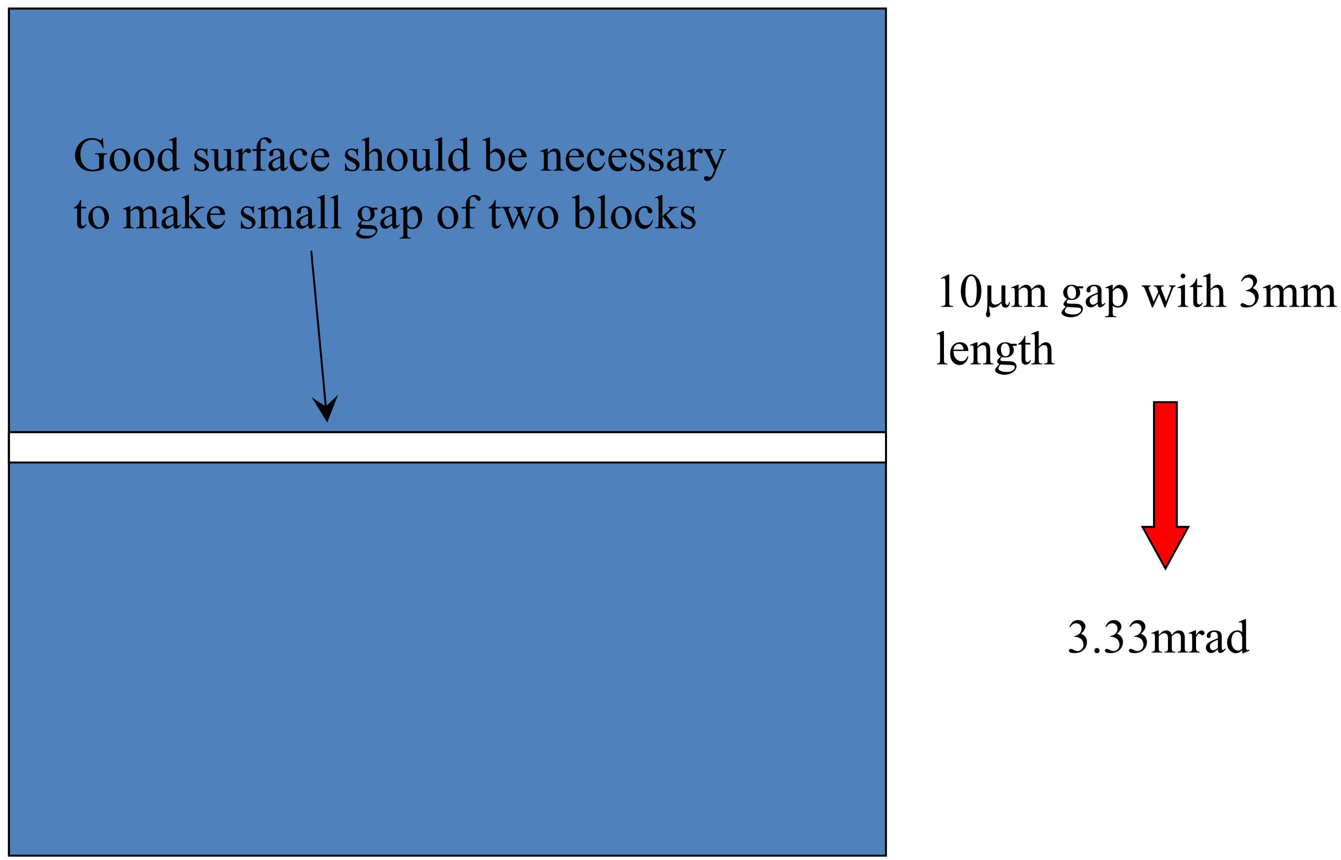

Totally reflection by surface of pinhole blocks

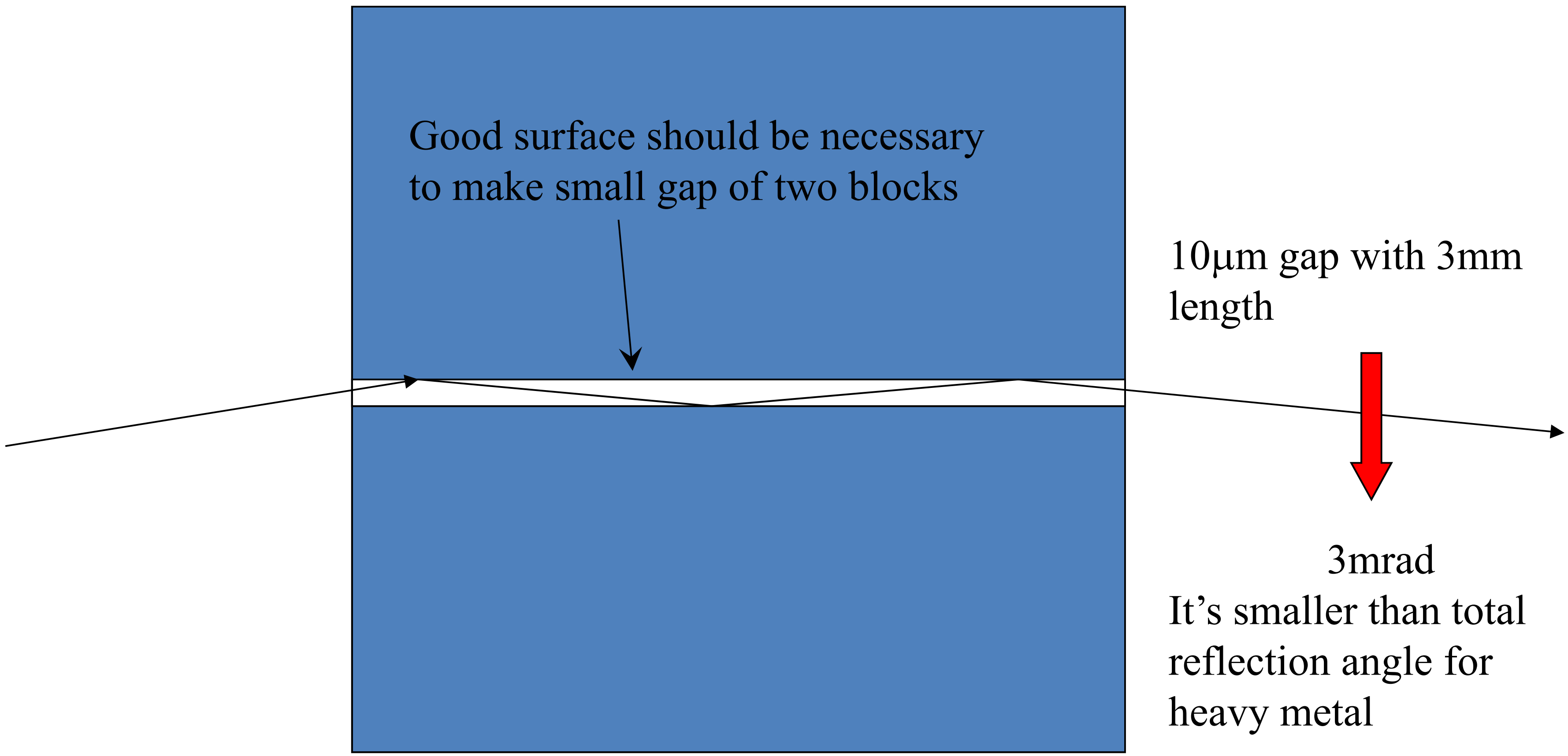

From these evidences, decomvolution by PSF including many effects such as diffraction, total reflection and halation in detection system etc. is very important in X-ray pin-hole camera.

X-ray Fresnel zone plate

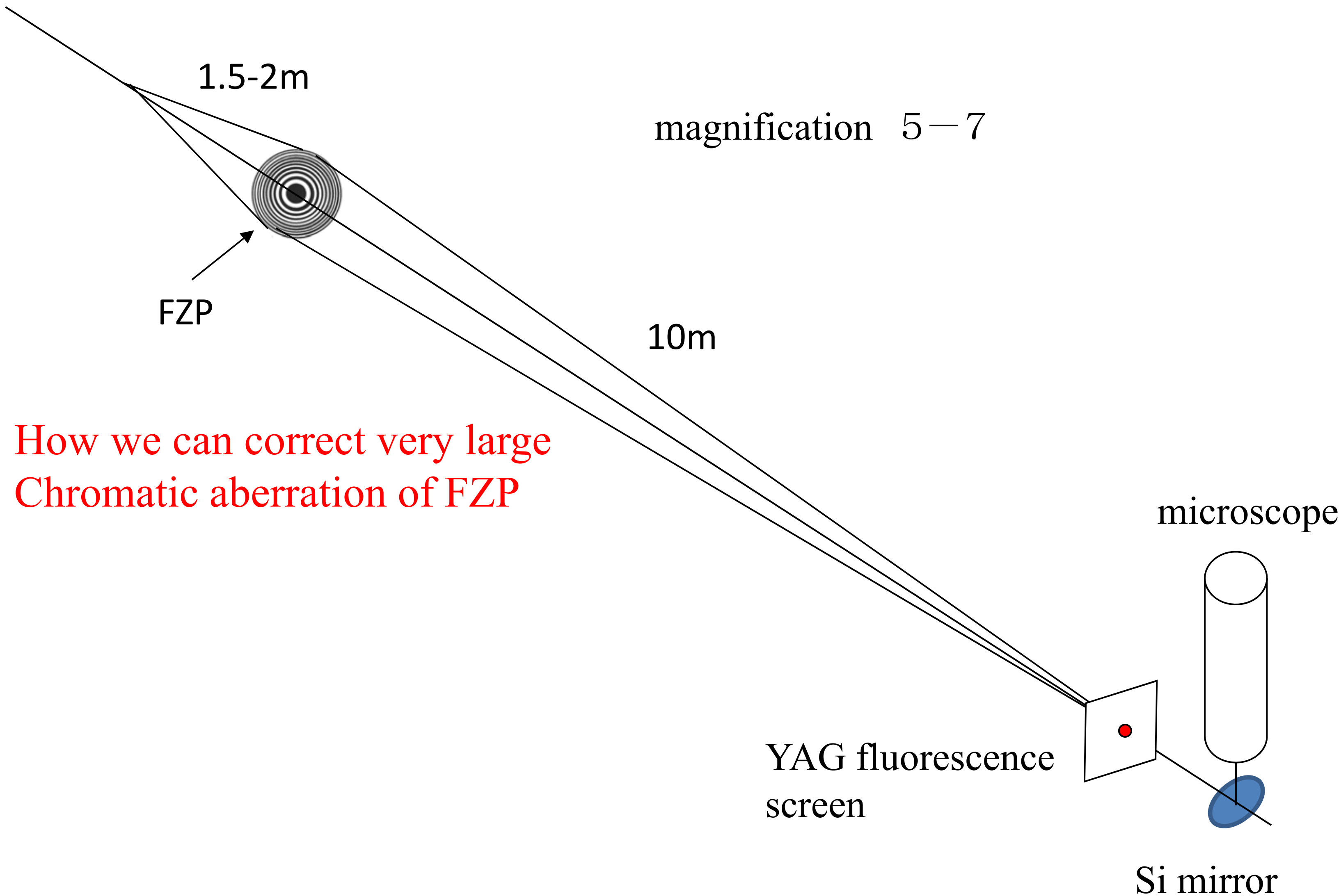

How we can correct very large Chromatic aberration of FZP

Concept of achromatic lens

Focusing lens +dispersion

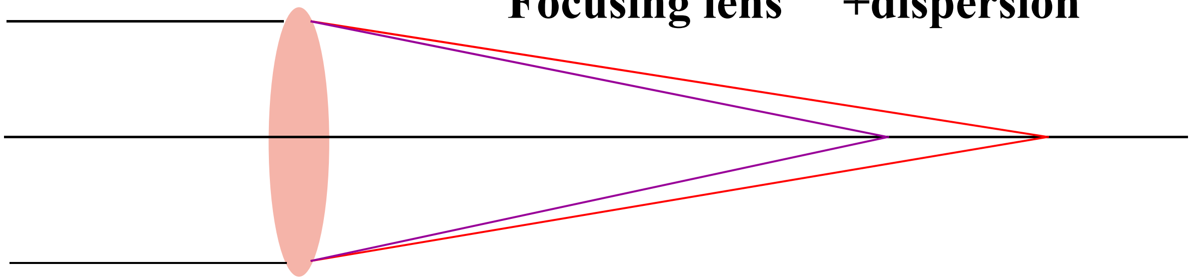

Defocusing lens -dispersion

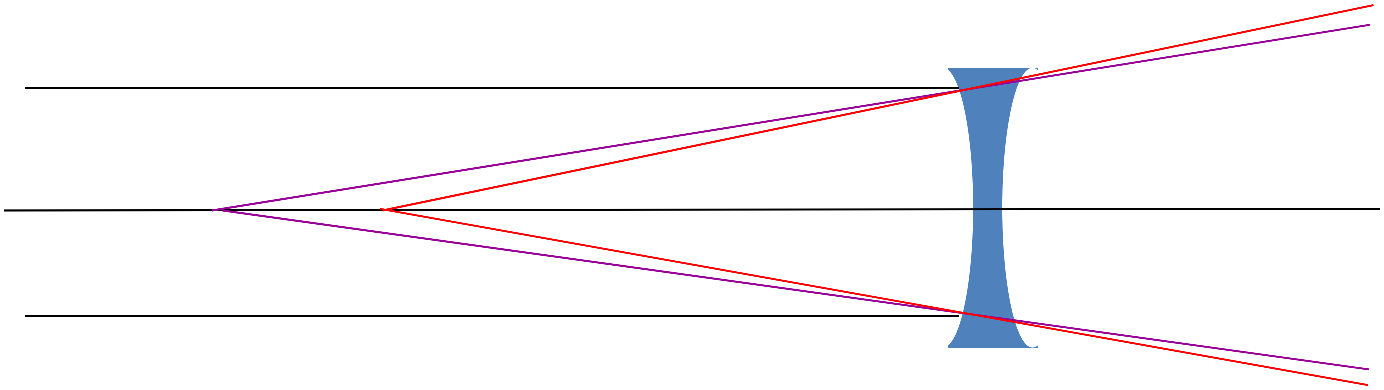

Certain combination of focusing and defocusing lens can cancel focal shift

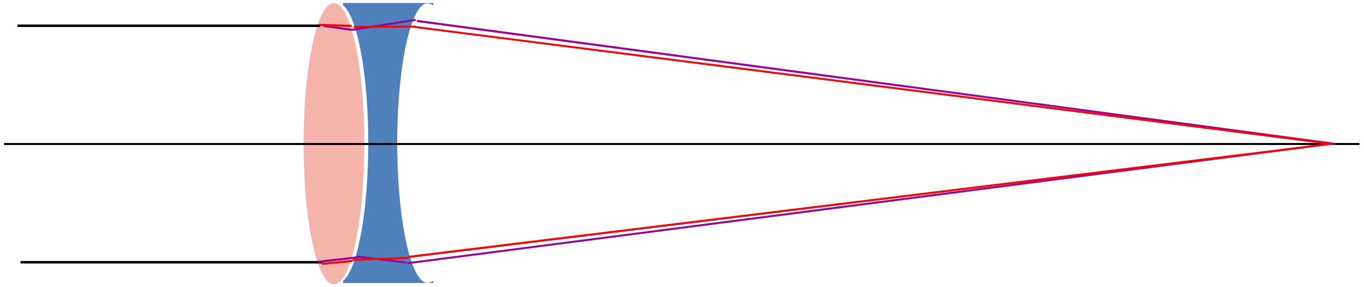

Idea of hybrid lens

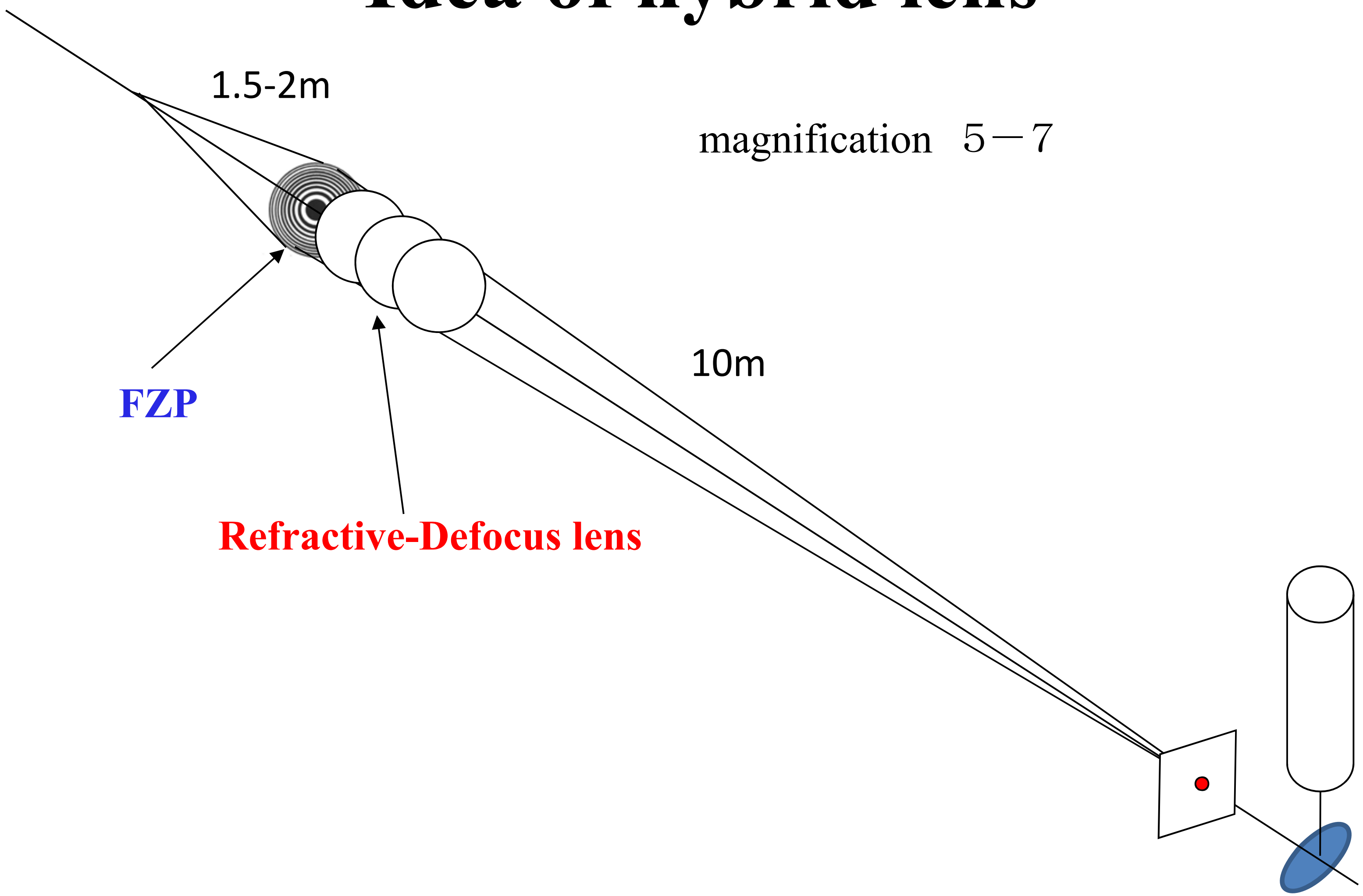

Hybrid type FZP

(a)

(b)

Abbe number of FZP

About -8 very high dispersion

Abbe number

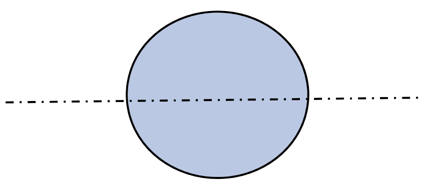

X-ray defocusing lens

About 0.8 extremely high dispersion

Combination of these two components, we can make achromatic lens with focusing length of 1m.

FZP: 0.9m
XDL: -9m

f=1m

For questions

Unbalanced input method for measurement of very small beam size less than 5μm

Let's us consider equation for interferogram.

$$I(y,D) = \int (I_1 + I_2) \cdot \left\{ \sin c\left(\frac{\pi \cdot a \cdot y \cdot \chi(D)}{\lambda \cdot f} \right) \right\}^2 \cdot \left\{ 1 + \gamma \cdot \cos\left(k \cdot D \cdot \left(\frac{y}{f} + \psi \right) \right) \right\} d\lambda$$

$$\gamma = \left(\frac{2 \cdot \sqrt{I_1 \cdot I_2}}{I_1 + I_2} \right) \cdot \left(\frac{I_{max} - I_{min}}{I_{max} + I_{min}} \right) \quad , \quad \psi = \tan^{-1} \frac{S(D)}{C(D)}$$

In this equation, the term "γ" has not only real part of complex degree of spatial coherence but also intensity factor!

$$\gamma = \left(\frac{2 \cdot \sqrt{I_1 \cdot I_2}}{I_1 + I_2} \right) \cdot \left(\frac{I_{max} - I_{min}}{I_{max} + I_{min}} \right)$$

If $I_1=I_2$, γ is just equal to real part of complex degree of spatial coherence , but if $I_1 \neq I_2$, we must take into account of intensity factor;

$$\frac{2\cdot\sqrt{I_1\cdot I_2}}{I_1+I_2}$$

This intensity factor is always smaller than 1 for $I_1 \neq I_2$.

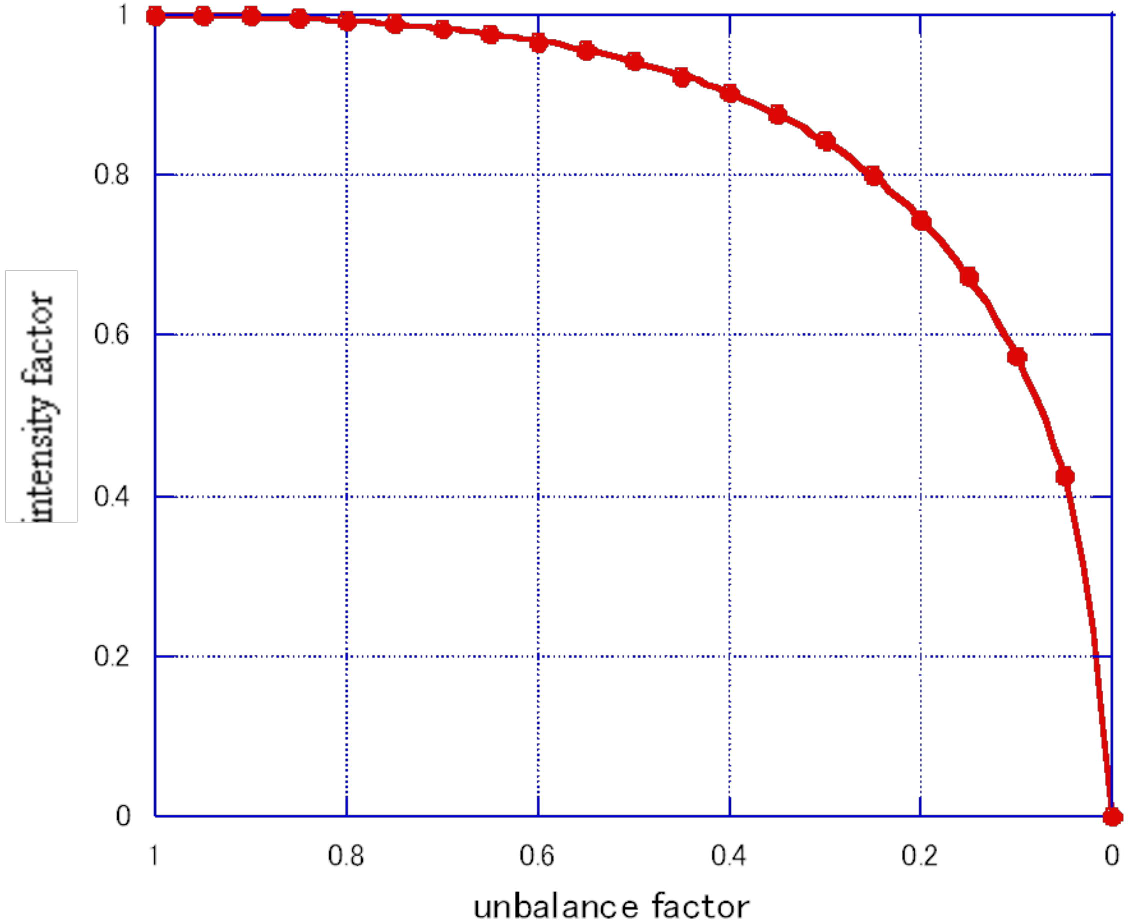
intensity factor
1
0.8
0.6
0.4
0.2
0
1
0.8
0.6
0.4
0.2
0
unbalance factor

$$\gamma = \left(\frac{2 \cdot \sqrt{I_1 \cdot I_2}}{I_1 + I_2} \right) \cdot \left(\frac{I_{max} - I_{min}}{I_{max} + I_{min}} \right)$$

Since intensity factor is smaller than 1 for $I_1 \neq I_2$, the "γ" will observed smaller than real part of complex degree of spatial coherence.

This means beam size will observed larger than primary size and <u>we know ratio between observed size and primary size.</u>

This is magnification!

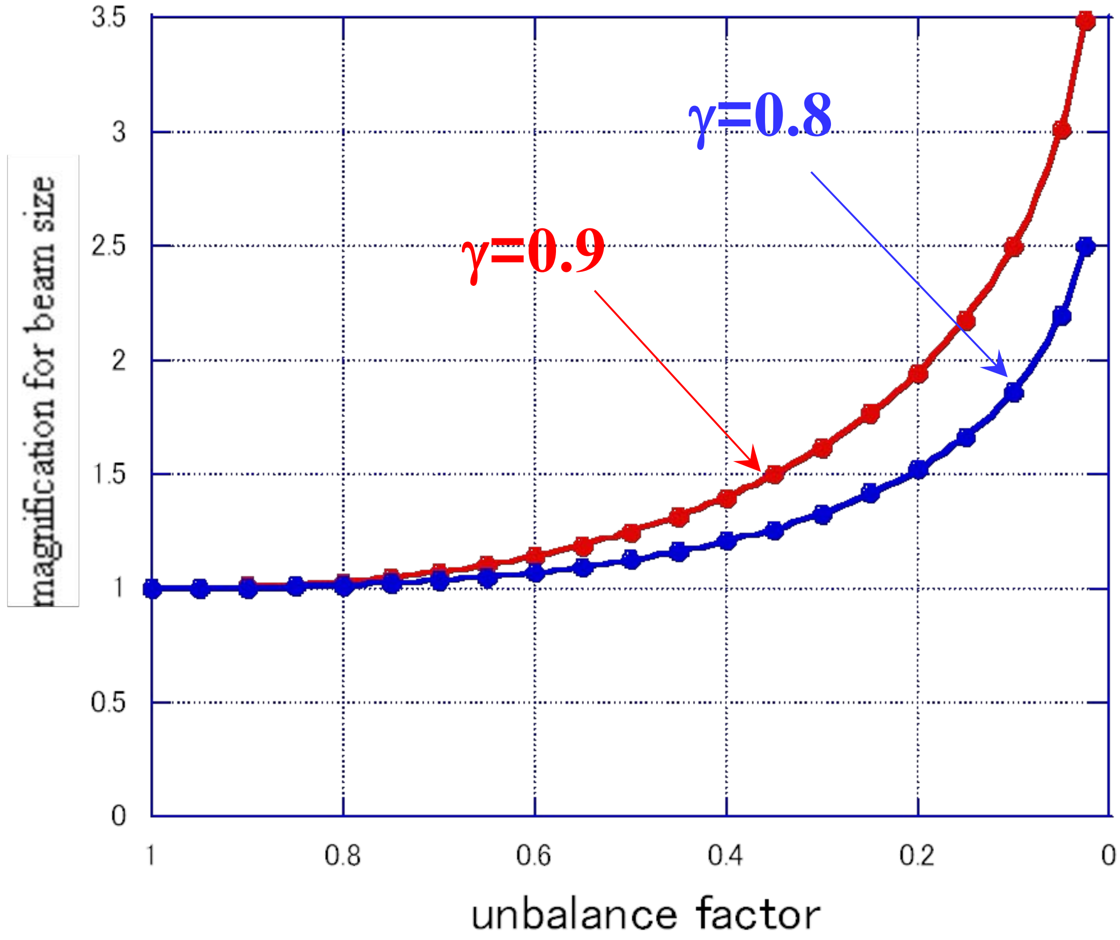

We can use magnification range up to 2 for $I_1 : I_2 = 1 : 0.2$ or 3 for $1 : 0.05$.

In interferometry, we can magnify beam size by very simple way;

applying unbalance input for double slit!

What is significant problem in measurement for very small beam size?

In very small beam size measurement (less than 5μm), enhancement in error (CCD noise in baseline) transmission will make a saturation in visibility.

We have certain limit in small beam size measurement, and it is about 5μm.

error will enhanced systematically in high visibility region by error transmission.

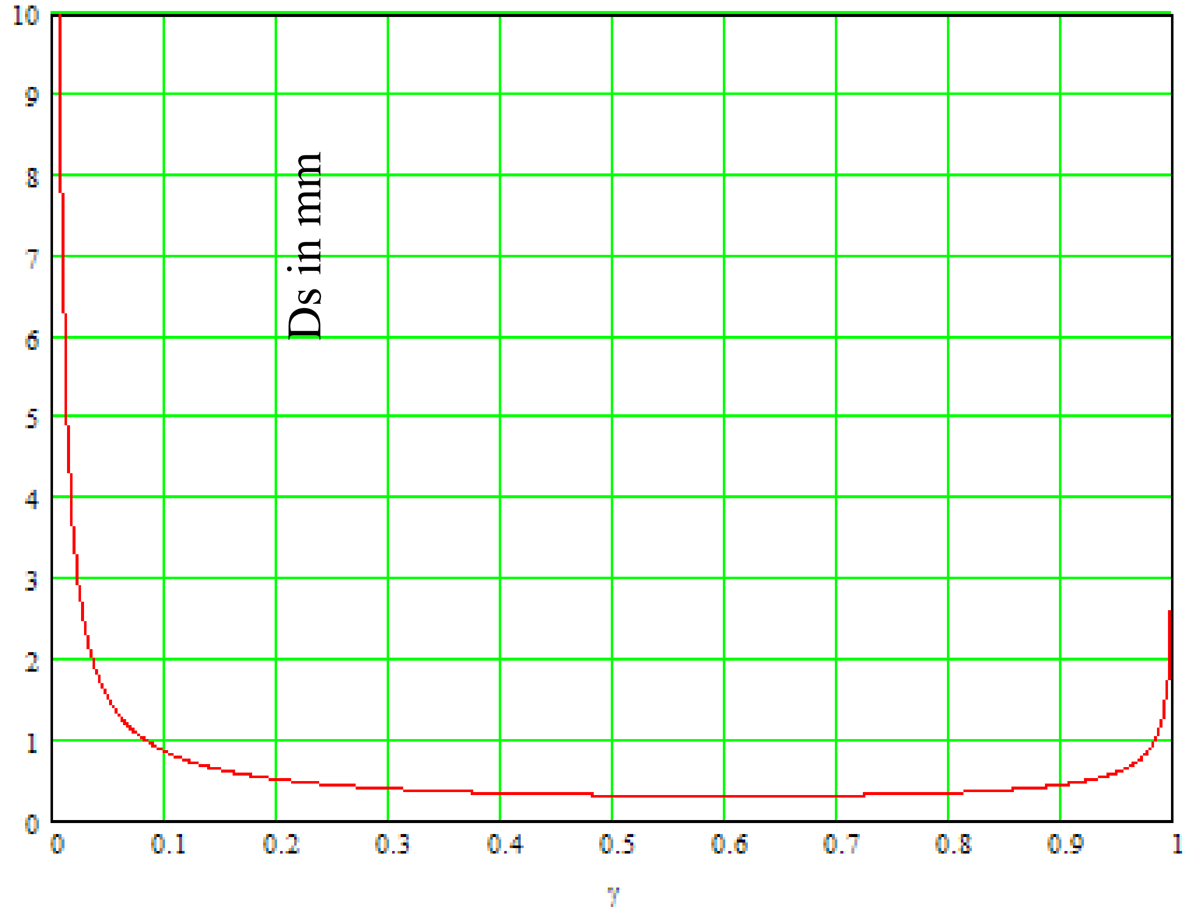

Most important point to escape from this problem is we should measure the beam size with good range of visibility.

To realize this to very small beam size measurement, magnification by unbalanced input will very helpful!

Result of visibility for beam size 5.8μm (l=550nm) with several separation of double slit.

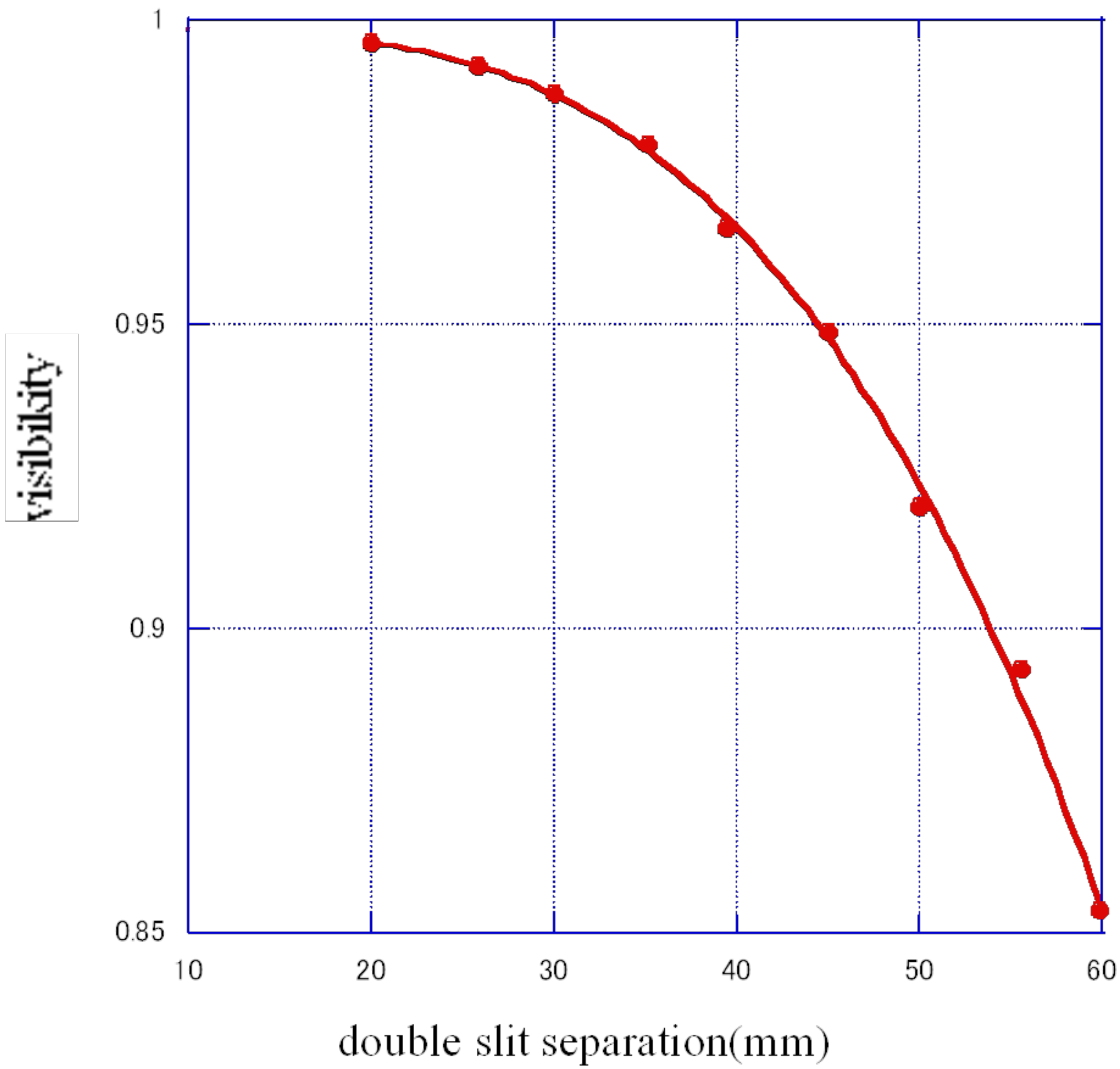

Result of visibility for beam size 5.8µm (l=550nm) with several separation of double slit.

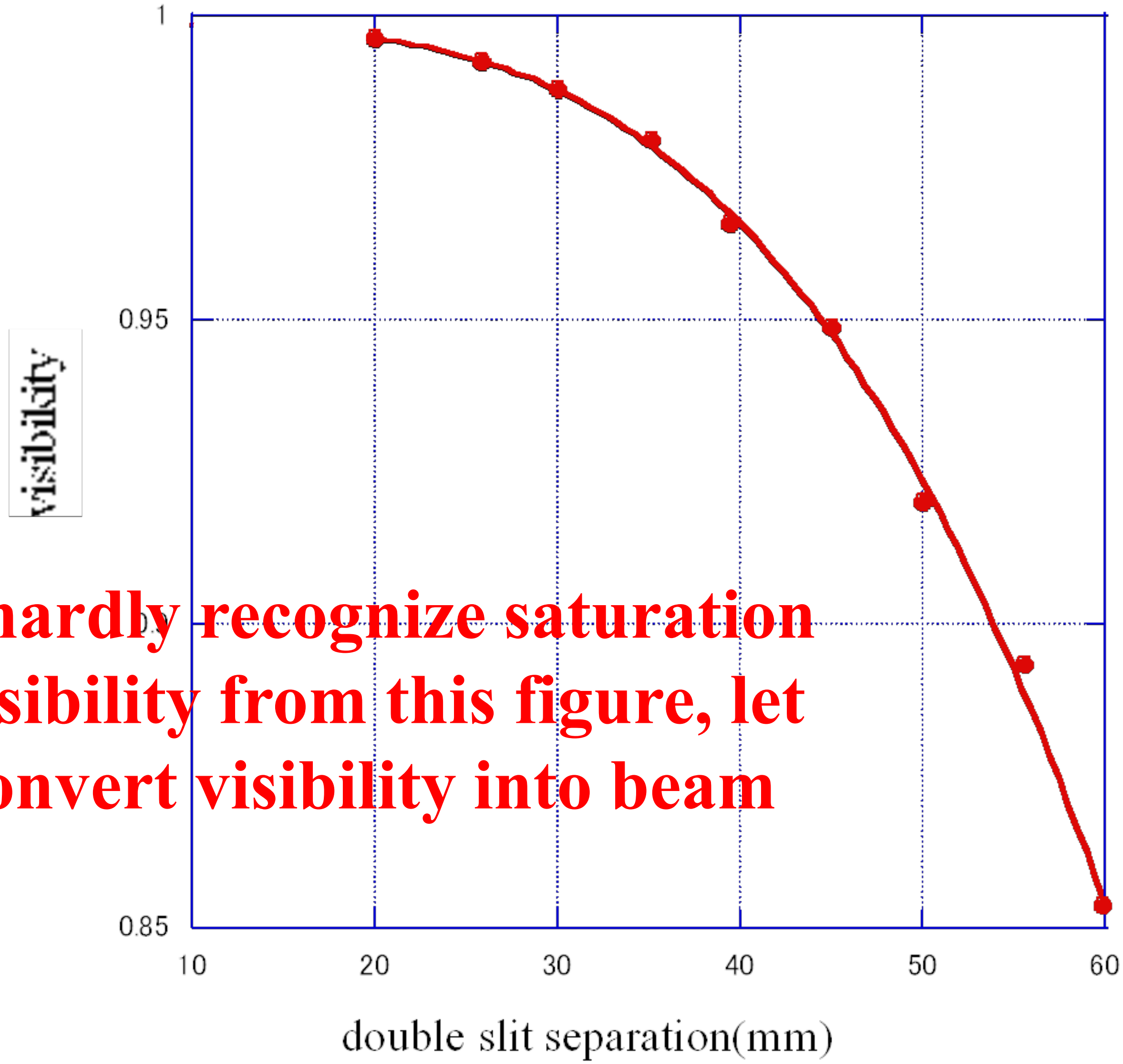

We hardly recognize saturation in visibility from this figure, let us convert visibility into beam size!

Convert visibility into beam size. We can see clear saturation in smaller double slit range which has visibility near 1.

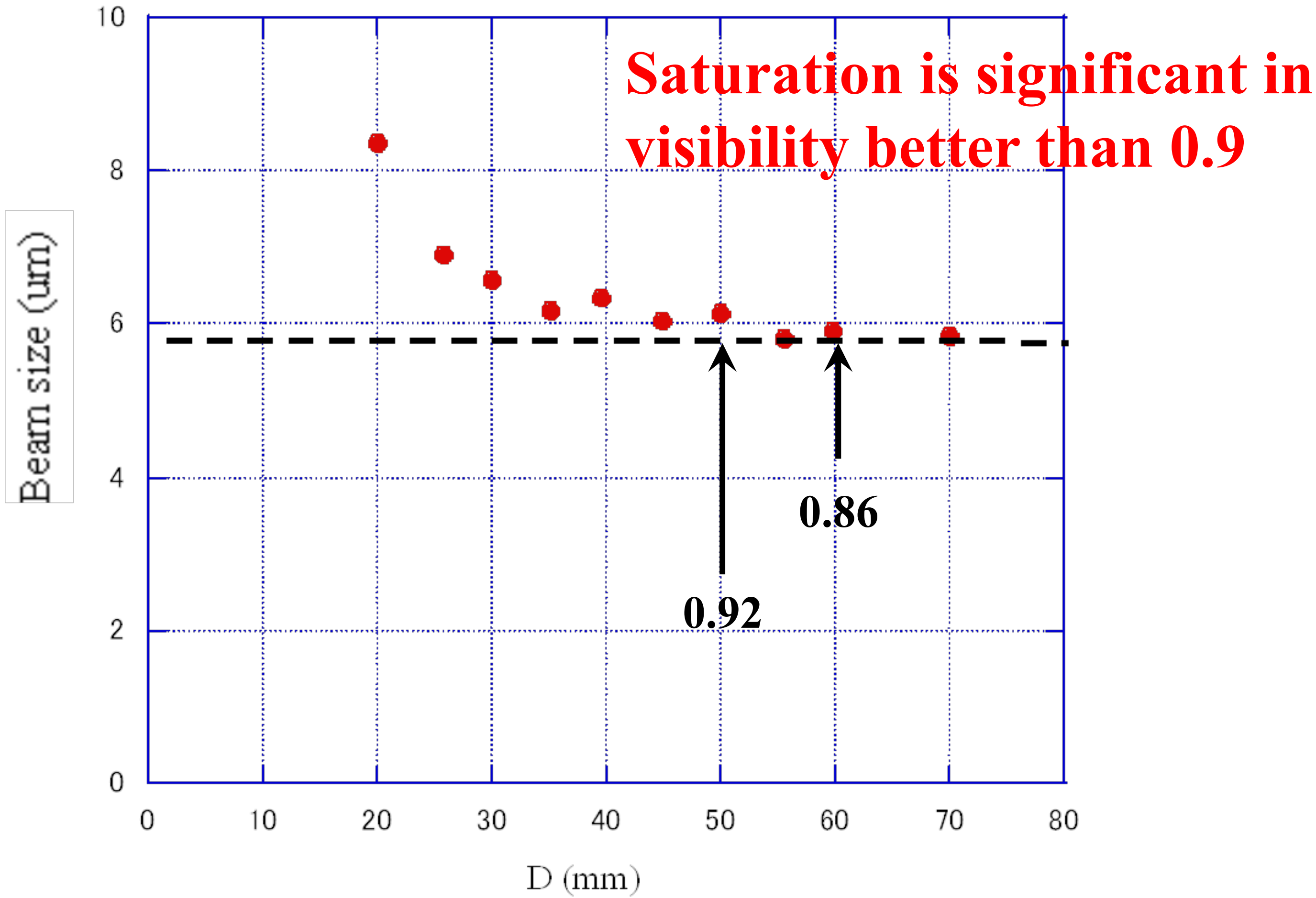

Setup for unbalanced input by half ND filter

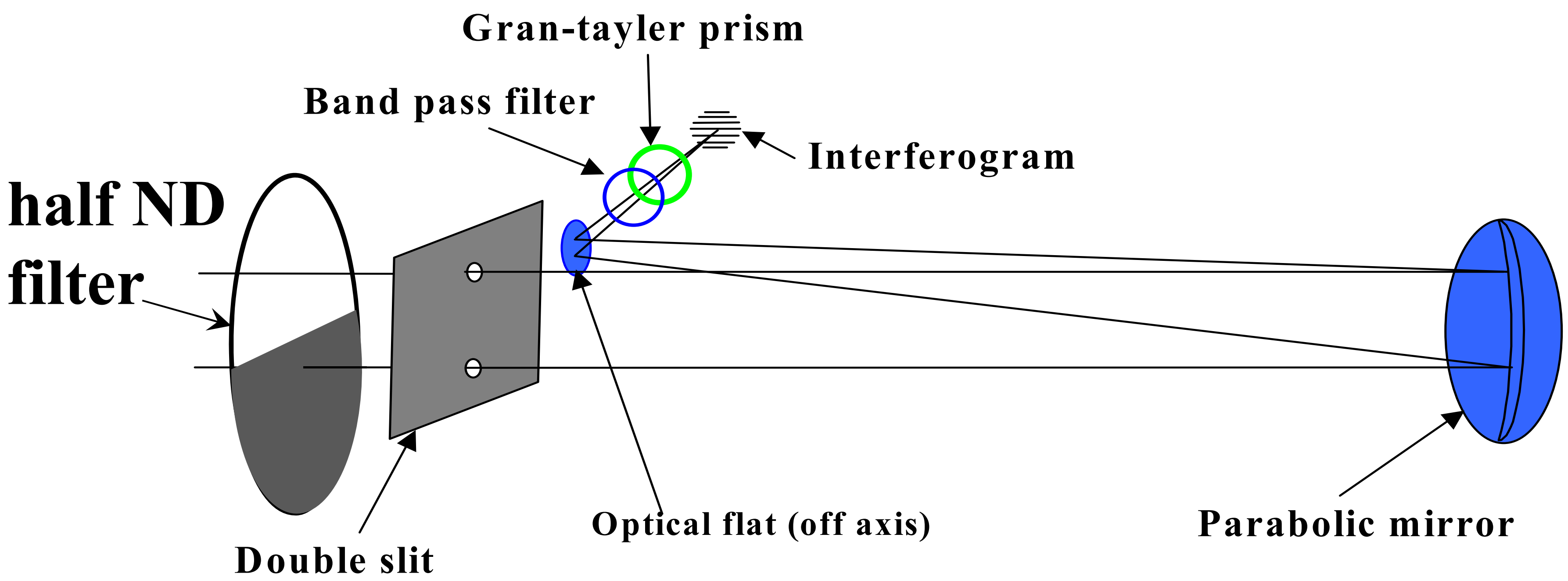

Appling unbalance method for D=30mm.
$I_1 : I_2 = 0.853:0.249$

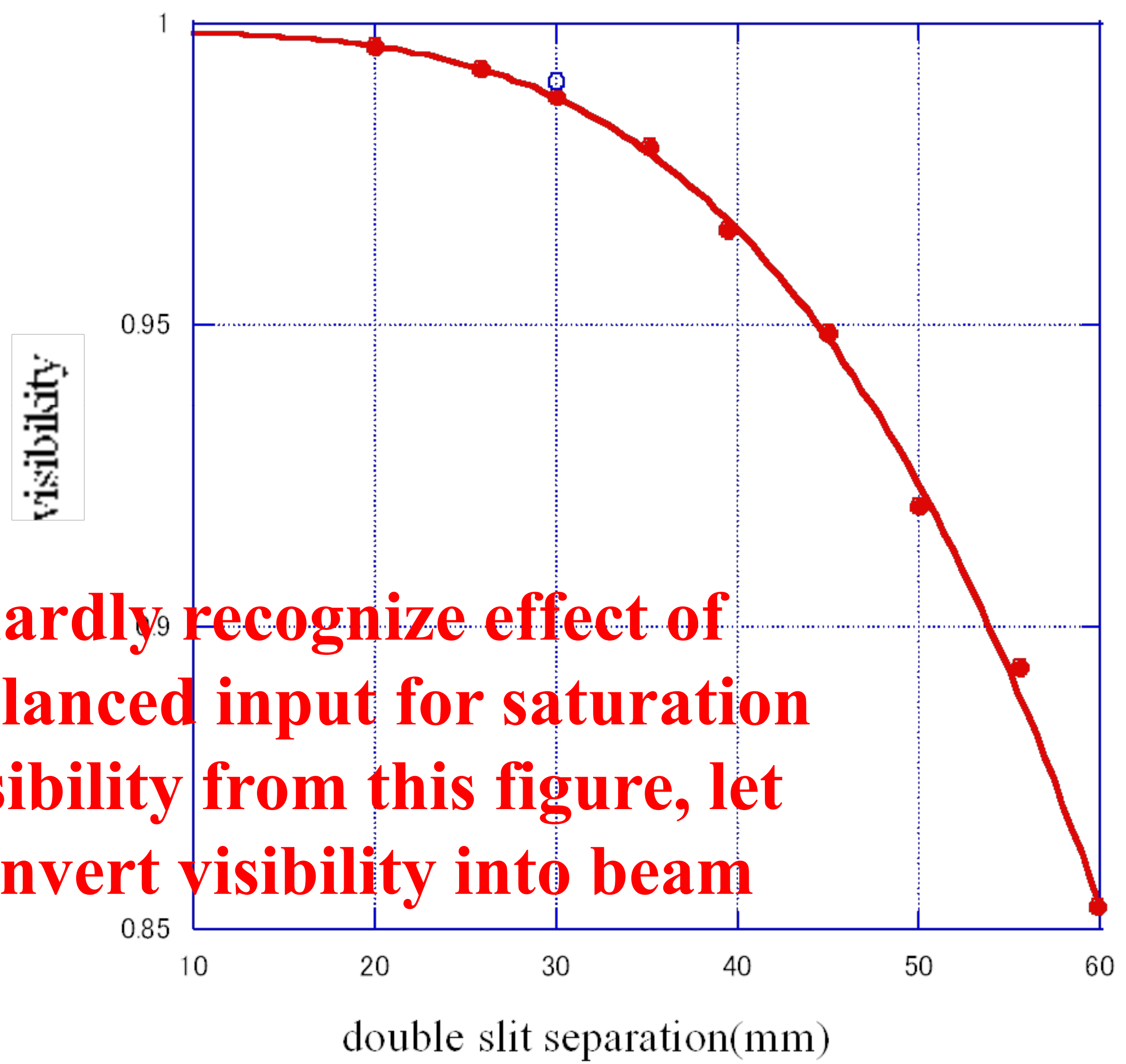

We hardly recognize effect of unbalanced input for saturation in visibility from this figure, let us convert visibility into beam size!

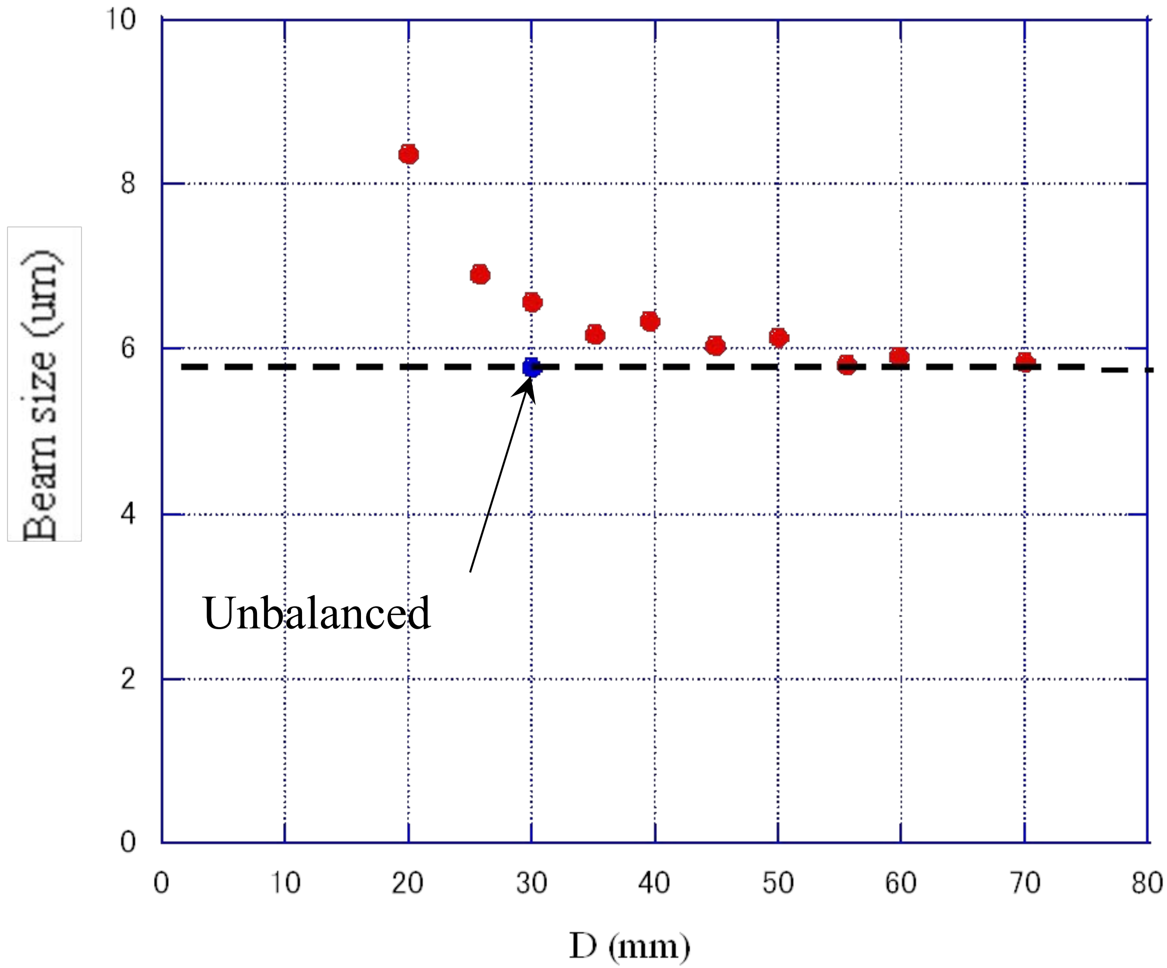

Beam size (um)
D (mm)
Unbalanced
10
8
6
4
2
0
0
10
20
30
40
50
60
70
80

Conclusion

Smallest result of beam size at ATF is 4.7μm with reflective SR interferometer using double slit separation of 45-55mm, λ=400nm. This size is almost small limit with equal input method.

When we will apply unbalanced method;

With magnification factor 2 ⟹ 2.4μm
With magnification factor 3 ⟹ 1.6μm

We are waiting beam size in this range!

Part 10
Intensity interferometry

2002 Bunch length measurement with intensity interferometry.

2003 Observation of beam blowup in the LER due to electron trapping by the use of high-speed gated camera.

2004 Observation of beam tail by coronagraph.

2004 Dynamical observation of injected beam profile by high-speed gated camera.

2002 Intensity interferometry experiment

1. Investigate the photon statistics in the synchrotron radiation.

2. Demonstrate possibility to measure very short bunch length (fs region).

Principle of second-order autocorrelator: colinear arrangement

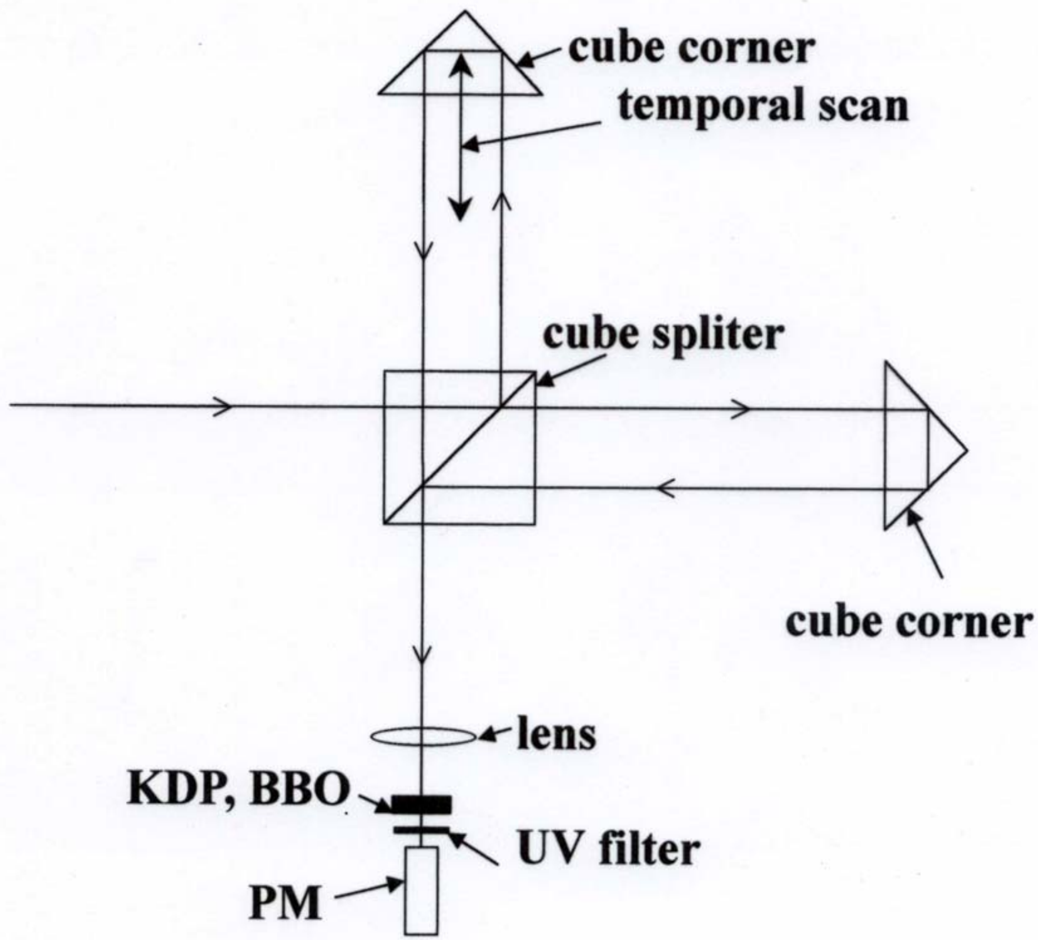

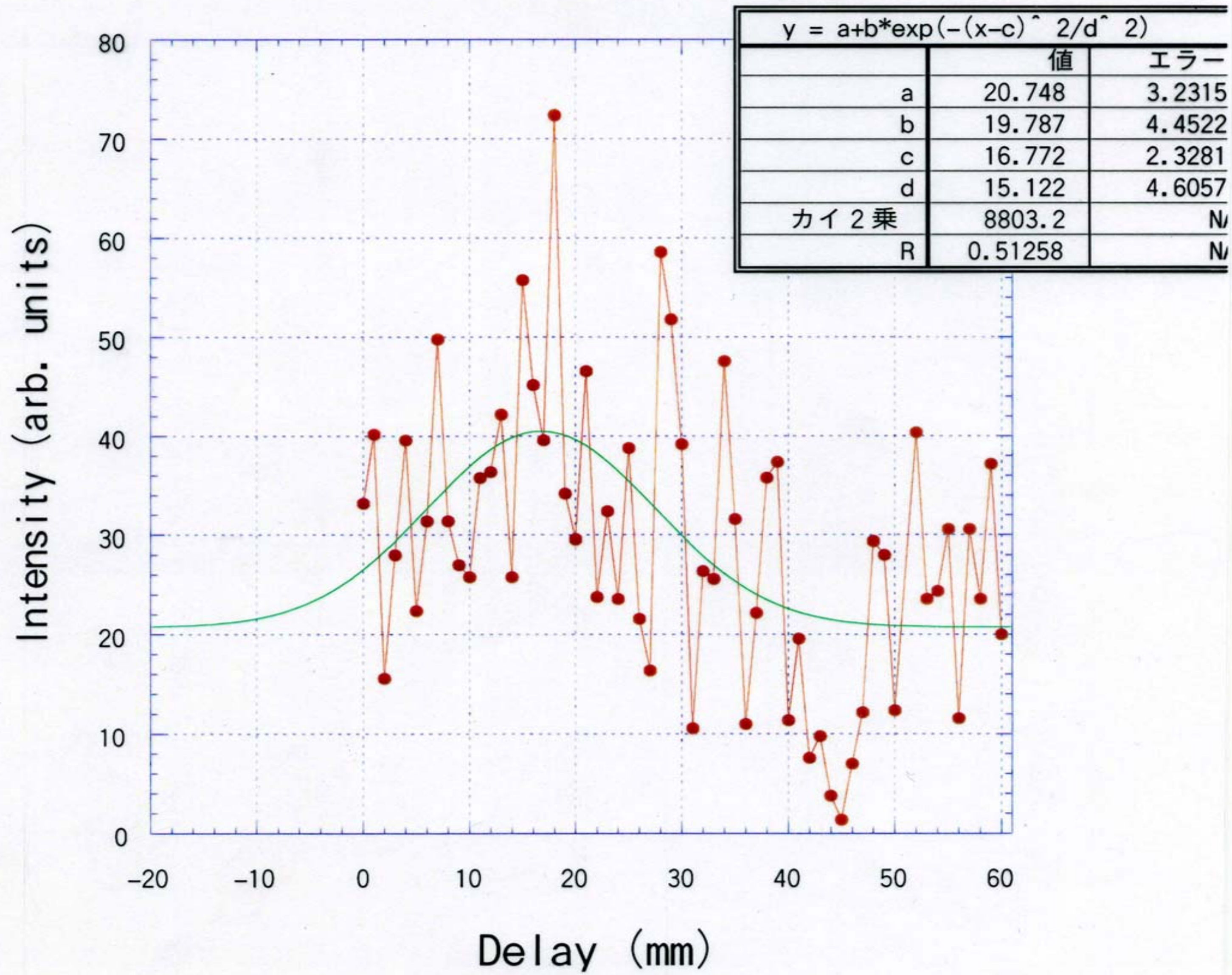
y = a+b*exp(-(x-c)^ 2/d^ 2)
値
エラー
a
20.748
3.2315
b
19.787
4.4522
c
16.772
2.3281
d
15.122
4.6057
カイ 2 乗
8803.2
N/
R
0.51258
N/
Intensity (arb. units)
Delay (mm)
80
70
60
50
40
30
20
10
0
-20
-10
0
10
20
30
40
50
60

Bunch length measurement by intensity interferometry

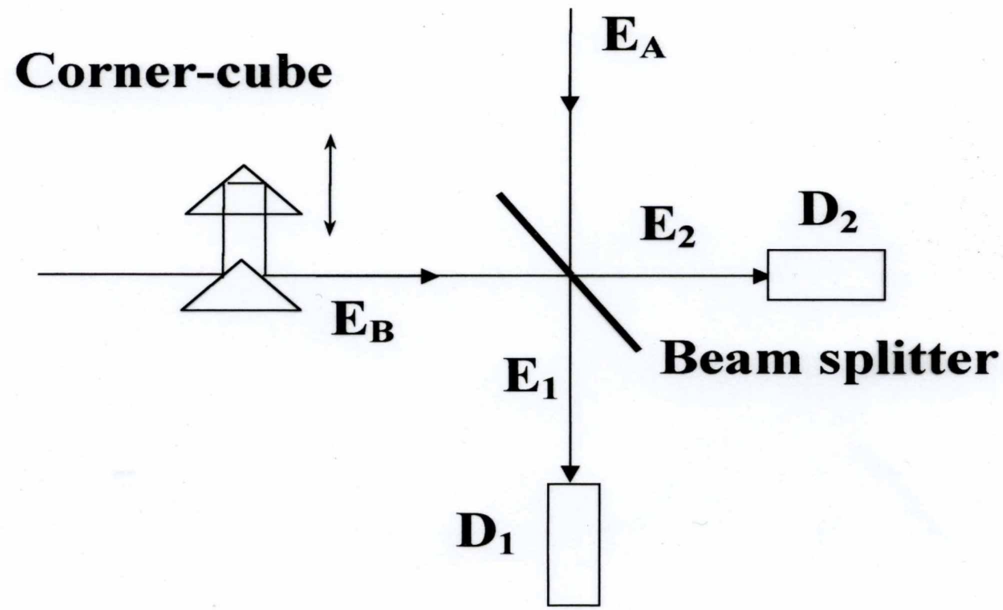

Input fields for a beam splitter in intensity interferometry.

Let us represent the incident optical field by the complex field ,

$$E_A(t) = C_A(t) A_A(t)$$
$$E_B(t) = C_B(t) A_B(t) \,. \quad -(3)$$

Here C(t) is the pulse envelope having a pulse width (bunch length) σ_p, and A(t) is a stationary random variable having coherence time τ_c.

We assume the correlation function of A(t) and C(t) have Gaussian shape. We also assume that E_A and E_B of two photons have no first order coherence. We thus obtain from Eq. (2), remormalizing the proportional constant K,

$$\mathrm{Count}_{12}(\delta\tau) = K\sigma_p^{\,2}\left(1+\frac{\tau^*}{\sigma_p}\left[1-\frac{1}{2}\exp\left(-\frac{\delta\tau^2}{4\sigma_p^{\,2}}\right)\right]\right),$$

$$\frac{1}{\tau^{*2}} = \frac{1}{\sigma_p^{\,2}} + \frac{1}{\tau_c^{\,2}} \,.$$

Let us represent the incident optical field by the complex field ,

$$E_A(t) = C_A(t)A_A(t)$$
$$E_B(t) = C_B(t)A_B(t)\ .$$

Here C(t) is the pulse envelope having a pulse width (bunch length) σ_p, and A(t) is a stationary random variable having coherence time τ_c.

We assume the correlation function of A(t) and C(t) have Gaussian shape.

We thus obtain coincidence count;

$$\mathrm{count}_{12}(\delta\tau) = K\sigma_p{}^2\left[1-\frac{1}{2}\exp\left(-\frac{\delta\tau^2}{4\tau_c{}^2}\right)+\frac{\tau^*}{\sigma_p}\left(1-\frac{1}{2}\exp\left(-\frac{\delta\tau^2}{4\sigma_p{}^2}\right)\right)\right]$$

$$\frac{1}{\tau^{*2}} = \frac{1}{\sigma_p{}^2}+\frac{1}{\tau_c{}^2}\ .$$

Illustration of intensity interference pattern with coherent light pulse. Phase correlation peak in the center.

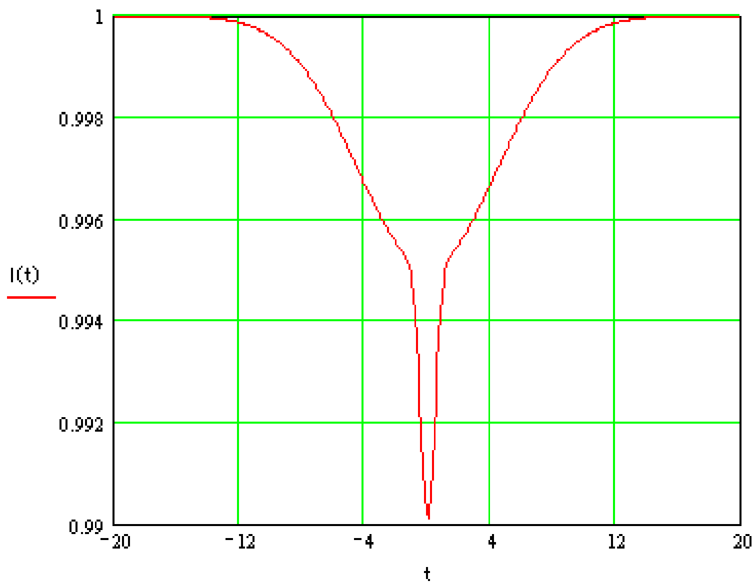

Illustration of intensity interference pattern with chaotic light pulse.

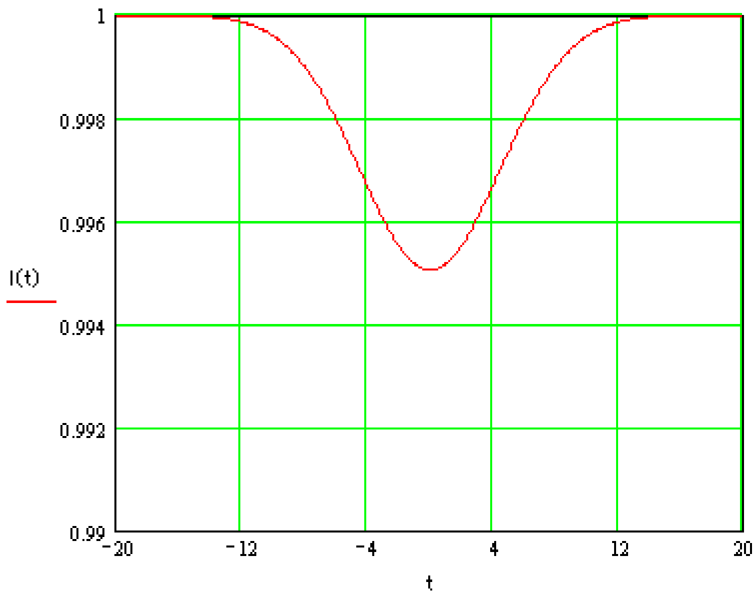

Experimental setup of the intensity interferometer

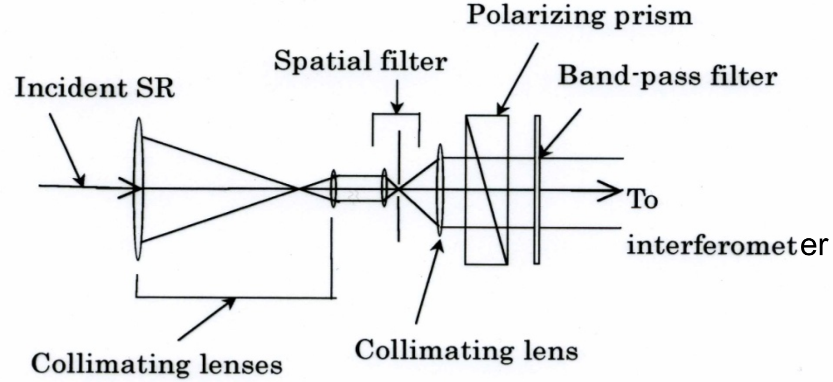

(a) Set up of first-stage system to produce an incidence beam for the interferometer

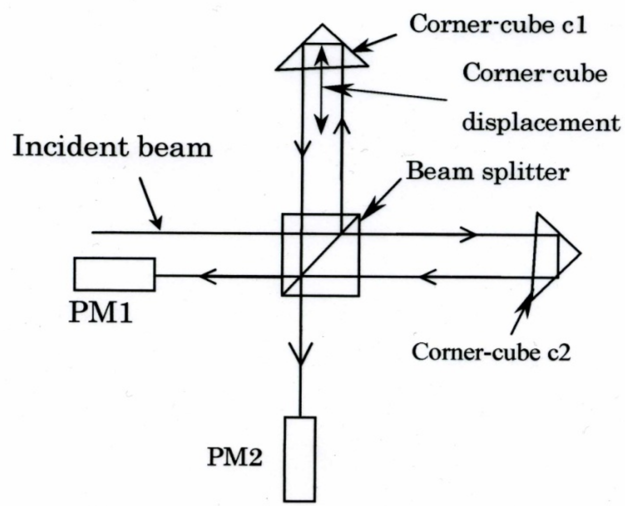

(b): Set-up of intensity interferometer.

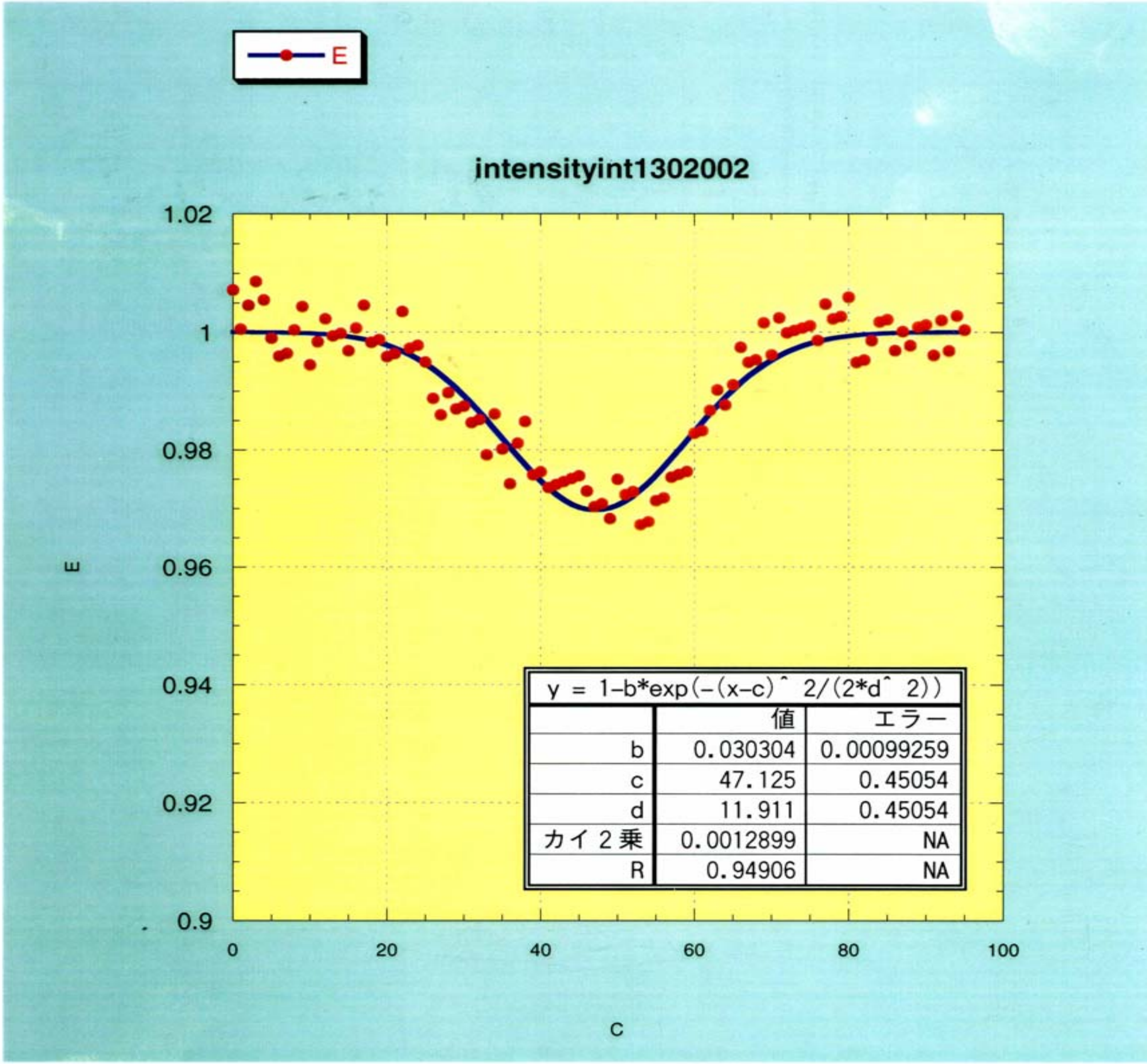

L_{corr} = 23.8 mm bunch length 16.8 ± 0.6 mm

σ_e = 50.5 ± 2 psec

Streack 46.8 ~ 51 psec

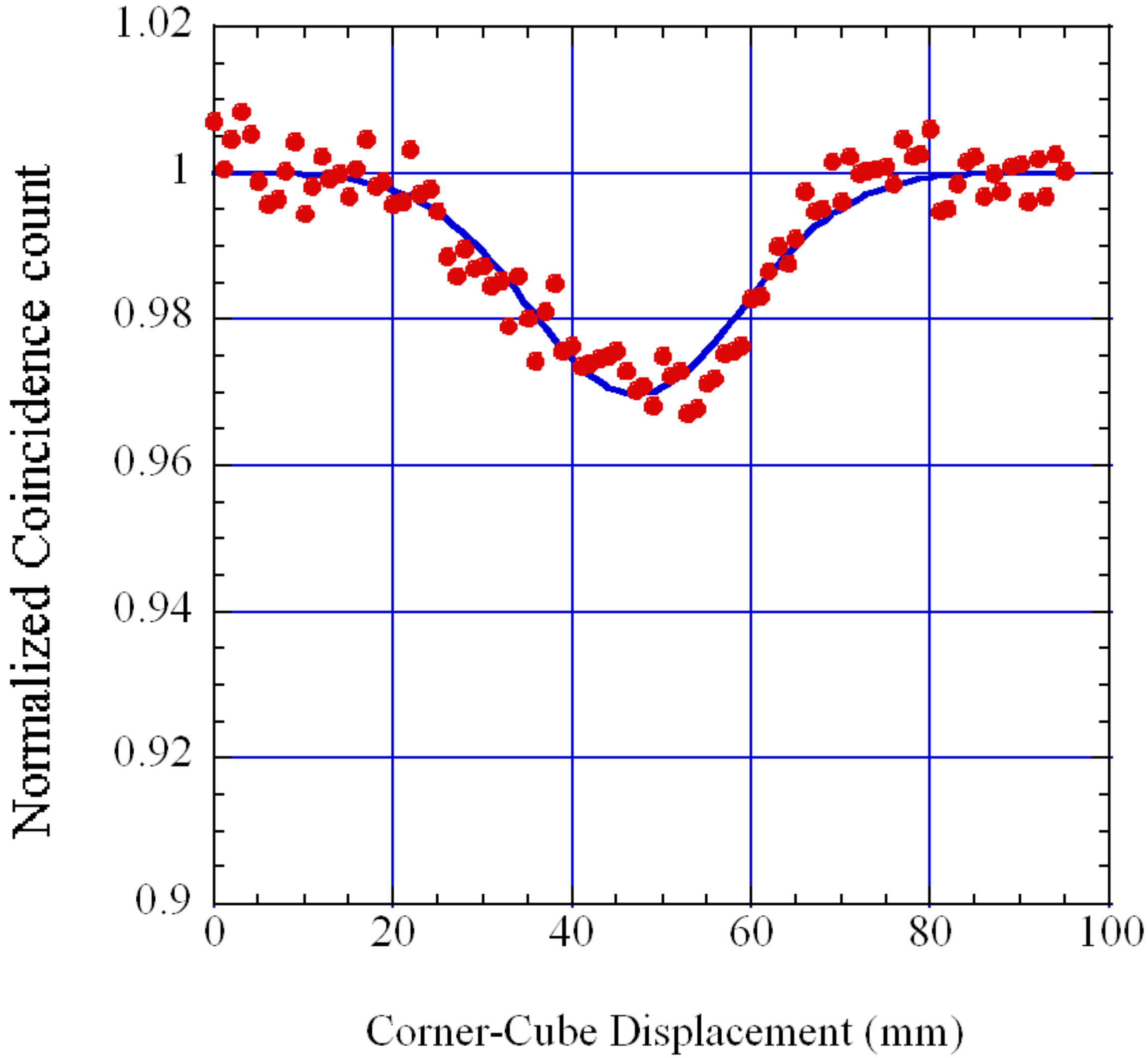

1.02
1
0.98
0.96
0.94
0.92
0.9
0
20
40
60
80
100
Normalized Coincidence count
Corner-Cube Displacement (mm)

Pulse envelope length σ_p is always longer than Coherent length of wave pockets τ_c.

$$\sigma_p \geq \tau_c$$

We can measure the very short pulse length with intensity interferometry
with nearly no theoretical limit on temporal resolution.

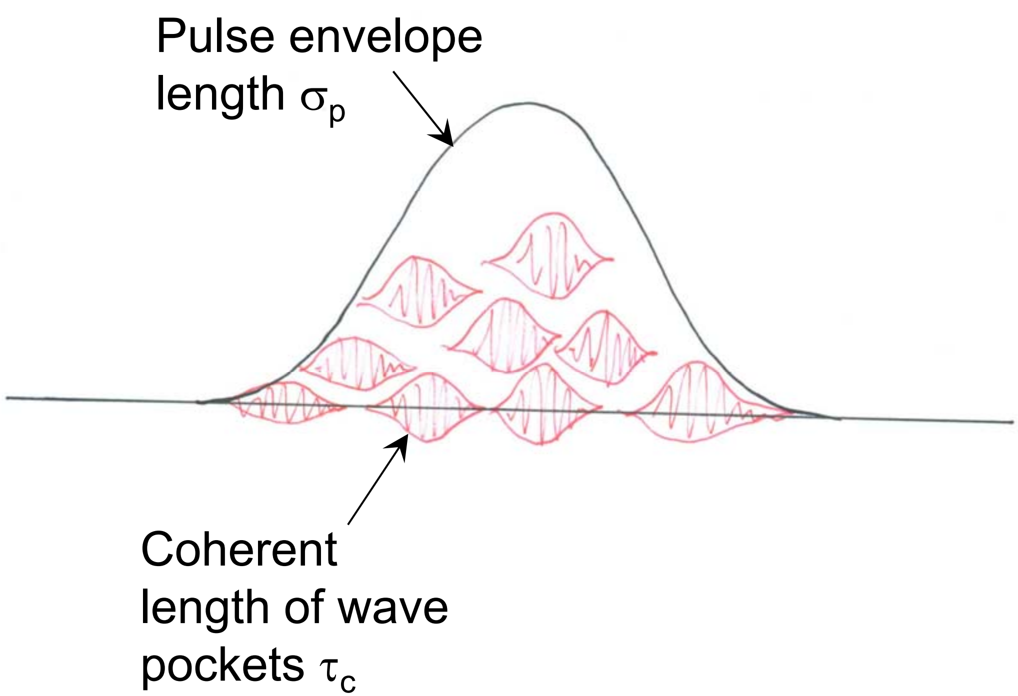

3-2. インコヒーレント SR 強度干渉計による ショートバンチ長の計測

Bunch length measurement by intensity interferometry

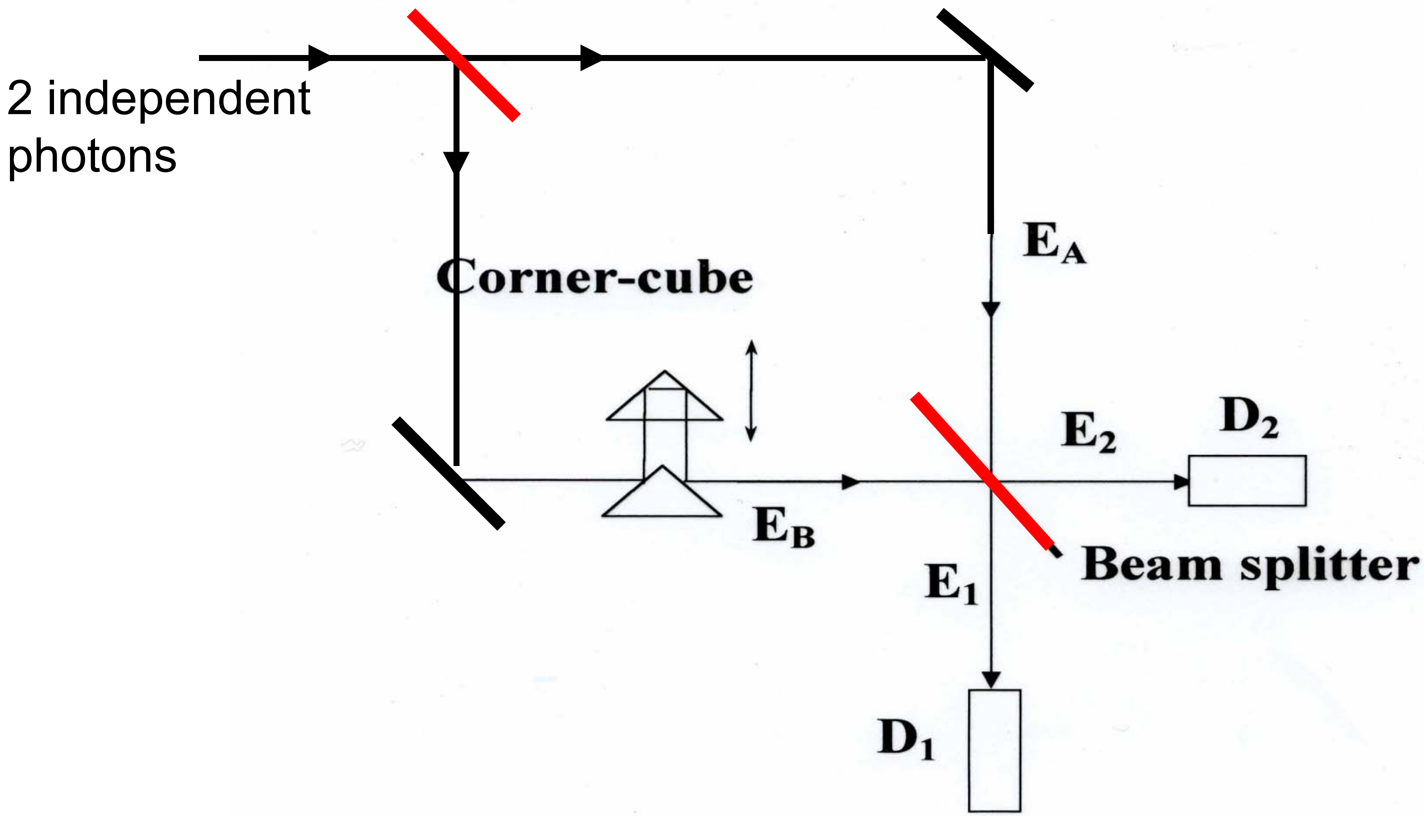

入力光のフィールドE_A,E_B

$$E_A(t) = C_A(t)A_A(t)$$
$$E_B(t) = C_B(t)A_B(t) \ .$$

σ_pのパルス幅(バンチ長)を持つパルスエンヴェロープ C(t)

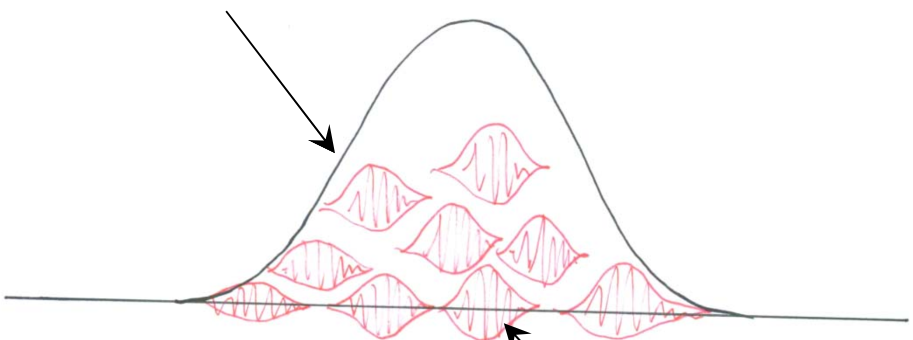

τ_c の コ ヒ ー レ ン ト 長 を も つ　stationary random variable A(t)

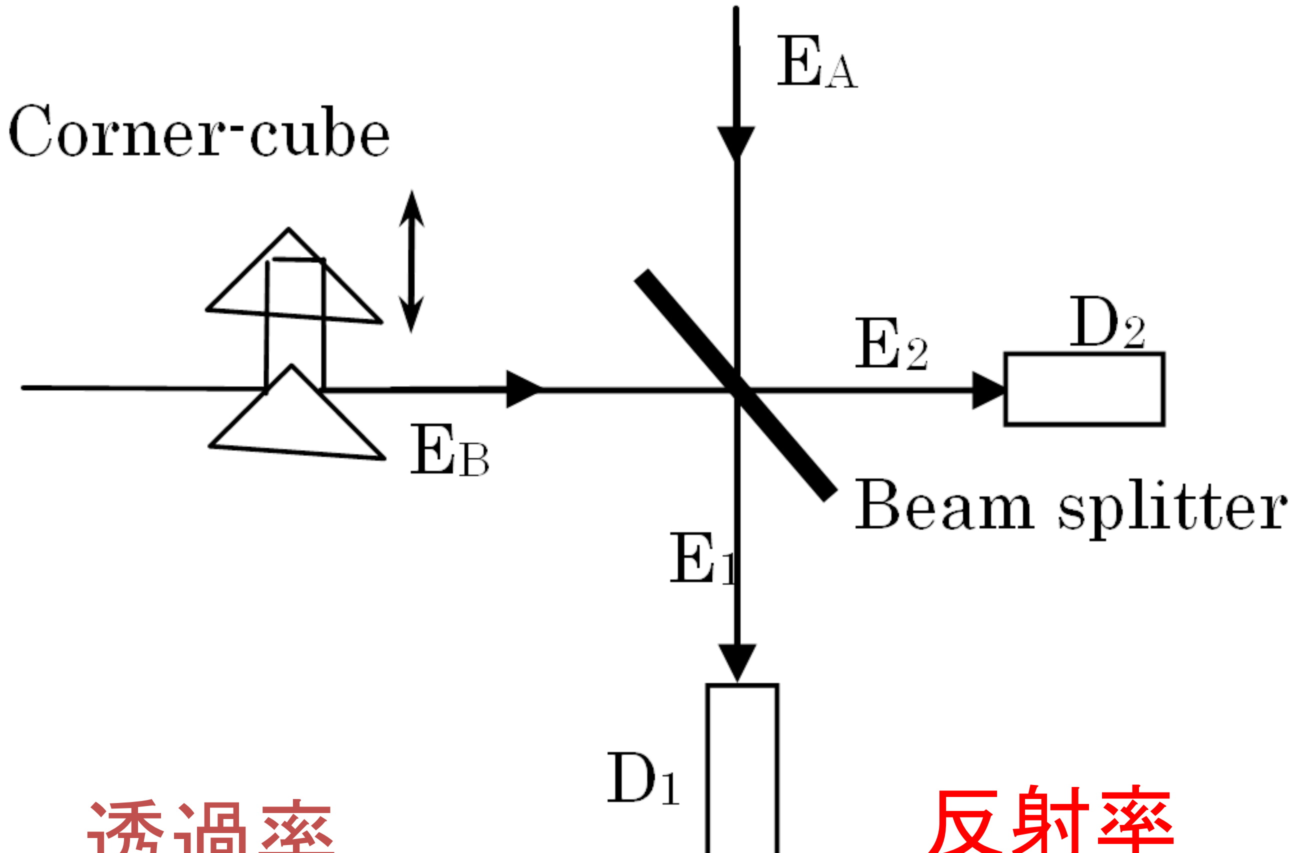

透過率　　　　　　　　反射率

$$E_1(t) = \sqrt{T} \cdot E_A(t) + i\sqrt{R} \cdot E_B(t + \delta\tau)$$

$$E_2(t) = \sqrt{T} \cdot E_B(t + \delta\tau) + i\sqrt{R} \cdot E_A(t) \ .$$

detector D1 と detector D2の同時計数 Count12(dt)はE1,E2を用いて

$$Count_{12}(\delta\tau) = K\int_{-\frac{T_m}{2}}^{\frac{T_m}{2}} dt \int_{-\frac{T_r}{2}}^{\frac{T_r}{2}} d\tau \left\langle E_1^{\ *}(t) E_2^{\ *}(t+\tau) \right.$$

$$\left. \times E_2(t+\tau) E_1(t) \right\rangle \ ,$$

C(t),A(t)の両方がGauss型であるとし、入力光子のフィールドE_A,E_Bが一次時間コヒーレント と思い、ゴチャゴチャした積分をやると、

パルスエンベロープの相関項

$$count_{12}(\delta\tau) = K\sigma_p^{\ 2} \times$$

$$\left[1 - \boxed{\frac{1}{2}\exp\left(-\frac{\delta\tau^2}{4\tau_c^{\ 2}}\right)} + \frac{\tau^*}{\sigma_p}\left(1 - \boxed{\frac{1}{2}\exp\left(-\frac{\delta\tau^2}{4\sigma_p^{\ 2}}\right)}\right)\right]$$

波束の相関項

$$\frac{1}{\tau^{*2}} = \frac{1}{\sigma_p^{\ 2}} + \frac{1}{\tau_c^{\ 2}} \quad .$$

E_A,E_Bが一次時間インコヒーレントな場合については波束の相関項が消えて同時計数は

$$Count_{12}(\delta\tau) = K\sigma_p{}^2\left(1+\frac{\tau^*}{\sigma_p}\left[1-\boxed{\frac{1}{2}\exp\left(-\frac{\delta\tau^2}{4\sigma_p{}^2}\right)}\right]\right),$$

パルスエンベロープの相関項

E_A,E_Bが一次時間コヒーレント

E_A,E_Bが一次時間インコヒーレント

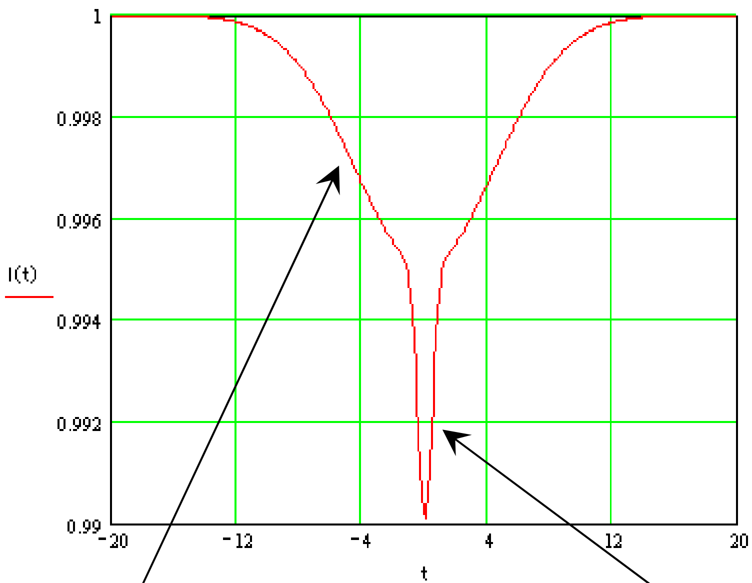

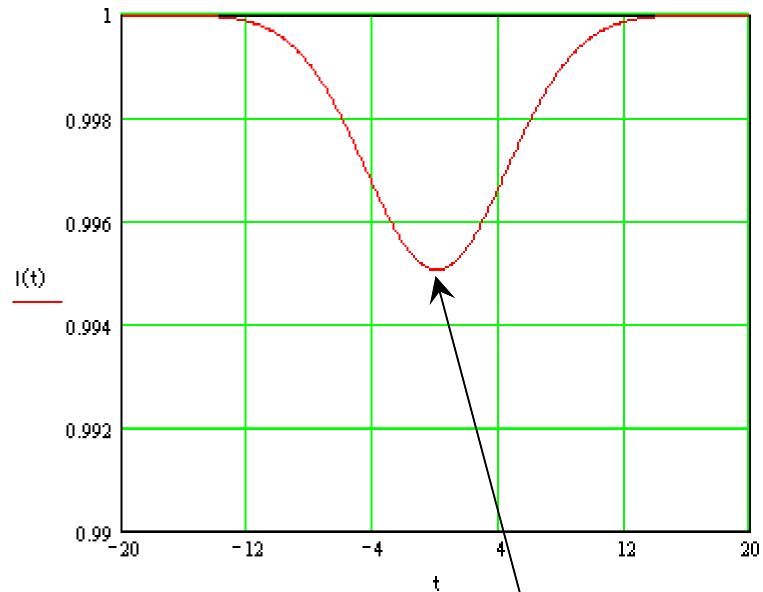

パルスエンベロープの自己相関

波束の自己相関

パルスエンベロープの自己相関だけ残る

実際の強度干渉計のセットアップ

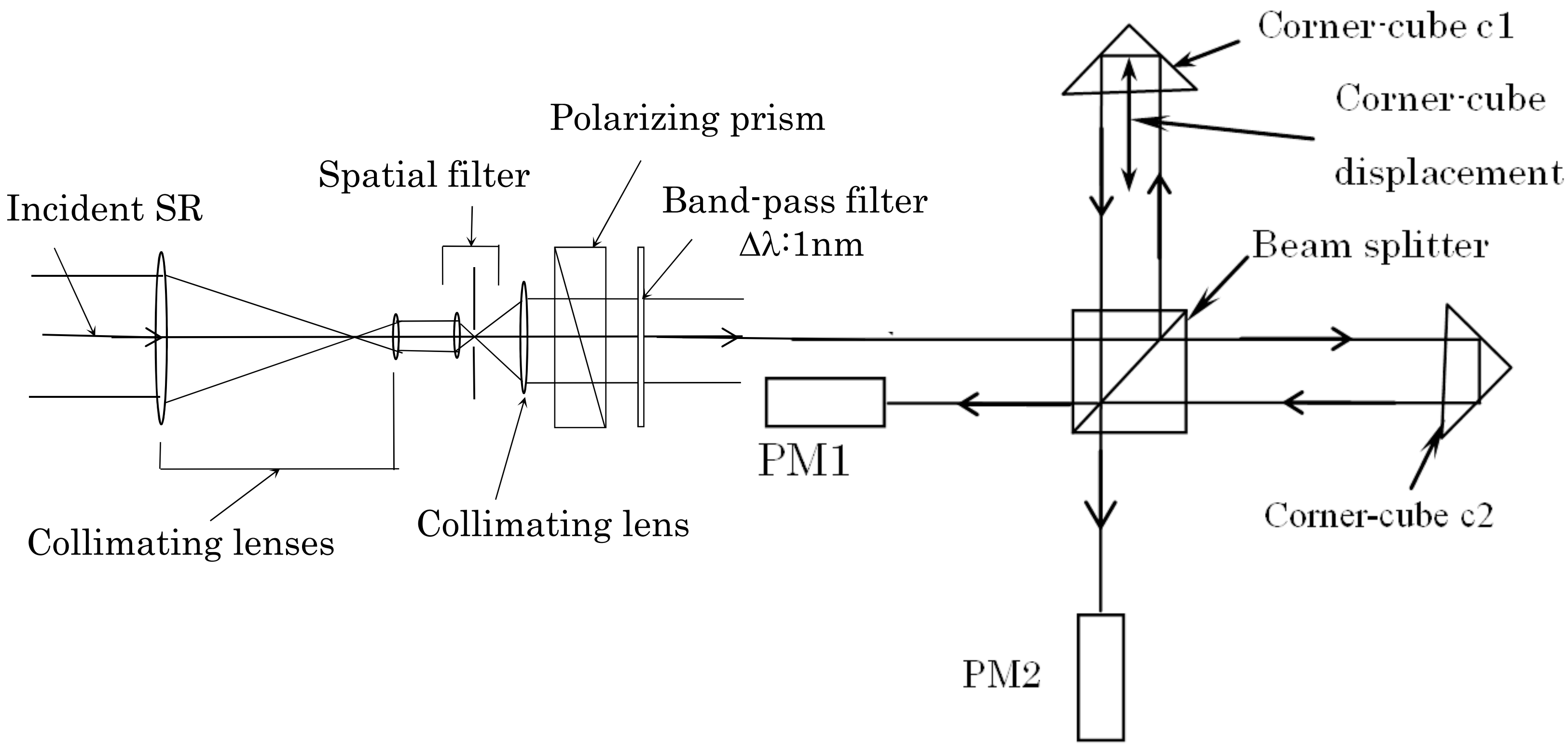

Count$_{12}$の実測データの例
オバーコリメーションである。

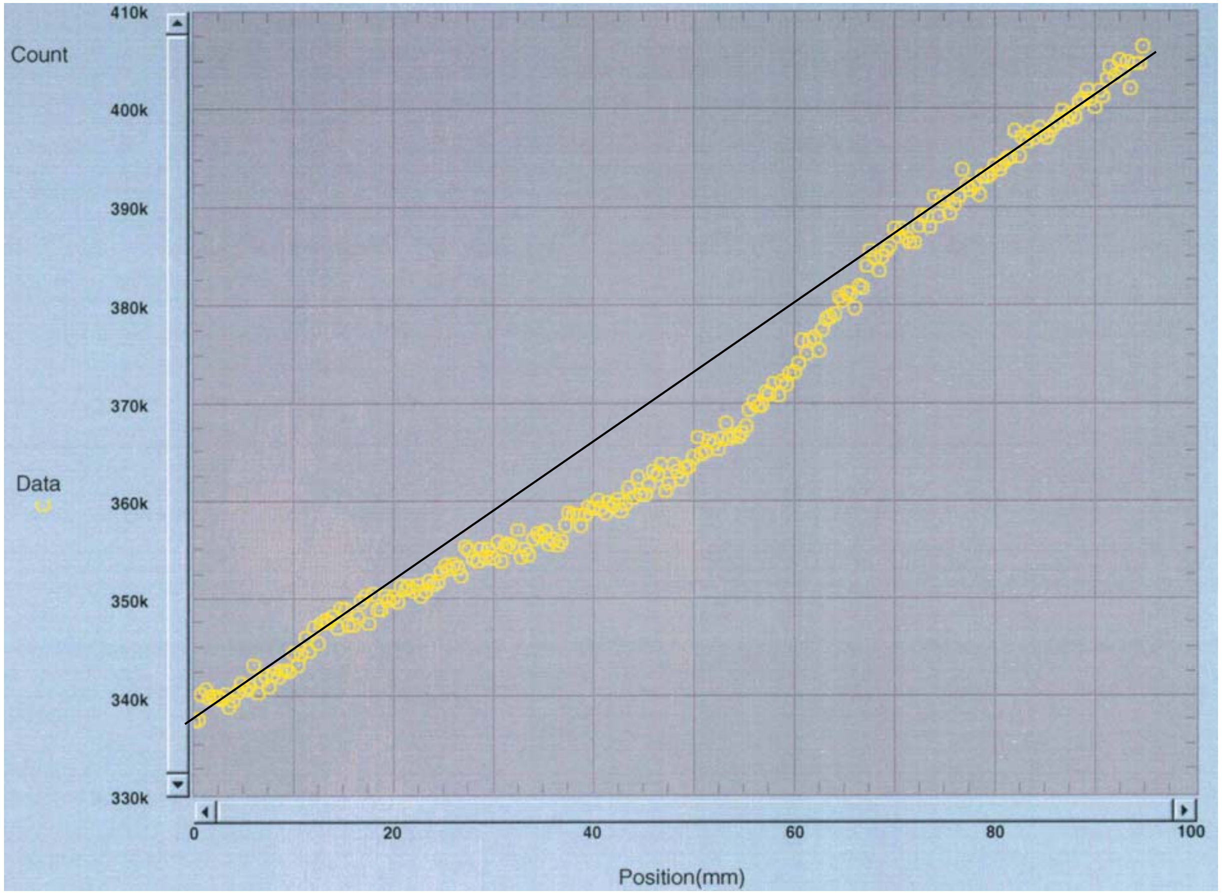

Count$_{12}$の実測データの例
アンダーコリメーションである。

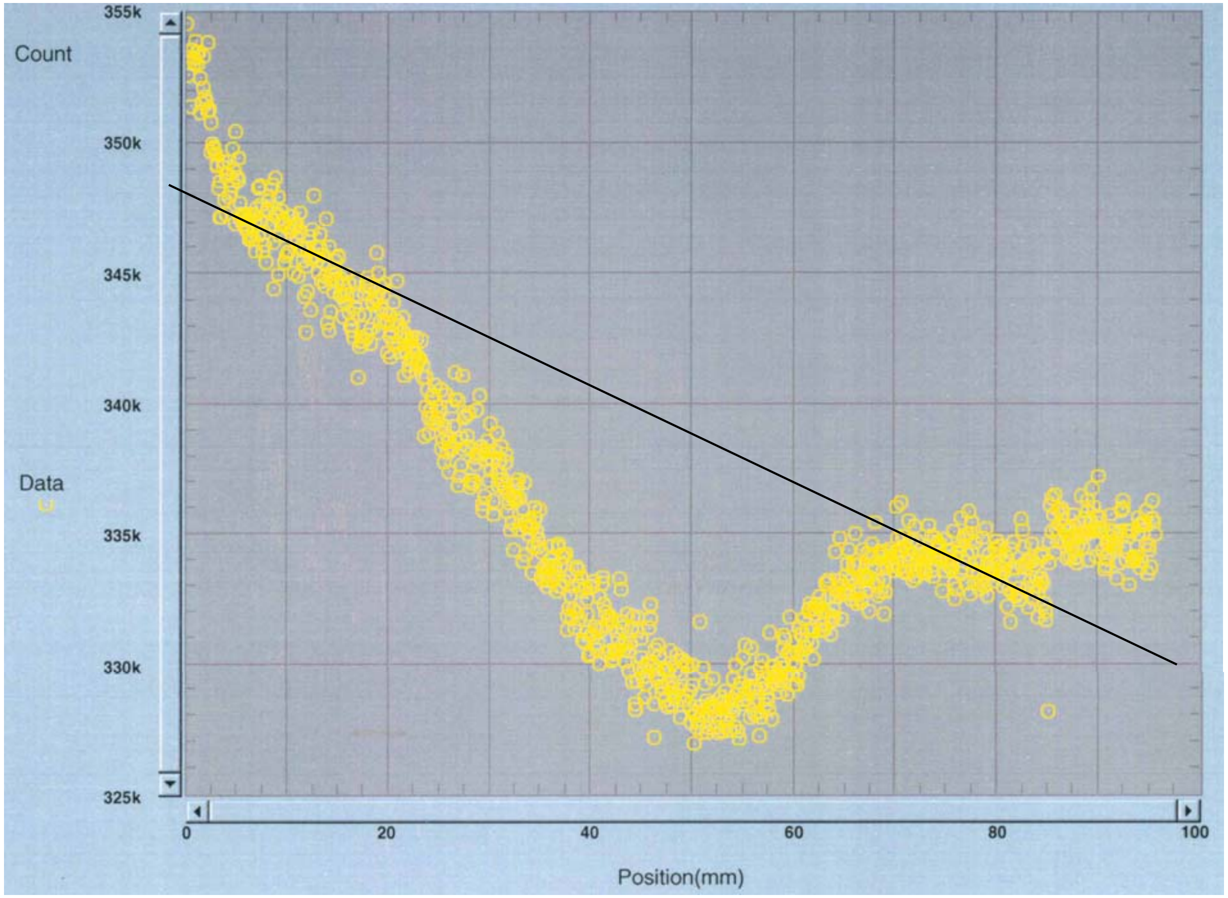

PFでのバンチ長測定結果

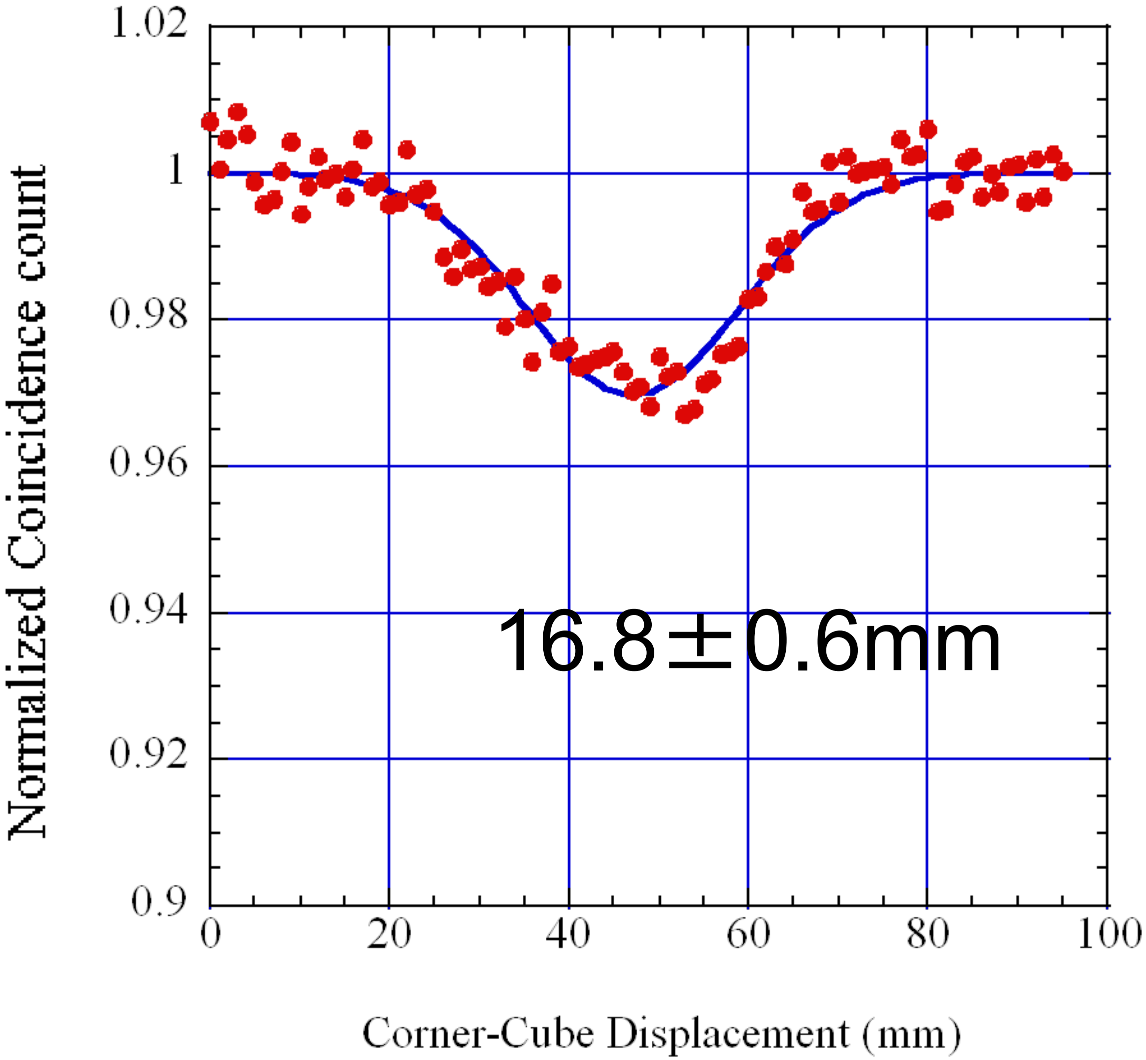

PFでのバンチ長測定結果

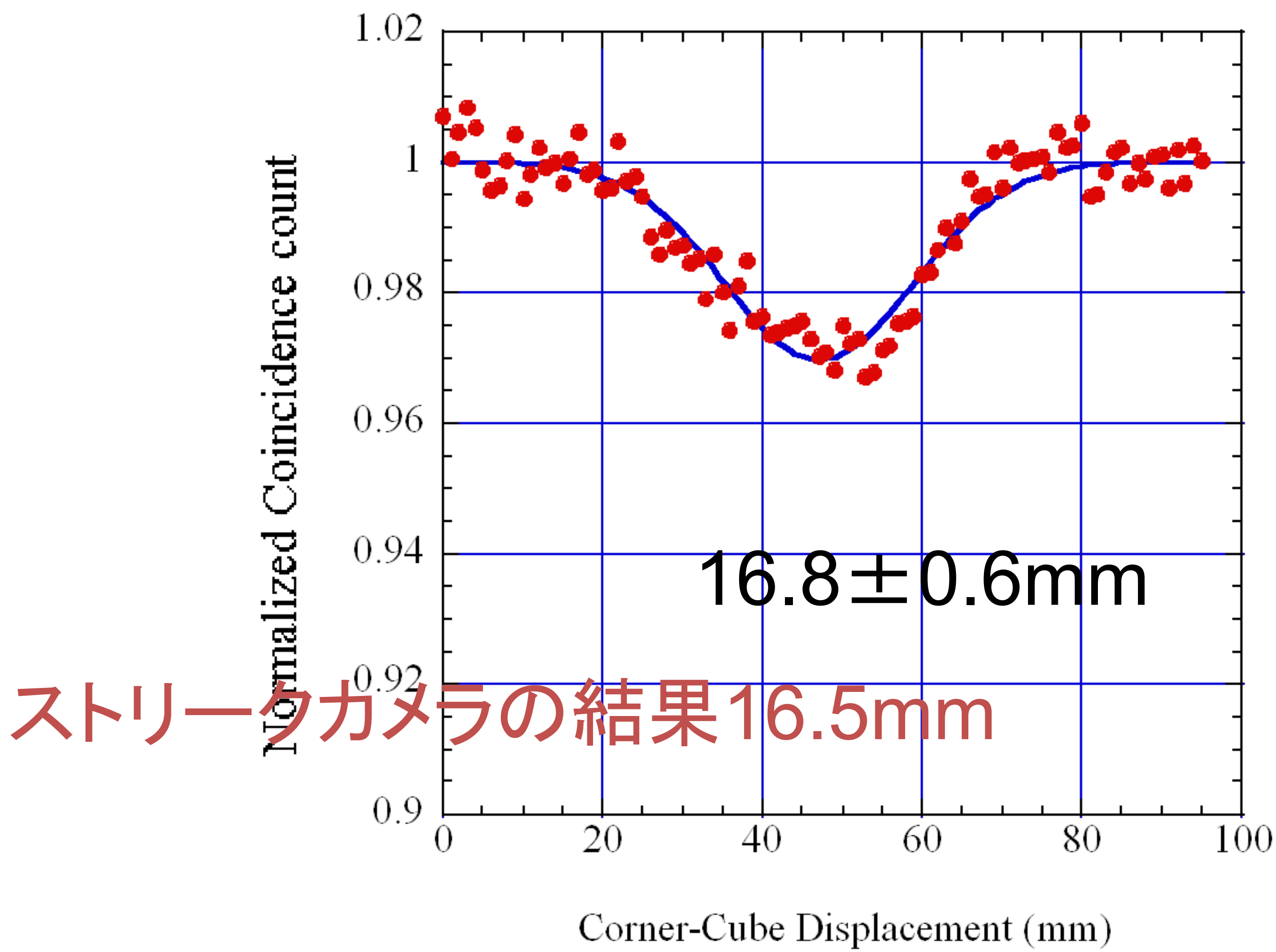

強度干渉計の時間分解能について

Pulse envelope length σ_p is always longer than Coherent length of wave pockets τ_c.

$$\sigma_p \geq \tau_c$$

We can measure the very short pulse length with intensity interferometry
with nearly no theoretical limit on temporal resolution.

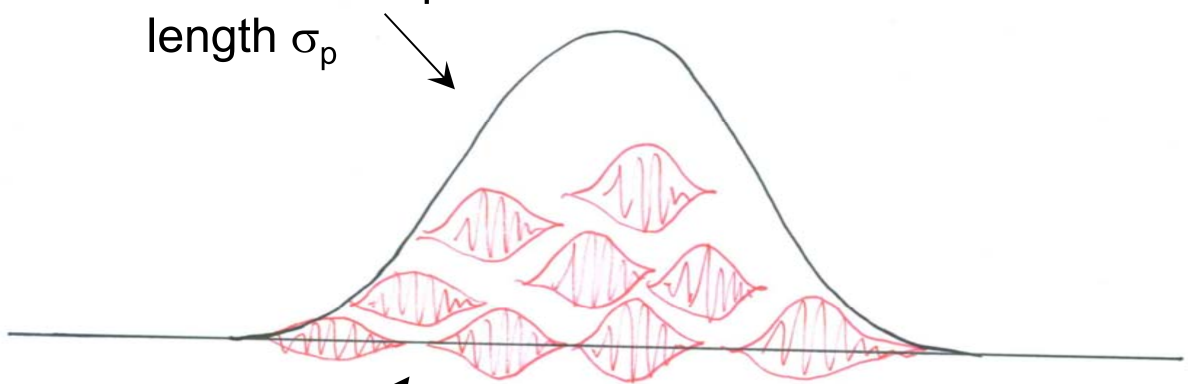

Actual resolution will be limited by dispersion of the glass. <10fsec

Conclusions of intensity interferometry

1. Bending radiation are chaotic as the ensamble of photons.
2. Intensity interferometry is fully applicable to measure very short bunch length.